Guanidinium Iminosugars as Glycosidase Inhibitors

Alen Sevšek

Cover image: Abstract representation of the pharmacological chaperone's mechanism of action

This Ph.D. program was financially supported by:
Slovene Human Resources Development and Scholarship Fund

The printing of this thesis was financially supported by:
Utrecht Institute for Pharmaceutical Sciences
Shimadzu Benelux BV
Screening Devices
MestReNova
Bio-Techne
Actu-All Chemicals
PamGene

Printed by: Print Service Ede
Cover by: Marjon Stel & Alen Sevšek
ISBN: 978-94-92679-20-8

Guanidinium Iminosugars as Glycosidase Inhibitors

Guanidinium Iminosuikers als Glycosidase Remmers

(met een samenvatting in het Nederlands)

Gvanidinijski Iminosladkorji kot Inhibitorji Glikozidaz

(s povzetkom v Slovenščini)

PROEFSCHRIFT

ter verkrijging van de graad van doctor aan de Universiteit Utrecht op gezag van de rector magnificus, prof.dr. G.J. van der Zwaan, ingevolge het besluit van het college voor promoties in het openbaar te verdedigen op maandag 30 oktober 2017 des ochtends te 10.30 uur

door

Alen Sevšek

geboren op 30 april 1987 te Celje, Slovenië

Promotor: Prof. dr. R.J. Pieters

Copromotor: Dr. N.I. Martin

This work is dedicated to my family, without whom this accomplishment would not be possible.

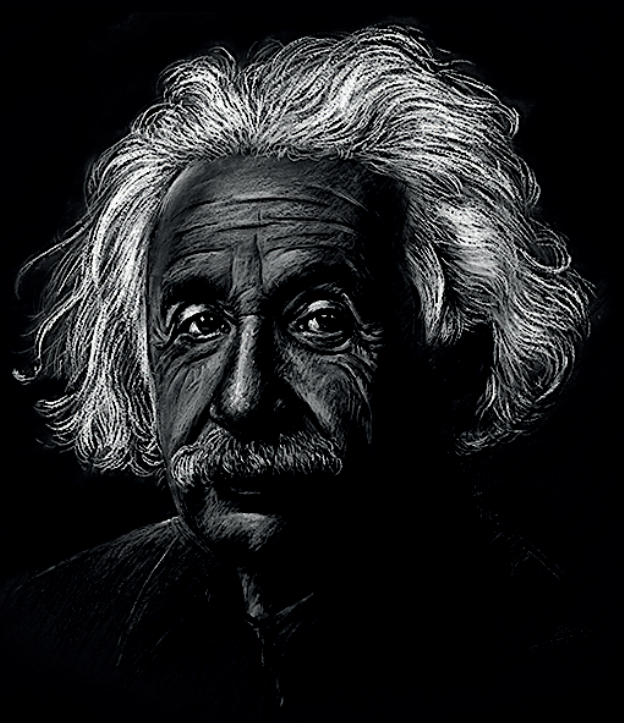

“Imagination is more important than knowledge.

For knowledge is limited to all we know and understand, while imagination embraces the entire world and all there ever will be to know and understand.”

— *Albert Einstein* —

Table of Contents

List of Abbreviations

Ac	acetyl
AcOH	acetic acid
All	allyl
Boc	tert-butyloxycarbonyl
Bn	benzyl
Bz	benzoyl
Cbz	carboxybenzyl
CSA	camphorsulfonic acid
DCE	dichlororethane
DCM	dichloromethane
DEAD	diethylazodicarboxylate
DiPEA	N,N-diisopropylethylamine
DIX	imino-D-xylitol
DMF	N,N-dimethylformamide
DNJ	deoxynojirimycin
DMSO	dimethyl sulfoxide
EDCI	ethyl dimethylaminopropyl carbodiimide
EMA	european medicine agency
ERAD	endoplasmic-reticulum-associated protein degradation
ERT	enzyme replacement therapy
ESI	electrospray ionization
EtOAc	ethylacetate
EtOH	ethanol
eq	equivalent
Fmoc	9-fluorenylmethyloxycarbonyl
GALC	β-galactocerebrosidase
GBA, GCase	β-glucocerebrosidase
GD	Gaucher disease
GlcCer	glucosylceramide
HBTU	O-(7-benzotriazol-1-yl)-N,N,N′,N′-tetramethyluronium hexafluorophosphate
HILIC	hydrophilic interaction liquid chromatography
HOBt	1-hydroxybenzotriazole
HPLC	high performance liquid chromatography
HRMS	high resolution mass spectrometry
IC_{50}	concentration at which 50% of the target is inhibited
IFG	isofagomine
LSD	lysosomal storage disease
MeOH	methanol
MS	mass spectrometry
MTBE	methyl-tert-butyl ether

NMR	nuclear magnetic resonance
NN-DNJ	*N*-nonyl-deoxynojirimycin
PC	pharmacological chaperone
PCT	pharmacological chaperone treatment
PDB	protein data bank
R_f	retention factor
RP-HPLC	reversed phase high-performance liquid chromatography
SPPS	solid phase peptide synthesis
SRT	substrate reduction therapy
TBAF	tetra-n-butylammoniumfluoride
TBDMSCl	tert-butyldimethylchlorosilane
tBu	tert-butyl
TFA	trifluoroacetic acid
THF	tetrahydrofuran
THP	3,4,5-trihydroxypiperidine
TIS	triisopropylsilane
TLC	thin layer chromatography
TMS	tetramethylsilane
UHP	ultra high performance
UV	ultra violet

Amino acids

Ala	A	Alanine
Arg	R	Arginine
Asn	N	Asparagine
Asp	D	Aspartic acid
Cys	C	Cysteine
Glu	E	Glutamic acid
Gln	Q	Glutamine
Gly	G	Glycine
His	H	Histidine
Ile	I	Isoleucine
Leu	L	Leucine
Lys	K	Lysine
Met	M	Methionine
Phe	F	Phenylalanine
Pro	P	Proline
Ser	S	Serine
Thr	T	Threonine
Trp	W	Tryptophan
Tyr	Y	Tyrosine
Val	V	Valine

CHAPTER 1

GENERAL INTRODUCTION

1

1 GENERAL INTRODUCTION

CHAPTER OVERVIEW

The scope of this thesis is to provide an overview of the strategies employed towards developing guanidine-containing iminosugars and evaluate their activity against disease relevant enzymes. The introductory chapter aims to describe the history and background information on topics that were involved in this study.

The first chapter provides background information on natural guanidines, reasons for their vast abundance in nature and their modifications for therapeutic opportunities.

Next, basic information on the important carbohydrate class is discussed with a subsequent focus on their nitrogen containing relatives: iminosugars. This attractive class of carbohydrate mimetics is discussed for the purpose of this work. Different tactics for iminosugar modifications and prospects of synthetic glycomimetics are briefly discussed.

The chapter continues to elaborate the importance of glycosidases; a class of enzymes responsible for glycan hydrolysis that is vital for normal cell function. Furthermore, current treatments for glycosidase deficiencies are deliberated, with the main emphasis on β-glucocerebrosidase, as compounds prepared in this work seem to be selective for this particular enzyme. Defective mutants of this protein are responsible for the most common lysosomal storage disorder named Gaucher disease.

The section concludes with an overview of current small-molecule actives and outlines the subsequent research chapters discussed in this thesis.

1.1 GUANIDINE GROUP

Guanidines are neutral, nitrogen-containing compounds ubiquitously found in nature, predominantly in the form of arginine (**1**) containing compounds (**Figure 1**), and are critical for the normal function of living organisms.[1] The active sites of many enzymes contain functional groups that can interact with guanidine and it is therefore not surprising that a broad range of biologically active compounds in a significant number of natural products and clinical pharmaceutical ingredients include guanidine moeities.[2] Guanidine groups determine the chemical and biological properties of many compounds suitable for medicinal purposes. Guanidine-rich compounds have the potential to treat a wide variety of diseases attributed to the multiple ways that the guanidinium cation engages in non-covalent interactions.[3,4]

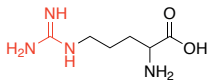

1

Figure 1. Arginine (**1**) as one of the main guanidine containing compounds found in nature.

Guanidines are considered as organic superbases due to their conjugated acid pK_a values of approximately 13 and are commonly used as strong bases in synthetic organic chemistry.[5] This extremely high basic nature can be explained by the resonance stabilization of the protonated form with three canonical resonance structures as illustrated in **Scheme 1**.[6]

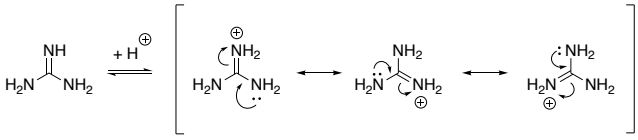

Scheme 1. Guanidine protonation and resonance structures of guanidinium cation (p*K*a = 13.6) with its three canonical forms.

Due to the high basicity of guanidine groups, a wide variety of guanidine compounds remain protonated over a wide pH range in its conjugate acid form, and form strong non-covalent interactions to anions such as carboxylates and phosphates, through ion pairing and hydrogen bonding.[7] Interestingly, the guanidinium ion is one of the most hydrophilic functional groups known,[8] and one would think that solvation by water molecules in aqueous solution is so efficient that despite the favorable ion-pairing with carboxylates and phosphates would tend to be insignificant.[9] However, solvation does not pose any problems in nature due to the rather hydrophobic interior of proteins where such interactions usually occur, permitting guanidine-rich compounds to play decisive roles in transition state binding in various catalytic processes and therefore represent promising natural drug agents and therapeutic tools for the future.[10] On the downside, high polarity of simple guanidines is responsible for poor uptake of such charged drugs, which requires appropriate synthetic modifications in order to achieve better permeability.[11]

1

1.1.1 Natural guanidines

The sheer number of guanidine-containing derivatives in nature, in both terrestrial and marine environments, is very impressive. Probably the most notable is the diversity of guanidine alkaloids in aquatic organisms that represent an intriguing aspect of guanidine chemistry.[12] These alkaloids include structural motifs that range from simple arginine,[13] creatine or agmatine residues, and their derivatives incorporated into terpenes[14] and peptides[15] to the highly complex polycyclic frameworks of crambescidins,[16] massadines,[17] palau'amines,[18] ptilomycalins,[19] and related analogues.[20] Noteworthy are also intriguingly complex and potently active saxitoxins[21] and tetrodotoxins[22] found in many different animal species that still remain a subject of much research due to significant implications in cancer-associated pain (**2**, **3** and **4**, **Figure 2**).[23] At the moment, many natural guanidine-rich molecules are in different phases of preclinical and clinical development and one natural product ziconotide (**5**),[24] isolated from *Conus magus* snail venom, is already approved and marketed as synthetically prepared equivalent - Prialt®, which is used to ameliorate severe and chronic pain (**Figure 3**).[25]

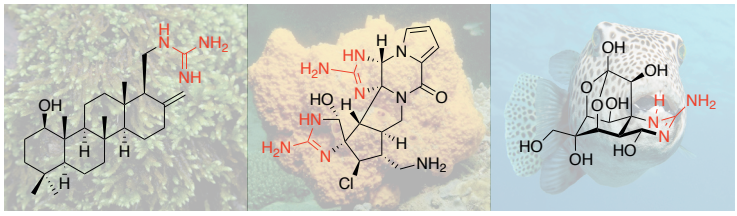

2
Scytoscalarol
Antimicrobial activity
f.e. Scytonema

3
Palau'amine
Immunosuppressive activity
f.e. Stylotella agminata

4
Tetrodotoxin
Pain relief
f.e. Hepalochlaena lunulata

Figure 2. A selection of few natural guanidine-containing compounds **2**, **3** and **4** with bioactive properties and their corresponding natural source representatives in the background.

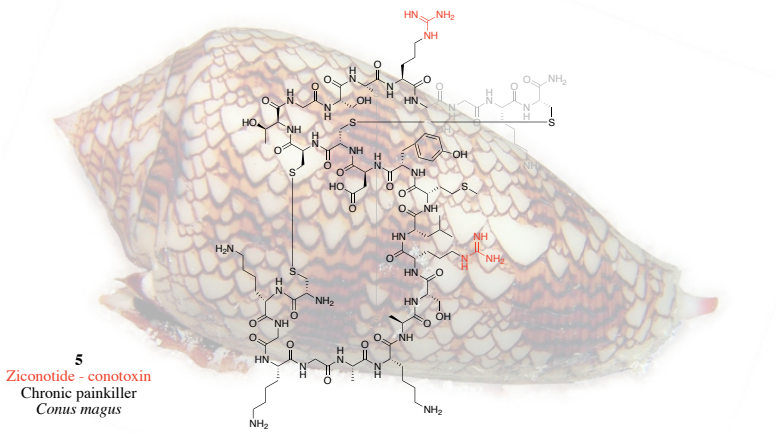

5
Ziconotide - conotoxin
Chronic painkiller
Conus magus

Figure 3. Natural product ziconotide **5** from *Conus magus* (in the background) venom as a potential chronic painkiller.

It is therefore not surprising, that natural abundance of guanidine-rich compounds as well as the natural propensity of the guanidinium cation to engage in non-covalent interactions holds important roles in biological systems and exhibits a broad spectrum of biological activities, which serves as a gateway to new medicines.[26]

1.1.2 Synthetic guanidines

The polyvalent nature of guanidine compounds, due to its three nitrogens, proved to be a promising flexible synthetic template to which side chains may be appended in order to occupy similar relative regions of space as of the known ligands. Substitution of the nitrogen atoms in guanidine by electron-donating groups such as alkyls or heteroalkyls slightly increases its basicity, while substitution by electron withdrawing groups such as aryl, acyl, sulfonyl, NO_2, CN, NH_2, OH or OCH_3 decreases the p*K*a values considerably to approximately 8, which could be utilized for the desired effect of the potential drug.[27] Although the natural guanidines from plants and microorganisms can have good biological activity profiles, modifications of the natural template successfully lead to bioactive compounds with greater selectivity and potency. Therefore, synthetic guanidine-containing compounds have attracted considerable interest as a result of their modification possibilities and diverse chemical, biochemical and pharmacological properties (**Figure 4**).[28–31]

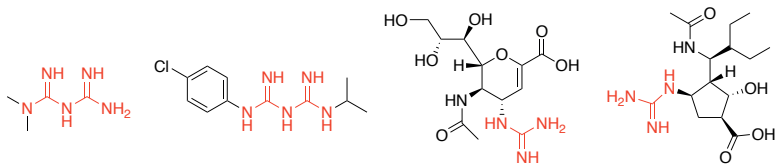

Figure 4. A selection of few guanidine-containing therapeutics that have reached the market.

It has been known since the 1960s that guanidine hydrochloride inhibits the replication of many plant and animal viruses.[32] Extended close relatives to classic guanidines, as can be seen in metformin (**6**) and proguanil (**7**), are one of the first guanidine-containing drugs used in the clinic. Metformin, marketed as Glucophage®,[33] is the first-line medication for the treatment of type 2 diabetes and proguanil, sold under the trade name Paludrine®,[34] is a medication used to treat and prevent malaria. In addition, first marketed antiviral guanidine-containing drug – zanamivir (**8**), developed by *van Itzstein*, was approved by the FDA and marketed as Relenza® (**Figure 4**) in 1999.[35] A few years later, peramivir (**9**), a close relative of zanamivir was approved for treatment under the name Rapivab®.[36] Both analogues exhibit additional hydrogen-bonding interactions with the active site of neuraminidase, resulting in the inhibition of oseltamivir-resistant strains of influenza.[37] This is a great example of how incorporating a guanidine moiety into the design can be exploited for successful drug development.[38] So far, an array of synthetic guanidines have been evaluated in many bioassays which lead to a vast

interest in developing them in novel drugs for antibacterial,[39–42] anticancer,[28,43–45] antihypertensive,[46] anti-inflammatory,[47] antithrombotic,[48,49] antidiabetic,[50–52] antifungal,[31,53] antiparasitic,[54,55] anti-neurodegenerative,[30,56] antiviral[29,57] purposes and drugs that can be used as guanidinium-based transporters.[58,59] Since the so-broad topic of guanidine chemistry exceeds the scope of this thesis, its main idea was to discuss the beneficial use of this attractive moiety to enrich molecules and utilize additional hydrogen binding with enzymes of interest.

1.2 THE DIVERSITY OF GLYCANS

Glycans, also called sugars or carbohydrates, are ubiquitous biomolecules essential for all known forms of life and are, together with a vast library of proteins, lipids and nucleotides, among the most abundant natural products in the kingdom of life (**Figure 5**).[60] Although they are generally perceived as being merely a source of nutrition, these biologically important functional molecules decorate the surface of cells to aid tissue integrity, act as receptors for various viruses, bacteria, pathogens and toxins,[61] regulate cell adhesion,[62] influence metastasis of cancer cells,[63] have vital roles in the immune response,[64] and are crucial in a vast array of numerous other biological functions.[65,66]

It is therefore not surprising to consider this class of molecules a vital part of biologically and therapeutically important medicines comprised of antibiotic, antidiabetic, antitumor and antiviral drugs, which places glycans at the forefront of modern chemical and biomedical research.[67–70]

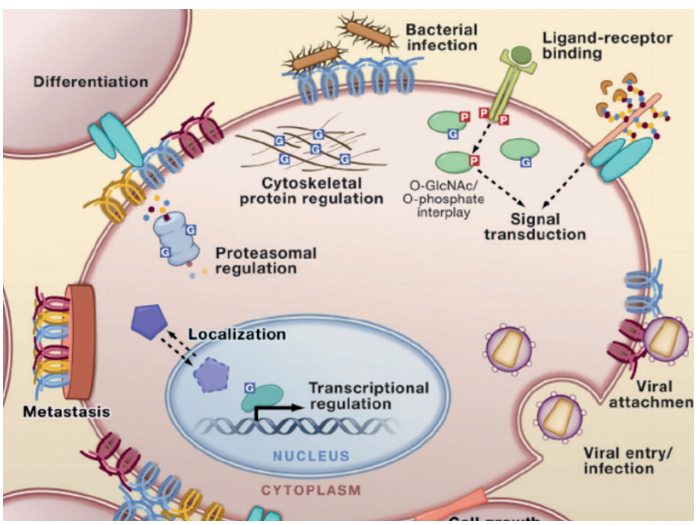

Figure 5. The role of glycans and dynamic complex processes they take part in living organisms.[71]

1.2.1 *Iminosugars: an important subgroup of glycans*

A special class of carbohydrate mimetics in which the endocyclic oxygen of the molecule is replaced with nitrogen, are generally named iminosugars (**Figure 6**).[72] These small and stable polar molecules share many properties with carbohydrates, but remain at the same time sufficiently distinct, which allows them to avoid being processed by carbohydrate enzymes and are rather readily excreted in urine without many modifications.[73] There are numerous individual targets encompassing a range of therapeutic areas and many of the natural or synthetically modified iminosugars might eventually find curative use by affecting these targets if they continue to exhibit specificity and potency in appropriate assays.[74]

Five different ring structures that can be found in nature fall into this classification: piperidines (**10**), indolizidines (**11**), pyrrolidines (**12**), pyrrolizidines (**13**) and nor-tropanes (**14**) as represented in **Figure 7**. There are now more than 200 variants of natural iminosugars reported, and the variety of synthetic compounds have been researched extensively.[75] These natural or synthetic polyhydroxylated alkaloids can interact with a range of carbohydrate enzymes such as glycosyltransferases, glycosidases and nucleoside-processing enzymes, thereby potentially affecting many biological processes of medicinal interest.[76] Almost four decades since their first isolation, iminosugars are considered to have great biological and therapeutic application as a result of their excellent drug profile.[77]

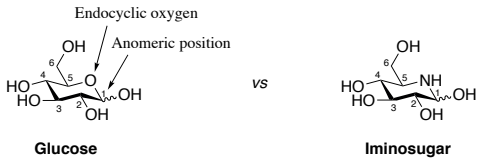

Figure 6. Basic structure of iminosugars and comparison with glucose.

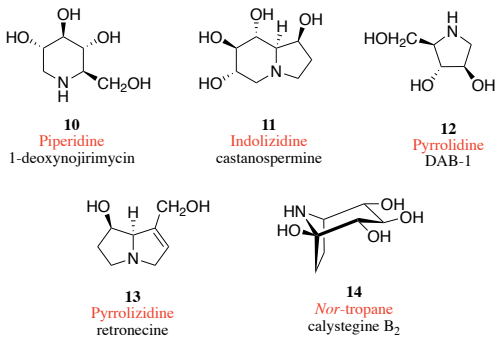

Figure 7. Most common natural structural classes of iminosugars and corresponding selected representative for each class.

1.2.2 The birth of iminosugar research

Ever since classification of iminosugars in the 19th century, organic chemists have been on a pursuit for more complex natural and non-natural derivatives.[78] In this respect, it is interesting that the discovery of iminosugars was first achieved *via* synthesis as opposed to the majority of naturally occurring compounds being first isolated from natural sources. Many groups investigated possible modifications of the oxygen atom in carbohydrates with other heteroatoms and *Paulsen et al.* managed to, somewhat unexpectedly, synthesize and identify a 1-deoxyglucose analog with a substituted nitrogen in the ring named 1-deoxynojirimycin (**15**, DNJ, **Figure 8**).[79] A few months after this discovery the first natural iminosugar, nojirimycin (**16**, NJ, **Figure 8**), was discovered by *Inouye* and co-workers in Japan in 1966, as a result of investigating novel antibiotic properties of *Streptomyces*.[80] Nevertheless, nojirimycin suffered from one of the major drawbacks associated with some simple iminosugars: their instability in solution.[81]

In comparison, DNJ lacking the anomeric hydroxyl, proved to be a relatively stable compound. This instability of NJ can be explained by the lability of the *N*,*O*-acetal function, which prevents their use as biological probes or drug candidates. In order to overcome this problem; one can simply exclude the anomeric hydroxyl group. Such a strategy of removing the anomeric hydroxyl, was originally employed in a more controlled fashion of DNJ synthesis by the *Inouye*-group in 1968 confirming the identical structure of *Paulsen's* molecule.[81] Also, DNJ was isolated from mulberry leaves in 1976 by *Yagi et al.* while studying the antidiabetic activity of the plant,[82] and was later found to be a potent, unspecific and stable inhibitor of the α- and β-glucosidases.[83] Another example of stable iminosugars is Castanospermine (**17**) that has been isolated in the 1980s from the Australian legume *Castanospermum australe*.[84] Castanospermine was later established to be an α-glucosidase I inhibitor with marked antiviral activity against a number of viruses.[85] α-glucosidase I plays a critical role in viral maturation by initiating the processing of the *N*-linked oligosaccharides of viral glycoproteins which are essential for virus–host interactions and inhibition of this enzyme is considered to be an attractive anti-hepatitis C virus (HCV) strategy.[86]

The aforementioned strategy triggered the ever-rising therapeutic interest in iminosugars, and many synthetic efforts have been devoted to developing efficient therapeutic agents.[74,87,88]

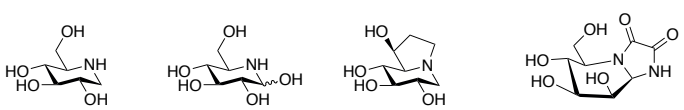

Figure 8. First known natural iminosugars 1-deoxynojirimycin (**15**), nojirimycin (**16**), castanospermine (**17**), and kifunensine (**18**).

1.2.3 sp^2 iminosugars

Although natural products from plants and microorganisms can have decent selectivity characteristics, most representatives of early researched iminosugars exhibit broad inhibitory profiles; for example, simultaneously inhibiting several α- and β-glycosidases, which represents a serious limitation for clinical applications.[89] Fortunately, modifications of natural templates have been very successful in producing bioactive compounds with better drug profiles. Tuning synthetic variants in such a way to enhance binding to target enzymes without affecting the off-target relatives could result in fewer unwanted side effects, which would drastically improve important features of future therapeutics. With the aim of improving the enzyme selectivity, replacement of the standard sp^3 hybridized endocyclic amine-type nitrogen atom with a trigonal planar pseudo amide-type nitrogen with a substantial sp^2-hybridisation profile has given rise to a new family of glycomimetics, named sp^2-iminosugars.[76] One of such examples found in nature is kifunensine (**18**, **Figure 8**), which was isolated from *Kitasatosporia kifunense*[90] in 1987 and was also characterized[91] and chemically synthesized[92] some years later. Kifunensine also proved to have a potent inhibitory activity against α-mannosidase[93] and has later shown promise as an anticancer agent.[94] Closely related, ureas (**19**),[95] thioureas (**20**),[96] isoureas (**21**),[97,98] isothioureas (**22**),[99] guanidines (**23**),[95] carbamates (**24**),[100] thiocarbamates (**25**),[101] sulfamides (**26**),[102] and thiohydantoines (**27**)[103] all fall into this category and it has been confirmed that some of these glycomimetics have unparalleled abilities to discriminate between different glycosidase isoenzymes (**Figure 9**).[104,105]

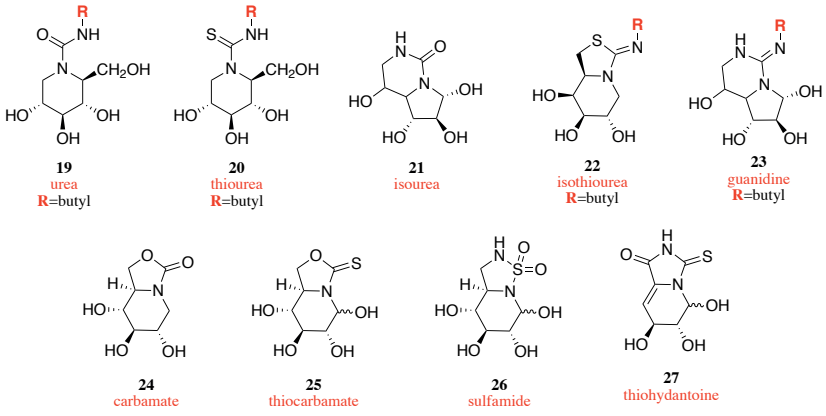

Figure 9. A selection of few sp^2 iminosugars.

This principle can be illustrated by a comparison of simple iminosugar **16** with a synthetically prepared nojirimycin carbamate **28**,[105] which acts as a specific inhibitor of neutral α-glucosidases, exhibiting antiproliferative activity against human breast carcinoma cells *in vitro* (**Figure 10**).[106] In comparison to nojirimycin (**16**), derivative **28** has the anomeric hydroxyl group somewhat 'axially anchored',[100] which would equal the configuration of natural α-glucosides. Such more pronounced anomeric

effect in sp^2-iminosugars is ascribable to a very efficient overlap between the lone-pair of the endocyclic nitrogen and the σ-antibonding orbital of the anomeric bond.[107] Interestingly, biological experiments *in vitro* revealed that compound **28** behaves as a potent and selective inhibitor of α-glucosidase, with α/β anomeric selectivity of at least 300-fold, which is much higher than their close relatives **15**, **16** and **18**.[105] It was claimed that such anomeric effect outperforms electron acceptor nature of the compound and might be an explanation to stereo-complementarity of the axially oriented hydroxyl group with the key active site residues in α-glucosidase that is responsible for the remarkable α-selectivity.[98]

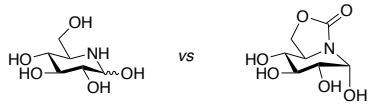

16 **28**

Figure 10. Enhanced anomeric hydroxyl stabilization of sp^2 modified iminosugar **28**.

In some cases, sp^2-iminosugars can potentially result in extremely strong anomeric effect that results in very high chemical and configurational stabilities and in some cases lead to notable improvements compared to classical iminosugars such as naturally occurring nojirimycin **16**, which does not possess a defined configuration at the pseudoanomeric center in aqueous solution and therefore categorizes the sp^2 modified iminosugars as a special class of new and promising drug candidates.[108]

1.2.4 Modified iminosugars and their benefits

An important aspect in finding a perfect drug candidate lies in their ability to be a potent inhibitor. Strong affinity of therapeutics would mean that a smaller amount of the drug is needed to attain the same results in comparison with their weaker competitors. In order to strengthen the affinity of iminosugars for α- or β-glycosidases, fine-tuning is possible by the incorporation of substituents that provide additional hydrophobic interactions with the protein. Besides enhancing potency, structural modifications can also enhance oral bioavailability.

A good example of such effect of modified *N*-alkylated iminosugars can be demonstrated with a series of DNJ *N*-linked analogues (**Figure 11**).

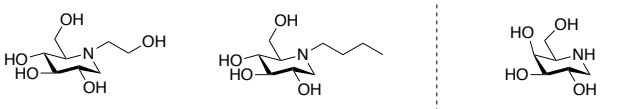

29
Miglitol
Glyset®
diabetes mellitus 2

30
Miglustat
Zavesca®
SRT for Gaucher Disease

31
Migalastat
Galafold®
PC for Fabry disease

Figure 11. Current clinically approved iminosugars miglitol **29**, miglustat **30** and migalastat **31**.

The first iminosugar drug to reach the market under the name Glyset® was *N*-hydroxyethyl-DNJ, also named Miglitol (**29**), which was successfully developed as an antidiabetic and has been approved for non-insulin-dependent *diabetes mellitus* since 1996.[109] Miglitol reduces the rate of complex carbohydrate digestion, thereby controlling the absorption of glucose and preventing hyperglycemia. Many modifications were also made to the DNJ sugar template to enhance cell uptake and yielded *N*-butyl-DNJ (Miglustat, **30**), which is, since 2003, used for the treatment of type 1 Gaucher's disease and Niemann–Pick type C disease under the name Zavesca®. Gaucher's disease is caused by a deficiency in *β*-glucocerebrosidase and Niemann–Pick type C disease is a result of a deficiency in the metabolism of cholesterol and other lipids with both diseases falling in the category of lysosomal storage associated disorders (more detailed explanation in **Chapter 1.4**).[110] Miglustat is inhibiting the enzyme glucosylceramide synthase (GCS) involved in the glucosylation of many sphingolipids and decreases the excessive cellular storage of glycolipids.[111] However efficient, miglustat suffers from very common gastrointestinal side effects among the treated again attributable to the nonspecific activity of the drug and, as an additional drawback, very high serum levels of the drug were required for its efficacy. Although Zavesca® is not perfect in this sense, its sales amounted to approximately 100 million euros for the year of 2016 and is still one of the main drugs for ameliorating Gaucher disease.[112] The increase in the glucosidase inhibitory potency upon incorporation of long aliphatic substituents onto heterocyclic frameworks is well documented in similar frameworks such as piperidine,[113] cyclohexene[114] glycosylamine[115] and imidazole functionalized inhibitors.[116]

Another good example of modified iminosugars, advantageous over their unsubstituted parents is a close relative of castanospermine (**17**) as portrayed in **Figure 12**.

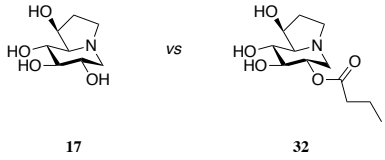

17 **32**

Figure 12. Alkylation of castanospermine (**17**) resulted in a prodrug relative Celgosivir® (**32**).

Although castanospermine is an efficient *α*-glucosidase I inhibitor, the clinical development seemed to be problematic due to the compound's ability to inhibit intestinal enzymes that cause digestive problems.[117] In the search for newer agents that target virus-specific enzymes, castanospermine was later modified with a desire to increase the cell uptake and increase the hydrophobicity. The addition of a butanoyl group to a bicyclic ring gave a prodrug 6-*O*-butanoyl-castanospermine (**32**), also known as Celgosivir®.[118] Celgosivir® is a relatively inactive inhibitor of intestinal sucrases with improved bioavailability and appears to be nontoxic to the gastrointestinal tract. Furthermore, it possesses antiviral activity that is 30-fold

greater than the parent compound and displays potent antiviral activity against several viruses including HIV-1, cytomegalovirus, influenza, herpes simplex virus, BVDV (bovine viral diarrhea virus) and HCV (hepatitis C virus), and the agent is currently undergoing phase II clinical trials as a treatment for HCV infection.[119] The antiviral efficacy and safety of Celgosivir® were demonstrated in clinical trials and is a great example of how iminosugars have been applied to drug discovery by tailoring their properties to become more drug-like and eventually effective in humans.

The use of combined strategies discussed in **Chapter 1.2** can be illustrated on a modified castanospermine-like compound 5*N*,6*O*-(*N*-butyl-iminomethylidene) nojirimycin (**33**, **Figure 13**).

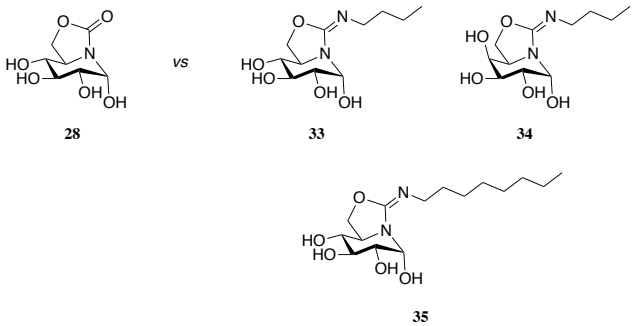

Figure 13. Comparison of compounds **28**, **33**, **34** and **35**.

Affinity towards α- or β-glycosidases as well as towards specific isoenzymes within a series can be tuned by incorporation of substituents that provide additional interactions with protein regions in the vicinity of the active site.[120] For instance, the cyclic carbamate nojirimycin derivative **28** serves as a potent and selective inhibitor of the neutral α-glucosidase II of the endoplasmic reticulum while being inactive against β-glucosidase. In stark contrast to this, the modification of *N*-butyl isothiourea analogue **33** led to a dramatic shift in α/β glucosidase selectivity along with good relative potency and bioavailability. Compound **33** binds to the almond β-glucosidase 50 times tighter than to yeast α-glucosidase.[98] Furthermore, the same compound **33** behaves as a good inhibitor of human lysosomal β-glucosidase and may hold promise as a pharmacological chaperone for the treatment of Gaucher disease.[121] The chaperone activity was assumed to rely on the specific binding to the active site of misfolded GBA mutants at the endoplasmic reticulum thereby facilitating trafficking to the lysosome.[122] Even though α/β selectivity might not be that clear, the fact that a compound, which lacks the alkyl chain (**28**) acts as a good α-glucosidase inhibitor suggests that this substituent plays a key role as a discriminating element. What can also be observed with the same example is that compound **33**, despite its α-configuration at the (pseudo)anomeric position, shows a preference for β-glucosidases. This counter-intuitive phenomenon was

rationalized after the observation that although the α-anomer is the predominant form of the inhibitor in solution, small amounts (10–15%) of the β-anomer were present. Since hemiaminals are known to mutarotate in solution,[123] X-ray structural evidence demonstrated that the axial orientation of the OH group indeed switched to equatorial (β-configuration) when complexed with the enzyme.[124]

In addition to these findings, an important observation involving the C-4 hydroxyl orientation with respect to inhibition of β-glucosidases should be taken into account as well (**Figure 13**). Comparison of the inhibition data in one study shows that the D-galacto-configured relative **34** tends to be more potent against β-glucosidases than its D-gluco-configured counterpart **33**. This insight shows that β-glucosidases are not necessarily very selective regarding the configuration at C-4. This was also observed for the well-reported cytosolic β-glucosidase from the mammalian liver, which is known for its ability to hydrolyze a range of β-D-glycosides with comparable efficiencies.[125] A solution for the lack of selectivity was found by the incorporation of the 2-octylamino substituent to yield 5*N*,6*O*-(N^0-octyl-iminomethylidene)nojirimycin (**35**), which shifted the selectivity of the therapeutic **35** towards β-glucosidases with good results. The example above illustrates how appropriate modifications for specific and potent inhibition can be used to one's advantage.

However, this process is not always straightforward due to many factors, such as the hydrophobic interactions at work near the active site of the enzyme or hemiaminal mutarotations. Current efforts of intensely researched iminosugars include C-alkylated analogues, aminocyclitols and aminosugars, which also show great therapeutic promise.[126,127] However, this class of interesting modifications is not discussed here, as the focus is on iminosugars relevant for this thesis.

Since the discovery of iminosugars, many new natural members of this class have been identified with a wide range of biological activities and many common naturally occurring iminosugars possessing a polyhydroxylated pyrrolidine core have been additionally annulated to either result in a more selective, potent or bioavailable drug. The great amount of attention paid to iminosugars is due to their powerful inhibition and modulation of carbohydrate-processing enzymes including glycosidases,[128] glycosyltransferases,[129] metalloproteinases,[130] or nucleoside-processing enzymes,[131] which makes them great candidates for the development of new therapeutic agents for a wide range of diseases. Despite the fact that the initial pharmaceutical interest in iminosugars was related to their properties as glycosidase inhibitors, these compounds are also considered to be important tools for studying carbohydrate biology by understanding interactions obtained in biological settings.[132] Various structures are currently involved in clinical trials for the treatment of diabetes,[133] cancers,[134] viral infections,[135] and rare genetic diseases such as lysosomal storage disorders[136] and cystic fibrosis.[137] Nevertheless, very few reached the market to this date; Glyset® (**29**) and Zavesca® (**30**) derived from the glucosidase-inhibiting natural product 1-deoxynojirimycin, and their galacto-relative 1-deoxygalactonojirimycin, marketed as Galafold® (Migalastat,

31, **Figure 11**) which is approved for the long-term treatment of Fabry disease.

These are the only examples of iminosugar drugs at the moment and show a promising opportunity for the development of similar agents suitable for use in a clinical setting. With vast opportunities to modify iminosugar scaffolds and the use of current knowledge to tailor these modifications into pharmaceutically interesting compounds, it becomes clear that there is a lot of promise in tuning this bioactive template for specific therapeutic applications.

1.3 GLYCOSIDASES

Glycosidases, also referred to as glycoside hydrolases, are a vast family of enzymes that catalyze the hydrolysis of the glycosidic linkage of O-, N- and S-linked glycosides, leading to the formation of a sugar hemiacetal or hemiketal and the corresponding free aglycon (**Scheme 2**).[138] These efficient and specific catalysts play imperative roles in biological processes by hydrolyzing glycosidic linkages within a plethora of substrates comprising of oligosaccharides, polysaccharides, glycolipids, glycoproteins and small molecule glycoconjugates.[139] Therefore, knowledge of glycosidase function is valuable for understanding and controlling diseases and the development of specific glycosidase inhibitors for medicinal purposes.[140]

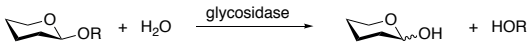

Scheme 2. Simplified hydrolyzation of glycosidic linkages by glycosidases.

Glycosidases are classified in many different ways; according to the diversity of reactions that they catalyze and their mechanistic approach, as well as based on their amino acid sequences and folding patterns.[141] A new type of classification centered on the amino acid similarity within the protein has been proposed recently, and the so-called CAZy database provides a direct relationship between sequence and folding.[142] Next, the two categories, based on the two most commonly employed catalytic reactions, will be described which will be helpful for understanding the inhibitor design discussed in this thesis. Glycosidases classified according to their hydrolysis mechanism, as first outlined by *Koshland*, result in either products that retain the orientation of the anomeric substituent or in their inverted configurational analogues as discussed on the next page (**Scheme 2**).[143]

1.3.1 Inverting glycosidases

In this respect, hydrolysis of a glycoside with a net inversion of the anomeric configuration is achieved in a one step, single-displacement mechanism *via* one oxocarbenium-ion-like transition state and generates a hemiacetal product having the opposite stereochemistry at the anomeric center as illustrated in **Scheme 3**. The reaction typically occurs with general acid and general base assistance from two amino acid side chains (glutamate or aspartate) and is possible due to catalytic residues separated by a 9 Å distance on average, which allows the substrate and a water molecule to bind between them and the reaction to proceed in one step.[144]

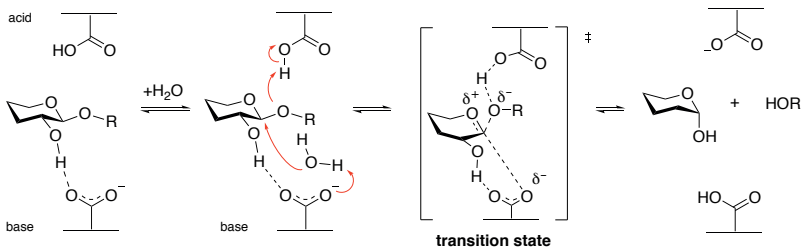

Scheme 3. Inverting mechanism of glycosylation by β-glycosidases.

1.3.2 Retaining glycosidases

Retaining glycosidase hydrolysis is most commonly achieved *via* a two-step, double-displacement mechanism, through a substantial oxocarbenium ion character transition state. The two carboxyl groups in retaining glycosidases are provided by two amino acid side chains, glutamate or aspartate, that are located 5.5 Å apart.[145] In the first step, the so-called *glycosylation* step, one of the carboxyl groups acts as a nucleophile, attacking the anomeric center to displace the aglycon and form a covalent glycosyl-enzyme intermediate, while the other carboxyl group simultaneously functions as an acid catalyst that protonates the glycosidic oxygen as the bond cleaves. In the second phase known as the *deglycosylation* step, the glycosyl-enzyme complex is hydrolyzed by water, with the other residue now acting as a base catalyst that deprotonates the incoming water molecule, which attacks at the anomeric center and results in a hydrolyzed correspondent with retained configuration as depicted in **Scheme 4**.

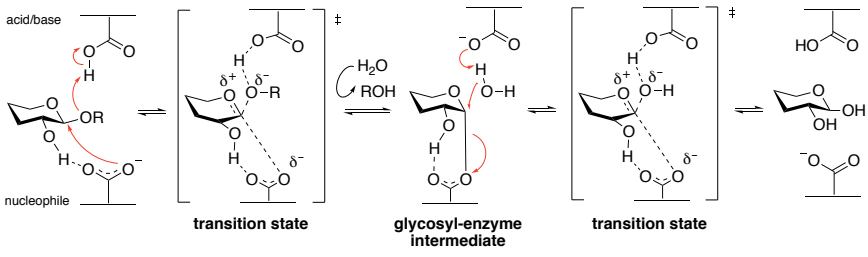

Scheme 4. Retaining mechanism of glycosylation by β-glycosidases.

The glycosidases are essential for normal functioning of most eukaryotes by catalyzing processes such as the degradation of diet polysaccharides to furnish monosaccharide units, which can then be metabolically absorbed and used by the organism. Among those processes are also lysosomal glycoconjugate catabolism and glycoprotein processing reactions, and synthetic craftings of oligosaccharide units onto glycoproteins or glycolipids.[146]

1.3.3 Glycosidases as important targets for drug design

Effective drug design to modulate biological processes requires knowledge of how substrates are assembled, disassembled and recognized by cells.[147] The maintenance of proper cellular levels of glycoconjugates within eukaryotes is, along with hydrolases, coordinated by glycosyltransferases; enzymes that link monosaccharide units to various biomolecules.[148] Most glycoproteins are biosynthesized in a stepwise manner as they pass through the inside of a series of subcellular organelles known as the secretory pathway. These pathways involve the action of several enzymes, where one enzyme produces the substrate for the next enzyme and so on. Depending on the substrate specificity of the enzymes, their tissue-specific expression and the relative locations of glycoside hydrolases and glycosyltransferases within the catabolic process; one can locate such machinery in the endoplasmic reticulum, compartments of the Golgi apparatus and lysosomes. Glycoside trimming enzymes are crucially important in a broad range of metabolic pathways, including glycoprotein and glycolipid processing and carbohydrate digestion in the intestinal tract. Thus, glycan-processing inhibitors can be used to target an enzyme in a specific pathway to induce predictable changes in glycosylation.[149] The outcomes of such alterations can then be studied and the information obtained is important to understand what makes an inhibitor useful in the biological process, and how inhibitors having these features can be designed in a way that can then be applied into future therapeutics.[150] Several diseases will be mentioned hereafter and it will be demonstrated how inhibitors, capable of impairing the function of specific enzymes can be useful in biology and medicine.

One example is diabetes, a chronic metabolic disorder that is characterized by high blood glucose levels, which may eventually result in heart disease and stroke, renal failure and optic neuropathy among others.[151] In type II diabetes, this occurs due to a deficiency of the insulin receptors on the target cells or their insensitivity to insulin.[152] One therapeutic approach to treat diabetes is to delay the absorption of glucose *via* inhibition of enzymes in the digestive tract such as α-glucosidases. The inhibition of membrane-bound α-glucosidases that are present in the epithelium of the small intestine decreases and delays the absorption of glucose into the blood and helps to avoid the onset of late diabetic complications.[153]

Another example is a retaining α-glycosidase neuraminidase, also termed as sialidase, which plays a crucial role in the replication and infectivity in the final stages of the influenza virus life cycle.[154] Influenza is a serious respiratory viral infection that causes substantial morbidity.[155] Although inhibition of neuraminidase does not

preclude the virus infection, the virus particles form aggregates and remain bound to the infected cell surface thereby preventing an efficient viral spread.[156]

In both cases mentioned above, inhibitors play a role to stop the corresponding processes and hinder additional manifestations. There is yet another type of disease in which enzyme malfunction results in an accumulation of the corresponding substrate and triggers manifestations due to the accumulation of the substrate in the organelles. In such cases, inhibiting the underperforming enzyme does not seem wise yet it could well play in a role towards normal function and cell longevity.

1.4 LYSOSOMAL STORAGE DISORDERS

Lysosomal catabolic pathways involve the well-orchestrated actions of a series of enzymes for proper functioning.[157] Lysosomal enzymes carry out precise biochemical reactions in breaking the substrates into smaller components, which need to be either recycled or excreted by the cell. Such specialized enzymatic digestions are largely controlled inside specific mildly acidic cellular organelles named lysosomes that were first reported by *Christian de Duve* in 1955.[158,159] Abnormal excessive accumulation of undegraded substrates causes a variety of cellular dysfunctions that can potentially lead to a range of pathologies commonly known as lysosomal storage disorders, generally abbreviated as LSDs.[160,161] In this group of rare and severe hereditary disorders, accumulated substrate is present in different organs that are part of the hematologic, skeletal, visceral, and neurological systems of the human body.[162] There are more than 50 different lysosomal enzymatic malfunctions and each results in a unique disorder.[163] Amongst the most widespread are those associated with the anomalous storage of glycosphingolipids, a complex family of structural components of mammalian cell membranes that are involved in processes such as cell adhesion and signal transduction modulation.[164] A small part of such catabolic pathways is discussed on the next page in **Scheme 5**, to exemplify the enzymes in action and state the associated diseases in case of inappropriate performance of the hydrolytic enzymes.[165]

Altogether, the prevalence of LSD incidences is around one in 10000 live births, which is similar to that of cystic fibrosis; one of the most frequently occurring genetic disease. LSDs are classified according to the accumulated metabolite and are commonly named after the physicians who first reported their clinical manifestations. The group of such disorders comprises Pompe, Fabry, and Gaucher disease, among others, with the ones mentioned being the most common.[166] In chapter 1.4.1, we will have a detailed look at Gaucher's disease and the responsible enzyme for its onset.

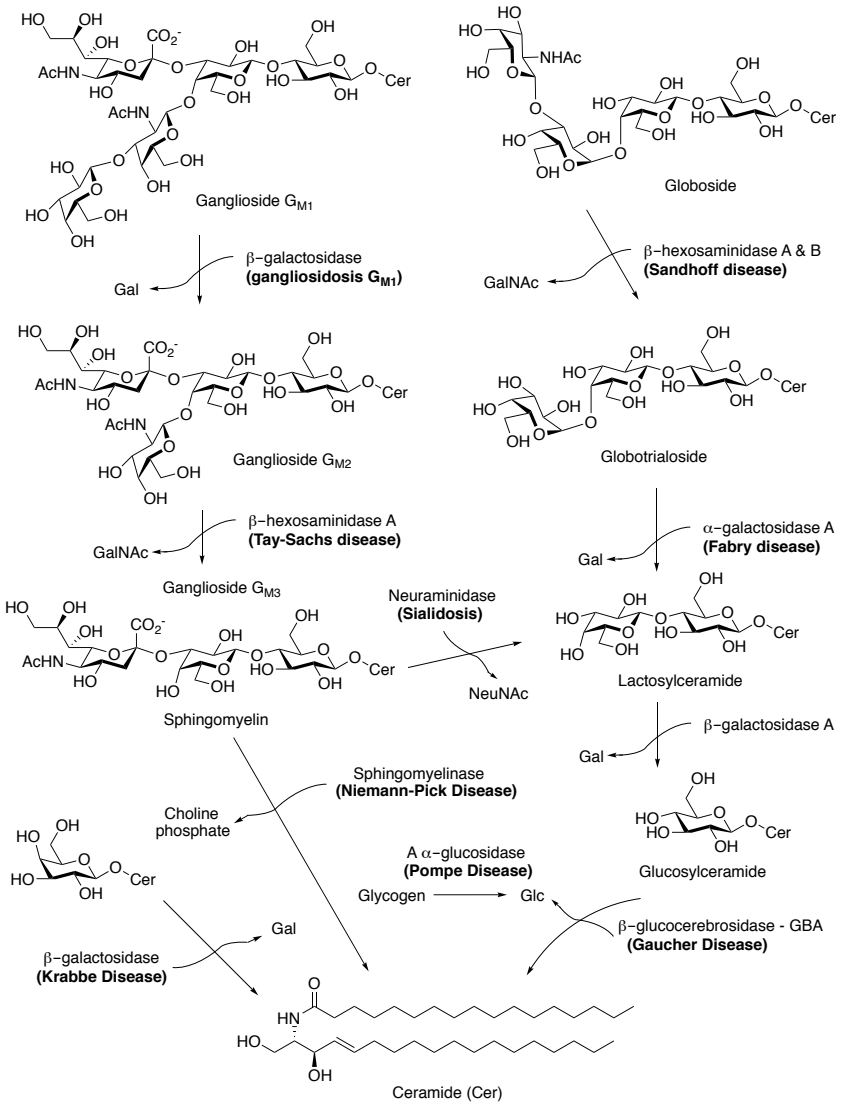

Scheme 5. Catabolic pathway of glycosphingolipids, their corresponding enzymes crucial for substrate degradation and manifested lysosomal storage disorders (LSDs).

1.4.1 Gaucher disease

Gaucher disease (GD) is the most dominant lysosomal storage disease with approximately 10000 individuals affected worldwide.[167,168] Notably, the prevalence is particularly high among Ashkenazi Jews (one in 500 live births).[169–17] The condition is caused by a mutation in the glucocerebrosidase gene, which can lead to reduced activity of β-glucocerebrosidase (GBA, GBA1, GCase, acid β-glucosidase or glucosylceramidase, a member of CAZy family 30, EC 3.2.1.45), the enzyme responsible for the hydrolysis of glucosylceramide (GlcCer).[172]

A deficiency in GBA activity can result in the progressive accumulation of undegraded glucosylceramide substrate leading to serious clinical symptoms including hepatomegaly, splenomegaly, pancytopenia, bone lesions, respiratory failure and in some cases neurological complications (**Scheme 6**).[173–176]

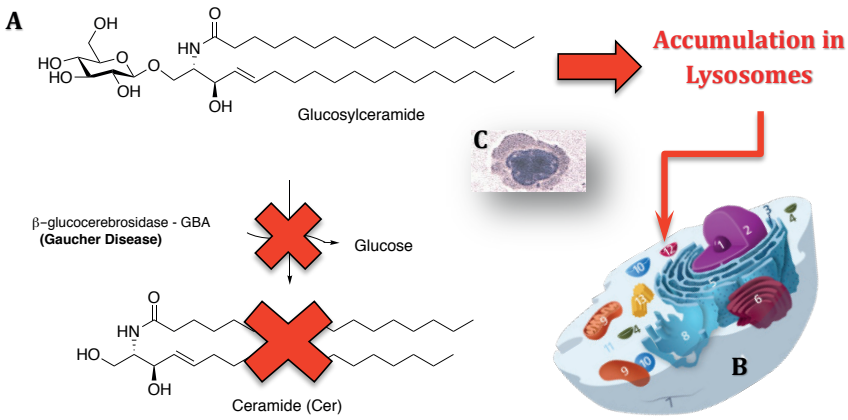

Scheme 6. Illustration of Gaucher disease onset. A) Deficient hydrolysis of glucosylceramide by β-glucocerebrosidase. **B)** Substrate accumulation in the lysosome. **C)** Gaucher cell with the accumulated glucosylceramide.

A variety of characterized gene mutations, ranging from single base substitutions to whole gene deletions, are known to lead to a deficient enzyme and its decreased activity associated with the disease.[177] In this respect, GD has three clinical subtypes that are linked to particular mutations of the GBA. Type I GD, where the N370S mutation is present, is the most widespread form of the disease accounting for more than 90% of the cases. Its symptoms appear only during adulthood due to a progression of substrate accumulation over time.[178] Neuropathic types are mainly a result of an L444P mutation that affects the patient's brain. In the most dramatic cases of the acute infantile form (Type II), affected rarely survive the first year of life.[179] In addition, recent reports have suggested an association between GD disease and the development of Parkinson's disease due to mutations in GBA that can promote α-synuclein aggregation.[180–183]

1

1.4.2 GBA structure

GBA is a membrane-associated lysosomal hydrolase enzyme and consists of 497 amino acids with a molecular weight of approximately 60 kDa.[184] The GBA structure comprises three non-contiguous domains as illustrated in **Figure 14**. Domains I and II are non-catalytic and predominantly consist of a major three stranded anti-parallel β-sheet and two closely associated β-sheets, respectively. Domain III involves the (β/α) (TIM) barrel catalytic site.[185] Although domains I and II are non catalytic and their functions are not fully understood, the location of several mutations throughout all three domains suggests that they play a significant regulatory role. GBA acts like a classic retaining β-glucosidase for which the catalytic cycle proceeds through a two-step reaction mechanism where Glu235 serves as the acid/base and Glu340 as the nucleophile in the catalytic cycle.[186,187] In this case, *glucosylation* of the active site by substrate proceeds first and is then followed by *deglucosylation via* a carbenium ion intermediate with release of β-glucose.[188]

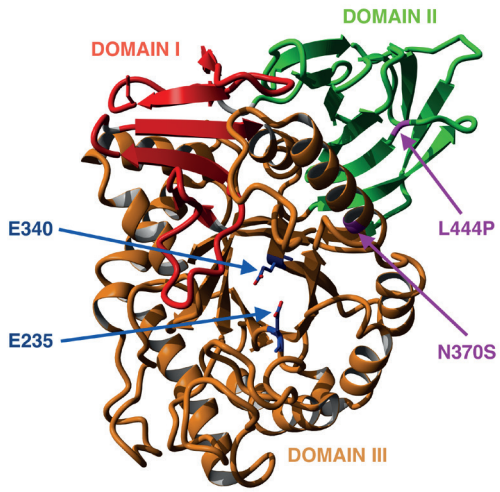

Figure 14. X-ray structure of acid-β-glucosidase. **Domain I** is shown in red, **Domain II** in green and **Domain III**, which is the catalytic domain, in orange. The active-site residues **E235** and **E340** are shown as ball and stick models in blue. The most common GBA mutations that result in either nonneuronopathic (**N370S**) or neuronopathic (**L444P**) forms of GD are shown and highlighted in magenta.[126]

To this date, many GBA structures for both, the apoenzyme and for the enzyme in complex with various ligands, have been published, although it was not until 2003 when the first X-ray structure of GBA was reported.[185] Interestingly, a molecular modeling study of the N370S mutation,[189] the most prevalent mutation associated with type I GD,[190] came to a similar mechanistic conclusion than the one based on the later reported X-ray structure.[191] It has been shown that the N370S mutation site is located in the catalytic domain of the enzyme somewhat remote from the active site at the interface of domains II and III and it is not directly involved in the catalytic activity.[190] In addition, the site of the L444P mutation is located in domain II, also distant from the active site, yet it leads to severe disease with a neurological

phenotype.[192] In this respect, it has proven difficult to determine whether a mutation in one region or domain of the protein will lead to mild or severe disease.[193] The X-ray crystal structure of GBA also indicated the existence of hydrophobic residues around the entrance to the glucose binding site.[185] Such a hydrophobic site could be exploited by derivatisation of iminosugars with a hydrophobic group and potentially lead to a better inhibitor.

1.4.3 Current treatments of Gaucher disease

Even though more studies are required to fully comprehend the events leading from a glycosidase deficiency to clinical symptoms, it appears that the accumulation of undegraded glycosphingolipids is most likely to be a key factor in the initiation and progression of LSDs.[161] The primary focus for therapeutic strategies has been on reducing the cellular concentration of glycosphingolipids within the lysosome.[194] Among the different therapeutic approaches under investigation at present, there are a few well-established therapeutic strategies for the treatment of Gaucher disease and LSDs in general (**Scheme 7**).[195]

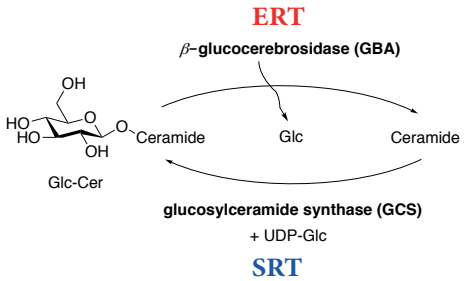

Scheme 7. Illustrated therapeutic possibilities for affecting Gaucher disease.
Enzyme Replacement Treatment (**ERT**) as the most straightforward approach by addition of recombinant active form of GBA to help with the substrate hydrolysis. Substrate Reduction Therapy (**SRT**) inhibitors of GCS are used to alter the production of potentially harmful substrate GlcCer.

1.4.3.1 Enzyme replacement treatment (ERT)

The most straightforward approach is undoubtedly a so-called enzyme replacement therapy (ERT), where an exogenously produced replacement enzyme is administrated to the patient as a means of reducing the substrate burden.[196] In the case of GD, three enzymes; Imiglucerase (Cerezyme®, Genzyme),[197] Velaglucerase alfa (VPRIV®, Shire)[198] and Taliglucerase alfa (Elelyso®, Protalix),[199] are used for ERT and alleviate many symptoms associated with the disease. The 3D structures of all the three enzymes currently in clinical use have been resolved experimentally, and the structures do not differ in any significant manner from the natural functional enzyme.[200] However successful, such treatment is ineffective in treating the neuropathic form of the disease due to the inability of the replacement enzyme to cross the blood brain barrier.[201] Furthermore, lifelong intravenous administration of the manufactured enzyme involves a weekly or bi-weekly infusion, which is

a burden for the patients. Such a high frequency of administration can also lead to hypersensitivity reactions, anaphylactic shock, as well as inactivation and accelerated clearance of the infused enzyme. The cost of constant attention to the patient and the drug administration typically exceeds €250.000 per year and brings a great financial burden to the patient. It is, therefore, no surprise that other cheaper and more effective treatments involving small molecule agents would be preferred.[202]

1.4.3.2 Substrate reduction therapy (SRT)

Alternatively, substrate reduction therapy (SRT) is aimed at inhibiting glycolipid biosynthesis to balance the deficient activity of GBA (**Scheme 7**).[203] The most prominent case of substrate reduction therapy used in the treatment of GD is the use of iminosugar-based glucosylceramide synthase inhibitor *N*-butyl-1-deoxynojirimicin (NB-DNJ, miglustat, **30**, Zavesca®).[204] Experiments with radiolabeled iminosugar derivatives suggest that *N*-alkyl deoxynojirimycins have an advantage over ERT due to its possibility of crossing the blood brain barrier and lowering the substrate concentration in patients suffering from the neuropathic form of GD.[205]

Even though miglustat was originally considered as a GCS inhibitor, further studies were performed in order to understand the biochemical and therapeutic effects of the drug and unveiled that the beneficial effects of miglustat also might be attributed to the inhibition of β-glucosidase 2 (GBA2), a non-lysosomal hydrolase that also degrades glucosylceramide.[206] This somewhat suggested that it was not only substrate reduction itself but also a potential alternative mechanism that contributed to the symptoms amelioration. Miglustat was later shown to act, in combination with its capacity to inhibit GCS, as a pharmacological chaperone towards some mutant variants of GBA.[207] The drug was approved by EMA in 2002 and FDA in 2003 for the treatment of Type 1 and Type 3 GD and is administered with a recommended dose of 100 mg, three times per day.[208] While useful in treating GD patients with mild to moderate forms of the disease especially for whom enzyme replacement therapy is not an option; there is also a range of side effects associated with Zavesca® and the latency for adverse long-term neurological effects is unknown.[209]

Nevertheless, miglustat was not the only drug to be discovered as a substrate reduction agent for GD over the last decade. Eliglustat tartrate is a glucosylceramide analogue that has demonstrated promising effects on manifestations of GD Type 1 although it cannot cross the blood-brain barrier and thus lacks efficacy for the neuronopathic disease.[210] However, it is hoped that an improved efficacy versus toxicity ratio will offer patients with Type 1 Gaucher disease an oral alternative to ERT and other SRTs, which remains to be investigated.[211] Although the number of patients is small relative to other more common disorders and therapies for such diseases tends to be very expensive, appropriate use of various agents clearly improve the health status of affected individuals

and development of other treatments is essential for their long-term health.[212]

In response, the search for alternative strategies has lead to another promising curative approach for GD and other lysosomal storage diseases as discussed hereafter.[213]

1.4.3.3 Pharmacological Chaperone Therapy (PCT)

Another therapeutic tactic to treat lysosomal enzymopathies in order to restore the balance between the influx and degradation of the accumulated substrates is termed pharmacological chaperone therapy (PCT).[214] Pharmacological chaperones (PC) are small molecules capable of stabilizing a misfolded enzyme and thus prevent degradation by the Endoplasmic Reticulum Associated Degradation machinery (ERAD).[215] In the case of GD, the mutant GBA enzyme is predisposed to misfolding and premature degradation in the ER but often still retains some degree of catalytic activity. It is assumed that the threshold for lysosomal diseases is around 10% of a fully functional enzyme activity.[216] Therefore, only a relatively small increase in the enzyme activity of a partly defective mutant is required to obtain major health benefits.

An effective pharmacological chaperone-based treatment for Gaucher disease would see the pharmacologically active compound bind to the enzyme and stabilize misfolded GBA, thus facilitating its trafficking from the ER to the lysosome where it can degrade GlcCer. Ever since *Fan et al.* in 1999[217] first suggested that iminosugar inhibitors show the ability to act as pharmacological chaperones, an increased interest emerged in a new class of extensively researched compounds with potential for use in pharmacological chaperone-based therapies.[218] Certain iminosugars are highly potent and selective inhibitors of glycosidases[219] and in some cases reversibly bind to the active site of their target enzyme in a pH-dependent manner.[89] It may seem paradoxical to use an inhibitor to stabilize an enzyme, however, the positive outcomes of such therapeutic approaches lie in identifying therapeutic levels at inhibitory intracellular concentrations that has positive enhancing final-impact. An important aspect to consider is that upon correct lysosome trafficking, the inhibitory pharmacological chaperone will likely be displaced from the active site due to the availability of the natural substrate at excess levels, which has a higher affinity for the active site. Furthermore, the acidic environment within the lysosome has an additional effect on the interactions that keep the inhibitor bound to the active site. In the case of GD, iminosugars that bind misfolded GBA more tightly at neutral pH can provide an improvement in its folding and promote proper trafficking from the ER to the lysosome.[74] Ideally, an iminosugar-based pharmacological chaperone should have a lower binding affinity for GBA in the acidic environment of the lysosome (pH 5.2) causing it to dissociate from the complex and ultimately raise residual enzyme activity.

Illustration of the proposed mechanistic approach of pharmacological chaperones is depicted in **Scheme 8**.

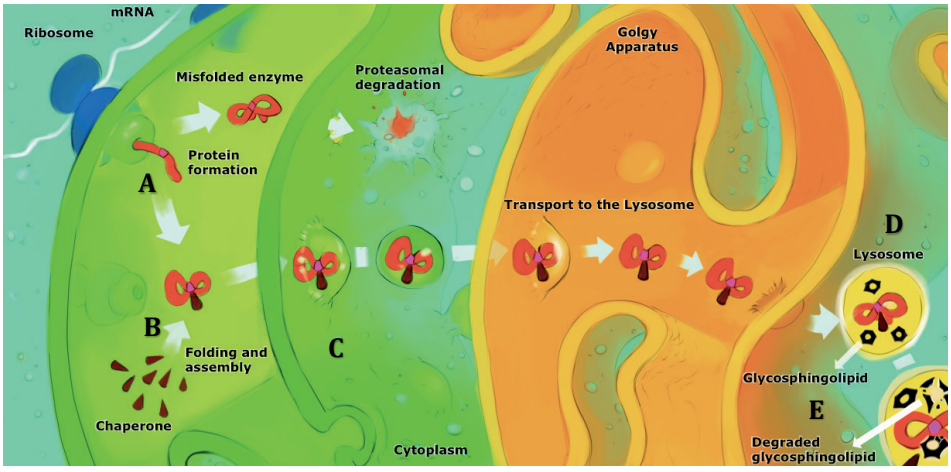

Scheme 8. Suggested pharmacological chaperone mechanistic mode of action. A) Missense mutation results in a misfolded, but still catalytically active enzyme. **B)** Pharmacological chaperone binds and stabilizes the misfolded enzyme. **C)** PC:enzyme complex is transported to the lysosome without being prematurely degraded. **D)** Once in the lysosome, the chaperone dissociates from the complex due to acidic pH and superior substrate concentration. **E)** The free enzyme is now capable of hydrolyzing the accumulated substrate.

The active sites of the affected enzymes, such as substrates or competitive inhibitors, have the ability to template the folding of the affected protein and can be used to rescue misfolding and accelerating its transport to the lysosome. In this regard, the development of potent, preferably pH-dependent glycosidase inhibitors presents an attractive target for the development of new therapeutics.[122]

However, it has been shown in the past that potent inhibition does not necessarily translate to greater chaperoning potential.[89] Nonetheless, intense interest in the chemistry, bio-chemistry and pharmacology of glucosidase inhibitors has already led to the discovery of a large number of compounds mimicking the structures of monosaccharide or oligosaccharides that were capable of improving the malfunctioning enzyme and enhance its hydrolysis function as a final result.[220] Many reports and patent applications have since appeared that evaluate different inhibitors, mainly iminosugar-based, for application against Gaucher disease.[221] No such compounds have been approved for the treatment of GD, however, one of PC representatives is Migalastat, which targets α-galactosidase (Gal A) and is used for the treatment of Fabry disease. This small first-in-class chaperone has been approved for use in 2016 under the brand name Galafold® (**31**, Amicus Therapeutics) and is the only approved pharmacological chaperone to date.[222] Pharmacological chaperones offer promising opportunities in the treatment of a broad range of inherited lysosomal storage diseases.[202,218,223,224] Importantly, given their complementary mechanisms, pharmacological chaperone-based approaches and enzyme replacement strategies may also have potential for use in combination for the treatment of lysosomal storage diseases.[225]

1.4.4 Transition state mimics

Since glycosidases catalyze reactions by very tightly binding and stabilizing transition states, the effectiveness of successful glycosidase inhibitors depends largely on their ability to mimic the structural and electronic properties of the natural substrate during the hydrolysis process.[93,227] Iminosugars proved to be great candidates for glycosidase inhibitors due to their capability of resembling relevant transition states. Although the debate continues on whether some of these inhibitors are real transition state mimics, there is no doubt that many strategies to generate successful inhibitors have included a suitably positioned positive charge able to interact with key enzymatic carboxylates.[149] As iminosugars are in a protonated state at physiological pH, the resulting ammonium ions mimic the carbocation/oxocarbenium character of the hydrolysis transition states. In this respect, direct electrostatic interactions with Glu-340 are possible for example in the case of isofagomine (**36**), a potent β-glucosidase inhibitor, which protonated nitrogen mimics the charge developing on the anomeric carbon. In contrast, 1-deoxynojirimycin (**15**), a potent α-glucosidase inhibitor, contains nitrogen whose charge mimics the oxocarbenium ion (**Scheme 9**).

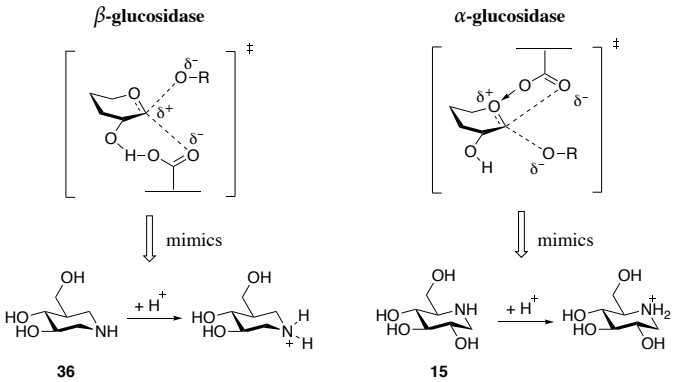

Scheme 9. Isofagomine (**36**) and deoxynojirimycin (**15**) and their favorable interactions with the corresponding substrates of β- and α-glucosidases. In the case of β-glycosidases, the nucleophilic residue is precisely positioned to interact with the anomeric center and the adjacent exocyclic hydroxyl, which favors the formation of a carbocation at the anomeric position in the transition state. In the case of the α-glycosidases, the nucleophilic residue is adequately positioned to build-up a positive charge at the endocyclic oxygen and the anomeric group is ejected, resulting in a transition state with oxocarbenium character. [226]

In this respect, structural factors for glucosidase inhibition may be related to the charge and/or shape and these characteristics can be tailored towards favorable interactions by the hybridization and conformation of the ring. Another key observation from X-ray studies is that mimicry of both the carbohydrate and ceramide portions of the substrate play an important role in maximizing the inhibition as in the case of alkylated DNJ relative NB-DNJ, which was shown to inhibit GBA and even increased cellular GBA activity, suggesting pharmacological chaperone properties.[228] Nevertheless, isofagomine-related glycomimetics, which

comprise of IFG, the calystegines and DIX, bind to GBA with the nitrogen atom occupying a position analogous to the anomeric carbon of glucose (C-1). In contrast deoxynojirimycin-type iminosugars do so in a mode in which the nitrogen atom matches the endocyclic oxygen (O-5). These findings demonstrate the possibilities of scaffolds such as IFG, THP, DIX and, to some extend, modified DNJ to interact with the active site and might hold promise for the future research for GBA inhibitors.

1.4.5 Iminosugar-based inhibitors of GBA

The next section provides an overview of few selected iminosugar-based inhibitors of GBA that have so far been discovered. To this date there are no clinically approved pharmacological chaperone-based drugs for the treatment of Gaucher disease, however, many compounds have shown promising results in various biological experiments.[215] Simple iminosugars such as 1-deoxynojirimicin (DNJ, **15**), isofagomine (IFG, **36**), 1,5-dideoxy-1,5-iminoxylitol (DIX, **37**), calystegine A_3 (**38**) or castanospermine (**17**), have all been identified as GBA inhibitors, although in several cases they are non-specific inhibitors and have problems crossing membranes which hinders their ability to act as potent chaperones (**Figure 15**).[229–232]

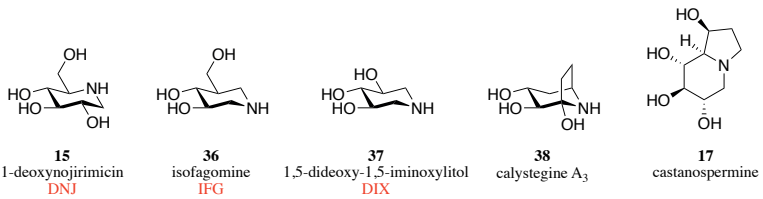

Figure 15. Simple iminosugars acting as GBA inhibitors.

Currently, the only orally available drugs for the treatment of Gaucher disease are NB-DNJ (**6**) and the non-iminosugar compound Eliglustat (**39**, trade name Cerdelga®) both capable of inhibiting GCS (**Figure 16**).[204,233] However, as already mentioned, NB-DNJ has also been shown to exhibit a chaperone effect with GBA.[207] Although being closely related to deoxynojirimycin, crystal structures of GBA in complex with either NB-DNJ (**30**) or NN-DNJ (**40**) do not support a direct interaction by Glu-235 or Glu-340 to their protonated nitrogen (**Figure 16**).[186] Nonetheless, iminosugars with *N*-linked alkyl chains of varying lengths, such as NB-DNJ[189] and NN-DNJ[216] hold the ability to interact with the active site of GBA and it has been shown that such compounds act as opportunistic binders of the active site rather than being true transition state mimics.[186] The common concept to conjugate an iminosugar with a lipophilic moiety to improve the metabolic properties of chaperone candidates had a considerable impact in the field.[228] In such cases, iminosugar's hydrophilic nature mimics the sugar part or the transition state towards glycosidic cleavage, and the hydrophobic part mimics the ceramide aglycone part of the natural substrate.[193]

There is, however, a limit to such theory where increased amphiphilic nature of the substituent potentiates the inhibition properties as in the case of amantadine DNJ-analogue **41** (**Figure 16**). Compound **41** was shown to inhibit GBA with 1,2 mM but still managed to keep its chaperoning capabilities.[234] In addition, incorporating sp^2 hybridization at the pseudo anomeric center of the iminosugar can potentially lead to binding affinity increases and is, to some extend, associated with closer transition state mimicry. An sp^2-hybridized carbon with a carbonyl group instead of the hydroxymethyl group in DNJ was designed into an inhibitor by *Butters, Ye, and coworkers* and resulted in octyl derivative **42** that elicited significant enzyme activity enhancements in N370S mutations by reaching a sizeable 6.2-fold increase of GBA activity (**Figure 16**).[235]

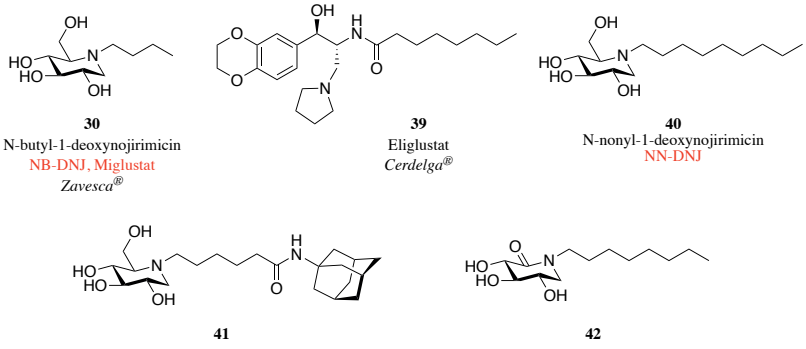

Figure 16. A few selected inhibitors of GBA.

An evaluation of naturally occurring iminosugars by *Fan and co-workers* identified IFG (**36**) as the most potent GBA inhibitor among unmodified iminosugars and reached a Phase 2 stage in the drug development process before being terminated due to patients unresponsiveness.[229] IFG requires high concentrations to increase GBA activity in cells (10–100 mM) compared with the amount needed to inhibit GBA in the in vitro assays (5–100 nM), which is probably attributed to the highly hydrophilic nature of the molecule, which hinders the transport into the ER.[236]

In stark contrast to improved DNJ modifications, the research group of *Fan et al.* found that *N*-alkylation of iminosugars such as derivatives **43** and **44**, is either detrimental or has little effect on GBA binding affinity (**Figure 17**).[113] Interestingly, moving the alkyl substituent from the N-atom to the adjacent C-atom in 1-azasugars of IFG derivatives **45-47** restores the inhibition capabilities, leading to strong GBA inhibitors with good GBA chaperoning properties (**Figure 17**).[237] Furthermore, compound **47** from the same study was found to have the most potent properties with an IC_{50} value of 0.6 nM and a 1.8-fold activity increase in N370S fibroblasts at a concentration as low as 10 nM.[113] Similarly, *Compain, Martin, Asano and co-workers* identified 1-C modified DNJ compounds[238] **48-50** as moderate inhibitors and 1-C modified DIX species[221] **51-53** as very potent GBA inhibitors (**Figure 17**).

It should be mentioned, that DIX derivatives are also known to be highly selective and display no inhibition towards α-glucosidases, including intestinal α-glucosidases, and thus give the promise of fewer side effects in case of further development.[239] The same group recently expanded their study of 1-C-alkylated DIX derivatives and converted them into 1,2,3-triazole adducts,[240] with 3-(trimethylsilyl)propyl derivative **54** exhibiting great activity enhancement of up to 4-fold in Gaucher fibroblasts containing the G202R mutation at 100 nM concentration (**Figure 17**). Similar modifications were investigated by *Withers and coworkers* to generate thiol **55**, which reached 3.4-fold increase in homozygous Gaucher N370S and L444P fibroblasts (**Figure 17**).[241] Such enhancement for the L444P variant is particularly notable given that this particular mutation, with high prevalence in Type 3 GD is refractory to most pharmacological chaperone candidates.

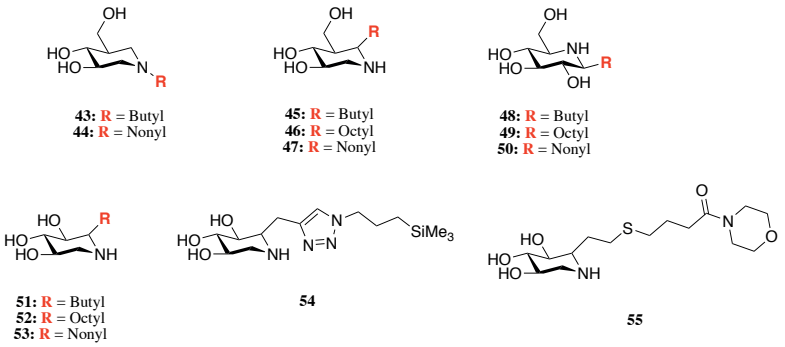

Figure 17. Derivatives of IFG and DIX as GBA inhibitors.

Compounds without a nitrogen in the glycone system such as amino-myo-inositol derivatives **56** and **57** were developed by *Llebaria and co-workers* and resulted in extremely potent inhibitors of recombinant GBA with K_i values of 4 and 5 nM, respectively (**Figure 18**).[242] Compound **56** promoted a 2.1-fold GBA activity enhancement in N370S Gaucher cells when used at 100 nM concentration and 1.5-fold activity enhancement in L444P lymphoblasts at 10 nM. Further improvement was achieved by preparing cyclitols bearing two vicinal alkylamino groups (**58**) or aminocyclitols with adjacent N- and O-alkyl substituents **59** (**Figure 18**). The latter compound produced 1.9-fold increases of GBA activities in N370S lymphoblasts at 1 nM and 1.4-fold in L444P lymphoblasts at 0.01 nM.[115,243]

The incorporation of adamantyl substituents into similar systems such as compound **60**, was designed to increase amphiphilicity and induced a 2.5-fold GBA activity increases in L444P fibroblasts when used at 50 mM concentrations (**Figure 18**).[244] The observation that the presence of a nitrogen atom in the glycone moiety of glycomimetics is not a necessity for strong GBA binding led to a high throughput screening (HTS) study of an FDA-approved drug library of 1040 compounds, which identified Ambroxol® (**61**) as a compound capable of stabilizing GBA and even increased the activity of the enzyme in the brain (**Figure 18**).[245,246]

Ambroxol®, a commonly used secretolytic agent for the treatment of respiratory diseases, also produced a 1.4-fold increase in enzyme activity at 60 mM and is currently in pilot trials in humans affected with neuronopathic GD.[247] In addition to this class of inhibitors, lipophilic aminocyclitol derivatives such as ceramide-bearing β-valienamine **62** represented the first known selective inhibitor of GBA (**Figure 18**).[248]

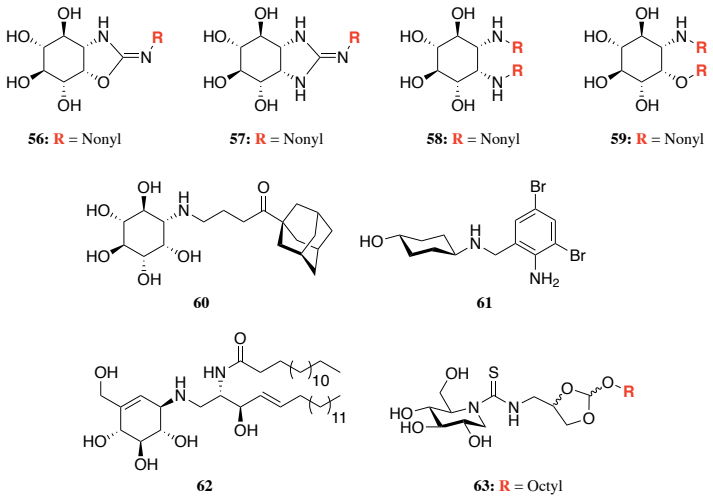

Figure 18. Representatives of GBA inhibitors.

A critical aspect to consider when finding a suitable chaperone candidate lays in the protonation capabilities of the inhibitor to convey significant binding affinity differences towards the target glycosidase at neutral pH in the endoplasmic reticulum and acidic environment of the lysosome. In this regard, the design of acid-labile compounds capable of changing their hydrophobic nature under acidic conditions were developed by *Ortiz-Mellet, Garcia-Fernandez, Higaki, and colleagues*.[249] Their design incorporated acid-labile orthoester moiety into the scaffold, which changes the nature of the molecule from hydrophobic to hydrophilic when in the lysosome. Compound **63** has an IC_{50} of 150 nM and is able to drastically improve the enzyme activity of V230G (Type 2) and N188S (Type 3) in a fibroblast experiments by up to 6-fold (**Figure 18**). In addition, no inhibition was observed when tested under acidic conditions to mimic the lysosomal environment, proving that this type of design is a promising approach towards the beneficial pharmacological chaperone candidates.

In conclusion, this chapter attempted to illustrate the privileged drug-like properties of selected iminosugar glycosidase inhibitors and their potential to target these impressive biological machines present in all living organisms that are vital for normal functioning. Therefore, the quest of discovering new selective and potent inhibitors towards these enzymes is extremely important field associated with finding agents for the amelioration of their corresponding diseases.

1

1.5 THESIS OUTLINE

In this thesis, we describe the synthesis of sp^2 guanidinylated iminosugars and evaluate them against a series of commercially available glycosidases *in vitro*. In addition, experiments using Gaucher patient-derived fibroblasts bearing the N370S and L444P GBA mutation were performed to evaluate their ability to counteract the loss of enzyme activity by potentially functioning as pharmacological chaperones.

Chapter 2 describes the preparation and biological evaluation of a novel class of DNJ-derived guanidinylated iminosugars using a concise synthetic protocol proceeding *via* a guanidino intermediate. Interestingly, such *N*-alkylated guanidine DNJ analogues spontaneously cyclized to generate the corresponding stable bicyclic isoureas (**Scheme 10**) the mechanism of which we investigated.

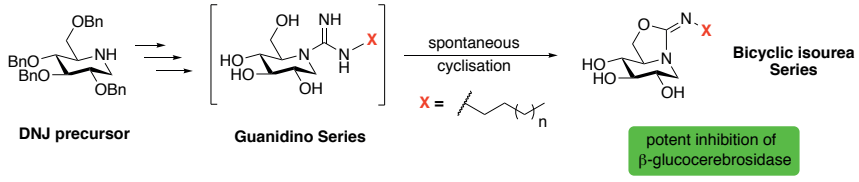

Scheme 10. Overview scheme of compounds discussed in **Chapter 2**.

In order to circumvent the process of spontaneous cyclization of DNJ-derived guanidinylated iminosugars, **Chapter 3** describes the preparation of a novel class of *N*-substituted guanidine analogues of DIX, lacking the 6-OH group of DNJ, which were found to be stable. Also, the corresponding urea derivatives were synthesized and both series were evaluated in biological experiments (**Scheme 11**).

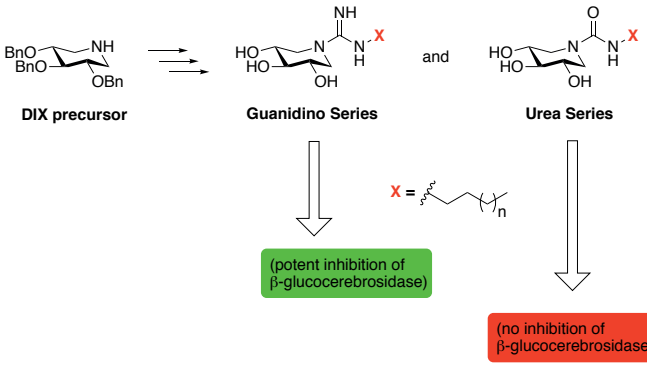

Scheme 11. Overview scheme of compounds discussed in **Chapter 3**.

As a continuation of our previous studies, **Chapter 4** describes the preparation of new DIX-iminosugar based glycosidase inhibitors that contain both; an exocyclic *N*-alkylated guanidine and an acid labile orthoester moiety (**Scheme 12**). Such compounds are interesting due to the pH-responsive orthoester capable of self-hydrolyzation in the lysosomal environment, thereby transforming from the hydrophobic inhibitor to the hydrophilic non-inhibitor.

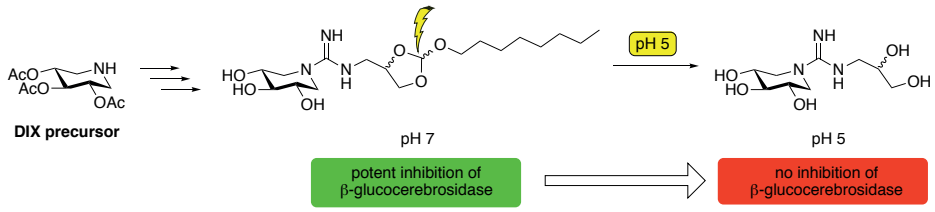

Scheme 12. Overview scheme of compounds discussed in **Chapter 4**.

Finally, **Chapter 5** provides a summary of the research described in Chapters 2 to 4 and aims to discuss prospects for future research and potential application in biological and clinical research.

1

1.6 REFERENCES

1. Berlinck, R. G. S. & Romminger, S. The chemistry and biology of guanidine natural products. *Nat. Prod. Rep.* **33,** 456–490 (2016).
2. JV, G. & P, L. Amidines and guanidines in medicinal chemistry. *Prog Med Chem* **30,** 203–326 (1993).
3. Schmidtchen, F. P. & Berger, M. Artificial Organic Host Molecules for Anions. *Chemical Reviews* **97,** 1609–1646 (1997).
4. Schug, K. A. & Lindner, W. Noncovalent binding between guanidinium and anionic groups: Focus on biological- and synthetic-based arginine/guanidinium interactions with phosph[on] ate and sulf[on]ate residues. *Chem. Rev.* **105,** 67–113 (2005).
5. Ishikawa, T. *Superbases for Organic Synthesis: Guanidines, Amidines, Phosphazenes and Related Organocatalysts*. *Wiley* (2009). doi:10.1002/9780470740859
6. Reetz, M. T., Bingel, C. & Harms, K. Structure of carbanions having carbocations as counterions. *J. Chem. Soc., Chem. Commun.* **20,** 1558–1560 (1993).
7. Mori, A., Cohen B D & Lowenthal A. Guanidines: historical, biological, biochemical, and clinical aspects of the naturally occurring guanidino compounds. *Pure Appl. Chem.* **60,** 1627–1634 (1988).
8. Wolfenden, R., Andersson, L., Cullis, P. M. & Southgate, C. C. B. Affinities of amino acid side chains for solvent water. *Biochemistry* **20,** 849–855 (1981).
9. Mautner, M. M. The Ionic Hydrogen Bond. *Chem. Rev.* **105,** 213–284 (2005).
10. Turk, T. *et al.* Biological activities of ethanolic extracts from deep-sea antarctic marine sponges. *Mar. Drugs* **11,** 1126–1139 (2013).
11. Pardridge, W. M. The Blood-Brain Barrier: Bottleneck in Brain Drug Development. *J. Am. Soc. Exp. Neurother.* **2,** 3–14 (2005).
12. Shi, Y., Moazami, Y. & Pierce, J. G. Structure, synthesis and biological properties of the pentacyclic guanidinium alkaloids. *Bioorganic Med. Chem.* **25,** 2817–2824 (2017).
13. Tapiero, H., Mathe, G., Couvreur, P. & Tew, K. Arginine. *Biomed Pharmacother* **56,** 439–445 (2002).
14. Carbone, M. *et al.* Marine Terpenoid Diacylguanidines: Structure, Synthesis, and Biological Evaluation of Naturally Occurring Actinofide and Synthetic Analogues. *J. Nat. Prod.* **80,** 1339–1346 (2017).
15. Alegre-Requena, J. V., Marqués-López, E. & Herrera, R. P. Guanidine motif in biologically active peptides. *Aust. J. Chem.* **67,** 965–971 (2014).
16. Roel, M. *et al.* Marine guanidine alkaloids crambescidins inhibit tumor growth and activate intrinsic apoptotic signaling inducing tumor regression in a colorectal carcinoma zebrafish xenograft model. *Oncotarget* **7,** 83071–83087 (2016).
17. Gribble, G. W. Biological activity of recently discovered halogenated marine natural products. *Mar. Drugs* **13,** 4044–4136 (2015).
18. Seiple, I. B. *et al.* Total synthesis of palau'amine. *Nat. Commun.* **6,** 1–9 (2015).
19. Campos, P.-E. *et al.* Unguiculin A and Ptilomycalins E–H, Antimalarial Guanidine Alkaloids from the Marine Sponge Monanchora unguiculata. *J. Nat. Prod.* **80,** 1404–1410 (2017).
20. Berlinck, R. G. S., Trindade-Silva, A. E. & Santos, M. F. C. The chemistry and biology of organic guanidine derivatives. *Nat. Prod. Rep.* **29,** 1382–1406 (2012).
21. Cusick, K. D. & Sayler, G. S. An overview on the marine neurotoxin, saxitoxin: Genetics, molecular targets, methods of detection and ecological functions. *Mar. Drugs* **11,** 991–1018 (2013).
22. Bane, V., Lehane, M., Dikshit, M., O'Riordan, A. & Furey, A. Tetrodotoxin: Chemistry, toxicity, source, distribution and detection. *Toxins (Basel).* **6,** 693–755 (2014).
23. Nieto, F. R. *et al.* Tetrodotoxin (TTX) as a therapeutic agent for pain. *Mar. Drugs* **10,** 281–305 (2012).
24. Skov, M. J., Beck, J. C., De Kater, A. W. & Shopp, G. M. Nonclinical safety of ziconotide: an intrathecal analgesic of a new pharmaceutical class. *Int. J. Toxicol.* **26,** 411–421 (2007).
25. Marine Pharmacology: Clinical Development. *http://marinepharmacology. midwestern.edu/ clinPipeline.htm* (2017).
26. Mayer, A. M. S. *et al.* The odyssey of marine pharmaceuticals: a current pipeline perspective. *Trends Pharmacol. Sci.* **31,** 255–265 (2010).

27. Eckert-Maksic, M. *et al.* Basicity of guanidines with heteroalkyl side chains in acetonitrile. *European J. Org. Chem.* **2008,** 5176–5184 (2008).
28. Salvino, J. M. *et al.* Novel small molecule guanidine Sigma1 inhibitors for advanced prostate cancer. *Bioorganic Med. Chem. Lett.* **27,** 2216–2220 (2017).
29. Li, Z. *et al.* Discovery of acylguanidine oseltamivir carboxylate derivatives as potent neuraminidase inhibitors. *Bioorg. Med. Chem.* **25,** 2772–2781 (2017).
30. O'Brien-Brown, J. *et al.* Discovery and pharmacological evaluation of a novel series of adamantyl cyanoguanidines as P2X 7 receptor antagonists. *Eur. J. Med. Chem.* **130,** 433–439 (2017).
31. Choi, H., Kim, K. J. & Lee, D. G. Antifungal activity of the cationic antimicrobial polymer-polyhexamethylene guanidine hydrochloride and its mode of action. *Fungal Biol.* **121,** 53–60 (2017).
32. Rightsel, W. A. *et al.* Antiviral effect of guanidine. *Sci. Reports* **134,** 558–559 (1961).
33. Maruthur, N. M. *et al.* Diabetes medications as monotherapy or metformin-based combination therapy for type 2 diabetes: A systematic review and meta-analysis. *Ann. Intern. Med.* **164,** 740–751 (2016).
34. Elewa, H. & Wilby, K. J. A Review of Pharmacogenetics of Antimalarials and Associated Clinical Implications. *Eur. J. Drug Metab. Pharmacokinet.* 1–12 (2017).
35. von Itzstein, M. *et al.* Rational design of potent sialidase-based inhibitors of influenza virus replication. *Nature* **363,** 418–423 (1993).
36. Alame, M. M., Massaad, E. & Zaraket, H. Peramivir: A novel intravenous neuraminidase inhibitor for treatment of acute influenza infections. *Front. Microbiol.* **7,** 1–14 (2016).
37. Kerry, P. S. *et al.* Structural basis for a class of nanomolar influenza A neuraminidase inhibitors. *Sci. Rep.* **3,** 3–8 (2013).
38. Burnham, A. J., Baranovich, T. & Govorkova, E. A. Neuraminidase inhibitors for influenza B virus infection: Efficacy and resistance. *Antiviral Res.* **100,** 520–534 (2013).
39. Li, P. *et al.* Synthesis, characterization, and bactericidal evaluation of chitosan/guanidine functionalized graphene oxide composites. *Molecules* **22,** 1–15 (2017).
40. Nizalapur, S. *et al.* Amphipathic guanidine-embedded glyoxamide-based peptidomimetics as novel antibacterial agents and biofilm disruptors. *Org. Biomol. Chem.* **15,** 2033–2051 (2017).
41. Kaul, M. *et al.* A bactericidal guanidinomethyl biaryl that alters the dynamics of bacterial FtsZ polymerization. *J. Med. Chem.* **55,** 10160–10176 (2012).
42. Maccari, G. *et al.* Synthesis of linear and cyclic guazatine derivatives endowed with antibacterial activity. *Bioorganic Med. Chem. Lett.* **24,** 5525–5529 (2014).
43. Bravo, I. *et al.* Phenyl-guanidine derivatives as potential therapeutic agents for glioblastoma multiforme: catalytic syntheses, cytotoxic effects and DNA affinity. *RSC Adv.* **6,** 8267–8276 (2016).
44. Legin, A. A. *et al.* Guanidine platinum(II) complexes: Synthesis, in vitro antitumor activity, and DNA interactions. *J. Inorg. Biochem.* **133,** 33–39 (2014).
45. Jarvis, A. *et al.* Small molecule inhibitors of the neuropilin-1 vascular endothelial growth factor A (VEGF-A) interaction. *J. Med. Chem.* **53,** 2215–2226 (2010).
46. R., P. N. & B., S. A. Synthesis of Novel 3,4-Dihydroquinolin-2(1H)-one Guanidines as Potential Antihypertensive Agents. *Asian J. Chem.* **23,** 1655–1660 (2011).
47. Clark, R. D. *et al.* Discovery and SAR development of 2-(phenylamino) imidazolines as postacyclin receptor antagonists. *Bioorganic Med. Chem. Lett.* **14,** 1053–1056 (2004).
48. Kazmierczak, P. A., Dobaczewski, M. P., Przygodzki, T., Carsky, J. & Watala, C. β-Resorcylidene aminoguanidine (RAG) dilates coronary arteries in an endothelium-independent manner. *Pharmacol. Reports* **67,** 631–635 (2015).
49. Lu, T. *et al.* Discovery and clinical evaluation of 1-{N-[2-(amidinoaminooxy)ethyl]amino} carbonylmethyl-6-methyl-3-[2,2-difluoro-2-phenylethylamino]pyrazinone (RWJ-671818), a thrombin inhibitor with an oxyguanidine P1 motif. *J. Med. Chem.* **53,** 1843–1856 (2010).
50. Tang, Y.-L. *et al.* Metformin Use Is Associated with Reduced Incidence and Improved Survival of Endometrial Cancer: A Meta-Analysis. *Biomed Res. Int.* 1–9 (2017).
51. Chamberlain, J. J. *et al.* Pharmacologic Therapy for Type 2 Diabetes: Synopsis of the 2017 American Diabetes Association Standards of Medical Care in Diabetes. *Ann. Intern. Med.* **166,** 572–579 (2017).
52. Sinz, C. *et al.* Discovery of N-Aryl-2-acylindole human glucagon receptor antagonists.

Bioorganic Med. Chem. Lett. **21,** 7124–7130 (2011).
53. Reginato, C. F. *et al.* Antifungal activity of synthetic antiseptics and natural compounds against Candida dubliniensis before and after in vitro fluconazole exposure. *Rev. Soc. Bras. Med. Trop.* **50,** 75–79 (2017).
54. Martins, L. F. *et al.* Analogues of Marine Guanidine Alkaloids Are in Vitro Effective against Trypanosoma cruzi and Selectively Eliminate Leishmania (L.) infantum Intracellular Amastigotes. *J. Nat. Prod.* **79,** 2202–2210 (2016).
55. McKeever, C., Kaiser, M. & Rozas, I. Aminoalkyl derivatives of guanidine diaromatic minor groove binders with antiprotozoal activity. *J. Med. Chem.* **56,** 700–711 (2013).
56. Anzini, M. *et al.* Synthesis and biological evaluation of amidine, guanidine, and thiourea derivatives of 2-amino-(6-trifluoromethoxy)benzothiazole as neuroprotective agents potentially useful in brain diseases. *J. Med. Chem.* **53,** 734–744 (2010).
57. Mooney, C. A. *et al.* Oseltamivir Analogues Bearing N‑Substituted Guanidines as Potent Neuraminidase Inhibitors. *J. Med. Chem.* **57,** 3154–3160 (2014).
58. Cooley, C. B. *et al.* Oligocarbonate molecular transporters: Oligomerization-based syntheses and cell-penetrating studies. *J. Am. Chem. Soc.* **131,** 16401–16403 (2009).
59. Stanzl, E. G., Trantow, B. M., Vargas, J. R. & Wender, P. a. Fifteen Years of Cell-Penetrating, Guanidinium-Rich Molecular Transporteurs: Basic Science, Research Tools, and Clinical Applications. *Acc. Chem. Res.* **46,** 2944–2954 (2013).
60. Varki, A. *et al. Biological roles of glycans - Essentials of glycobiology*. (Cold Spring Harbor Laboratory Press, 2008).
61. Neelamegham, S. & Liu, G. Systems glycobiology: Biochemical reaction networks regulating glycan structure and function. *Glycobiology* **21,** 1541–1553 (2011).
62. Armenta, S., Moreno-Mendieta, S., Sanchez-Cuapio, Z., Sanchez, S. & Rodriguez-Sanoja, R. Advances in molecular engineering of carbohydrate-binding modules. *Proteins* 1–50 (2017). doi:10.1002/prot.25327
63. Ghazarian, H., Idoni, B. & Oppenheimer, S. B. A glycobiology review: Carbohydrates, lectins and implications in cancer therapeutics. *Acta Histochem.* **113,** 236–247 (2011).
64. Wolfert, M. A. & Boons, G.-J. Adaptive immune activation: glycosylation does matter. *Nat. Chem. Biol.* **9,** 776–784 (2013).
65. Buskas, T., Ingale, S. & Boons, G. J. Glycopeptides as versatile tools for glycobiology. *Glycobiology* **16,** 113–136 (2006).
66. Partridge, E. A. Regulation of Cytokine Receptors by Golgi N-Glycan Processing and Endocytosis. *Science (80-.).* **306,** 120–124 (2004).
67. Gloster, T. M. Development of inhibitors as research tools for carbohydrate-processing enzymes. *Biochem. Soc. Trans.* **40,** 913–928 (2012).
68. Wang, Z. *et al.* A General Strategy for the Chemoenzymatic Synthesis of Asymmetrically Branched N-Glycans. *Science (80-.).* **341,** 379–383 (2013).
69. An, H. J., Kronewitter, S. R., de Leoz, M. L. A. & Lebrilla, C. B. Glycomics and disease markers. *Curr. Opin. Chem. Biol.* **13,** 601–607 (2009).
70. Lebrilla, C. B. & An, H. J. The prospects of glycanbiomarkers for the diagnosis of diseases. *Mol. Biosyst.* **5,** 17–20 (2009).
71. Hart, G. W. & Copeland, R. J. Glycomics hits the big time. *Cell* **143,** 672–676 (2010).
72. Compain, P. & Martin, O. R. *Iminosugars: From synthesis to therapeutic applications*. (Wiley, 2007).
73. Mellor, H. R. *et al.* Cellular effects of deoxynojirimycin analogues: uptake, retention and inhibition of glycosphingolipid biosynthesis. *Biochem. J.* **381,** 861–866 (2004).
74. Nash, R. J., Kato, A., Yu, C.-Y. & Fleet, G. W. Iminosugars as therapeutic agents: recent advances and promising trends. *Futur. Sci.* **3,** 1513–1521 (2011).
75. Winchester, B. G. Iminosugars: from botanical curiosities to licensed drugs. *Tetrahedron Asymmetry* **20,** 645–651 (2009).
76. Horne, G., Wilson, F. X., Tinsley, J., Williams, D. H. & Storer, R. Iminosugars past, present and future: medicines for tomorrow. *Drug Discov. Today* **16,** 107–118 (2011).
77. Withers, S. G., Namchuk, M. & R, M. *Iminosugars as Glycosidase Inhibitors: Nojirimycin & Beyond*. (Wiley-VCH, 1999).
78. Kunz, H. Emil Fischer - Unequalled classicist, master of organic chemistry research, and inspired trailblazer of biological chemistry. *Angew. Chemie - Int. Ed.* **41,** 4439–4451 (2002).

79. Paulsen, H. Carbohydrates Containing Nitrogen or Sulfur in the'Hemiacetal' Ring. *Angew. Chem. Int. Ed.* **5,** 495–510 (1966).
80. Inouye, S., Tsuruoka, T. & Nida, T. The structure of nojirimycin, a piperidinose sugar antibiotic. *J. Antibiot. (Tokyo).* **19,** 288–292 (1966).
81. Inouye, S., Tsuruoka, T., Ito, T. & Niida, T. Structure and synthesis of nojirimycin. *Tetrahedron* **24,** 2125–2144 (1968).
82. Yagi M, Kouno T, Aoyagi Y, M. H. The structure of moranoline, a piperidine alkaloid from Morus species. *Nippon Nogei Kagaku Kaishi.* **50,** 571–572 (1976).
83. Gao, K. *et al.* 1-Deoxynojirimycin: Occurrence, Extraction, Chemistry, Oral Pharmacokinetics, Biological Activities and In Silico Target Fishing. *Molecules* **21,** 1600–1614 (2016).
84. Hohenschutz, L. D. *et al.* Castanospermine, a 1,6,7,8-tetrahydroxyoctahydroindolizine alkaloid, from seeds of Castanospermum australe. *Phytochemistry* **20,** 811–814 (1981).
85. Asano, N., Oseki, K., Tomioka, E., Kizu, H. & Matsui, K. N-Containing sugars from Morus alba and their glycosidase inhibitory activities. *Carbohydr. Res.* **259,** 243–255 (1994).
86. Karpas, A. *et al.* Aminosugar derivatives as potential anti-human immunodeficiency virus agents. *Proc. Natl. Acad. Sci.* **85,** 9229–9233 (1988).
87. Bergeron-Brlek, M., Meanwell, M. & Britton, R. Direct synthesis of imino-C-nucleoside analogues and other biologically active iminosugars. *Nat. Commun.* **6,** 1–6 (2015).
88. Zhang, L. & Ye, X.-S. Synthesis of Iminosugar-Containing KRN7000 Analogues. *Chinese J. Chem.* **20,** 1–8 (2017).
89. Horne, G. Iminosugars: Therapeutic Applications and Synthetic Considerations. *Top. Med. Chem.* **12,** 23–51 (2014).
90. Iwami, M. *et al.* A new immunomodulator, FR-900494: taxonomy, fermentation, isolation, and physico-chemical and biological characteristics. *J. Antibiot. (Tokyo).* **40,** 612–622 (1987).
91. Kayakiri, H. *et al.* Structure of kifunensine, a new immunomodulator isolated from an actinomycete. *J. Org. Chem.* **54,** 4015–4016 (1989).
92. Kayakiri, H., Kasahara, C., Oku, T. & Hashimoto, M. Synthesis of kifunensine, an immunomodulating substance isolated from microbial source. *Tetrahedron Lett.* **31,** 225–226 (1990).
93. Gloster, T. M. & Davies, G. J. Glycosidase inhibition: assessing mimicry of the transition state. *Org. Biomol. Chem.* **8,** 305–320 (2010).
94. Goss, P. E., Baker, M., Dennis, J. W. & Carver, J. Inhibitors of Carbohydrate Processin: A new Class of Anticancer Agents. *Clin. Cancer Res.* **1,** 935–944 (1995).
95. Kooij, R. *et al.* Glycosidase inhibition by novel guanidinium and urea iminosugar derivatives. *Medchemcomm* **4,** 387–393 (2013).
96. Diaz-Perez, P., Garcia-Moreno, M. I., Mellet, C. O. & Fernandez, J. M. G. Synthesis of (1S,2S,3R,8S,8aR)-1,2,3,8-Tetrahydroxy-6-oxa-5-thioxoindolizidine: A Stable Reducing Swainsonine Analog with Controlled Anomeric Configuration. *Synlett* **3,** 341–344 (2003).
97. Sevšek, A. *et al.* Bicyclic isoureas derived from 1-deoxynojirimycin are potent inhibitors of β-glucocerebrosidase. *Org. Biomol. Chem.* **14,** 8670–8673 (2016).
98. García-Moreno, M. I., Díaz-Pérez, P., Mellet, O. & García Fernández, J. M. Castanospermine-trehazolin hybrids: a new family of glycomimetics with tuneable glycosidase inhibitory properties. *Chem. Commun.* **45,** 848–849 (2002).
99. Aguilar-Moncayo, M. *et al.* Bicyclic (galacto)nojirimycin analogues as glycosidase inhibitors: effect of structural modifications in their pharmacological chaperone potential towards β-glucocerebrosidase. *Org. Biomol. Chem.* **9,** 3698–3713 (2011).
100. Díaz Pérez, V. M. *et al.* Generalized anomeric effect in action: Synthesis and evaluation of stable reducing indolizidine glycomimetics as glycosidase inhibitors. *J. Org. Chem.* **65,** 136–143 (2000).
101. Blanco, J. L. J. *et al.* N-thiocarbonyl azasugars: a new family of carbohydrate mimics with controlled anomeric configuration. *Chem. Commun.* **45,** 1969–1970 (1997).
102. Benltifa, M., García Moreno, M. I., Ortiz Mellet, C., García Fernández, J. M. & Wadouachi, A. Synthesis and evaluation of sulfamide-type indolizidines as glycosidase inhibitors. *Bioorganic Med. Chem. Lett.* **18,** 2805–2808 (2008).
103. Aguilar-moncayo, M. *et al.* Synthesis of Thiohydantoin-Castanospermine Glycomimetics as Glycosidase Inhibitors. *J. Org. Chem.* **74,** 3595–3598 (2009).
104. Haff, R. F. & Swim, H. E. Histochemical Demonstration of Enzymes Separated by Zone

Electrophoresis in Starch Gels. *Science (80-.).* **125,** 1294–1295 (1957).
105. Sánchez-Fernández, E. M. *et al.* sp2-Iminosugar O-, S-, and N-glycosides as conformational mimics of α-linked disaccharides; implications for glycosidase inhibition. *Chemistry* **18,** 8527–8539 (2012).
106. Sánchez-Fernández, E. M. *et al.* Synthesis of N-, S-, and C-glycoside castanospermine analogues with selective neutral alpha-glucosidase inhibitory activity as antitumour agents. *Chem. Commun.* **46,** 5328–5330 (2010).
107. Aguilar-Moncayo, M. *et al.* Glycosidase inhibition by ring-modified castanospermine analogues: tackling enzyme selectivity by inhibitor tailoring. *Org. Biomol. Chem.* **7,** 2738–2747 (2009).
108. Pérez, P. D., García-Moreno, M. I., Mellet, C. O. & García Fernández, J. M. Synthesis and comparative glycosidase inhibitory properties of reducing castanospermine analogues. *European J. Org. Chem.* 2903–2913 (2005).
109. Scott, L. & Spencer, C. Miglitol: a review of its therapeutic potential in type 2 diabetes mellitus. *Drugs* **59,** 521–549 (2000).
110. Marques, A. R. A. *et al.* Reducing GBA2 activity ameliorates neuropathology in niemann-pick type C mice. *PLoS One* **10,** 1–18 (2015).
111. Fischl, M. A. *et al.* The safety and efficacy of combination N-butyl-deoxynojirimycin (SC-48334) and zidovudine in patients with HIV-1 infection and 200-500 CD4 cells/mm3. *J. Acquir. Immune Defic. Syndr.* **7,** 139–147 (1994).
112. Acetilon Financial Performance for 2016. *Acetilon* https://www1.actelion.com/en-rebranded/investors/n (2017).
113. Zhu, X., Sheth, K. a, Li, S., Chang, H.-H. & Fan, J.-Q. Rational design and synthesis of highly potent beta-glucocerebrosidase inhibitors. *Angew. Chem. Int. Ed. Engl.* **44,** 7450–7453 (2005).
114. Ogawa, S., Kanto, M. & Suzuki, Y. Development and medical application of unsaturated carbaglycosylamine glycosidase inhibitors. *Mini Rev. Med. Chem.* **7,** 679–691 (2007).
115. Trapero, A., González-Bulnes, P., Butters, T. D. & Llebaria, A. Potent aminocyclitol glucocerebrosidase inhibitors are subnanomolar pharmacological chaperones for treating gaucher disease. *J. Med. Chem.* **55,** 4479–4488 (2012).
116. Dedola, S., Hughes, D. L., Nepogodiev, S. A., Rejzek, M. & Field, R. A. Synthesis of alpha- and beta-D-glucopyranosyl triazoles by CuAAC 'click chemistry': reactant tolerance, reaction rate, product structure and glucosidase inhibitory properties. *Carbohydr. Res.* **345,** 1123–1134 (2010).
117. Pan, Y. T., Ghidoni, J. & Elbein, A. D. The effects of castanospermine and swainsonine on the activity and synthesis of intestinal sucrase. *Archives of biochemistry and biophysics* **303,** 134–144 (1993).
118. Taylor, D. L. *et al.* 6-O-Butanoylcastanospermine (MDL 28,574) inhibits glycoprotein processing and the growth of HIVs. *AIDS* **5,** 693–698 (1991).
119. Durantel, D. Celgosivir, an alpha-glucosidase I inhibitor for the potential treatment of HCV infection. *Curr. Opin. Investig. drugs* **10,** 860–870 (2009).
120. García-Moreno, M. I., Díaz-Pérez, P., Ortiz Mellet, C. & García Fernández, J. M. Synthesis and Evaluation of Isourea-Type Glycomimetics Related to the Indolizidine and Trehazolin Glycosidase Inhibitor Families. *J. Org. Chem.* **68,** 8890–8901 (2003).
121. Fan, J. Q. A contradictory treatment for lysosomal storage disorders: Inhibitors enhance mutant enzyme activity. *Trends Pharmacol. Sci.* **24,** 355–360 (2003).
122. Fan, J. Q. A counterintuitive approach to treat enzyme deficiencies: use of enzyme inhibitors for restoring mutant enzyme activity. *Biol Chem* **389,** 1–11 (2008).
123. Liu, H., Liang, X., Sohoel, H., Bulow, A. & Bols, M. Noeuromycin, a glycosyl cation mimic that strongly inhibits glycosidases. *J. Am. Chem. Soc.* **123,** 5116–5117 (2001).
124. Brumshtein, B. *et al.* Cyclodextrin-mediated crystallization of acid β-glucosidase in complex with amphiphilic bicyclic nojirimycin analogues. *Org. Biomol. Chem.* **9,** 4160–4167 (2011).
125. de Graaf, M. *et al.* Cloning and characterization of human liver cytosolic beta-glycosidase. *Biochem. J.* **356,** 907–910 (2001).
126. Sanchez-Fernandez, E. M., Garcia Fernandez, J. M. & Mellet, C. O. Glycomimetic-based pharmacological chaperones for lysosomal storage disorders: lessons from Gaucher, GM1-gangliosidosis and Fabry diseases. *Chem. Commun.* **52,** 5497–5515 (2016).
127. Li, K.-Y. *et al.* Exploring functional cyclophellitol analogues as human retaining beta-

glucosidase inhibitors. *Org. Biomol. Chem.* **12,** 7786–91 (2014).
128. Lahiri, R., Ansari, A. A. & Vankar, Y. D. Recent developments in design and synthesis of bicyclic azasugars, carbasugars and related molecules as glycosidase inhibitors. *Chem. Soc. Rev.* **42,** 5102 (2013).
129. Nishimura, Y. Gem-diamine 1-N-iminosugars as versatile glycomimetics: synthesis, biological activity and therapeutic potential. *J. Antibiot. (Tokyo).* **62,** 407–423 (2009).
130. Nocquet, P.-A. *et al.* Synthesis of a new class of iminosugars based on constrained azaspirocyclic scaffolds by way of catalytic C–H amination. *Org. Biomol. Chem.* **13,** 9176–9180 (2015).
131. Schramm, V. L. & Tyler, P. C. Imino-sugar-based nucleosides. *Curr. Top. Med. Chem.* **3,** 525–540 (2003).
132. Willems, L. I. *et al.* From covalent glycosidase inhibitors to activity-based glycosidase probes. *Chem. - A Eur. J.* **20,** 10864–10872 (2014).
133. Langeveld, M. *et al.* Treatment of genetically obese mice with the iminosugar N-(5-adamantane-1-yl-methoxy-pentyl)-deoxynojirimycin reduces body weight by decreasing food intake and increasing fat oxidation. *Metabolism.* **61,** 99–107 (2012).
134. Wrodnigg, T. M., Steiner, A. J. & Ueberbacher, B. J. Natural and synthetic iminosugars as carbohydrate processing enzyme inhibitors for cancer therapy. *Anticancer. Agents Med. Chem.* **8,** 77–85 (2008).
135. Alonzi, D. S., Scott, K. A., Dwek, R. A. & Zitzmann, N. Iminosugar antivirals: the therapeutic sweet spot. *Biochem. Soc. Trans.* **45,** 571–582 (2017).
136. Kallemeijn, W. W. *et al.* Investigations on therapeutic glucocerebrosidases through paired detection with fluorescent activity-based probes. *PLoS One* **12,** 1–23 (2017).
137. Gomes, C. M. Protein Misfolding in Disease and Small Molecule Therapies. *Curr. Top. Med. Chem.* **12,** 2460–2469 (2012).
138. Rye, C. S. & Withers, S. G. Glycosidase mechanisms. *Curr. Opin. Chem. Biol.* **4,** 573–580 (2000).
139. Kötzler, M. P., Hancock, S. M. & Withers, S. G. Glycosidases: Functions, Families and Folds. *eLS* 1–14 (2014). doi:10.1002/9780470015902.a0020548.pub2
140. Asano, N. Glycosidase inhibitors: Update and perspectives on practical use. *Glycobiology* **13,** 93–104 (2003).
141. Davies, G. & Henrissat, B. Structures and mechanisms of glycosyl hydrolases. *Structure* **3,** 853–859 (1995).
142. Cantarel, B. I. *et al.* The Carbohydrate-Active EnZymes database (CAZy): An expert resource for glycogenomics. *Nucleic Acids Res.* **37,** 233–238 (2009).
143. Koshland, D. E. Stereochemistry and T H E Mechanism of Enzymatic Reactions. *Biol. Rev.* **28,** 416–436 (1953).
144. McCarter, J. D. & Stephen Withers, G. Mechanisms of enzymatic glycoside hydrolysis. *Curr. Opin. Struct. Biol.* **4,** 885–892 (1994).
145. Zechel, D. L. & Withers, S. G. Glycosidase mechanisms: Anatomy of a finely tuned catalyst. *Acc. Chem. Res.* **33,** 11–18 (2000).
146. Dwek, R. A. Biological importance of glycosylation. *Dev. Biol. Stand.* **96,** 43–47 (1998).
147. Guo, J., Asong, J. & Boons, G. J. Selective inhibition of glycosidases by feedback prodrugs. *Angew. Chemie - Int. Ed.* **45,** 5345–5348 (2006).
148. Ardèvol, A. & Rovira, C. Reaction Mechanisms in Carbohydrate-Active Enzymes: Glycoside Hydrolases and Glycosyltransferases. Insights from ab Initio Quantum Mechanics/Molecular Mechanics Dynamic Simulations. *J. Am. Chem. Soc.* **137,** 7528–7547 (2015).
149. Gloster, T. M. & Vocadlo, D. J. Developing inhibitors of glycan processing enzymes as tools for enabling glycobiology. *Nat. Chem. Biol.* **8,** 683–694 (2012).
150. Brás, N. F., Cerqueira, N. M., Ramos, M. J. & Fernandes, P. A. Glycosidase inhibitors: a patent review (2008-2013). *Expert Opin. Ther. Pat.* **24,** 857–874 (2014).
151. Salsali, A. & Nathan, M. A review of types 1 and 2 diabetes mellitus and their treatment with insulin. *Am. J. Ther.* **13,** 349–361 (2006).
152. Olokoba, A. B., Obateru, O. A. & Olokoba, L. B. Type 2 diabetes mellitus: A review of current trends. *Oman Med. J.* **27,** 269–273 (2012).
153. Van de Laar, A. Alpha-glucosidase inhibitors in the early treatment of type 2 diabetes. *Vasc. Health Risk Manag.* **4,** 1189–1195 (2008).
154. Babu, Y. S., Chand, P. & Kotian, P. L. Influenza Neuraminidase Inhibitors as Antiviral Agents. *Annu. Rep. Med. Chem.* **41,** 287–297 (2006).

155. Taubenberger, J. K. & Morens, D. M. Influenza: the once and future pandemic. *Public Health Rep.* **125,** 16–26 (2010).
156. Kim, C. U., Chen, X. & Mendel, D. B. Neuraminidase inhibitors as anti-influenza virus agents. *Antivir. Chem. Chemother.* **10,** 141–154 (1999).
157. Winchester, B. Lysosomal metabolism of glycoproteins. *Glycobiology* **15,** 1–15 (2005).
158. de Duve, C., Pressman, B. C., Gianetto, R., Wattiaux, R. & Appelmans, F. Tissue fractionation studies. *Biochem. J.* **60,** 604–617 (1955).
159. de Duve, C. The lysosome turns fifty. *Nat. Cell Biol.* **7,** 847–849 (2005).
160. Futerman, A. H. & van Meer, G. The cell biology of lysosomal storage disorders. *Nat. Rev.* **5,** 554–565 (2004).
161. Aerts, J. M. F. G. *et al.* Biomarkers in the diagnosis of lysosomal storage disorders: Proteins, lipids, and inhibodies. *J. Inherit. Metab. Dis.* **34,** 605–619 (2011).
162. Vellodi, A. Lysosomal storage disorders. *Br. J. Haematol.* **128,** 413–431 (2005).
163. Meikle, P. J., Fietz, M. J. & Hopwood, J. J. Diagnosis of lysosomal storage disorders: current techniques and future directions. *Expert Rev. Mol. Diagn.* **4,** 677–691 (2004).
164. Wennekes, T. *et al.* Glycosphingolipids - Nature, Function, and Pharmacological Modulation. *Angew. Chemie Int. Ed.* **48,** 8848–8869 (2009).
165. Pralhada Rao, R. *et al.* Sphingolipid metabolic pathway: an overview of major roles played in human diseases. *J. Lipids* **2013,** 178910–178922 (2013).
166. Wang, R. Y., Bodamer, O. A., Watson, M. S. & Wilcox, W. R. Lysosomal storage diseases: Diagnostic confirmation and management of presymptomatic individuals. *Genet. Med.* **13,** 457–484 (2011).
167. Rosenbloom, B. E. & Weinreb, N. J. Gaucher disease: a comprehensive review. *Crit. Rev. Oncog.* **18,** 163–175 (2013).
168. Grabowski, G. A. Phenotype, diagnosis, and treatment of Gaucher's disease. *Lancet* **372,** 1263–1271 (2008).
169. Zeller, J. L. Gaucher Disease. *J. Am. Med. Assoc.* **298,** 1358 (2007).
170. Jmoudiak, M. & Futerman, A. H. Gaucher Disease: Pathological Mechanisms and Modern Management. *Br. J. Haematol.* **129,** 178–188 (2005).
171. Brady, R. O. Gaucher's Disease : Past , Present and Future. *Baillieres. Clin. Haematol.* **10,** 621–634 (1997).
172. Fabrega, S. *et al.* Human Glucocerebrosidase: Heterologous Expression of Active Site Mutants in Murine Null Cells. *Glycobiology* **10,** 1217–1224 (2000).
173. Charrow, J. *et al.* The Gaucher Registry. *Arch Intern Med.* **160,** 2835–2843 (2000).
174. Pastores, G. M., Patel, M. J. & Firooznia, H. Bone and Joint Complications Related to Gaucher Disease. *Curr. Rheumatol. Rep.* **2,** 175–180 (2000).
175. Beutler, E. Gaucher Disease: Multiple Lessons from a Single Gene Disorder. *Acta Paediatr.* **95,** 103–109 (2006).
176. Dekker, N. *et al.* Elevated plasma glucosylsphingosine in Gaucher disease: relation to phenotype, storage cell markers, and therapeutic response. *Blood* **118,** 118–128 (2012).
177. Hruska, K. S., LaMarca, M. E., Scott, C. R. & Sidransky, E. Gaucher disease: Mutation and polymorphism spectrum in the glucocerebrosidase gene (GBA). *Hum. Mutat.* **29,** 567–583 (2008).
178. Beutler, E., Gelbart, T. & Scott, C. R. Hematologically important mutations: Gaucher disease. *Blood Cells, Mol. Dis.* **35,** 355–364 (2005).
179. Butters, T. D. Gaucher disease. *Curr. Opin. Chem. Biol.* **11,** 412–418 (2007).
180. Sidransky, E. & Lopez, G. The link between the GBA gene and parkinsonism. *Lancet Neurol.* **11,** 986–998 (2012).
181. Migdalska-Richards, A. & Schapira, A. H. V. The relationship between glucocerebrosidase mutations and Parkinson disease. **136,** 1–15 (2016).
182. Rodriguez-Porcel, F., Espay, A. J. & Carecchio, M. Parkinson disease in Gaucher disease. *J. Clin. Mov. Disord.* **4,** 1–4 (2017).
183. Dehay, B. *et al.* Targeting α-synuclein: Therapeutic options. *Mov. Disord.* **31,** 882–886 (2016).
184. Horowitz, M. *et al.* The human glucocerebrosidase gene and pseudogene: Structure and evolution. *Genomics* **4,** 87–96 (1989).
185. Dvir, H. *et al.* X-ray structure of human acid-β-glucosidase, the defective enzyme in Gaucher disease. *EMBO Rep.* **4,** 704–709 (2003).

186. Brumshtein, B. *et al.* Crystal structures of complexes of N-butyl- and N-nonyl-deoxynojirimycin bound to acid β-glucosidase: Insights into the mechanism of chemical chaperone action in Gaucher disease. *J. Biol. Chem.* **282,** 29052–29058 (2007).
187. Kallemeijn, W. W. *et al.* A sensitive gel-based method combining distinct cyclophellitol-based probes for the identification of acid/base residues in human retaining β-glucosidases. *J. Biol. Chem.* **289,** 35351–35362 (2014).
188. Liou, B. & Grabowski, G. A. Participation of asparagine 370 and glutamine 235 in the catalysis by acid β-glucosidase: The enzyme deficient in Gaucher disease. *Mol. Genet. Metab.* **97,** 65–74 (2009).
189. Offman, M. N., Krol, M., Silman, I., Sussman, J. L. & Futerman, A. H. Molecular basis of reduced glucosylceramidase activity in the most common Gaucher disease mutant, N370S. *J. Biol. Chem.* **285,** 42105–42114 (2010).
190. Wei, R. R. *et al.* X-ray and biochemical analysis of N370S mutant human acid beta-glucosidase. *J. Biol. Chem.* **286,** 299–308 (2011).
191. Offman, M. N. *et al.* Comparison of a molecular dynamics model with the X-ray structure of the N370S acid β-glucosidase mutant that causes Gaucher disease. *Protein Eng. Des. Sel.* **24,** 773–775 (2011).
192. Liou, B. *et al.* Analyses of variant acid β-glucosidases: Effects of Gaucher disease mutations. *J. Biol. Chem.* **281,** 4242–4253 (2006).
193. Futerman, A. H. & Platt, F. M. The metabolism of glucocerebrosides - From 1965 to the present. *Mol. Genet. Metab.* **120,** 22–26 (2017).
194. Boustany, R.-M. N. Lysosomal storage diseases—the horizon expands. *Nat. Rev. Neurol.* **9,** 583–598 (2013).
195. Cox, T. M. Innovative treatments for lysosomal diseases. *Best Pract. Res. Clin. Endocrinol. Metab.* **29,** 275–311 (2015).
196. Charrow, J. & Scott, C. R. Long-term treatment outcomes in Gaucher disease. *Am. J. Hematol.* **90,** 19–24 (2015).
197. Deegan, P. B. & Cox, T. M. Imiglucerase in the treatment of Gaucher disease: A history and perspective. *Drug Des. Devel. Ther.* **6,** 81–106 (2012).
198. Burrow, T. A. & Grabowski, G. A. Velaglucerase alfa in the treatment of Gaucher disease type 1. *Clin. Investig. (Lond).* **1,** 285–293 (2011).
199. Grabowski, G. A., Golembo, M. & Shaaltiel, Y. Taliglucerase alfa: An enzyme replacement therapy using plant cell expression technology. *Mol. Genet. Metab.* **112,** 1–8 (2014).
200. Vitner, E. B., Vardi, A., Cox, T. M. & Futerman, A. H. Emerging therapeutic targets for Gaucher disease. *Expert Opin. Ther. Targets* **19,** 321–334 (2015).
201. Desnick, R. J. & Schuchman, E. H. Enzyme replacement and enhancement therapies: lessons from lysosomal disorders. *Nat Rev Genet* **3,** 954–966 (2002).
202. Trapero, A. & Llebaria, A. Glucocerebrosidase inhibitors: future drugs for the treatment of Gaucher disease? *Futur. Sci.* **6,** 975–978 (2014).
203. Platt, F. M. & Jeyakumar, M. Substrate reduction therapy. *Acta Paediatr.* **97,** 88–93 (2008).
204. Platt, F. M., Neises, G. R., Dwek, R. A. & Butters, T. D. N-butyldeoxynojirimycin is a novel inhibitor of glycolipid biosynthesis. *J. Biol. Chem.* **269,** 8362–8365 (1994).
205. Mellor, H. R. *et al.* Preparation, biochemical characterization and biological propreties of radiolabelled N-alkylated deoxynojirimycins. *Society* **233,** 225–233 (2002).
206. Boot, R. G. *et al.* Identification of the Non-lysosomal Glucosylceramidase as - Glucosidase 2. *J. Biol. Chem.* **282,** 1305–1312 (2007).
207. Alfonso, P. *et al.* Miglustat (NB-DNJ) works as a chaperone for mutated acid β-glucosidase in cells transfected with several Gaucher disease mutations. *Blood Cells, Mol. Dis.* **35,** 268–276 (2005).
208. Cox, T. *et al.* Novel oral treatment of Gaucher's disease with N-butyldeoxynojirimycin (OGT 918) to decrease substrate biosynthesis. *Lancet* **355,** 1481–1485 (2000).
209. Hollak, C. E. M. & Wijburg, F. A. Treatment of lysosomal storage disorders: successes and challenges. *J. Inherit. Metab. Dis.* **37,** 587–598 (2014).
210. Shayman, J. A. Eliglustat tartrate: Glucosylceramide synthase inhibitor treatment of type 1 gaucher disease. *Drugs Future* **35,** 613–620 (2010).
211. Coutinho, M. F., Santos, J. I. & Alves, S. Less Is More: Substrate Reduction Therapy for Lysosomal Storage Disorders. *Int. J. Mol. Sci.* **17,** 1–22 (2016).

212. Smid, B. E. *et al.* Biochemical response to substrate reduction therapy versus enzyme replacement therapy in Gaucher disease type 1 patients. *Orphanet J. Rare Dis.* **11,** 1–12 (2016).
213. Boyd, R. E. *et al.* Pharmacological chaperones as therapeutics for lysosomal storage diseases. *J. Med. Chem.* **56,** 2705–2725 (2013).
214. Convertino, M., Das, J. & Dokholyan, N. V. Pharmacological chaperones: design and development of new therapeutic strategies for the treatment of conformational diseases. *ACS Chem. Biol.* **11,** 1471–1489 (2016).
215. Parenti, G., Andria, G. & Valenzano, K. J. Pharmacological Chaperone Therapy: Preclinical Development, Clinical Translation, and Prospects for the Treatment of Lysosomal Storage Disorders. *Mol. Ther.* **23,** 1138–1148 (2015).
216. Sawkar, A. R. *et al.* Chemical chaperones increase the cellular activity of N370S beta-glucosidase: A therapeutic strategy for Gaucher disease. *Proc. Natl. Acad. Sci. U. S. A.* **99,** 15428–15433 (2002).
217. Fan, J. Q., Ishii, S., Asano, N. & Suzuki, Y. Accelerated transport and maturation of lysosomal alpha-galactosidase A in Fabry lymphoblasts by an enzyme inhibitor. *Nat. Med.* **5,** 112–115 (1999).
218. Parenti, G., Moracci, M., Fecarotta, S. & Andria, G. Pharmacological chaperone therapy for lysosomal storage diseases. *Future Med. Chem.* **6,** 1031–1045 (2014).
219. Ichikawa, Y., Igarashi, Y., Ichikawa, M. & Suhara, Y. 1-N-Iminosugars: Potent and Selective Inhibitors of β-Glycosidases. *J. Am. Chem. Soc.* **120,** 3007–3018 (1998).
220. Asano, N. Sugar-mimicking glycosidase inhibitors: bioactivity and application. *Cell. Mol. Life Sci.* **66,** 1479–1492 (2009).
221. Compain, P. *et al.* Design and synthesis of highly potent and selective pharmacological chaperones for the treatment of Gaucher's disease. *ChemBioChem* **7,** 1356–1359 (2006).
222. Young-Gqamana, B. *et al.* Migalastat HCl Reduces Globotriaosylsphingosine (Lyso-Gb3) in Fabry Transgenic Mice and in the Plasma of Fabry Patients. *PLoS One* **8,** 1–14 (2013).
223. Gavrin, L. K., Denny, R. A. & Saiah, E. Small molecules that target protein misfolding. *J. Med. Chem.* **55,** 10823–10843 (2012).
224. Trapero, A. & Llebaria, A. Glucocerebrosidase inhibitors for the treatment of Gaucher disease. *Futur. Sci.* **5,** 573–590 (2013).
225. Parenti, G. Treating lysosomal storage diseases with pharmacological chaperones: From concept to clinics. *EMBO Mol. Med.* **1,** 268–279 (2009).
226. Borges de Melo, E., da Silveira Gomes, A. & Carvalho, I. α- and β-Glucosidase inhibitors: chemical structure and biological activity. *Tetrahedron* **62,** 10277–10302 (2006).
227. Gloster, T. M. *et al.* Glycosidase inhibition: an assessment of the binding of 18 putative transition-state mimics. *J. Am. Chem. Soc.* **129,** 2345–2354 (2007).
228. Overkleeft, H. S. *et al.* Generation of specific deoxynojirimycin-type inhibitors of the non-lysosomal glucosylceramidase. *J. Biol. Chem.* **273,** 26522–7 (1998).
229. Chang, H. H., Asano, N., Ishii, S., Ichikawa, Y. & Fan, J. Q. Hydrophilic iminosugar active-site-specific chaperones increase residual glucocerebrosidase activity in fibroblasts from Gaucher patients. *FEBS J.* **273,** 4082–4092 (2006).
230. Kato, A. *et al.* Docking and SAR studies of calystegines: Binding orientation and influence on pharmacological chaperone effects for Gaucher's disease. *Bioorganic Med. Chem.* **22,** 2435–2441 (2014).
231. Orwig, S. D. *et al.* Binding of 3,4,5,6-tetrahydroxyazepanes to the acid-β-glucosidase active site: implications for pharmacological chaperone design for Gaucher disease. *Biochemistry* **50,** 10647–10657 (2011).
232. Compain, P. Searching for glycomimetics that target protein misfolding in rare diseases: Successes, failures, and unexpected progress made in organic synthesis. *Synlett* **25,** 1215–1240 (2014).
233. Pleat, R. *et al.* Stability is maintained in adults with Gaucher disease type 1 switched from velaglucerase alfa to eliglustat or imiglucerase: A sub-analysis of the eliglustat ENCORE trial. *Mol. Genet. Metab. Reports* **9,** 25–28 (2016).
234. Sawkar, A. R. *et al.* Chemical Chaperones and Permissive Temperatures Alter the Cellular Localization of Gaucher Disease Associated Glucocerebrosidase Variants. *ACS Chem. Biol.* **1,** 235–251 (2006).
235. Wang, G. N. *et al.* Rational design and synthesis of highly potent pharmacological chaperones

for treatment of N370S mutant Gaucher disease. *J. Med. Chem.* **52,** 3146–3149 (2009).
236. Steet, R. A. *et al.* The iminosugar isofagomine increases the activity of N370S mutant acid beta-glucosidase in Gaucher fibroblasts by several mechanisms. *Proc. Natl. Acad. Sci. U. S. A.* **103,** 13813–13818 (2006).
237. Hill, T., Tropak, M. B., Mahuran, D. & Withers, S. G. Synthesis, Kinetic Evaluation and Cell-Based Analysis of C-Alkylated Isofagomines as Chaperones of β-Glucocerebrosidase. *ChemBioChem* **12,** 2151–2154 (2011).
238. Yu, L. *et al.* α-1-C-Octyl-1-deoxynojirimycin as a pharmacological chaperone for Gaucher disease. *Bioorganic Med. Chem.* **14,** 7736–7744 (2006).
239. Oulaïdi, F. *et al.* Second-generation iminoxylitol-based pharmacological chaperones for the treatment of Gaucher disease. *ChemMedChem* **6,** 353–361 (2011).
240. Serra-Vinardell, J. *et al.* Glucocerebrosidase enhancers for selected gaucher disease genotypes by modification of alpha-1-C-substituted Imino-D-xylitols (DIXs) by click chemistry. *ChemMedChem* **9,** 1744–1754 (2014).
241. Goddard-Borger, E. D. *et al.* Rapid assembly of a library of lipophilic iminosugars via the thiol-ene reaction yields promising pharmacological chaperones for the treatment of Gaucher disease. *J. Med. Chem.* **55,** 2737–2745 (2012).
242. Trapero, A., Alfonso, I., Butters, T. D. & Llebaria, A. Polyhydroxylated bicyclic isoureas and guanidines are potent glucocerebrosidase inhibitors and nanomolar enzyme activity enhancers in Gaucher cells. *J. Am. Chem. Soc.* **133,** 5474–5484 (2011).
243. Trapero, A. & Llebaria, A. The myo-1,2-Diaminocyclitol Scaffold Defines Potent Glucocerebrosidase Activators and Promising Pharmacological Chaperones for Gaucher Disease. *ACS Med. Chem. Lett.* **2,** 614–619 (2011).
244. Trapero, A., Egido-Gabás, M. & Llebaria, A. Adamantane substituted aminocyclitols as pharmacological chaperones for Gaucher disease. *Medchemcomm* **4,** 1584–1589 (2013).
245. Migdalska-Richards, A., Ko, W. K. D., Li, Q., Bezard, E. & Schapira, A. H. V. Oral ambroxol increases brain glucocerebrosidase activity in a nonhuman primate. *Synapse* **71,** 1–3 (2017).
246. Narita, A. *et al.* Ambroxol chaperone therapy for neuronopathic Gaucher disease: A pilot study. *Ann. Clin. Transl. Neurol.* **3,** 200–215 (2016).
247. Zimran, A., Altarescu, G. & Elstein, D. Pilot study using ambroxol as a pharmacological chaperone in type 1 Gaucher disease. *Blood Cells, Mol. Dis.* **50,** 134–137 (2013).
248. Tsunoda, H., Inokuchi, J. -I, Yamagishi, K. & Ogawa, S. Synthesis of glycosylceramide analogs composed of imino-linked unsaturated 5a-carbaglycosyl residues: potent and specific gluco- and galactocerebrosidase inhibitors. *Liebigs Ann.* 279–284 (1995). doi:10.1002/jlac.199519950237
249. Mena-Barragán, T. *et al.* pH-Responsive Pharmacological Chaperones for Rescuing Mutant Glycosidases. *Angew. Chemie - Int. Ed.* **54,** 11696–11700 (2015).

CHAPTER 2

Bicyclic Isoureas Derived from 1-Deoxynojirimycin are Potent Inhibitors of β-Glucocerebrosidase

Parts of this chapter have been published:

Sevšek, A.; Čelan, M.; Erjavec, B.; Quarles van Ufford, L.; Sastre Toraño, J.; Moret, E. E.; Pieters, R. J.; Martin, N. I. *Org. Biomol. Chem.* **2016**, *14*, 8670–8673.

ABSTRACT

A series of bicyclic isourea derivatives were prepared from 1-deoxynojirimycin using a concise synthetic protocol proceeding *via* a guanidino intermediate.Inhibition assays with a panel of glycosidases revealed that these deoxynojirimycin-derived bicyclic isoureas display very potent inhibition against human recombinant β-glucocerebrosidase with IC_{50} values in the low nanomolar range.

2.1 INTRODUCTION

Glycosidases are an important class of enzymes capable of cleaving glycosidic bonds.[1] As such, they have a strong effect on the glycan decoration of biomolecules and the numerous biological effects that this controls.[2] Iminosugars are a naturally occurring group of carbohydrate analogues and serve as a major source of inspiration for glycosidase inhibitor development.[3] To date, a number of iminosugars have been identified as highly potent and selective inhibitors of glycosidases.[4,5] The effectiveness of iminosugars as glycosidase inhibitors depends largely on their ability to mimic the relevant transition state in the hydrolysis process.[6,7] In the case of iminosugar-based inhibitors, the geometry and hybridization state of the "pseudoanomeric" carbon and/or the endocyclic nitrogen atom are important points of consideration. Glycosidases can bind with very high affinities to compounds that mimic the relevant transition state such as the naturally occurring 1-deoxynojirimycin (DNJ, **1**) and its derivatives (**2** and **3**), as well as castanospermine (**4**, **Figure 1A**).[8] However, these simple iminosugars generally lack selectivity towards specific glycosidases, which can lead to off-target binding and side effects.

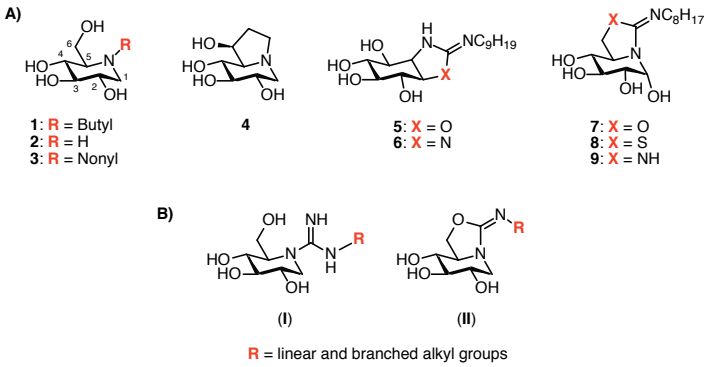

Figure 1. A) Chemical structures of selected iminosugar-based glycosidase inhibitors. **B)** General structures of guanidine (**I**) and bicyclic isourea (**II**) DNJ derivatives prepared in this work.

Synthetic modification of iminosugars holds much promise for the tuning and optimization of their properties. For example, fused guanidine or isourea systems such as compounds **5**-**9** were found to be good inhibitors of various glycosidases.[9–13] Given these findings, we recently described the application of a method developed in our group for the convenient conversion of amines into substituted guanidines.[14] Specifically, we prepared novel DNJ derivatives in which the endocyclic amine was converted into a substituted guanidine group (compounds **I**, **Figure 1B**).[15] Introduction of an exocyclic guanidine group was envisioned as a means of probing both the effects of altered iminosugar ring conformation and charge delocalization in relation to glycosidase inhibition. These compounds showed a distinct inhibition pattern relative to that of the DNJ parent compound, with respect to both potency and selectivity (compounds **II**, **Figure 1B**).

In this chapter, we describe the continuation of previous investigations with a broader panel of DNJ-derived compounds and their evaluation as glycosidase inhibitors. While such guanidinylated DNJ analogues could be prepared and screened as glycosidase inhibitors (compounds **13a-e**, **Scheme 1**), we found that they were prone to spontaneous cyclization to generate the corresponding bicyclic isoureas (compounds **14a-e**). Gratifyingly, these isoureas were found to be very stable and exhibited potent β-specific glycosidase inhibition with a strong preference for the human lysosomal β-glycosidase; β-glucocerebrosidase (GBA, EC 3.2.1.45).

2.2 RESULTS AND DISCUSSION

2.2.1 *Synthesis of guanidine-DNJ compounds*

In the initial synthetic plans we designed a series of guanidine-modified DNJ analogues incorporating different N^G-substituents comprised of simple alkyl chains ranging from eight to fourteen carbon atoms in length as well as a bis-lipidated species (compounds **13a-e**). The synthetic approach used in preparing the initially pursued guanidine analogues of DNJ is outlined in **Scheme 1**. The benzyl protected DNJ species **10** was synthesized on a multi-gram scale as previously described[16] and served as a common starting material in the preparation of the protected N^G-substituted guanidine analogues (**12a-e**). For this conversion, a series of Cbz-protected thioureas (**11a-e**) were also needed and generated as previously described by treatment of the corresponding amine with CbzNCS.[17,18] Activation of the thioureas with EDCI followed by addition of benzyl protected DNJ species **10** led to clean formation of protected guanidines **12a-e**. Removal of benzyl and Cbz groups was achieved *via* hydrogenation to yield the guanidine products **13a-e**.

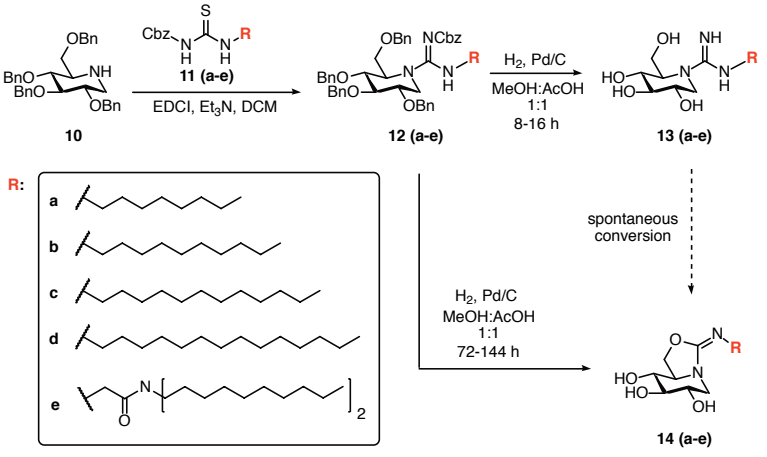

Scheme 1. Synthetic route employed in preparing deoxynojirimycin analogues with N^G-substituted guanidine and bicyclic isoureas analogues.

2.2.2 *Spontaneous conversion of DNJ-guanidines into bicyclic isoureas*

Somewhat surprisingly, it was found that upon deprotection, the guanidines were prone to spontaneous cyclization, rearranging to form the bicyclic isourea species **14a-e**. Isolation of guanidines **13a-e** was possible by limiting the time of the final deprotection step followed by immediate HPLC purification and lyophilization. However, over the time course of the subsequent enzyme inhibition assays we found that partial cyclization of the guanidines to the corresponding isoureas was unavoidable.

The cyclization can follow two possible pathways, with one involving elimination of ammonia and the other the alkylated amine (**Scheme 2** and **Figure 2**). While these pathways compete, formation of the lipidated isoureas **14a-e** was found to be generally favored.

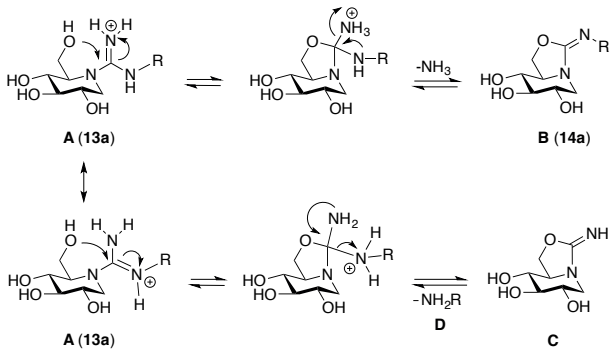

Scheme 2. Spontaneous conversion of guanidine-modified iminosugar **A** (**13a**) to bicyclic isourea products **B** (**14a**) and **C**.

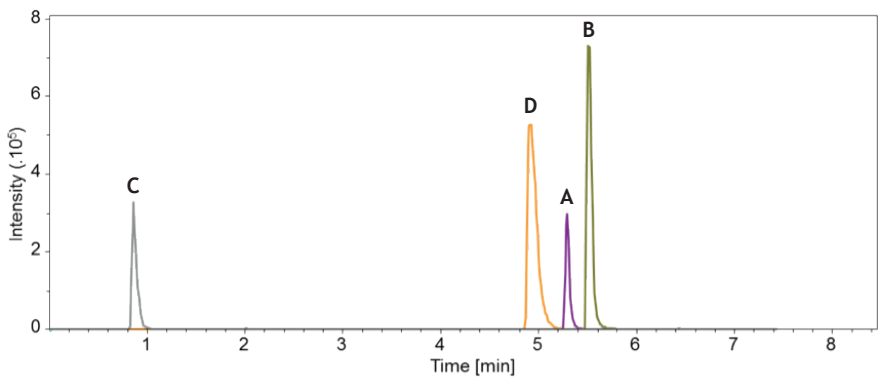

Figure 2. Extracted ion chromatogram for compound **A** (**13a**) obtained with the optimized UHPLC-MS method of a 1mM solution (pH 7.0), degraded at 21 °C for 2 days. The following compounds were identified by their *m/z* value: **A)** *m/z* 318 for compound **13a**; **B)** *m/z* 301 for compound **14a**; **C)** *m/z* 189 for isourea free amine after alkylamine elimination; **D)** *m/z* 130 for alkylamine.

2.2.3 *Kinetic characterization of the bicyclic isourea formation*

The kinetic characterization of cyclization to form isoureas **14a-e** in aqueous solutions was studied by ultra-high performance liquid chromatography – mass spectrometry (UHPLC-MS). A stability indicating method was developed and used to test the chemical stability of the compounds at pH 5.2 and pH 7.0 during a maximum period of time of 24 days.

The isourea compounds **14a-e** were identified by their *m/z* value as the main degradation products. The sum of peak areas in the chromatograms of the guanidine and the isourea compounds remained constant in time of the samples analyzed at different time points which indicates that their detector responses are similar. This allows for the application of relative responses for quantitative analysis of these compounds to determine the degradation process as described in **Figure 3**. **Figure 3** shows the first-order degradation data of **13a** and the formation of **14a** at pH 7.0, both expressed as % area. The half-life time, where the concentration of **13a** and **14a** were equal, was > 20h. By using the logarithm (to base-e) of the concentration, a linear graph was obtained (**Figure 4**), confirming that the degradation of **13a** was a first-order reaction with equation:

$$[\mathbf{13a}(t)] = [\mathbf{13a}]_0 \times e^{-k.t}$$

The slopes of the ln-linearized curves of all guanidine compounds **13a-e** were used to calculate the degradation rate constants (k) and the half-times ($t_{0.5}$=(ln2/k)) for each compound.

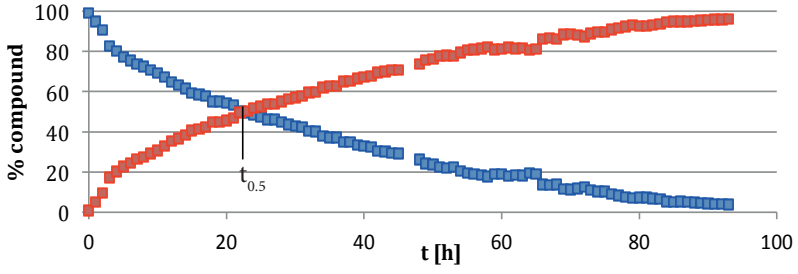

Figure 3. First-order degradation of **13a** and formation of **14a** in pH 7.0 buffer solution at 21 °C.

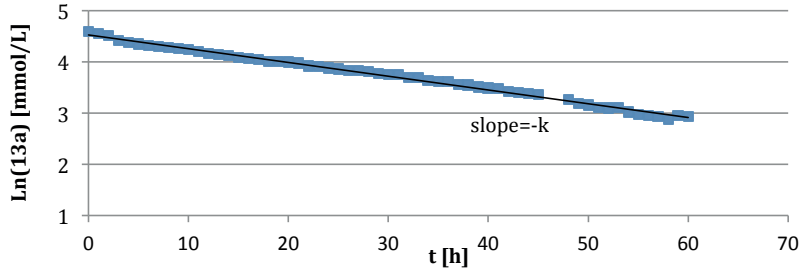

Figure 4. Ln-linearization of the first-order degradation data of **13a** in pH 7.0 buffer solution at 21 °C.

Degradation was much slower at pH 5.2, compared to pH 7.0 and compounds with shorter lipophilic tails appeared to be more stable than compounds with extended alkyl chains.

Compounds **14a-e** showed no degradation at both pHs even after 14 days. **Table 1** shows the $t_{0.5}$ values for compounds **13a-e** for the degradation at pH 5.2 and pH 7.0.

Compound	$t_{0.5}$ in buffer pH 7.0 [h]	$t_{0.5}$ in buffer pH 5.2 [h]
13a	21.4	519.4
13b	17.4	465.5
13c	14.1	226.8
13d	2.9	37.2
13e	1.0	9.7

Table 1. $t_{0.5}$ values for guanidine compounds **13a-e** at pH 7.0 and 5.2.

2.2.4 Enzyme inhibition studies

With compounds **14a-e** in hand, inhibition studies were performed against a panel of readily available glycosidase enzymes as well as human recombinant GBA and β-galactocerebrosidase (GALC) as represented in **Table 2**. Notably, in the case of the plant enzymes, relatively strong inhibition was seen for the β-glycosidases. No inhibition was observed for the α-specific enzymes. Strikingly, the strongest inhibition was observed for the human lysosomal β-glycosidase GBA with low nanomolar inhibition (IC_{50} 1.5-20 nM). Interestingly, these IC_{50} values are significantly lower than those observed for the *N*-alkylated reference compound NN-DNJ (**3**), which was found to have an IC_{50} for GBA of over 500 nM in our assay. Furthermore, despite the observed β-selectivity, our isoureas did not inhibit the lysosomal β-galactosidase GALC, indicating a high degree of selectivity among the human lysosomal enzymes. Also of note is the pH dependence observed for GBA inhibition by compounds **14a-e**; in general, the IC_{50} values measured at pH 7.0 were an order of magnitude lower than those measured at pH 5.2.

Enzyme	14a	14b	14c	14d	14e	NNDNJ
α-glu[b]	> 100000	> 100000	> 100000	> 100000	> 100000	> 100000
α-gal[c]	> 100000	> 100000	> 100000	> 100000	> 100000	> 100000
β-glu[d]	5650±387	2080±95	1650±70	661±30	> 100000	> 100000
β-gal[e]	420±9	136±4	88±10	138±34	938±91	128±6
Nar[f]	128±6	117±6	141±7	195±1	518±7	116±5
GBA[g] (pH 7.0)	**20.8±1.3**	**2.6±0.9**	**1.8±0.1**	**1.5±0.2**	**1.7±0.1**	**562.5±56.6**
GBA[g] (pH 5.2)	**135.5±3.9**	**16.7±0.5**	**12.8±1.2**	**15.4±1.7**	**14.0±1.2**	**1293.0±55.3**
GALC[g]	> 10000	> 10000	> 10000	> 10000	> 10000	> 10000

Table 2. Glycosidase inhibition values obtained for guanidines **14a-e**.[a]
[a]IC_{50} values are reported in nM and are averages obtained from triple independent duplicate analysis of each compound. For ease of comparison, the IC_{50} values obtained for all compounds shown in Table 2 are compared to a reference compound NNDNJ. [b]α-glucosidase (from baker's yeast, Sigma G5003): 0.05 U/mL, the activity was determined with p-nitrophenyl-α-D-glucopyranoside (0.7 mM final conc. in well) in sodium phosphate buffer (100 mM, pH 7.2). [c]α-galactosidase (from green coffee beans, Sigma G8507): 0.05 U/mL; α-galactosidase activity was determined with p-nitrophenyl-α-D-galactopyranoside (0.7 mM final conc. in well) in sodium phosphate buffer (100 mM, pH 6.8). [d]β-glucosidase (from almond, Sigma G4511): 0.05 U/mL; the activity was determined with p-nitrophenyl-β-D-glucopyranoside (0.7 mM final conc. in well) in sodium acetate buffer (100 mM, pH 5.0). [e]β-galactosidase (from bovine liver, Sigma G1875): 0.05 U/mL; activity was determined with p-nitrophenyl-β-D-galactopyranoside (0.7 mM final conc. in well) in sodium phosphate buffer (100 mM, pH 7.2). [f]Naringinase (from penicillium decumbens, Sigma N1385): 0.06 U/mL. the activity was determined with p-nitrophenyl-β-D-glucopyranoside (0.7 mM final conc. in well) in sodium acetate buffer (100 mM, pH 5.0). [g]β-glucocerebrosidase (GBA) and [g]β-galactocerebrosidase (GALC) activities were determined using 4-methylumbelliferyl-β-D-glucopyranoside and 4-methylumbelliferyl-β-D-galactopyranoside using assay conditions based on those previously reported, respectively.[27]

2.2.5 Fibroblast experiments

It is known that mutations in GBA can lead to serious lysosomal storage disorders such as Gaucher's disease (GD).[19] Interestingly, in some cases GBA inhibitors can serve to counteract the loss of GBA activity by functioning as pharmacological chaperones.[20] Among the more than 200 mutations identified in the GBA1 gene, the most prevalent is the N370S missense mutation, which results in Type 1 Gaucher disease. This mutation accounts for more than 90% of all cases of the disease and leads to an approximate 70% loss of GBA activity in affected cells. The less prevalent but equally devastating Type 2 and Type 3 forms of Gaucher disease affect the central nervous system. Among the mutations in GBA that lead to central nervous system involvement, L444P is the most common and leads to a loss of up to 90% of GBA activity in neural cells. Both the N370S and L444P mutations result in structural changes to GBA that increase the potential for ER-associated degradation.[21] The pharmacological chaperone potential of isoureas **14a-e** was therefore evaluated in human fibroblasts derived from Gaucher patients homozygous for N370S and L444P mutations according to previously established procedures.[22]

To investigate whether the inhibitory effect would translate into cellular pharmacological chaperone behavior, we examined the impact of compounds **14a-e** on GBA activity in both normal and GD derived fibroblasts.

2.2.5.1 Cytotoxicity assay in wild-type GD derived fibroblasts

We began by first establishing that compounds **14a-e** were not toxic to wild-type human fibroblasts in the concentrations range to be used. Cells were seeded at a density of 10000 cells per well in 96-well plates. Media were renewed after 24h and compounds were added to give final concentrations of **14a** and NNDNJ in 10-1-0.1-0.01 μM and **14b-e** tested from 1 μM – 0.1 μM. No toxicity was found for compounds **14a-e** at 1 μM or lower.

2.2.5.2 Inhibition of human recombinant GBA in wild-type human fibroblasts

Next, the GBA inhibitory effect of compounds **14a-e** in wild-type human fibroblasts was assessed. The fibroblasts were incubated for a 24-hour period with isoureas **14a-e** and NN-DNJ (**3**) over a range of concentrations between 0.1-100 nM, well bellow the toxic concentration determined. **Figure 5** illustrates the GBA inhibition measured for compounds **14a-e** in wild-type human fibroblasts. The results of these cell-based assays generally correlated well with the enzyme inhibition assays using purified recombinant GBA (**Table 2**). As seen in **Figure 5**, NN-DNJ (**3**) and the *N*-octyl isourea derivative **14a** elicited 10-20% inhibition of basal GBA activity over the range of concentrations evaluated. Conversely, the other isoureas **14b-e** displayed much more potent inhibition of cellular GBA activity with 60-90% inhibition at the highest concentration tested (100 nM).

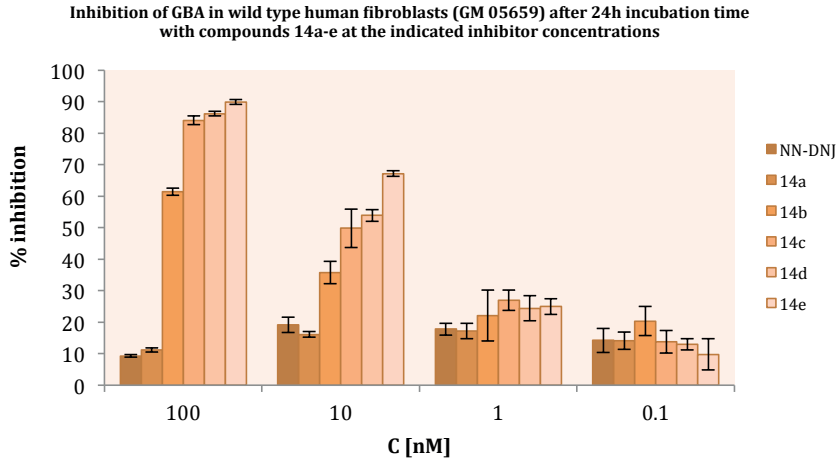

Figure 5. Inhibition of GBA in Wild Type Human Fibroblasts (GM 05659) after 24h incubation time at the indicated inhibitor concentrations. Patient derived cells were incubated with compounds **14a-e** and evaluated against GBA. Averages are obtained from triple independent duplicate analysis of each compound and presented as %-inhibition. For ease of comparison, values obtained for compounds **14a-e** are compared to a reference compound NN-DNJ (**3**).

2.2.5.3 Enzyme enhancement activity in human N370S fibroblasts

Patient derived cells were incubated with compounds **14a-e** or NN-DNJ (**3**) for 4 days followed by measurement of GBA activity. The most prominent enzyme enhancement effects were seen with the N370S cell line. **Figure 6** summarizes the increase in GBA activity measured at various concentrations of compounds **14a-e** as well as NN-DNJ (**3**), included as a reference pharmacological chaperone. Treatment of the N370S cell line with 100 nM of the *N*-octyl substituted compound **14a** resulted in a 1.2-fold increase of the GBA activity. This 20% enhancement was found to be greater than the approximate 10% increase in GBA activity measured for NN-DNJ (**3**) administered at the same 100 nM concentration. It should be noted that a much higher pharmacological chaperone effect, a near two-fold enhancement in GBA activity, was previously reported when administering NN-DNJ (at a concentration of 10 μM) to cell lines bearing the same N370S mutation.[38] The reproducibly higher pharmacological chaperone effect observed in our assays for compound **14a** relative to NN-DNJ therefore prompted us to investigate higher concentrations of both compounds (up to 1 μM). Interestingly, in our fibroblast assays no significant increase in GBA enhancement was seen for either NN-DNJ or compound **14a** relative to that measured at a concentration of 100 nM. The other bicyclic isoureas **14b-e** bearing longer lipids were found to be generally inhibitory of GBA activity at concentrations higher than 10 nM. These observations are also in line with the more potent inhibition observed for these compounds with the purified enzyme. At significantly lower concentrations however, GBA enhancement effects were observed for compounds **14b-e** with a maximum 7% enhancement measured for the N-decyl substituted analogue **14b** when administered at 100 pM.

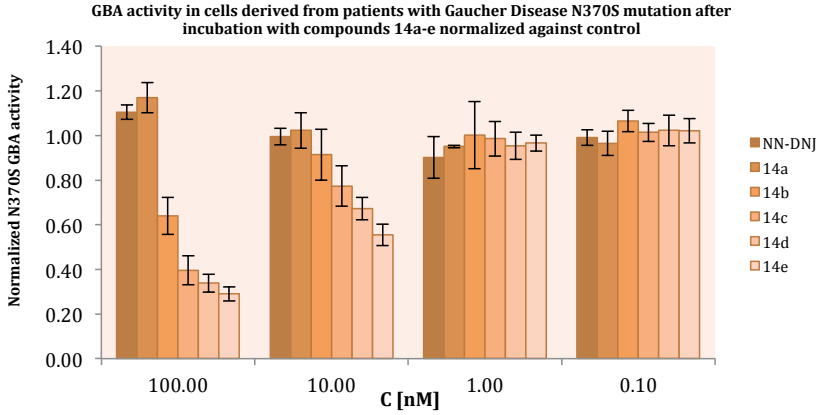

Figure 6. The effect of compounds **14a-e** on GBA activity in N370S fibroblasts (GM00372) from Gaucher patients. Cells were cultured for 4 days in the absence or presence of increasing concentrations (nM) of the compounds before GBA activity was measured. Experiments were performed in triplicate, and each bar represents the mean ± SD. Enzyme activity is normalized to untreated cells, assigned a relative activity of 1.

2.2.5.4 Enzyme enhancement activity in human L444P fibroblasts

The effect of NN-DNJ (**3**) and compounds **14a-e** on the activity of the L444P GBA mutant was also measured using Gaucher disease Type 2 patient-derived fibroblast cell line. After a 4-day incubation, however, little-to-no enhancement in GBA activity was observed at all compound concentrations measured (**Figure 7**). The data do suggest a slight chaperone effect for compound **14a** relative to NN-DNJ (**3**), however the low basal GBA activity of the L444P cell line led to large fluctuations in the measured activity making it difficult to draw firm conclusions.

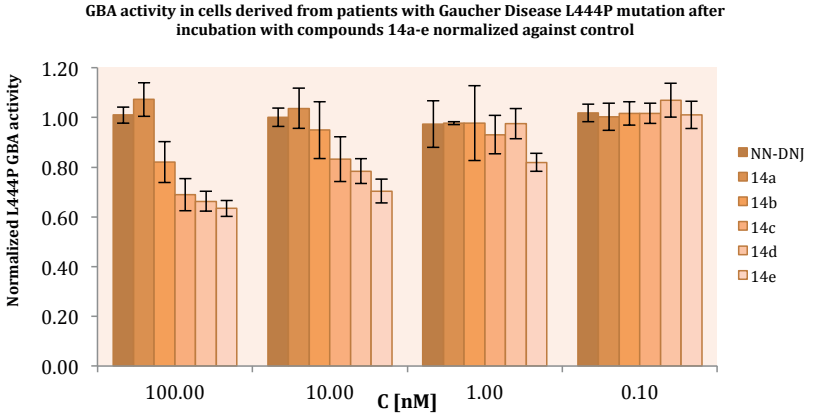

Figure 7. The effect of compounds **14a-e** on GBA activity in L444P fibroblasts (GM00877) from Gaucher patients. Cells were cultured for 4 days in the absence or presence of increasing concentrations (nM) of the compounds before GBA activity was measured. Experiments were performed in triplicate, and each bar represents the mean ± SD. Enzyme activity is normalized to untreated cells, assigned to a relative activity of 1.

2.2.6 Computational docking experiments

To gain insight into the possible binding mode(s) of isoureas **14a-e** within the GBA active site, modeling was performed. **Figure 8A** depicts the docking of compound **14a** and NNDNJ in the GBA active site while **Figure 8B** depicts the docking of compound **14a** in the GBA active site highlighting the predicted interactions with active site residues. This analysis reveals an ionic bond to Glu_{235} and a cation-π interaction with Tyr_{313}. Notably, these interactions are not seen in the X-ray structure of GBA when co-crystalized with NN-DNJ[24] and may indicate a higher binding affinity of **14a** relative to NN-DNJ (as reflected in our inhibition data). These additional interactions require that the isourea moiety be protonated in the bound state. In this regard, we also measured the pKa of **14a** to be 9.30, indicating that this is indeed likely to be the case.

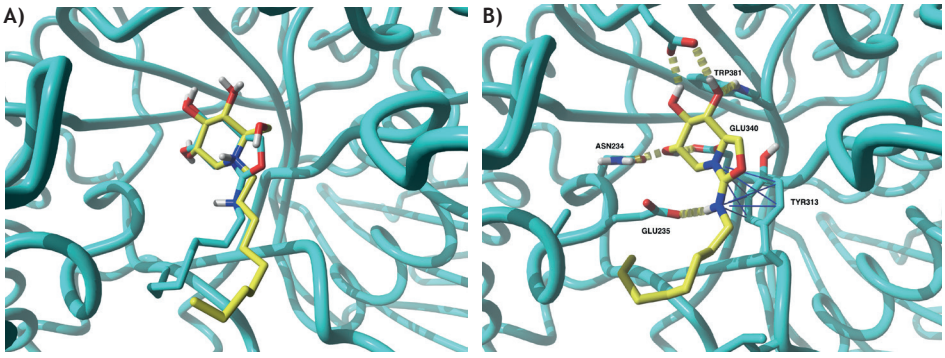

Figure 8. A) GBA (PDB-ID 2V3E) with the X-ray pose of NN-DNJ (yellow carbon atoms) with the docked pose of **14a** superimposed (cyan carbon atoms). **B)** GBA (PDB-ID 2V3E with the docked pose of **14a** (yellow carbon atoms), showing a hydrogen bond and cation-π interactions.

2.3 CONCLUSIONS & OUTLOOK

The DNJ-derived bicyclic isourea analogues described in this study are a novel class of glycosidase inhibitors. While we initially set out to explore exocyclic guanidine analogues of DNJ it was found that such compounds are prone to intramolecular cyclization yielding instead the corresponding bicyclic isoureas. Our data indicate that compounds **14a-e** are among the most potent GBA inhibitors reported to date. Of note is a closely related nojirimycin analogue **7** that was also previously reported as a GBA inhibitor.[11] While compound **7** was prepared in 8 steps in ca. 20% overall yield, the corresponding DNJ analogue **14a** can be prepared in 6 steps with a near 50% overall yield. Also of note is the striking difference observed for these compounds in their capacity to inhibit GBA. Using similar assay conditions, we measured a near 200-fold lower IC_{50} value for compound **14a** (20.8 nM) relative to that reported for **7** (3.8 μM).[11] Also of note are the similar IC_{50} values measured for NN-DNJ (**3**) which was used as a reference inhibitor in both studies suggesting the values here measured for compound **14a** can legitimately be compared to that reported for **7**. The difference in GBA inhibition between **14a** and **7** is likely attributable to the pseudoanomeric hydroxyl group present in **7**.

A derivative of nojirimycin, compound **7** retains the aminal functionality of the parent compound. This structural feature may lead to less stable compounds as derivatives of **7** were also reported to rearrange at lower pH[25] and to anomerize upon binding to GBA.[26] An additional factor that might contribute to the difference in GBA inhibition by compounds **7** and **14a** are their different pKa values (7.0 reported for **7**,[25] *vs* 9.3 determined for **14a**). The enhanced basicity of **14a** may facilitate the formation of the ionic interactions as identified by the modeling.

These investigations revealed compounds **14a-e** to be among the most potent known inhibitors of GBA, a human lysosomal *β*-glycosidase. Our findings suggest that further investigations into the potential for DNJ-derived bicyclic isoureas like compounds **14a-e** may be warranted. Preliminary data from experiments in our group using Gaucher patient derived fibroblasts bearing the N370S GBA mutation indicate that **14a** possesses a chaperone activity on par with that of the known chaperone NN-DNJ (**3**). Additionally, the apparent pH dependence of the GBA inhibition measured for isoureas **14a-e** suggested that these compounds might have a higher binding affinity for GBA in the ER (neutral pH) than in the lysosome (pH 5.2). More comprehensive studies into the full potential of compounds **14a-e** to serve as pharmacological chaperones will be reported in due course.

2.4 EXPERIMENTAL SECTION

2.4.1 General methods and materials

Reagents, Solvents and Solutions. Unless stated otherwise, chemicals were obtained from commercial sources and used without further purification. All solvents were purchased from Biosolve (Valkenswaard, The Netherlands) and were stored on molecular sieves (4 Å). 2,3,4,6-Tetra-O-benzyl-D-glucopyranose was obtained from Carbosynth Limited (MT06691). 2,3,4,6- Tetra-O-benzyl-1-deoxynojirimycin[16] (**10**), Cbz-NCS[14] and compounds **11a**[15], **12a**[15], **13a**[15] were prepared as previously described. The preparation of compounds **11e**, **12e**, **13e** and **14e** required access to non-commercial amine building block **16** that was prepared according to established literature procedures.

Purification Techniques. All reactions and fractions from column chromatography were monitored by thin layer chromatography (TLC) using plates with a UV fluorescent indicator (normal SiO_2, Merck 60 F254). One or more of the following methods were used for visualization: 10% H_2SO_4 in MeOH, molybdenum blue, $KMnO_4$ or ninhydrine followed by warming until spots could be visible detected under UV light. Flash chromatography was performed using Merck type 60, 230–400 mesh silica gel. Removal of solvent was performed under reduced pressure using a rotary evaporator.

Instrumentation for Compound Characterization. For LC–MS analysis, an HPLC system (detection simultaneously at 214, 254 nm and evaporative light detection) equipped with an analytical C_{18} column (100 Å pore size, 4.6 mm (⌀) x 250 mm (l), 10 µm particle size) or C_8 column (100 Å pore size, 4.6 mm (⌀) x 250 mm (l), 10 µm particle size) in combination with buffers A: H_2O, B: MeCN, A and B with 0.1% aqueous trifluoroacetic acid (TFA), in some cases - coupled with an electrospray interface (ESI) was used. For RP-HPLC purifications (detection simultaneously at 213, 254 nm), an automated HPLC system equipped with a preparative C_{18} column (20 mm (⌀) x 250 mm (l), 5 µm particle size) or C_8 column (20 mm (⌀) x 250 mm (l), 5 µm particle size) in combination with buffers A: H_2O, B: MeCN, A and B with 0.1% aqueous trifluoroacetic acid (TFA). High-resolution mass spectra were recorded by direct injection (2 µL of a 2 µM solution in H_2O/MeCN 50:50 *v/v* and 0.1% formic acid) on a mass spectrometer. ^1H and ^{13}C NMR spectra were recorded on 500–125 MHz or 400–100 MHz spectrometers. Chemical shifts (δ) are given in ppm relative to tetramethylsilane (TMS) as internal standard. All ^{13}C NMR spectra are proton decoupled. ^1H NMR data are reported in the following order: number of protons, multiplicity (*s*, singlet; *d*, doublet; *t*, triplet; *q*, quartet and *m*, multiplet) and coupling constant (*J*) in Hertz (*Hz*). When appropriate, the multiplicity is preceded by *br*, indicating that the signal was broad. ^{13}C NMR spectra were recorded at 101 or 126 MHz with chemical shifts reported relative to $CDCl_3$ δ 77.0. ^{13}C NMR spectra were recorded using the attached proton test (APT) sequence. All literature compounds had ^1H NMR and mass spectra consistent with the assigned structures.

2.4.2 Preparative details and analytical data for synthesized compounds

2.4.2.1 General procedure for the synthesis of thiourea intermediates *11a-e*

The amine of choice (1.2 eq) was dissolved in CH_2Cl_2 (100 mL) and treated with a 0.5 M solution of CbzNCS in CH_2Cl_2 (1 eq) and NEt_3 (10 eq). After stirring for 12 h at room temperature, TLC analysis indicated complete conversion to thiourea species. The CH_2Cl_2 was then removed under reduced pressure, and the residue dissolved in chloroform, and applied directly to a silica column, eluting with EtOAc/hexanes. Analytical data and characterization data for compounds **11a-e** are given below.

N-(Benzyloxycarbonyl)-N'-(octyl) thiourea (11a).

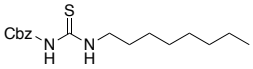

According to the literature procedure.[15] Yield: 1.6 g, 42%. R_f (EtOAc/hexanes = 1:8) = 0.28. ^{1}H NMR (400 MHz, $CDCl_3$) δ 0.70 - 0.98 (m, 3H), 1.12 - 1.47 (m, 10H), 1.60 - 1.71 (m, 2H), 3.63 (td, *J* = 5.4, 7.2 Hz, 2H), 5.18 (s, 2H), 7.27 - 7.47 (m, 5H), 8.05 (br s, 1H), 9.61 (br s, 1H). ^{13}C NMR (101 MHz, $CDCl_3$) δ 178.7, 152.5, 134.5, 129.1, 128.9, 128.8, 128.7, 128.6, 128.51, 128.46, 128.3, 77.3, 68.1, 45.8, 31.7, 29.1, 28.2, 26.9, 22.6, 14.1. HRMS (ESI, $[M+Na]^+$), calculated for $C_{17}H_{26}N_2O_2S$, 345.1613; found, 345.1580.

N-(Benzyloxycarbonyl)-N'-(decyl) thiourea (11b).

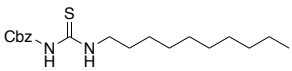

Yield: 2.7 g, 65%. R_f (EtOAc/hexanes = 1:8) = 0.33. ^{1}H NMR (400 MHz, $CDCl_3$) δ 0.88 (t, *J* = 6.7 Hz, 3H), 1.20 - 1.44 (m, 14H), 1.57 - 1.71 (m, 2H), 3.63 (td, *J* = 5.4, 7.2 Hz, 2H), 5.17 (s, 2H), 7.31 - 7.47 (m, 5H), 8.07 (br s, 1H), 9.62 (br s, 1H). ^{13}C NMR (101 MHz, $CDCl_3$) δ 178.7, 152.5, 134.5, 129.1, 129.0, 128.9, 128.8, 128.7, 128.3, 68.1, 45.8, 38.4, 31.9, 29.5, 29.2, 28.2, 26.9, 22.7, 14.1. HRMS (ESI, $[M+Na]^+$), calculated for $C_{19}H_{30}N_2O_2S$, 373.1926; found, 373.1890.

N-(Benzyloxycarbonyl)-N'-(dodecyl) thiourea (11c).

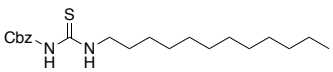

Yield: 3.4 g, 75%. R_f (EtOAc/hexanes = 1:8) = 0.56. ^{1}H NMR (400 MHz, $CDCl_3$) δ 0.88 (t, *J* = 6.4 Hz, 3H), 1.16 - 1.47 (m, 18H), 1.56 - 1.77 (m, 2H), 3.56 - 3.72 (m, 2H), 5.17 (s, 2H), 7.20 - 7.50 (m, 5H), 8.12 (s, 1H), 9.62 (br s, 1H). ^{13}C NMR (101 MHz, $CDCl_3$) δ 178.7, 152.5, 134.5, 134.3, 129.1, 129.0, 128.9, 128.8, 128.7, 128.3, 111.9, 77.4, 77.0, 76.7, 68.1, 45.8, 38.4, 31.9, 29.61, 29.60, 29.53, 29.45, 29.3, 29.2, 28.2, 26.9, 22.7, 14.1. HRMS (ESI, $[M+Na]^+$), calculated for $C_{21}H_{34}N_2O_2S$, 401.2239; found, 401.2209.

N-(Benzyloxycarbonyl)-N'-(tetradecyl) thiourea (11d).

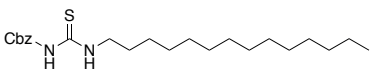

Yield: 3.9 g, 80%. R_f (EtOAc/hexanes = 1:8) = 0.6. ^{1}H NMR (400 MHz, $CDCl_3$) δ 0.88 (t, *J* = 6.8 Hz, 3H), 1.20 - 1.41 (m, 22H), 1.55 - 1.75 (m, 2H), 3.63 (td, *J* = 5.4, 7.2 Hz, 2H), 5.17 (s, 2H), 7.17 - 7.49 (m, 5H), 8.05 (s, 1H), 9.61 (s, 1H). ^{13}C NMR (101 MHz, $CDCl_3$) δ 178.7, 152.4, 134.5, 134.3, 129.1, 128.94, 128.89, 128.8, 128.7, 128.3, 68.1, 45.8, 41.2, 38.4, 31.9, 29.7, 29.64, 29.63, 29.61, 29.5, 29.4, 29.3, 29.2, 28.2, 26.9, 22.7, 14.1. HRMS (ESI, $[M+Na]^+$), calculated for $C_{23}H_{38}N_2O_2S$, 429.2552; found, 429.2502.

Benzyl 2-(didecylamino)-(2-oxoethyl)aminothionylcarbamate (11e).

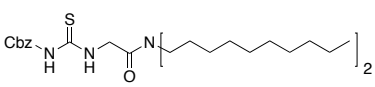

Yield: 0.86 g, 86%. R_f (EtOAc/hexanes = 1:8) = 0.16. ^{1}H NMR (400 MHz, $CDCl_3$) δ 0.88 (t, *J* = 6.7 Hz, 6H), 1.20 - 1.41 (m, 28H), 1.49 - 1.64 (m, 4H), 3.19 (t, *J* = 7.6 Hz, 2H), 3.35 (t, *J* = 7.8 Hz, 2H), 4.33 - 4.42 (m, 2H), 5.20 (s, 2H), 7.31 - 7.43 (m, 5H), 8.07 (s, 1H), 10.60 (s, 1H). ^{13}C NMR (101 MHz, $CDCl_3$) δ 177.8, 165.9, 152.0, 134.6, 129.0, 129.0, 128.8, 128.64, 128.62, 128.57, 128.5, 128.4, 128.2, 127.4, 77.3, 77.0, 76.7, 68.2, 67.9, 47.7, 46.9, 46.2, 34.6, 31.9, 31.8, 29.53, 29.51, 29.47, 29.4, 29.28, 29.26, 29.2, 28.6, 27.5, 27.0, 26.8, 22.7, 22.6, 14.1. HRMS (ESI, $[M+Na]^+$), calculated for $C_{31}H_{53}N_3O_3S$, 548.3886; found, 548.3897.

2.4.2.2 *General procedure for synthesis of benzyl protected N-guanidine-DNJ compounds* ***12a-e***

Corresponding thioureas **11a-e** (1.1 eq), OBn-DNJ (**10**, 1 eq) and EDCI (1.5 eq) were dissolved in CH_2Cl_2 (20 mL), followed by addition of NEt_3 (3 eq). Reaction mixture was stirred for 18h at room temperature, after which TLC analysis confirmed total consumption of starting material. Crude product, dissolved in $CHCl_3$ was purified by silica gel column chromatography, eluting with hexanes chaser and subsequently with EtOAc/hexanes. The solvent was then removed under reduced pressure, and the residue, dissolved in $CHCl_3$, was applied directly to a silica column, eluting with hexanes chaser and subsequently with EtOAc/hexanes. Analytical data and characterization data for compounds **12a-e** are given below.

Benzyl ((Z)-(octylamino)((2S, 3S, 4R)-3,4,5-tris(benyloxy)-2-((benzyloxy)methyl)piperidin-1-yl) methylene)carbamate (12a).

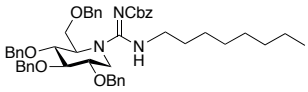

According to the literature procedure.[15] Yield: 340 mg, 75%. R_f (EtOAc/hexanes = 2:3) = 0.30. ^{1}H NMR (400 MHz, $CDCl_3$) δ 0.87 (t, *J* = 7.0 Hz, 3H), 1.07 - 1.48 (m, 12H), 2.92 - 3.14 (m, 2H), 3.43 (dd, *J* = 3.5, 13.8 Hz, 1H), 3.53 - 3.86 (m, 6H), 4.01 (dd, *J* = 5.2 Hz, 1H), 4.30 - 4.80 (m, 8H), 5.09 (d, *J* = 12.6 Hz, 1H), 5.16 (d, *J* = 12.6 Hz, 1H), 6.90 - 7.70 (m, 25H). ^{13}C NMR (101 MHz, $CDCl_3$) δ 163.0, 160.9, 138.0, 137.88, 137.86, 137.6, 128.40, 128.35, 128.2, 127.93, 127.90, 127.86, 127.82, 127.80, 127.74, 127.72, 127.70, 127.68, 127.4, 80.7, 77.8, 77.4, 77.0, 76.7, 75.4, 73.4, 73.1, 72.7, 71.3, 69.8, 66.6, 58.7, 44.5, 44.0, 31.8, 29.6, 29.2, 29.1, 26.8, 22.6, 14.1. HRMS (ESI, $[M+H]^+$), calculated for $C_{51}H_{61}N_3O_6$, 812.4639; found, 812.4623.

Benzyl ((Z)-(decylamino)((2S, 3S, 4R)-3,4,5-tris(benyloxy)-2-((benzyloxy)methyl)piperidin-1-yl) methylene)carbamate (12b).

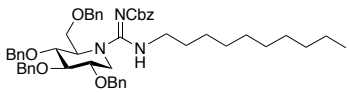

Yield: 790 mg, 85%. R_f (EtOAc/hexanes = 2:3) = 0.32. ^{1}H NMR (400 MHz, $CDCl_3$) δ 0.88 (t, *J* = 6.9 Hz, 3H), 1.05 - 1.39 (m, 16H), 2.89 - 3.19 (m, 2H), 3.43 (dd, *J* = 3.5, 13.7 Hz, 1H), 3.56 - 3.85 (m, 6H), 4.00 (ddd, *J* = 5.2 Hz, 1H), 4.30 - 4.78 (m, 8H), 5.09 (d, *J* = 12.6 Hz, 1H), 5.16 (d, *J* = 12.6 Hz, 1H), 7.13 - 7.51 (m, 25H). ^{13}C NMR (101 MHz, $CDCl_3$) δ 163.0, 160.9, 138.0, 137.9, 137.9, 137.5, 128.4, 128.3, 128.3, 128.1, 127.92, 127.89, 127.84, 127.80, 127.78, 127.72, 127.70, 127.68, 127.66, 127.3, 80.7, 77.8, 77.3, 77.0, 76.7, 75.4, 73.4, 73.1, 72.7, 71.3, 69.8, 66.6, 58.7, 44.5, 44.0, 31.9, 29.7, 29.51, 29.46, 29.3, 29.2, 26.8, 22.7, 14.1. HRMS (ESI, $[M+H]^+$), calculated for $C_{53}H_{65}N_3O_6$, 840.4952; found, 840.4916.

Benzyl ((Z)-(dodecylamino)((2S, 3S, 4R)-3,4,5-tris(benyloxy)-2-((benzyloxy)methyl)piperidin-1-yl) methylene)carbamate (12c).

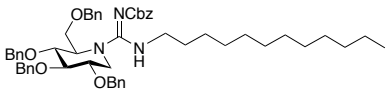

Yield: 420 mg, 86%. R_f (EtOAc/hexanes = 2:3) = 0.33. ^{1}H NMR (400 MHz, $CDCl_3$) δ 0.89 (d, *J* = 7.1 Hz, 3H), 1.02 - 1.54 (m, 20H), 2.89 - 3.20 (m, 2H), 3.43 (dd, *J* = 3.7, 13.1 Hz, 1H), 3.54 - 3.88 (m, 6H), 3.93 - 4.08 (m, 1H), 4.31 - 4.80 (m, 8H), 5.09 (d, *J* = 12.6 Hz, 1H), 5.16 (d, *J* = 12.6 Hz, 1H), 7.08 - 7.71 (m, 25H). ^{13}C NMR (101 MHz, $CDCl_3$) δ 163.0, 160.9, 138.0, 137.9, 137.9, 137.6, 128.39, 128.35, 128.2, 127.93, 127.90, 127.86, 127.8, 127.74, 127.72, 127.69, 127.67, 127.4, 80.7, 77.8, 77.3, 77.0, 76.7, 75.4, 73.4, 73.1, 72.7, 71.3, 69.8, 66.6, 58.7, 44.5, 44.0, 31.9, 29.7, 29.6, 29.5, 29.4, 29.2, 26.8, 22.7, 14.1. HRMS (ESI, $[M+H]^+$), calculated for $C_{55}H_{69}N_3O_6$, 868.5265; found, 868.5234.

Benzyl ((Z)-(tetradecylamino)((2S, 3S, 4R)-3,4,5-tris(benyloxy)-2-((benzyloxy)methyl)piperidin-1-yl) methylene)carbamate (12d).

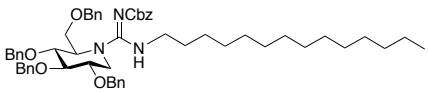

Yield: 392 mg, 79%. R_f (EtOAc/hexanes = 2:3) = 0.35. ^{1}H NMR (400 MHz, $CDCl_3$) δ 0.79 - 0.98 (m, 3H), 1.05 - 1.52 (m, 24H), 2.87 - 3.19 (m, 2H), 3.43 (dd, *J* = 3.5, 13.7 Hz, 1H), 3.56 - 3.85 (m, 6H), 3.94 - 4.09 (m, 1H), 4.35 - 4.74 (m, 8H), 5.09 (d, *J* = 12.6 Hz, 1H), 5.16 (d, *J* = 12.6 Hz, 1H), 7.16 - 7.51 (m, 25H). ^{13}C NMR (101 MHz, $CDCl_3$) δ 163.1, 161.0, 138.1, 138.0, 137.9, 137.9, 137.6, 128.40, 128.36, 128.35, 128.2, 127.94, 127.91, 127.86, 127.82, 127.80, 127.74, 127.72, 127.70, 127.68, 127.4, 80.7, 77.9, 77.4, 77.0, 76.7, 75.4, 73.4, 73.1, 72.8, 71.3, 69.8, 66.6, 58.7, 44.5, 44.0, 31.9, 29.71, 29.69, 29.67, 29.6, 29.5,

29.4, 29.2, 26.8, 22.7, 14.1. HRMS (ESI, $[M+H]^+$), calculated for $C_{57}H_{73}N_3O_6$, 896.5578; found, 896.5557.

Benzyl ((Z)-((2-(didecylamino)-2-oxoethyl)amino)((2S,3S,4R)-3,4,5-tris(benzyloxy)-2-((benzyloxy) methyl)piperidin-1-yl)methylene)carbamate (12e).

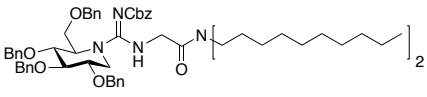

Yield: 622 mg, 54%. R_f (EtOAc/hexanes = 2:3) = 0.52. ^{1}H NMR (400 MHz, $CDCl_3$) δ 0.88 (t, *J* = 7.0 Hz, 6H), 1.06 - 1.36 (m, 28H), 1.42 - 1.54 (m, 4H), 2.91 (t, *J* = 7.6 Hz, 2H), 3.15 - 3.37 (m, 2H), 3.47 (dd, *J* = 3.7, 14.1 Hz, 1H), 3.57 - 4.01 (m, 8H), 4.20 (q, *J* = 5.0 Hz, 1H), 4.33 - 4.78 (m, 8H), 5.11 (d, *J* = 12.6 Hz, 1H), 5.17 (d, *J* = 12.6 Hz, 1H), 7.10 - 7.49 (m, 25H). ^{13}C NMR (101 MHz, $CDCl_3$) δ 167.3, 160.3, 138.5, 138.2, 138.1, 138.0, 128.48, 128.45, 128.4, 128.3, 128.2, 128.13, 128.10, 127.9, 127.84, 127.79, 127.7, 127.5, 81.7, 78.4, 77.5, 77.2, 76.8, 75.1, 73.4, 73.2, 73.0, 71.3, 69.4, 66.7, 58.4, 46.7, 46.1, 44.5, 43.9, 32.02, 32.01, 29.73, 29.70, 29.68, 29.6, 29.5, 29.4, 28.7, 27.7, 27.2, 27.0, 22.8, 14.3. HRMS (ESI, $[M+H]^+$), calculated for $C_{65}H_{88}N_4O_7$, 1037.6731; found, 1037.6685.

*2.4.2.3 General procedure for Pd/C catalyzed hydrogenolysis for the synthesis of N-substituted guanidine compounds **13a-e***

The corresponding perbenzylated iminosugar (**12a-e**) was dissolved in a mixture of glacial AcOH in MeOH (1/1, v/v) and transferred to a Parr high-pressure hydrogenation flask. A catalytic amount of 10% palladium on carbon was added to the flask (ca. 10 mg catalyst/mg of benzylated starting material). The flask was put under reduced pressure and ventilated with hydrogen gas. This procedure was repeated twice after which the pressure was adjusted to 4.5-5.0 bar hydrogen pressure. The reaction was allowed to proceed for 6-12 h while mechanically shaken and the pressure maintained at the value initially set. The mixture was filtered over celite on a glass microfiber filter, followed by rinsing the filter with MeOH. The mixture was concentrated under reduced pressure. The crude products thus obtained were purified using RP-HPLC employing a preparative C8 column and an H_2O/MeCN gradient moving from 5% to 95% MeCN (0.1% TFA) over 60 min (flow rate, 18.0 mL/min). Product **13e** was purified using an H_2O/MeCN gradient moving from 50% to 95% MeCN (0.1% TFA) over 90 min (flow rate, 18.0 mL/min). Fractions containing the desired product were combined and lyophilized to yield the pure compounds as amorphous white powders. Analytical data and in-depth characterization data for compounds **13a-e** are given below.

(2R,3R,4R,5S)-3,4,5-trihydroxy-2-(hydroxymethyl)-N-octylpiperidine-1-carboximidamide (13a).

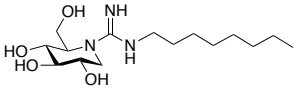

According to previously reported procedure.[15] Yield: 16 mg, 82%. ^{1}H NMR (500 MHz, D_2O) δ 0.74-0.86 (t, 3H), 1.16-1.34 (m, 12H), 1.50-1.62 (m, 2H), 3.17-3.26 (m, 2H), 3.50-3.55 (m, 2H), 3.60 (d, 2H), 3.76- 3.82 (m, 2H), 3.82-3.90 (m, 2H). ^{13}C NMR (126 MHz, D_2O) δ 87.5, 85.0, 82.6, 78.3, 73.8, 59.8, 56.8, 45.6, 42.8, 42.5, 40.3, 36.6, 28.0. HRMS (ESI, $[M+H]^+$), calculated for $C_{15}H_{31}N_3O_4$, 318.2393; found, 318.2414.

(2R,3R,4R,5S)-N-decyl-3,4,5-trihydroxy-2-(hydroxymethyl)piperidine-1-carboximidamide (13b).

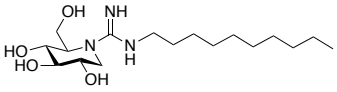

Yield: 8 mg, 75%. ^{1}H NMR (500 MHz, DMSO-d_6) δ 0.86 (t, *J* = 6.8 Hz, 3H), 1.16 - 1.37 (m, 14H), 1.40 - 1.59 (m, 2H), 3.12 - 3.24 (m, 2H), 3.37 - 3.56 (m, 4H), 3.57 - 3.68 (m, 2H), 3.68 - 3.78 (m, 2H), 5.19 - 5.40 (m, 1H), 5.40 - 5.60 (m, 1H), 7.35 - 7.53 (m, 3H), 7.67 (s, 1H). ^{13}C NMR (126 MHz, DMSO-d_6) δ 87.4, 85.1, 83.9, 78.5, 74.6, 74.0, 60.0, 59.4, 57.1, 46.4, 44.0, 43.6, 41.1, 37.3, 29.1. HRMS (ESI, $[M+H]^+$), calculated for $C_{17}H_{35}N_3O_4$, 346.2706; found, 346.2721.

(2R,3R,4R,5S)-N-dodecyl-3,4,5-trihydroxy-2-(hydroxymethyl)piperidine-1-carboximidamide (13c).

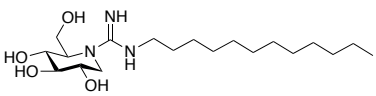

Yield: 12 mg, 82%. ^{1}H NMR (500 MHz, DMSO-d_6) δ 0.86 (t, *J* = 6.8 Hz, 3H), 1.18 - 1.35 (m, 18H), 1.41 - 1.59 (m, 2H), 3.10 - 3.22 (m, 2H), 3.35 - 3.56 (m, 4H), 3.58 - 3.68 (m, 2H), 3.70 - 3.79 (m, 2H), 5.29 (dd, *J* = 4.0, 5.6 Hz, 2H), 5.39 - 5.55 (m, 2H), 7.36 - 7.50 (m, 3H). ^{13}C NMR (126 MHz, DMSO-d_6) δ 87.4, 85.1, 83.9, 78.6, 74.66, 74.65, 60.0, 57.1, 46.5, 44.0, 43.6, 41.2, 36.6, 29.1. HRMS (ESI, $[M+H]^+$), calculated for $C_{19}H_{39}N_3O_4$, 374.3019; found, 374.3021.

(2R,3R,4R,5S)-3,4,5-trihydroxy-2-(hydroxymethyl)-N-tetradecylpiperidine-1-carboximidamide (13d).

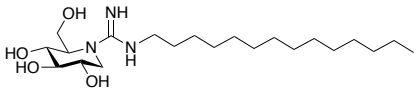

Yield: 7 mg, 79%. ^{1}H NMR (500 MHz, DMSO-d_6) δ 0.85 (t, J = 6.7 Hz, 3H), 1.17 - 1.33 (m, 22H), 1.42 - 1.56 (m, 2H), 3.12 - 3.21 (m, 2H), 3.42 - 3.56 (m, 4H), 3.57 - 3.69 (m, 2H), 3.70 - 3.78 (m, 2H), 5.19 - 5.39 (m, 2H), 5.47 (s, 1H), 7.33 - 7.56 (m, 2H). ^{13}C NMR (126 MHz, DMSO-d_6) δ 86.8, 85.1, 83.3, 78.6, 74.6, 74.1, 59.38, 57.1, 46.5, 43.9, 43.6, 41.2, 37.2, 29.1. HRMS (ESI, [M+H]$^+$), calculated for $C_{21}H_{43}N_3O_4$, 402.3332; found, 402.3328.

N,N-didecyl-2-((2R,3R,4R,5S)-3,4,5-trihydroxy-2-(hydroxymethyl)piperidine-1-carboximidamido) acetamide (13e).

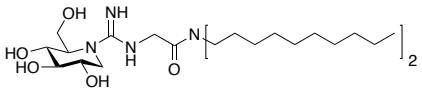

Yield: 15 mg, 89%. ^{1}H NMR (500 MHz, DMSO-d_6) δ 0.86 (t, J = 6.7 Hz, 6H), 1.13 - 1.36 (m, 28H), 1.37 - 1.65 (m, 4H), 3.20 (t, J = 7.8 Hz, 4H), 3.39 - 3.53 (m, 4H), 3.60 - 3.79 (m, 4H), 4.14 (dd, J = 4.8 Hz, 2H), 5.23 - 5.39 (br s, 2H), 5.55 - 5.69 (s, 2H), 7.51 - 7.69 (s, 2H). ^{13}C NMR (126 MHz, DMSO-d_6) δ 87.7, 85.3, 83.8, 79.4, 74.64, 74.63, 61.4, 60.7, 60.3, 58.9, 45.9, 44.0, 43.8, 43.4, 42.3, 41.51, 41.52, 37.2, 29.1. HRMS (ESI, [M+H]$^+$), calculated for $C_{29}H_{58}N_4O_5$, 543.4485; found, 543.4470.

*2.4.2.4 General procedure for Pd/C catalyzed hydrogenolysis for the synthesis of N-substituted urea compounds **14a-e***

Similarly to the guanidine compounds **13a-e**, the bicyclic isourea analogs **14a-e** were prepared using the same procedure with the exception of employing a longer reaction time in the final deprotection step to facilitate intramolecular cyclization. Reactions were stirred for 72-144 hours until fully converted to the cyclized compounds **14a-e**. Analytical data and in-depth characterization data for isourea compounds **14a-e** are given below.

(6S,7R,8R,8aR,E)-3-(octylimino)hexahydro-3H-oxazolo[3,4-a]pyridine-6,7,8-triol (14a).

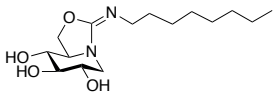

Yield: 21 mg, 82%. ^{1}H NMR (500 MHz, DMSO-d_6) δ 0.87 (t, J = 7.2 Hz, 3H), 1.23 - 1.31 (m, 12H), 1.43 - 1.60 (m, 2H), 2.92 (dd, J = 10.8, 13.2 Hz, 1H), 3.15 (ddd, J = 4.8, 9.0, 13.6 Hz, 1H), 3.22 (ddt, J = 6.2 Hz, 2H), 3.27 - 3.31 (m, 1H), 3.35 - 3.41 (m, 1H), 3.88 (ddd, J = 6.8, 8.8, 9.3 Hz, 1H), 3.98 (dd, J = 5.7, 13.1 Hz, 1H), 4.56 (dd, J = 6.8, 8.7 Hz, 1H), 4.92 (t, J = 8.6 Hz, 1H), 5.32 (d, J = 4.6 Hz, 1H), 5.46 (d, J = 5.4 Hz, 1H), 5.63 (d, J = 5.3 Hz, 1H), 9.39 (s, NH$^+$, 1H). ^{13}C NMR (101 MHz, DMSO-d_6) δ 158.6, 77.1, 72.6, 68.4, 60.6, 45.1, 42.9, 31.6, 28.98, 28.95, 26.4, 22.5, 14.4. HRMS (ESI, [M+H]$^+$), calculated for $C_{15}H_{28}N_2O_4$, 301.2127; found, 301.2147.

(6S,7R,8R,8aR,E)-3-(decylimino)hexahydro-3H-oxazolo[3,4-a]pyridine-6,7,8-triol (14b).

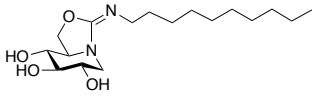

Yield: 16 mg, 85%. ^{1}H NMR (500 MHz, DMSO-d_6) δ (t, J = 6.2 Hz, 3H), 1.19 - 1.33 (m, 14H), 1.45 - 1.56 (m, 2H), 2.91 (t, J = 11.6, 12.1 Hz, 1H), 3.11 - 3.18 (m, 1H), 3.21 (d, J = 6.7 Hz, 2H), 3.27 - 3.31 (m, 1H), 3.35 - 3.42 (m, 1H), 3.82 - 3.92 (m, 1H), 3.98 (dd, J = 5.7, 13.1 Hz, 1H), 4.56 (t, J = 7.7 Hz, 1H), 4.92 (t, J = 8.7 Hz, 1H), 5.32 (d, J = 4.6 Hz, 1H), 5.46 (d, J = 5.4 Hz, 1H), 5.63 (d, J = 5.3 Hz, 1H), 9.38 (s, NH$^+$, 1H). ^{13}C NMR (101 MHz, DMSO-d_6) δ 158.2, 76.6, 73.3, 72.1, 67.9, 60.2, 44.6, 42.5, 31.3, 28.93, 28.91, 28.7, 28.6, 25.9, 22.1, 14.0. HRMS (ESI, [M+H]$^+$), calculated for $C_{17}H_{32}N_2O_4$, 329.2440; found, 329.2442.

(6S,7R,8R,8aR,E)-3-(dodecylimino)hexahydro-3H-oxazolo[3,4-a]pyridine-6,7,8-triol (14c).

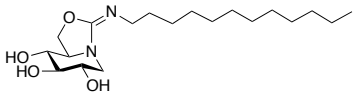

Yield: 11 mg, 80%. ^{1}H NMR (500 MHz, DMSO-d_6) δ 0.86 (t, J = 6.7 Hz, 3H), 1.18 - 1.35 (m, 18H), 1.44 - 1.58 (m, 2H), 2.91 (dd, J = 10.8, 13.1 Hz, 1H), 3.12 - 3.18 (m, 1H), 3.18 - 3.25 (m, 2H), 3.27 - 3.31 (m, 1H), 3.35 - 3.42 (m, 1H), 3.83 - 3.91 (m, 1H), 3.97 (dd, J = 5.6, 13.1 Hz, 1H), 4.56 (dd, J = 6.8, 8.8 Hz, 1H), 4.92 (t, J = 8.7 Hz, 1H), 5.31 (d, J = 4.6 Hz, 1H), 5.46 (d, J = 5.4 Hz, 1H), 5.62 (d, J = 5.3 Hz, 1H), 9.36 (s, NH$^+$, 1H). ^{13}C NMR (101 MHz, DMSO-d_6) δ 158.2, 76.6, 73.3, 72.1, 67.9,

60.2, 44.6, 42.5, 31.3, 29.03, 28.99, 28.98, 28.9, 28.7, 28.6, 25.9, 22.1, 14.0. HRMS (ESI, $[M+H]^+$), calculated for $C_{19}H_{36}N_2O_4$, 357.2753; found, 357.2770.

(6S,7R,8 R,8aR,E)-3-(tetradecylimino)hexahydro-3H-oxazolo[3,4-a]pyridine-6,7,8-triol (14d).

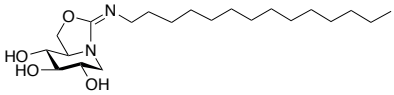

Yield: 18 mg, 86%. ^{1}H NMR (500 MHz, DMSO-d_6) δ 0.85 (t, J = 6.7 Hz, 3H), 1.18 - 1.30 (m, 22H), 1.50 (d, J = 7.6 Hz, 2H), 2.91 (dd, J = 10.9, 13.1 Hz, 1H), 3.12 - 3.18 (m, 1H), 3.18 - 3.26 (m, 2H), 3.27 - 3.30 (m, 1H), 3.34 - 3.41 (m, 1H), 3.81 - 3.93 (m, 1H), 3.97 (dd, J = 5.7, 13.2 Hz, 1H), 4.55 (dd, J = 7.4, 8.2 Hz, 2H), 4.92 (t, J = 8.5 Hz, 2H), 5.31 (d, J = 4.7 Hz, 1H), 5.46 (d, J = 5.4 Hz, 1H), 5.62 (d, J = 5.3 Hz, 1H), 9.36 (s, NH^+, 1H). ^{13}C NMR (101 MHz, DMSO-d_6) δ 158.2, 76.6, 73.3, 72.1, 67.9, 60.2, 44.6, 42.5, 31.3, 29.04, 29.03, 29.00, 28.98, 28.9, 28.7, 28.6, 26.0, 22.1, 14.0. HRMS (ESI, $[M+H]^+$), calculated for $C_{19}H_{36}N_2O_4$, 385.3066; found, 385.3068.

N,N-didecyl-2-(((6S,7R,8R,8aR,E)-6,7,8-trihydroxyhexahydro-3H-oxazolo[3,4-a]pyridin-3-ylidene)amino)acetamide (14e).

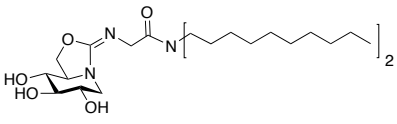

Yield: 15 mg, 91%. ^{1}H NMR (500 MHz, DMSO-d_6) δ 0.85 (2 x t, J = 6.7 Hz, 6H), 1.16 - 1.32 (m, 28H), 1.38 - 1.54 (m, 4H), 3.03 (t, J = 10.8, 13.2 Hz, 1H), 3.14 - 3.29 (m, 6H), 3.35 - 3.42 (m, 1H), 3.96 (ddd, J = 6.0, 8.9 Hz, 1H), 4.06 (dd, J = 5.6, 13.3 Hz, 1H), 4.16 (s, 2H), 4.56 (dd, J = 5.9, 8.8 Hz, 1H), 4.88 (dd, J = 8.6 Hz, 1H), 5.36 (d, J = 4.6 Hz, 1H), 5.53 (d, J = 5.3 Hz, 1H), 5.69 (d, J = 5.2 Hz, 1H), 9.78 (s, NH^+, 1H). ^{13}C NMR (101 MHz, DMSO-d_6) δ 165.5, 159.3, 104.18, 104.17, 76.5, 73.3, 72.1, 68.0, 60.4, 46.11, 46.10, 45.5, 44.8, 43.5, 43.5, 31.3, 28.97, 28.95, 28.92, 28.8, 28.71, 28.68, 28.67, 28.2, 27.1, 26.3, 26.1, 22.1, 14.0. HRMS (ESI, $[M+H]^+$), calculated for $C_{29}H_{55}N_3O_5$, 526.4220; found, 526.4229.

*2.4.2.5 Synthesis of bis-lipidated compounds **15**, **16** and **11e***

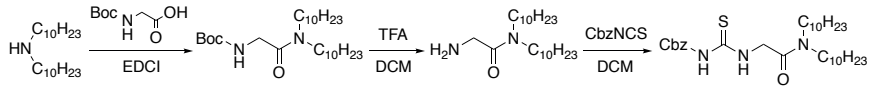

15 **16** **11e**

Scheme 3. Synthetic route towards thiourea compound **11e**.

***Tert*-butyl (2-(didecylamino)-2-oxoethyl)carbamate (15).**

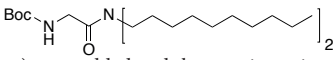

Boc-Gly-OH (0.88 g, 5 mmol, 1 eq) was dissolved in CH_2Cl_2 (60 mL). Didecylamine (1.64 g, 5.5 mmol, 1.1 eq) and EDCI (1.05 g, 5 mmol, 1 eq) were added and the reaction mixture was stirred for 24h. Consumption of starting material was confirmed with TLC analysis, followed by extraction with HCl (3x200 mL), sat. aq. $NaHCO_3$ (3x200 mL) and sat. aq. NaCl (200 mL). The combined organic phases were dried with Na_2SO_4, filtered and concentrated under reduced pressure. The residue was purified by silica gel column chromatography (EtOAc/hexanes = 4:1). Yield: 3.64 g, 92%. R_f (EtOAc/hexanes = 4:1) = 0.82. ^{1}H NMR (400 MHz, $CDCl_3$) δ 0.88 (2 x t, J = 7.1 Hz, 6H), 1.21 - 1.38 (m, 28H), 1.45 (s, 9H), 1.47 - 1.62 (m, 4H), 3.09 - 3.19 (m, 2H), 3.27 - 3.36 (m, 2H), 3.94 (d, J = 4.2 Hz, 2H), 5.57 (s, 1H). ^{13}C NMR (101 MHz, $CDCl_3$) δ 167.5, 155.8, 79.4, 77.3, 77.0, 76.7, 46.9, 46.1, 42.1, 31.83, 31.81, 29.50, 29.48, 29.4, 29.34, 29.28, 29.25, 29.2, 28.7, 28.3, 27.6, 26.94, 26.85, 22.6, 14.1. HRMS (ESI, $[M+H-Boc]^+$), calculated for $C_{27}H_{54}N_2O_3$, 355.3688; found, 355.3639.

2-amino-*N*,N-didecylacetamide (16).

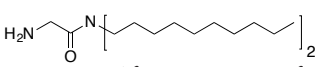

TFA (15 mL) was added to previously isolated **15** (3.27 g, 7.19 mmol, 1 eq), dissolved in CH_2Cl_2 (15 mL) and stirred for 24 h at room temperature. After consumption of starting material was observed with TLC, the residue was purified by flash column chromatography to obtain a yellow oil which was concentrated and co-evaporated with $CHCl_3$. Yield:

2.55 g, quant. yield, R_f (EtOAc/hexanes = 8:1) = 0.12. ^{1}H NMR (400 MHz, $CDCl_3$) δ 0.88 (2 x t, *J* = 7.0 Hz, 6H), 1.18 - 1.38 (m, 28H), 1.40 - 1.69 (m, 4H), 3.12 (t, *J* = 7.7 Hz, 2H), 3.30 (t, *J* = 7.6 Hz, 2H), 3.87 (s, 2H), 8.21 (s, 2H). ^{13}C NMR (101 MHz, $CDCl_3$) δ 164.9, 77.3, 77.0, 76.7, 47.2, 46.5, 40.0, 31.9, 31.8, 29.5, 29.44, 29.41, 29.34, 29.28, 29.21, 29.17, 28.3, 27.2, 26.9, 26.7, 22.63, 22.61, 14.0. HRMS (ESI, $[M+H]^+$), calculated for $C_{22}H_{46}N_2O$, 355.3688; found, 355.3633.

*2.4.2.6 Synthetic route for OBn protected DNJ building block **10***

An efficient construction of building block **10** was attempted via $LiAlH_4$-mediated reduction of commercially available 2,3,4,6-tetra-O-benzyl-D-glucopyranose (**17**) to produce glucitol **18**. Swern oxidation of diol **18** followed by treatment of the resulting crude hexosulose **19** with sodium cyanoborohydride and ammonium formate at 0 °C led, after warming to room temperature, to efficient formation of **10** in good overall yields (**Scheme 4**).

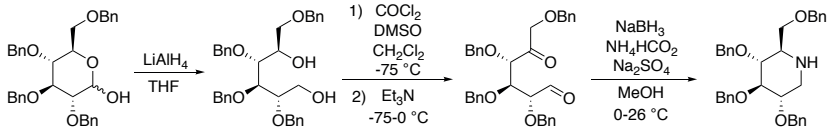

17 **18** **19** **10**

Scheme 4. Synthetic route towards protected DNJ species **10**.

2,3,4,6-Tetra-O-benzyl-D-glucitol (18).

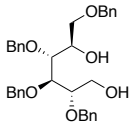

The compound was prepared according to previously published procedure.[16] $LiAlH_4$ (3.5 eq) was added in portions to a cooled (0 °C) and dry solution of commercially available 2,3,4,6-tetra-O-benzyl-D-glucopyranose (**17**, 14.1 g, 26.0 mmol) in THF (0.15 M). The reaction mixture was stirred for 20 hours, allowing it to warm to room temperature. The excess $LiAlH_4$ was quenched with water at 0 °C. The mixture was diluted with EtOAc and washed with saturated aqueous solution of NH_4Cl. The organic phase was dried over Na_2SO_4 and concentrated under reduced pressure. The resulting product **18** was used crude in the next reaction. Sample was purified by silica gel column chromatography (20%→50% EtOAc in PE) to provide product **18** as colorless oil. Characterization data for compound **18** is in accordance to previously published data.[16] R_f = 0.45 (1:1; EtOAc:PE). ^{1}H NMR (400 MHz, $CDCl_3$, COSY): δ = 7.48-7.08 (m, 20H), 4.70 (d, *J* = 11.3 Hz, 1H), 4.64 (d, *J* = 11.3 Hz, 1H), 4.63 (d, *J* = 11.7 Hz, 1H), 4.61-4.56 (m, 2H), 4.53 (d, *J* = 11.4 Hz, 1H), 4.52 (d, *J* = 11.8 Hz, 1H), 4.47 (d, *J* = 11.8 Hz, 1H), 4.03 (m, 1H), 3.89 (dd, *J* = 3.6 Hz, *J* = 6.3 Hz, 1H), 3.80-3.75 (m, 2H), 3.71 (dd, *J* = 4.3 Hz, *J* = 11.9 Hz, 1H), 3.65-3.59 (m, 2H), 3.55 (dd, *J* = 4.7 Hz, *J* = 11.9 Hz, 1H), 3.04 (br s, 1H, OH), 2.35 (br s, 1H, OH). ^{13}C NMR (100 MHz, $CDCl_3$, HMQC): δ = 138.1, 137.8, 137.8 (4×C), 128.25, 128.23, 127.9, 127.8, 127.7, 127.6, 79.4, 78.9, 77.3, 74.4, 73.3, 73.1, 72.9 (4×C), 71.0, 70.6, 61.6. HRMS (ESI, $[M+H]^+$), calculated for $C_{34}H_{38}O_6$, 543.2741; found 543.27224.

2,3,4,6-Tetra-O-benzyl-1-deoxynojirimycin (10).

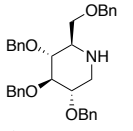

The compound was prepared according to previously published procedure.[16] **Swern oxidation:** A solution of oxalylchloride (4 eq) in DCM (1 M) was cooled to -78 °C. After dropwise addition of a solution of DMSO (5 eq) in DCM (2 M) over 10 minutes, the reaction mixture was stirred for 40 minutes while being kept below -70 °C. Next, a dry solution of the glucitol **18** in DCM (0.5 M) was added dropwise to the reaction mixture over a 15 minute period, while keeping the reaction mixture below -70 °C. After stirring the reaction mixture for 2 hours below -65 °C, Et_3N (12 eq) was added dropwise over a 10 minute period, while keeping the reaction mixture below -65 °C. After addition, the reaction mixture was allowed to warm to -5 °C over 2 hours. The crude product **19** was used in subsequent reaction without purification. **Double reductive amination:** The Swern reaction mixture was concentrated at a moderate temperature (~30 °C) with simultaneous co-evaporation of toluene. The residue was dissolved in MeOH (0.05 M relative to starting compound) and NH_4HCO_2 (20 eq) was added. The mixture was cooled to 0 °C and stirred until all NH_4HCO_2 had dissolved. Activated 3Å mol sieves were added and reaction mixture was stirred for 20 minutes, after which $NaBH_3CN$ (4 eq) was added. The reaction mixture was kept at 0 °C for one hour after which the cooling source was removed and the reaction was stirred for an additional 20 hours. After removal of the mol sieves over a glass microfibre filter, the filtrate was concentrated, dissolved in EtOAc and

washed with saturated aqueous solution of $NaHCO_3$. The aqueous phase was back-extracted with EtOAc and the combined organic layers were dried over Na_2SO_4 and concentrated under reduced pressure. The resulting residue was purified by silica gel column chromatography (20%→75% EtOAc in PE) to provide **10** as a light yellow crystalline solid. Characterization data for compound **10** is in accordance to previously published data.[16] Yield: 9.9 g, 73% yield over three steps, R_f = 0.25 (1:1; EtOAc:PE). ^{1}H NMR (400 MHz, $CDCl_3$, COSY): δ = 7.35-7.14 (m, 20H), 4.97 (d, *J* = 12.9 Hz, 1H), 4.87-4.82 (m, 2H), 4.68 (d, *J* = 11.7 Hz, 1H), 4.64 (d, *J* = 11.7 Hz, 1H), 4.48 (d, *J* = 11.0 Hz, 1H), 4.45 (d, *J* = 11.8 Hz, 1H), 4.40 (d, *J* = 11.8 Hz, 1H), 3.65 (dd, *J* = 2.6 Hz, *J* = 9.0 Hz, 1H), 3.57-3.45 (m, 3H), 3.34 (dd, *J* = 8.8 Hz, 1H), 3.22 (dd, *J* = 4.9 Hz, *J* = 12.2 Hz, 1H), 2.71 (ddd, *J* = 2.6 Hz, *J* = 5.9 Hz, *J* = 9.8 Hz, 1H), 2.48 (dd, *J* = 10.3 Hz, *J* = 12.2 Hz, 1H), 1.89 (br s, 1H, NH). ^{13}C NMR (100 MHz, $CDCl_3$, HMQC): δ = 138.8, 138.4, 138.3, 137.8 (4×C), 128.24, 128.21, 127.84, 127.78, 127.70, 127.6, 127.5, 127.4, 87.2, 80.5, 80.0, 75.5, 75.0, 73.2, 72.6, 70.1, 59.6, 48.0. (ESI, $[M+H]^+$), calculated for $C_{34}H_{37}NO_4$, 524.2795; found 524.2768.

2.4.3 Kinetic evaluation experimental details

Chemicals

Acetonitrile (ACN; LC-MS Chromasolv) was purchased from Biosolve BV (Valkenswaard, The Netherlands). Formic acid (FA; LC-MS grade), acetic acid, sodium acetate and ammonium acetate were acquired from Sigma-Aldrich (St. Louis, MA, USA). Ultra-pure water was obtained from a Synergy UV water delivery system from Millipore (Billerica, MA, USA). Buffer solutions of 200 mM ammonium acetate (pH 7.0) and 21 mM acetic acid with 85 mM sodium acetate (pH 5.2) were prepared in ultra-pure water. Standard solutions of 1 mM guanidine compounds **13(a-e)** were prepared in buffer solutions with pH 5.2 and pH 7.0.

Chromatography

Separation of guanidine compounds and their degradation products was achieved on a Zorbax Eclipse plus C_{18} column (4.6 x 50 mm, 1.8 µm particles). A 2-µL injection volume was used of all samples. UHPLC was performed on a 1290 Infinity UHPLC system (Agilent Technologies, Wald-bronn, BW, Germany) consisting of a binary pump and an autosampler. The optimal separation was achieved with a binary gradient with 0.5% FA (% v/v) in water (eluent A) and ACN (eluent B) at a flow rate of 0.5 mL/min. Detection was performed on a quadrupole-time-off-flight mass spectrometer, equipped with an electrospray ionization source (Bruker Daltonics, Bremen, HB, Germany). Masses were acquired from *m/z* 50-700 at a spectra rate of 1.5 Hz, nebulizer pressure was 4 bar, gas flow was 10 L/min, gas temperature was 2000 °C and capillary voltage was 3 kV. Guanidine compounds **13a-e** and their degradation products were detected as positive ions ($[M+H]^+$).

2.4.3.1 Stability indicating method procedure

A sample of 1 mM **13a**, degraded in buffer solution (pH 7.0) at 21 °C for 2 days, was used to develop the stability indicating method. The separation of **13a** and the degradation products was optimized by adjusting the amount and type of acidifier, organic modifier, the gradient time and slope. Good selectivity for all high and low polar compounds was achieved in one run with 0.5% FA/ACN gradients. The optimized gradient started with a composition of 70% eluent A and 30% eluent B (% v/v) for 3 min, increased linearly to 100% B in 3.5 min and remained at 100% B for 2 min. MS setting were optimized to obtain maximum detector response for all compounds. The optimized method was used to study the degradation of the synthesized guanidine compounds. Samples were dissolved in buffer solutions with pH 5.2 or pH 7.0, kept at 21°C and analyzed at regular time intervals.

2.4.4 Biological evaluation against commercial glycosidases

2.4.4.1 Inhibition assays against commercial glycosidases, human recombinant GBA (R&D 7410-GH) and human recombinant GALC (R&D 7310-GH)

Inhibition assays against commercial glycosidases were performed in either phosphate or acetate buffer at the optimum pH for each enzyme (See below for enzyme specific data). Determination of the IC_{50} values of the iminosugars was carried out by spectrophotometrically measuring the residual hydrolytic activities of the glycosidases on the corresponding p-nitrophenyl glycoside substrates in the presence of a concentration range

of iminosugar derivatives. The incubation mixture consisted of 50 μL of inhibitor solution in buffer (0.1 U mL^{-1}) and 50 μL of enzyme solution. The concentrations of the enzyme were adjusted so that the reading for the final absorbance was in the range of 0.5–1.5 units. Inhibitor and enzyme solutions were mixed in a disposable 96-well microtiter plate and then incubated at room temperature for 5 minutes. Next, the reactions were initiated by addition of 50 μL of a solution of the corresponding p-nitrophenyl glycoside substrates solution in the appropriate buffer at the optimum pH for the enzyme. After the reaction mixture was incubated at 37 ^{0}C for 30 min, the reaction was quenched with 0.5 M Na_2CO_3 (150 μL) and the absorbance of 4-nitrophenol released from the substrate was read immediately at 405 nm using a BioTek mQuant Microplate Spectrophotometer. IC_{50} values were determined graphically with GraphPad Prism (version 6.0) by making a plot of percentage inhibition versus the log of inhibitor concentration, using at least 8 different inhibitor concentrations. IC_{50} values were presented as a concentration of the iminosugars that inhibits 50% of the enzyme activity under the assay conditions. NN-DNJ was used as a reference compound. All materials were purchased from Sigma-Aldrich.

The commercial glycosidase solutions were prepared as following:

[b]For α-glucosidase (from *baker's yeast,* Sigma G5003, 0.05 U/mL) the activity was determined with p-nitrophenyl-α-D-glucopyranoside (0.7 mM final conc. in well) in sodium phosphate buffer (100 mM, pH 7.2).

[c]For α-galactosidase (from *green coffee beans*, Sigma G8507, 0.05 U/mL) activity was determined with p-nitrophenyl-α-D-galactopyranoside (0.7 mM final conc. in well) in sodium phosphate buffer (100 mM, pH 6.8).

[d]For β-glucosidase (from *almond*, Sigma G4511, 0.05 U/mL) the activity was determined with p-nitrophenyl-β-D-glucopyranoside (0.7 mM final conc. in well) in sodium acetate buffer (100 mM, pH 5.0).

[e]For β-galactosidase (from *bovine liver*, Sigma G1875, 0.05 U/mL) activity was determined with p-nitrophenyl-β-D-galactopyranoside (0.7 mM final conc. in well) in sodium phosphate buffer (100 mM, pH 7.2).

[f]For **Naringinase** (from *penicillium decumbens,* Sigma N1385, 0.06 U/mL) the activity was determined with p-nitrophenyl-β-D-glucopyranoside (0.7 mM final conc. in well) in sodium acetate buffer (100 mM, pH 5.0).

[g]**Recombinant Human Glucosylceramidase/** β-glucocerebrosidase/**GBA** (7410-GH), purchased from R&D was also used in the inhibition studies. The used substrate 4-methylumbelliferyl-β-D-glucopyranoside was purchased by Sigma-Aldrich. GBA activity was determined with 4-methylumbelliferyl-β-D-glucopyranoside as reported in (A. Trapero, J. Med. Chem. 2012, 55, 4479-4488).[27] Briefly, enzyme solutions (25 μL from a stock solution containing 0.6 μg/mL) in the presence of 0.25% (w/v) sodium taurocholate and 0.1% (v/v) Triton X-100 in Mcllvaine buffer (100 mM sodium citrate and 200 mM sodium phosphate buffer, pH 5.2 or pH 7.0) were incubated at 37°C without (control) or with inhibitor at a final volume of 50 μL for 30 min. After addition of 25 μL 4-methylumbelliferyl-β-D-glucopyranoside (7.2 mM, Mcllvaine buffer pH 5.2 or pH 7.0), the samples were incubated at 37°C for 10 min. Enzymatic reactions were stopped by the addition of aliquots (100 μL) of Glycine/NaOH buffer (100 mM, pH 10.6). The amount of 4-methylumbelliferone formed was determined with a FLUOstar microplate reader (BMG Labtech) at 355 nm (excitation) and 460 nm (emission).

[g]**Recombinant Human Galactosylceramidase/GALC** (7310-GH), purchased from R&D was used in the inhibition studies. The used substrate 4-methylumbelliferyl-β-D-galactopyranoside was purchased by Sigma-Aldrich. GALC activity was determined with 4-methylumbelliferyl-β-D-galactopyranoside as reported in assay procedure R&D product 7310-GH. Briefly, enzyme solutions (25 μL from a stock solution containing 60 ng/mL) in the presence of 0.5% (v/v) Triton X-100 in Assay buffer (50 mM sodium citrate and 125 mM NaCl, pH 4.5) were incubated at 37°C without (control) or with inhibitor at a final volume of 50 μL for 10 min. After addition of 25 μL 4-methylumbelliferyl-β-D-galactopyranoside (0.75mM, Assay buffer), the samples were incubated at 37°C for 20 min. Enzymatic reactions were stopped by the addition of aliquots (50 μL) of Glycine/NaOH buffer (100 mM, pH 10.6). The amount of 4-methylumbelliferone formed was determined with a FLUOstar microplate reader (BMG Labtech) at 355 nm (excitation) and 460 nm (emission).

2.4.4.2 IC_{50} curves for compounds 14a-e and NNDNJ against human recombinant GBA (R&D 7410-GH)

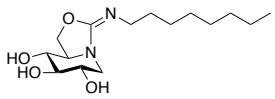

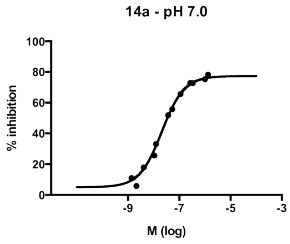

IC_{50} = 2.084e-008 ± 1.328e-009

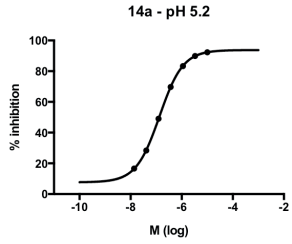

IC_{50} = 1.355e-007 ± 3.892e-009

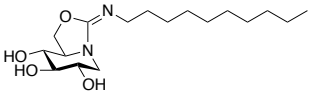

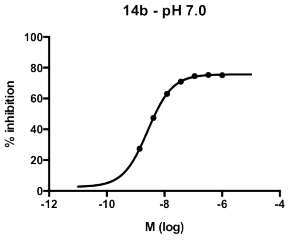

IC_{50} = 2.633e-009 ± 9.009e-010

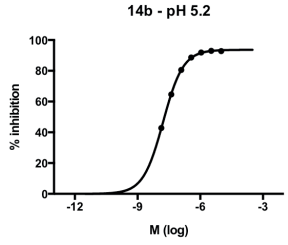

IC_{50} = 1.673e-008 ± 4.915e-010

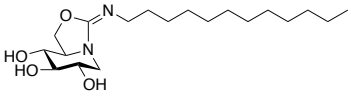

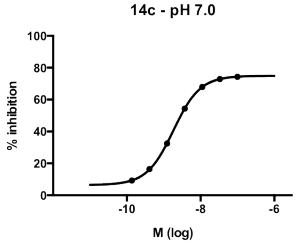

IC_{50} = 1.832e-009 ± 1.141e-010

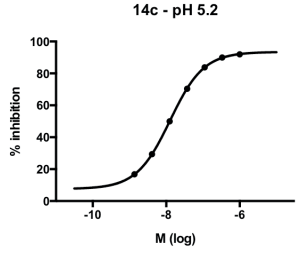

IC_{50} = 1.276e-008 ± 1.226e-009

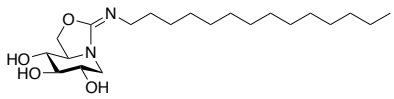

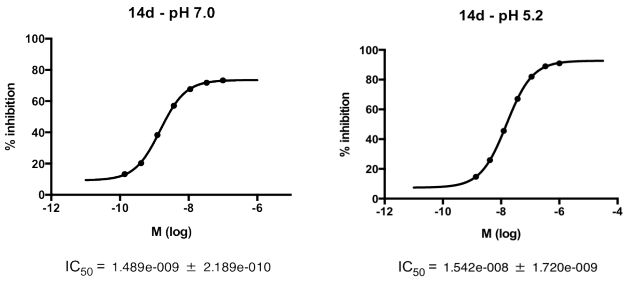

IC_{50} = 1.489e-009 ± 2.189e-010

IC_{50} = 1.542e-008 ± 1.720e-009

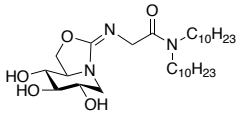

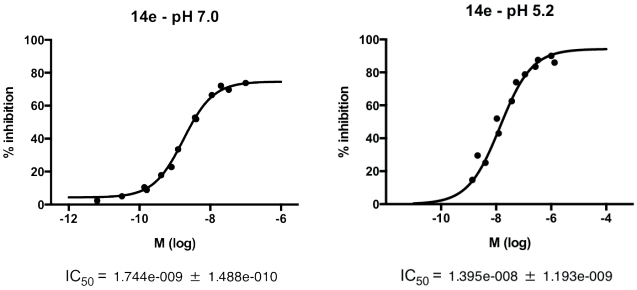

IC_{50} = 1.744e-009 ± 1.488e-010

IC_{50} = 1.395e-008 ± 1.193e-009

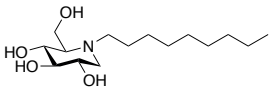

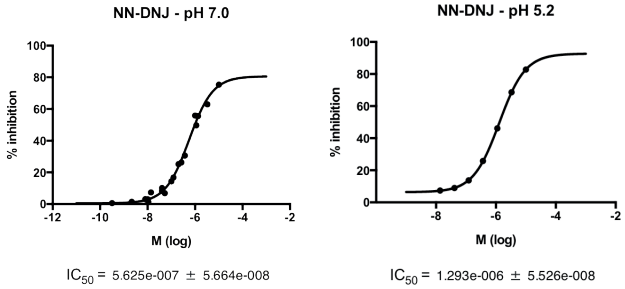

IC_{50} = 5.625e-007 ± 5.664e-008

IC_{50} = 1.293e-006 ± 5.526e-008

2.4.5 Fibroblast experiments

Cell lines and culture. Wild-type fibroblasts (GM 05659) and fibroblasts derived from Gaucher patients, homozygous for N370S GBA (GM00372) and L444P GBA (GM00877) were obtained from Coriell Institute, Camden, USA. Fibroblast cells were cultured in Dulbecco's modified Eagle's medium (DMEM, Sigma-Aldrich) supplemented with 10% fetal bovine serum (FBS, Sigma-Aldrich) and penicillin-streptomycin (100 U/ml resp. 0.1 mg/ml, Sigma-Aldrich) at 37°C in 5% CO_2 and all cells used in this study were between the 5th and 15th passages. The Fibroblasts assay (*chaperone assay)* was performed according to a modified version as described in a paper published by Trapero, et. al.[27]

2.4.5.1 Experimental details for cytotoxicity assay in wild-type GD derived fibroblasts

All compounds were dissolved in DMSO (final concentration <1%) and control experiments were performed with DMSO. Cells were incubated at 37 °C in 5% CO_2 for 24 h. The cytotoxicity was measured by using the CytoTox 96 non-radioactive cytotoxicity assay and the Celltiter-Blue Cell viability assay from Promega.

2.4.5.2 Measurements of GBA activity in intact human (wild-type) fibroblasts

Cells were plated into 24-well assay plates and incubated at 37°C in 5% CO_2 until a monolayer of at least 50% confluency was reached. The media were then replaced with fresh media with or without a test compound and incubated at 37°C in 5% CO_2 for 4 days. The enzyme activity assay was performed after removing media supplemented with the corresponding compound. The monolayers were washed twice with phosphate buffered saline (PBS) solution. Then, 80 µl of PBS and 80 µl of 200 mM acetate buffer (pH 4.0) were added to each well. The reaction was started by addition of 100 µl of 7.2 mM 4-methylumbelliferyl-β-D-glucopyranoside (200 mM acetate buffer pH 4.0) to each well, followed by incubation at 37°C for 2h. Enzymatic reactions were stopped by lysing the cells with 0.9 ml glycine/NaOH buffer (100 mM pH 10.6). Liberated 4-methylumbelliferone was measured (excitation 355 nm, emission at 460 nm) with the Fluoroskan Ascent FL plate reader (Labsystems) in 96-well format.

2.4.5.3 Measurements of N370S and L444P GBA activity in fibroblasts derived from patients with GD

The chaperone assay was performed according to a modified version as previously described.[4] Fibroblasts were plated into 24-well assay plates and incubated at 37°C under 5% CO_2 atmosphere until a monolayer of at least 50% confluency was reached. The media were then replaced with fresh media with or without various concentrations of test compounds and incubated at 37°C in 5% CO_2 for 4 days. The enzyme activity assay was performed after removing media supplemented with the corresponding compound. The monolayers were washed twice with phosphate buffered saline (PBS) solution. Then, 80 µl of PBS and 80 µl of 200 mM acetate buffer (pH 4.0) were added to each well. The reaction was started by addition of 100 µl of 7.2 mM 4-methylumbelliferyl-β-D-glucopyranoside (200 mM acetate buffer pH 4.0) to each well, followed by incubation at 37°C for 2h. Enzymatic reactions were stopped by lysing the cells with 0.9 ml glycine/NaOH buffer (100 mM pH 10.6). Liberated 4-methylumbelliferone was measured (excitation 355 nm, emission at 460 nm) with the Fluoroskan Ascent FL plate reader (Labsystems) in 96-well format.

2.4.6 Experimental details for computational studies

The crystal structure of GBA with NN-DNJ was downloaded from rcsb.org, code 2V3E.[24] Yasara 15.10.11 was used for all molecular manipulations, for example protonating GBA at pH 7.4 and 5.0.[28] Compounds **14a**-**e** were globally docked with Vina to the original 2V3E structure of GBA and the best hits were close to the position of NN-DNJ.[29] Then all compounds, including NN-DNJ, were docked locally to GBA at the two pH states with Vina local search, with Autodock local search, and with Vina local search followed by Autodock local search.[30] The default macros for local docking from Yasara were used, except for the 50 Autodock dockings where ga_pop_size was set to 15000. Affinities were predicted as K_i values. During all dockings the ligands were considered to be flexible. The Yasara energy minimization experiment was performed before the images were created.

2.4.7 Analytical RP-HPLC traces for compounds 13a-e and 14a-e

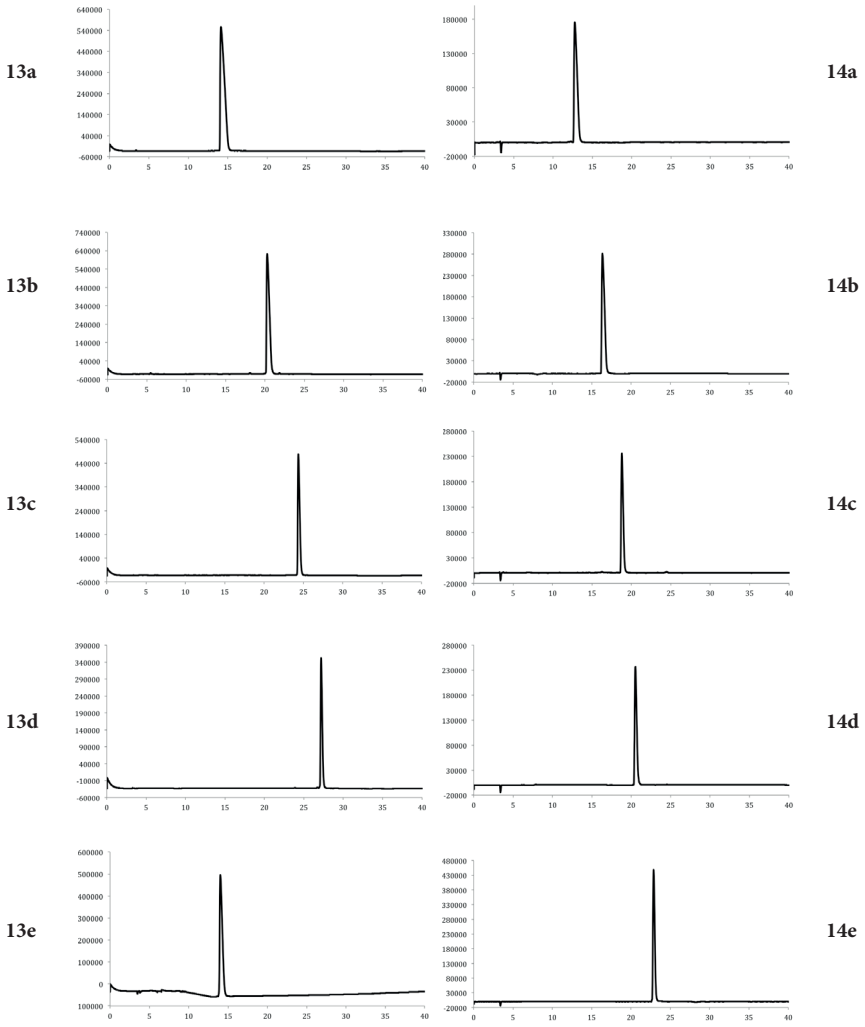

RP-HPLC experimental details

HPLC system (detection simultaneously at 214, 254 nm and evaporative light detection) equipped with an analytical C_{18} column (100 Å pore size, 4.6 mm (⌀) x 250 mm (l), 10 µm particle size) (for compounds **14a-e**) or C_8 column (100 Å pore size, 4.6 mm (⌀) x 250 mm (l), 10 µm particle size) (for compounds **13a-e**) in combination with buffers A: H_2O, B: MeCN, A and B with 0.1% aqueous trifluoroacetic acid (TFA), in some cases - coupled with an electrospray interface (ESI) was used. For RP-HPLC purifications (detection simultaneously at *l* 213, 254 nm), an automated HPLC system equipped with a preparative C_{18} column (20 mm (⌀) x 250 mm (l), 5 µm particle size) or C_8 column (20 mm (⌀) x 250 mm (l), 5 µm particle size) in combination with buffers A: H_2O, B: MeCN, A and B with 0.1% aqueous trifluoroacetic acid (TFA). Compounds **13a-d** and **14a-e** were purified using a 1 hour gradient, starting with 95% buffer A:5% buffer B (0.1%TFA) and 5% buffer A:95% buffer B (0.1%TFA) at the end mark. Compound **13e** required modified conditions starting with 40% buffer B and eluted at 53% buffer B.

2

2.4.8. *Graphical NMR example of compound* ***14a***

Compound 14a: ^{1}H NMR (500 MHz, DMSO-d_6)

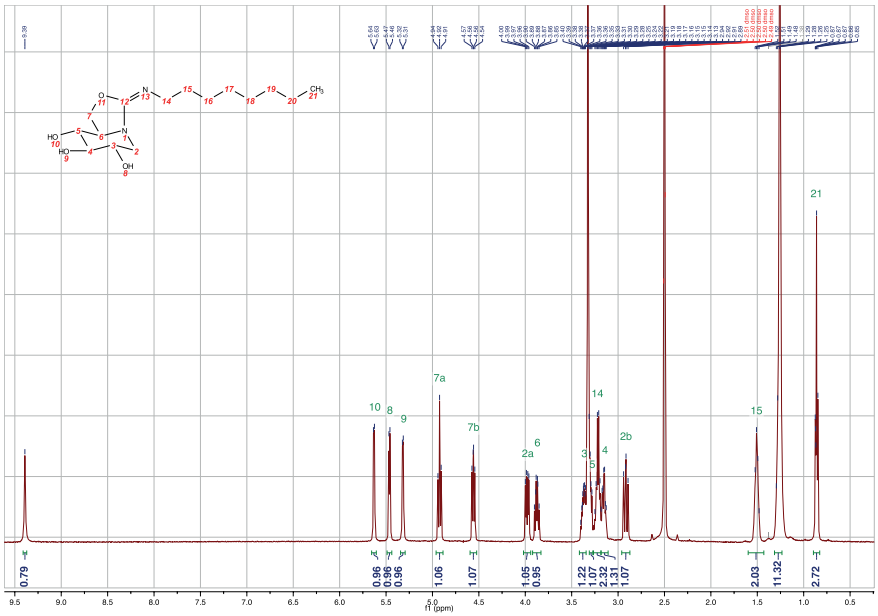

Compound 14a: ^{13}C NMR (126 MHz, DMSO-d_6)

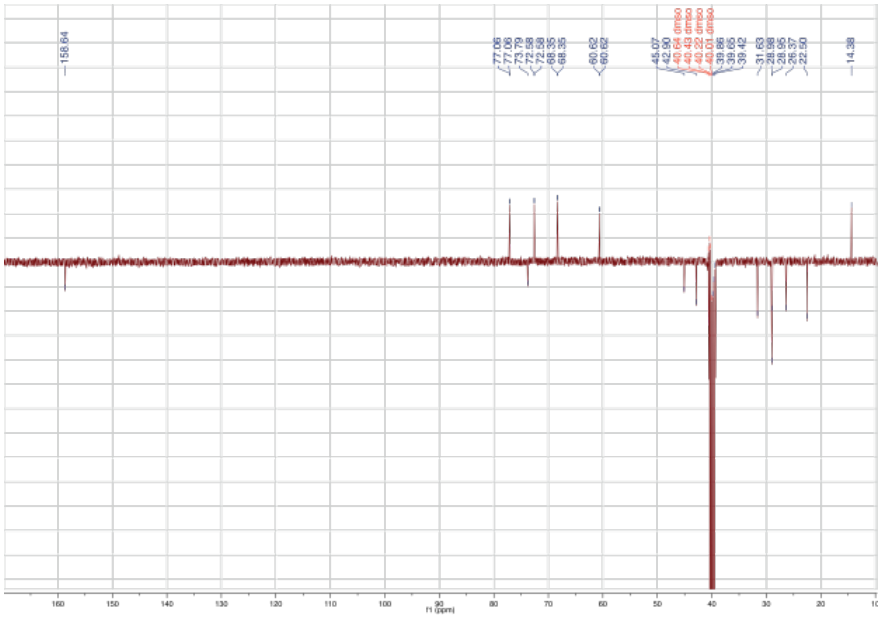

Compound 14a: $^{1}H - {}^{1}H$ COSY NMR (500 MHz, DMSO-d_6)

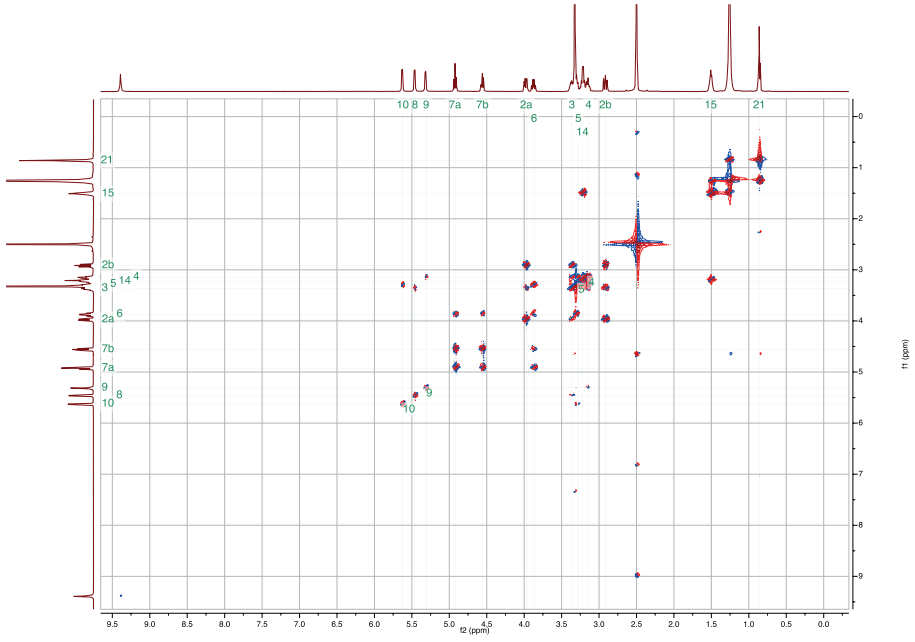

Compound 14a: $^{1}H - {}^{13}C$ HSQC NMR (126 MHz, DMSO-d_6)

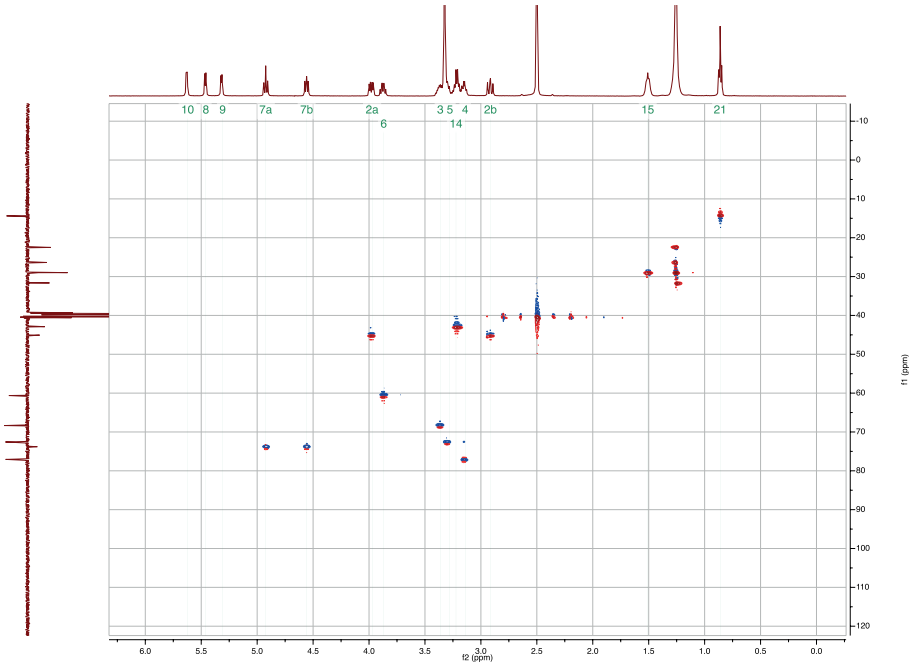

2.5 REFERENCES

1. Jongkees, S. A. K. & Withers, S. G. Unusual Enzymatic Glycoside Cleavage Mechanisms. *Acc. Chem. Res.* **47,** 226–235 (2014).
2. Nardy, A. F. F. R., Freire-de-Lima, L., Freire-de-Lima, C. G. & Morrot, A. The Sweet Side of Immune Evasion: Role of Glycans in the Mechanisms of Cancer Progression. *Front. Oncol.* **6,** 1–7 (2016).
3. Brás, N. F., Cerqueira, N. M., Ramos, M. J. & Fernandes, P. A. Glycosidase inhibitors: a patent review (2008-2013). *Expert Opin. Ther. Pat.* **24,** 857–874 (2014).
4. Ichikawa, Y., Igarashi, Y., Ichikawa, M. & Suhara, Y. 1-N-Iminosugars: Potent and Selective Inhibitors of β-Glycosidases. *J. Am. Chem. Soc.* **120,** 3007–3018 (1998).
5. Horne, G. Iminosugars: Therapeutic Applications and Synthetic Considerations. (2014). doi:10.1007/7355_2014_50
6. Gloster, T. M. *et al.* Glycosidase inhibition: an assessment of the binding of 18 putative transition-state mimics. *J. Am. Chem. Soc.* **129,** 2345–2354 (2007).
7. Gloster, T. M. & Davies, G. J. Glycosidase inhibition: assessing mimicry of the transition state. *Org. Biomol. Chem.* **8,** 305–320 (2010).
8. Aguilar-Moncayo, M. *et al.* Glycosidase inhibition by ring-modified castanospermine analogues: tackling enzyme selectivity by inhibitor tailoring. *Org. Biomol. Chem.* **7,** 2738–2747 (2009).
9. Sanchez-Fernandez, E. M., Garcia Fernandez, J. M. & Mellet, C. O. Glycomimetic-based pharmacological chaperones for lysosomal storage disorders: lessons from Gaucher, GM1-gangliosidosis and Fabry diseases. *Chem. Commun.* **52,** 5497–5515 (2016).
10. Aguilar-Moncayo, M. *et al.* Tuning glycosidase inhibition through aglycone interactions: pharmacological chaperones for Fabry disease and GM1 gangliosidosis. *Chem. Commun.* **48,** 6514–6516 (2012).
11. Luan, Z. *et al.* Chaperone activity of bicyclic nojirimycin analogues for Gaucher mutations in comparison with N-(nonyl)deoxynojirimycin. *ChemBioChem* **10,** 2780–2792 (2009).
12. Brumshtein, B. *et al.* 6-Amino-6-deoxy-5,6-di-N-(N′-octyliminomethylidene)nojirimycin: Synthesis, Biological Evaluation, and Crystal Structure in Complex with Acid β-Glucosidase. *ChemBioChem* **10,** 1480–1485 (2009).
13. Sánchez-Fernández, E. M. *et al.* Synthesis of N-, S-, and C-glycoside castanospermine analogues with selective neutral alpha-glucosidase inhibitory activity as antitumour agents. *Chem. Commun.* **46,** 5328–5330 (2010).
14. Martin, N. I., Woodward, J. J. & Marletta, M. A. NG-hydroxyguanidines from Primary Amines. *Org. Lett.* **8,** 4035–4038 (2006).
15. Kooij, R. *et al.* Glycosidase inhibition by novel guanidinium and urea iminosugar derivatives. *Medchemcomm* **4,** 387–393 (2013).
16. Wennekes, T. *et al.* Development of adamantan-1-yl-methoxy-functionalized 1-deoxynojirimycin derivatives as selective inhibitors of glucosylceramide metabolism in man. *J. Org. Chem.* **72,** 1088–1097 (2007).
17. Martin, N. I., Beeson, W. T., Woodward, J. J. & Marletta, M. A. N-aminoguanidines from primary amines and the preparation of nitric oxide synthase inhibitors. *J. Med. Chem.* **51,** 924–931 (2008).
18. Martin, N. I. & Liskamp, R. M. J. Preparation of NG-Substituted L-Arginine Analogues Suitable for Solid Phase Peptide Synthesis. *J. Org. Chem.* **73,** 7849–7851 (2008).
19. Platt, F. M. Sphingolipid Lysosomal Storage Disorders. *Nature* **510,** 68–75 (2014).
20. Parenti, G., Andria, G. & Valenzano, K. J. Pharmacological Chaperone Therapy: Preclinical Development, Clinical Translation, and Prospects for the Treatment of Lysosomal Storage Disorders. *Mol. Ther.* **23,** 1138–1148 (2015).
21. Beutler, E. Gaucher Disease: Multiple Lessons from a Single Gene Disorder. *Acta Paediatr.* **95,** 103–109 (2006).
22. Trapero, A., Alfonso, I., Butters, T. D. & Llebaria, A. Polyhydroxylated bicyclic isoureas and guanidines are potent glucocerebrosidase inhibitors and nanomolar enzyme activity enhancers in Gaucher cells. *J. Am. Chem. Soc.* **133,** 5474–5484 (2011).
23. Sawkar, A. R. *et al.* Chemical chaperones increase the cellular activity of N370S beta-glucosidase: A therapeutic strategy for Gaucher disease. *Proc. Natl. Acad. Sci. U. S. A.* **99,** 15428–15433 (2002).
24. Brumshtein, B. *et al.* Crystal structures of complexes of N-butyl- and N-nonyl-deoxynojirimycin bound to acid β-glucosidase: Insights into the mechanism of chemical chaperone action in Gaucher disease. *J. Biol. Chem.* **282,** 29052–29058 (2007).

25. García-Moreno, M. I., Díaz-Pérez, P., Ortiz Mellet, C. & García Fernández, J. M. Synthesis and Evaluation of Isourea-Type Glycomimetics Related to the Indolizidine and Trehazolin Glycosidase Inhibitor Families. *J. Org. Chem.* **68,** 8890–8901 (2003).
26. Brumshtein, B. *et al.* Cyclodextrin-mediated crystallization of acid β-glucosidase in complex with amphiphilic bicyclic nojirimycin analogues. *Org. Biomol. Chem.* **9,** 4160–4167 (2011).
27. Trapero, A., González-Bulnes, P., Butters, T. D. & Llebaria, A. Potent aminocyclitol glucocerebrosidase inhibitors are subnanomolar pharmacological chaperones for treating gaucher disease. *J. Med. Chem.* **55,** 4479–4488 (2012).
28. Krieger, E. & Vriend, G. New ways to boost molecular dynamics simulations. *J. Comput. Chem.* **36,** 996–1007 (2015).
29. Oleg Trott & Olson, A. J. AutoDock Vina: Improving the Speed and Accuracy of Docking with a New Scoring Function, Efficient Optimization, and Multithreading. *J. Comput. Chem.* **31,** 455–461 (2009).
30. Garrett M. Morris *et al.* AutoDock4 and AutoDockTools4: Automated Docking with Selective Receptor Flexibility. *J. Comput. Chem.* **30,** 2785–2791 (2009).

CHAPTER 3

N-Guanidino Derivatives of 1,5-Dideoxy-1,5-imino-D-xylitol are Potent, Selective, and Stable Inhibitors of *β*-Glucocerebrosidase

Parts of this chapter have been published:

Sevšek, A.; Šrot, L.; Rihter, J.; Čelan, M.; Quarles van Ufford, L.; Moret, E. E.; Martin, N. I.; Pieters, R. J. *ChemMedChem*. **2017**, *12*, 483–486.

ABSTRACT

A series of lipidated guanidino and urea derivatives of 1,5-di-deoxy-1,5-imino-D-xylitol were prepared from D-xylose using a concise synthetic protocol. Inhibition assays with a panel of glycosidases revealed that the guanidino analogues display potent inhibition against human recombinant *β*-glucocerebrosidase with IC_{50} values in the low nanomolar range. Related urea analogues of 1,5-dideoxy-1,5-imino-D-xylitol were also synthesized and evaluated in the same fashion and found to be selective for *β*-galactosidase from bovine liver. No inhibition of human recombinant *β*-glucocerebrosidase was observed for the urea analogues. Computational studies provided insight into the potent activity of analogues bearing the substituted guanidine moiety in the inhibition of lysosomal *β*-glucocerebrosidase (GBA).

3.1 INTRODUCTION

Creating potent and selective glycosidase inhibitors is an important goal in medicinal chemistry[1] due to their therapeutic potential in the treatment of a variety of carbohydrate-mediated diseases.[2–12] In this respect, iminosugars are privileged lead compounds because of their complementarity to glycosidase active sites and aspects of the relevant transition states in the hydrolysis processes catalyzed by glycosidases.[13] Glycomimetics that comprise an endocyclic nitrogen, such as the naturally occurring 1-deoxynojirimycin (DNJ, **1**, **Figure 1**) as well as 1,5-dideoxy-1,5-imino-D-xylitol (DIX, **4**) and their closely related unnatural relative isofagomine (IFG, **6**), are of particular interest[14,15] and a number of syntheses of these compounds have been reported.[16–18] It has also been demonstrated that synthetically modified N-substituted iminosugars often possess improved specificities and potent inhibition toward glycosidases.[19–21] In this context, some N-alkylated iminosugars, such as **2**, **3**, **5**, **7**, **8** and **9**, have already shown promise as potent glycosidase inhibitors.[22–32]

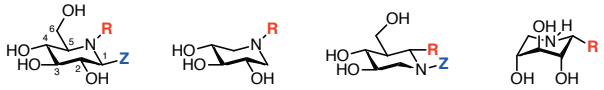

Figure 1. Chemical structures of selected iminosugar-based glycosidase inhibitors.

Our research group's activities in this area have focused on preparing iminosugar analogues with an sp^2 hybridized endocyclic nitrogen.[33] In doing so, both the conformation and charge delocalization of the endocyclic nitrogen atom is altered. These modifications have resulted in interesting specificity changes in comparison with the parent iminosugars.[34] To this end, we recently attempted the synthesis of a series of lipidated DNJ guanidine analogues (compounds **I**, **Scheme 1**).[35] Interestingly, we found that such N-alkylated guanidine DNJ analogues **I** spontaneously cyclized to generate the corresponding stable bicyclic isoureas **II**. Gratifyingly, the isoureas proved to be very potent and specific inhibitors of β-glucocerebrosidase.[35]

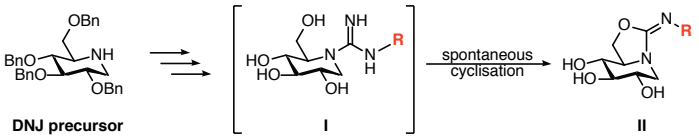

Scheme 1. Previously published spontaneous cyclisation of guanidine (**I**) compounds to bicyclic isoureas (**II**) derived from DNJ precursor.[35]

Our previous studies established that formation of the cyclic isourea **II** proceeds *via* the guanidine species **I**, which is prone to cyclization by action of the 6-OH group. We here report a strategy designed to circumvent this process wherein N-substituted guanidine analogues of DIX (**4**), lacking the 6-OH group of DNJ, were prepared and found to be stable. Previous reports indicate that a DIX analogue bearing an unsubstituted guanidinium moiety (**10**) displays a 100-fold enhancement in the inhibition of almond *β*-glycosidase (**Figure 2**).[36] However, N-guanidino-alkylated variants of DIX (**A**) have not yet been studied. We here report the synthesis and testing of new guanidinium compounds of type **A** as well as the corresponding urea derivatives **B** (**Figure 2**), both derived from DIX and lacking the hydroxymethyl found in DNJ that causes the cyclization. Interestingly, it has also been shown that the hydroxymethyl of DNJ can have a detrimental effect on its GBA binding when compared with unsubstituted DIX.[32]

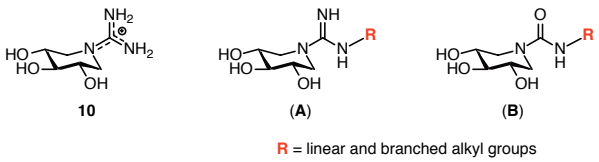

Figure 2. Unsubstituted guanidinium derivative **10**[36] and general structures of guanidine **(A)** and urea **(B)** DIX derivatives prepared in this work.

3.2 RESULTS AND DISCUSSION

3.2.1 *Synthesis of guanidine-DIX and urea-DIX compounds*

The synthetic strategy used in preparing the guanidinium and urea analogues of DIX (**4**), is outlined in **Scheme 2**. Benzyl protected 1,5-dideoxy-1,5-imino-D-xylitol **11** was synthesized according to the literature procedure[37] and used as a starting material for the preparation of both the guanidine and urea analogues. As indicated in **Scheme 2A**, treatment of **11** with the appropriate Cbz-protected thiourea (**12a-e**) and EDCI led to clean formation of protected guanidines **13a-e**.[38,39] Removal of Cbz and benzyl groups was achieved *via* hydrogenation to yield the guanidine products **14a-e**. For the synthesis of the corresponding urea species, a series of Boc-protected amines **15a-e** were generated according to a literature procedure.[40] Treatment of the Boc-protected amines with 2-chloropyridine followed by the addition of triflic anhydride resulted in formation of the corresponding isocyanate intermediates that were immediately treated with **11** to yield the protected ureas **16a-e**. Removal of the benzyl groups by hydrogenation provided the urea products **17a-e** (**Scheme 2B**). The guanidine (**14a-d**) and urea (**17a-d**) series both incorporate different N^G-substituents comprised of simple alkyl chains ranging from eight to fourteen carbon atoms in length. In addition, bis-lipidated species **14e** and **17e** were also synthesized as more representative substrate mimics for β-glucocerebrosidase.

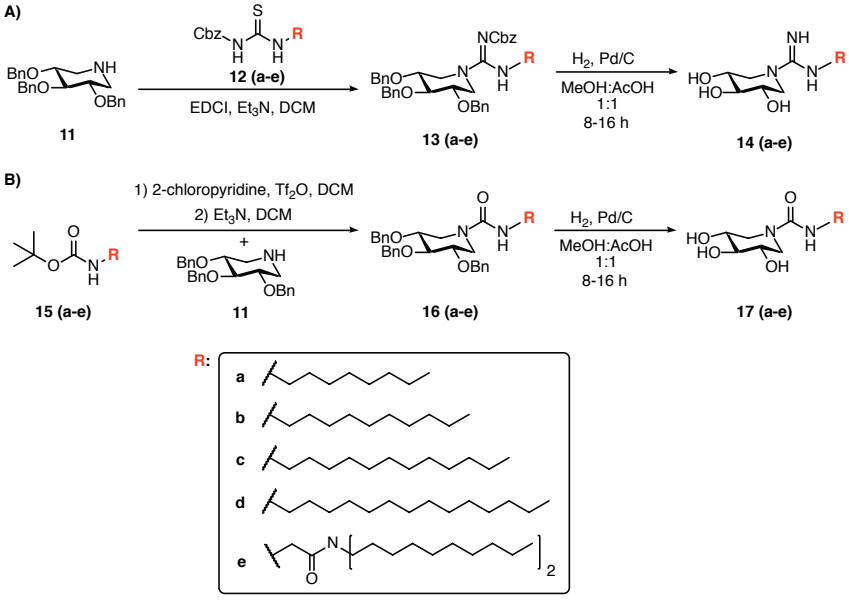

Scheme 2. Synthetic route employed in preparing 1,5-dideoxy-1,5-imino-D-xylitol derivatives with N^G-substituted guanidine (**14a-e**) and urea (**17a-e**) analogues.

3.2.2 *Stability experiments of guanidines **14a-e** and urea species **17a-e***

The kinetic stability evaluation for compounds **14a** and **17a** in aqueous solutions was studied by ultra-high performance liquid chromatography – mass spectrometry

(UHPLC-MS). A chemical stability experiment of compounds at pH 7.0 during a maximum period of time of 12 days proved that both, the guanidine **14a-e** and urea species **17a-e** are stable in aqueous solution even after long periods of time (**Table 1**).

t [h]	14a	17a	NNDNJ
0	100	100	100
24	100	100	100
54	100	100	100
85	100	100	100
310	100	100	100

Table 1. % of total peak area for compounds **14a** and **17a** at pH 7.0.

3.2.3 Enzyme inhibition studies

The inhibitory potencies of DIX derivatives **14a-e** and **17a-e** were determined against a panel of readily available glycosidase enzymes as well as the human recombinant enzymes *β*-glucocerebrosidase (GBA) and *β*-galactocerebrosidase (GALC). With the plant enzymes, low micromolar inhibition of the *β*-glycosidases was observed for **14a-e** whereas no inhibition was seen for the *α*-glycosidases, indicating an interesting preference (**Table 2**). The corresponding ureas were even more selective displaying inhibition of only the *β*-galactosidase from bovine liver. We further evaluated the compounds against human recombinant *β*-specific enzymes. Strikingly, potent inhibition was observed for guanidinium analogues **14a-e** against the human recombinant GBA with inhibition constants measured in the low nanomolar range (IC_{50}: 17-245 nM). Despite the observed *β*-selectivity, the guanidinium compounds did not inhibit the human recombinant galactose specific GALC, indicating a high degree of selectivity among the human enzymes. In contrast, urea species **17a-e** did not inhibit any of the human recombinant enzymes. Although the reason for the dramatic difference between the inhibition profile of the guanidine and urea analogues is not clear, the positive charge of the guanidinium group may point to an explanation. As can be seen in **Table 2**, the length of the lipid appended to the guanidine moiety also has some effect on the inhibition. The longer alkyl tails led to more potent inhibition. To confirm the validity of our assays, we measured the often-used reference compound NN-DNJ (**2**) and found it to have an IC_{50} for GBA of 750 nM, which is similar to previous reports.[32] Also of note is the pH dependence observed for GBA inhibition by compounds **14a-e**. In general, the IC_{50} values measured at pH 7.0 were two-to-three-fold lower than those measured at pH 5.2 (**Table 2**). To evaluate the effect of the substituted guanidinium groups in comparison to a simple N-alkylated analogue of DIX, we compared the C8 functionalized guanidine analogue **14a** with the previously reported N-alkylated DIX derivative **5** bearing a C9 lipid. Using similar assay conditions, we measured a near 7-fold lower IC_{50} value for compound **14a** (245 nM) relative to that reported for **5** (1500 nM).[32] Similar IC_{50} values were measured for NN-DNJ (**2**) in both studies indicating that the above comparison is legitimate.[32] While previous studies have indicated that N-alkylated DIX analogues are moderate glycosidase inhibitors,[30] our data indicate that incorporating an N-alkylated guanidino moiety can drastically improve inhibitor potency.

Enzyme	14a	14b	14c	14d	14e	17a	17b	17c	17d	17e	NNDNJ
α-glu[b]	> 100000	> 100000	> 100000	> 100000	> 100000	> 100000	> 100000	> 100000	> 100000	> 100000	> 100000
α-gal[c]	> 100000	> 100000	> 100000	> 100000	> 100000	> 100000	> 100000	> 100000	> 100000	> 100000	> 100000
β-glu[d]	38140±1470	26040±873	10730±281	2842±67	> 100000	> 100000	> 100000	> 100000	> 100000	> 100000	> 100000
β-gal[e]	24210±135	2754±218	677±44	1631±206	11620±4024	19570±1490	10440±884	12960±195	34200±189	12510±2924	> 100000
Nar[f]	52980±2192	41470±2129	37230±1668	33510±1680	3917±554	> 100000	> 100000	> 100000	> 100000	> 100000	176±12
GBA[g] (pH 7.0)	**244.5±20.2**	**33.3±4.0**	**19.6±2.6**	**19.2±2.6**	**16.9±2.4**	**> 10000**	**> 10000**	**> 10000**	**> 10000**	**> 10000**	**752±93**
GBA[g] (pH 5.2)	**999±92**	**93.2±7.2**	**37.9±2.7**	**36.1±2.3**	**38.1±5.2**	**> 10000**	**> 10000**	**> 10000**	**> 10000**	**> 10000**	**2564±287**
GALC[g]	> 10000	> 10000	> 10000	> 10000	> 10000	> 10000	> 10000	> 10000	> 10000	> 10000	> 10000

Table 2. Glycosidase inhibition values obtained for compounds **14a-e** and **17a-e**.[a]
[a]IC_{50} values are reported in nM and are averages obtained from triple independent duplicate analysis of each compound. For ease of comparison, the IC_{50} values obtained for all compounds shown in Table 2 are compared to a reference compound NNDNJ. [b]α-glucosidase (from baker's yeast, Sigma G5003): 0.05 U/mL, the activity was determined with p-nitrophenyl-α-D-glucopyranoside (0.7 mM final conc. in well) in sodium phosphate buffer (100 mM, pH 7.2). [c]α-galactosidase (from green coffee beans, Sigma G8507): 0.05 U/mL; α-galactosidase activity was determined with p-nitrophenyl-α-D-galactopyranoside (0.7 mM final conc. in well) in sodium phosphate buffer (100 mM, pH 6.8). [d]β-glucosidase (from almond, Sigma G4511): 0.05 U/mL; the activity was determined with p-nitrophenyl-β-D-glucopyranoside (0.7 mM final conc. in well) in sodium acetate buffer (100 mM, pH 5.0). [e]β-galactosidase (from bovine liver, Sigma G1875): 0.05 U/mL; activity was determined with p-nitrophenyl-β-D-galactopyranoside (0.7 mM final conc. in well) in sodium phosphate buffer (100 mM, pH 7.2). [f]Naringinase (from penicillium decumbens, Sigma N1385): 0.06 U/mL. the activity was determined with p-nitrophenyl-β-D-glucopyranoside (0.7 mM final conc. in well) in sodium acetate buffer (100 mM, pH 5.0). [g]β-glucocerebrosidase (GBA) and [g]β-galactocerebrosidase (GALC) activities were determined using 4-methylumbelliferyl-β-D-glucopyranoside and 4-methylumbelliferyl-β-D-galactopyranoside using assay conditions based on those previously reported, respectively.[43]

3.2.4 Fibroblast experiments

To investigate whether the inhibitory effect would translate into cellular pharmacological chaperone behavior, we examined the impact of compounds **14a-e** on GBA activity in Type 1 GD derived fibroblasts.

3.2.4.1 Cytotoxicity assay in wild-type GD derived fibroblasts

We first established that compounds **14a-e** were not toxic to wild-type human fibroblasts in the concentrations range to be used. Cells were seeded at a density of 10000 cells per well in 96-well plates. Media were renewed after 24 h and compounds were added to give final concentrations of **14a** and NNDNJ in 10-1-0,1-0,01 μM and **14b-e** tested from 1μM – 0,1μM. No toxicity was found for compounds **14a-e** at 1μM or lower.

3.2.4.2 Enzyme enhancement activity in human N370S fibroblasts

Patient derived cells were incubated with compounds **14a-e** or NN-DNJ (**2**) for 4 days followed by measurement of GBA activity. **Figure 3** summarizes the increase in GBA activity measured at various concentrations of compounds **14a-e** as well as NN-DNJ (**2**), included as a reference pharmacological chaperone. Although much research is still needed to fully determine their pharmacological chaperone function,[10] preliminary data from experiments using Gaucher patient-derived fibroblasts homozygous for N370S mutation, indicate that **14a** possesses a minor chaperone activity, somewhat weaker than the known chaperone NN-DNJ (**2**).

Treatment of the N370S cell line with 1000 nM of the N-octyl substituted compound **14a** resulted in a 1.2-fold increase of the GBA activity. This 20% enhancement was found to be lower than the approximate 60% increase in GBA activity measured for NN-DNJ (**2**) administered at the same 1000 nM concentration. In our fibroblast assays no significant increase in GBA enhancement was seen for compounds **14a** measured at a concentration of 1000 nM. The other bicyclic isoureas **14b-e** bearing longer lipids were found to be generally inhibitory of GBA activity at concentrations higher than 10 nM. These observations are also in line with the more potent inhibition observed for these compounds with the purified enzyme.

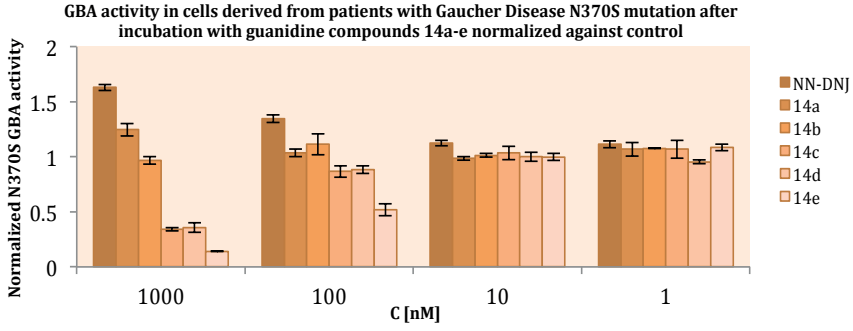

Figure 3. The effect of compounds **14a-e** on GBA activity in N370S fibroblasts (GM00372) from Gaucher patients. Cells were cultured for 4 days in the absence or presence of increasing concentrations (nM) of the compounds before GBA activity was measured. Experiments were performed in triplicate, and each bar represents the mean ± SD. Enzyme activity is normalized to untreated cells, assigned a relative activity of 1.

3.2.5 *Computational docking experiments*

To gain insight into the possible binding mode(s) of guanidinium compound **14a** within the GBA active site, molecular modeling was performed (**Figure 4A**). A comparison was made to the reported complex of NN-DNJ (**2**) (**Figure 4B**). It is clear that the guanidinium of **14a** is capable of making additional cation-π interactions with the nearby Tyr 313 in comparison to the smaller amino function of NN-DNJ (**2**). Furthermore, the guanidinium group engages in a hydrogen bond/salt bridge with nearby Glu 235 that has no counterpart in the structure of NN-DNJ (**2**). Both features likely contribute to the enhanced binding of **14a**. This enhanced binding was also the predicted outcome of the performed local docking simulation, which resulted in a calculated K_i of 155 nM for **14a** and of 1150 nM for NN-DNJ (**2**).

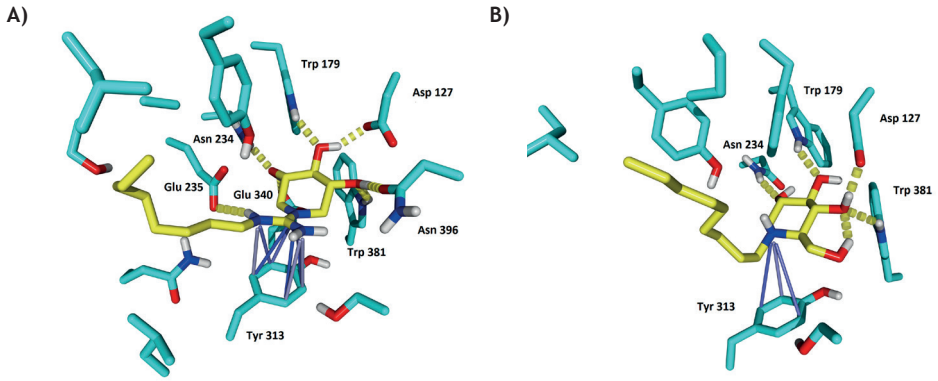

Figure 4. A) The polar interactions of compound **14a** (yellow carbon atoms) with GBA residues. In blue we see numerous cation-π interactions of the guanidinium group with Tyr 313. Dashed yellow lines are the hydrogen bonds from the sugar hydroxyl groups and the ion-ion interaction between the guanidinium group with Glu 235. **B)** The polar interactions of NN-DNJ (**2**, yellow carbon atoms) with GBA residues after docking and minimization. We see less interactions of NN-DNJ (**2**) with Tyr 313 and none with Glu 235.

3.3 CONCLUSIONS & OUTLOOK

In conclusion, we report a series of stable iminosugar based glycosidase inhibitors that contain either an exocyclic *N*-alkylated guanidinium or urea moiety. Interestingly, the DIX-derived ureas (**17a-e**) were selective inhibitors of *β*-galactosidase from bovine liver. By comparison, the guanidinium analogues (**14a-e**) were found to be highly selective inhibitors of the human *β*-glycosidase GBA. Our study clearly indicates that the addition of a guanidinium moiety leads to more potent inhibition of GBA when compared to the reported alkylated amine compound (**5**). The inhibitory potency is increased with longer alkyl substituents with the measured inhibition constants ranging from 245 nM to 19 nM for compounds **14a-d**. In addition, the bis-lipidated analogue **14e** served as a close substrate mimic for *β*-glucocerebrosidase and proved to be on par with our most potent inhibitors **14b-d** with an IC_{50} of 17 nM. Docking studies also point to additional cation-π_ interactions, as well as an extra hydrogen bond/salt bridge to the guanidinium group, as a plausible explanation for the enhanced glycosidase inhibition exhibited by **14a-e**. More comprehensive studies examining the potential for the DIX analogues reported here, to serve, as pharmacological chaperones will be reported in due course.

3.4 EXPERIMENTAL SECTION

3.4.1 General methods and materials

Reagents, Solvents and Solutions. Unless stated otherwise, chemicals were obtained from commercial sources and used without further purification. All solvents were purchased from Biosolve (Valkenswaard, The Netherlands) and were stored on molecular sieves (4 Å). 2,3,4-Tri-O-benzyl-5-des(hydroxymethyl)-1-deoxynojirimycin[37] (**11**), Cbz-NCS[33] and compounds **12a**[34], **13a**[34], **14a**[34] were prepared as previously described. The preparation of compounds **12e**[35], **13e**[35] and **14e**[35] required access to non-commercial amine building block **18**[35] that was prepared according to established literature procedures. Additionally, compounds **16a-d** and **17a-d** required access to Boc protected amines **15a-d** that were prepared according to established literature procedures.[40–42]

Purification Techniques. All reactions and fractions from column chromatography were monitored by thin layer chromatography (TLC) using plates with a UV fluorescent indicator (normal SiO_2, Merck 60 F254). One or more of the following methods were used for visualization: 10% H_2SO_4 in MeOH, molybdenum blue, $KMnO_4$ or ninhydrine followed by warming until spots could be visible detected under UV light. Flash chromatography was performed using Merck type 60, 230–400 mesh silica gel. Removal of solvent was performed under reduced pressure using a rotary evaporator.

Instrumentation for Compound Characterization. For LC–MS analysis, an HPLC system (detection simultaneously at 214, 254 nm and evaporative light detection) equipped with an analytical C_{18} column (100 Å pore size, 4.6 mm (⌀) x 250 mm (l), 10 µm particle size) or C_8 column (100 Å pore size, 4.6 mm (⌀) x 250 mm (l), 10 µm particle size) in combination with buffers A: H_2O, B: MeCN, A and B with 0.1% aqueous trifluoroacetic acid (TFA), in some cases - coupled with an electrospray interface (ESI) was used. For RP-HPLC purifications (detection simultaneously at /_213, 254 nm), an automated HPLC system equipped with a preparative C_{18} column (20 mm (⌀) x 250 mm (l), 5 µm particle size) or C_8 column (20 mm (⌀) x 250 mm (l), 5 µm particle size) in combination with buffers A: H_2O, B: MeCN, A and B with 0.1% aqueous trifluoroacetic acid (TFA). High-resolution mass spectra were recorded by direct injection (2 µL of a 2 µM solution in H_2O/MeCN 50:50 *v/v* and 0.1% formic acid) on a mass spectrometer. ^1H and ^{13}C NMR spectra were recorded on 500–125 MHz or 400–100 MHz spectrometers. Chemical shifts (δ) are given in ppm relative to tetramethylsilane (TMS) as internal standard. All ^{13}C NMR spectra are proton decoupled. ^1H NMR data are reported in the following order: number of protons, multiplicity (*s*, singlet; *d*, doublet; *t*, triplet; *q*, quartet and *m*, multiplet) and coupling constant (*J*) in Hertz (*Hz*). When appropriate, the multiplicity is preceded by *br*, indicating that the signal was broad. ^{13}C NMR spectra were recorded at 101 or 126 MHz with chemical shifts reported relative to $CDCl_3$ δ 77.0. ^{13}C NMR spectra were recorded using the attached proton test (APT) sequence. All literature compounds had ^1H NMR and mass spectra consistent with the assigned structures.

3.4.2 Preparative details and analytical data for synthesized compounds

3.4.2.1 General procedure for the synthesis of thiourea intermediates *12a-e*

The amine of choice (1.2 eq) was dissolved in CH_2Cl_2 (100 mL) and treated with a 0.5 M solution of CbzNCS in CH_2Cl_2 (1 eq) and NEt_3 (10 eq). After stirring for 12 h at room temperature, TLC analysis indicated complete conversion to thiourea species. The CH_2Cl_2 was then removed under reduced pressure, and the residue dissolved in chloroform, and applied directly to a silica column, eluting with EtOAc/hexanes. Analytical data and characterization data for compounds **12a-e** are given below.

N-(Benzyloxycarbonyl)-N'-(octyl) thiourea (12a).

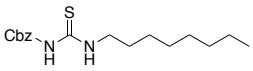

Compound **12a** is the same as compound **11a** from **Chapter 2** and was prepared according to the literature procedure.[34]

N-(Benzyloxycarbonyl)-N'-(decyl) thiourea (12b).

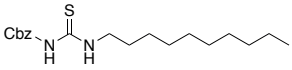

Compound **12b** is the same as compound **11b** from **Chapter 2** and was prepared according to the literature procedure.[35]

N-(Benzyloxycarbonyl)-N'-(dodecyl) thiourea (12c).

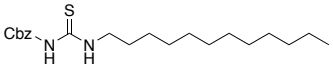

Compound **12c** is the same as compound **11c** from **Chapter 2** and was prepared according to the literature procedure.[35]

N-(Benzyloxycarbonyl)-N'-(tetradecyl) thiourea (12d).

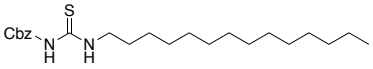

Compound **12d** is the same as compound **11d** from **Chapter 2** and was prepared according to the literature procedure.[35]

Benzyl 2-(didecylamino)-(2-oxoethyl)aminothionylcarbamate (12e).

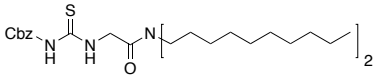

Compound **12e** is the same as compound **11e** from **Chapter 2** and was prepared according to the literature procedure.[35]

3.4.2.2 General procedure for the synthesis of benzyl protected N-guanidine-DIX compounds *13a-e*

Thioureas **12a-e** (1 eq), OBn-DIX (**11**, 1.05 eq) and EDCI (2 eq) were dissolved in CH_2Cl_2 (20 mL), followed by addition of NEt_3 (3 eq). The reaction mixture was stirred for 18h at room temperature, after which TLC analysis confirmed total consumption of starting material. The solvent was then removed under reduced pressure, and the residue, dissolved in $CHCl_3$, was applied directly to a silica column, eluting with hexanes and subsequently with EtOAc/hexanes. Analytical data and characterization data for compounds **13a-e** are given below.

Benzyl ((Z)-(octylamino)((2S, 3S, 4R)-3,4,5-tris(benyloxy)-2-((benzyloxy)methyl)-piperidin-1-yl)methylene)carbamate (13a).

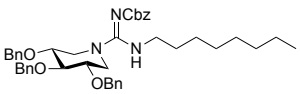

Yield: 320 mg, 59%. R_f (EtOAc/hexanes = 2:5) = 0.13. ^{1}H NMR (400 MHz, $CDCl_3$) δ 0.89 (t, *J* = 6.8 Hz, 3H), 1.16 – 1.38 (m, 10H), 1.39 – 1.52 (m, 2H), 2.75 (dd, *J* = 9.2, 13.1 Hz, 2H), 2.86 (td, *J* = 4.9, 6.9 Hz, 2H), 3.49 – 3.58 (m, 3H), 3.90 (dd, *J* = 4.0, 12.3 Hz, 2H), 4.64 (d, *J* = 11.6 Hz, 2H), 4.69 (d, *J* = 11.6 Hz, 2H), 4.86 (s, 2H), 5.12 (s, 2H), 7.23 – 7.44 (m, 20H), 8.32 (t, *J* = 5.1 Hz, 1H). ^{13}C NMR (101 MHz, $CDCl_3$) δ 165.0, 163.5, 138.7, 138.1, 137.3, 128.4, 128.3, 128.3, 128.04, 127.95, 127.88, 127.7, 127.6, 85.2, 77.4, 75.4, 73.0, 66.8, 49.3,

45.6, 31.7, 30.3, 29.1, 26.7, 22.6, 14.1. HRMS (ESI, $[M+H]^+$), calculated for $C_{43}H_{53}N_3O_5$, 692.4063; found, 692.4047.

Benzyl ((Z)-(decylamino)((2S, 3S, 4R)-3,4,5-tris(benyloxy)-2-((benzyloxy)methyl)-piperidin-1-yl)methylene)carbamate (13b).

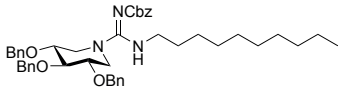

Yield: 365 mg, 63%. R_f (EtOAc/hexanes = 2:5) = 0.14. ^{1}H NMR (400 MHz, $CDCl_3$) δ 0.88 (t, *J* = 6.7 Hz, 3H), 1.18 – 1.38 (m, 14H), 1.40 – 1.51 (m, 2H), 2.75 (dd, *J* = 9.1, 13.1 Hz, 2H), 2.80 – 2.92 (m, 2H), 3.47 – 3.62 (m, 3H), 3.90 (dd, *J* = 3.6, 12.5 Hz, 2H), 4.64 (d, *J* = 11.6 Hz, 2H), 4.69 (d, *J* = 11.6 Hz, 2H), 4.86 (s, 2H), 5.12 (s, 2H), 7.19 – 7.52 (m, 20H), 8.32 (brs, 1H). ^{13}C NMR (101 MHz, $CDCl_3$) δ 165.0, 163.5, 138.6, 138.1, 137.3, 128.4, 128.32, 128.29, 128.0, 127.94, 127.88, 127.82, 127.7, 127.6, 85.2, 77.4, 75.4, 72.9, 66.7, 49.3, 45.6, 31.9, 30.3, 29.5, 29.4, 29.3, 29.1, 26.7, 22.7, 14.1. HRMS (ESI, $[M+H]^+$), calculated for $C_{45}H_{57}N_3O_5$, 720.4376; found, 720.4363.

Benzyl ((Z)-(dodecylamino)((2S, 3S, 4R)-3,4,5-tris(benyloxy)-2-((benzyloxy)methyl)-piperidin-1-yl)methylene)carbamate (13c).

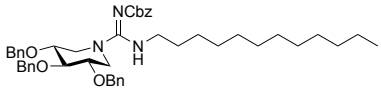

Yield: 491 mg, 76%. R_f (EtOAc/hexanes = 2:5) = 0.15. ^{1}H NMR (400 MHz, $CDCl_3$) δ 0.88 (t, *J* = 6.7 Hz, 3H), 1.15 – 1.36 (m, 18H), 1.43 – 1.53 (m, 2H), 2.75 (dd, *J* = 9.1, 13.0 Hz, 2H), 2.86 (td, *J* = 4.8, 6.9 Hz, 2H), 3.46 – 3.60 (m, 3H), 3.90 (dd, *J* = 3.6, 12.5 Hz, 2H), 4.64 (d, *J* = 11.7 Hz, 2H), 4.69 (d, *J* = 11.6 Hz, 2H), 4.86 (s, 2H), 5.12 (s, 2H), 7.34 (d, *J* = 56.8 Hz, 20H), 8.32 (t, *J* = 5.0 Hz, 1H). ^{13}C NMR (101 MHz, $CDCl_3$) δ 165.0, 163.5, 138.6, 138.1, 137.3, 128.4, 128.32, 128.29, 128.0, 127.94, 127.87, 127.81, 127.7, 127.6, 85.2, 77.4, 75.4, 72.9, 66.7, 49.3, 45.6, 31.9, 29.63, 29.61, 29.5, 29.4, 29.3, 29.2, 26.7, 22.7, 14.1. HRMS (ESI, $[M+H]^+$), calculated for $C_{47}H_{61}N_3O_5$, 748.4689; found, 748.4693.

Benzyl ((Z)-(tetradecylamino)((2S, 3S, 4R)-3,4,5-tris(benyloxy)-2-((benzyloxy)methyl)-piperidin-1-yl)methylene)carbamate (13d).

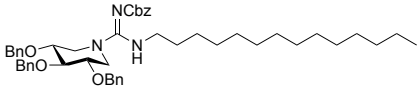

Yield: 610 mg, 91%. R_f (EtOAc/hexanes = 2:5) = 0.16. ^{1}H NMR (400 MHz, $CDCl_3$) δ 0.88 (t, *J* = 6.7 Hz, 3H), 1.14 – 1.37 (m, 22H), 1.44 – 1.53 (m, 2H), 2.75 (dd, *J* = 9.1, 13.1 Hz, 2H), 2.86 (td, *J* = 4.9, 6.9 Hz, 2H), 3.45 – 3.59 (m, 3H), 3.90 (dd, *J* = 3.7, 12.6 Hz, 2H), 4.64 (d, *J* = 11.6 Hz, 2H), 4.69 (d, *J* = 11.6 Hz, 2H), 4.86 (s, 2H), 5.12 (s, 2H), 7.21 – 7.47 (m, 20H), 8.32 (t, *J* = 4.9 Hz, 1H). ^{13}C NMR (101 MHz, $CDCl_3$) δ 165.0, 163.5, 138.6, 138.1, 137.3, 128.4, 128.32, 128.29, 128.0, 127.94, 127.87, 127.81, 127.7, 127.6, 85.2, 77.4, 75.4, 72.9, 66.7, 49.3, 45.6, 30.3, 29.68, 29.66, 29.64, 29.55, 29.4, 29.3, 29.2, 26.7, 22.7, 14.1. HRMS (ESI, $[M+H]^+$), calculated for $C_{49}H_{65}N_3O_5$, 776.5002; found, 776.5019.

Benzyl ((Z)-((2-(didecylamino)-2-oxoethyl)amino)((2S,3S,4R)-3,4,5-tris-(benzyloxy)-2-((benzyloxy)methyl)piperidin-1-yl)methylene)carbamate (13e).

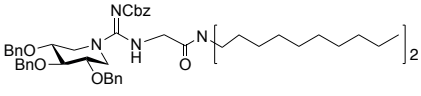

Yield: 247 mg, 75%. R_f (EtOAc/hexanes = 2:5) = 0.10. ^{1}H NMR (400 MHz, $CDCl_3$) δ 0.80 – 0.97 (m, 6H), 1.20 – 1.37 (m, 28H), 1.39 – 1.56 (m, 4H), 2.91 – 3.09 (m, 4H), 3.30 (t, *J* = 7.7 Hz, 2H), 3.54 – 3.61 (m, 3H), 3.90 (d, *J* = 3.1 Hz, 2H), 3.97 (dd, *J* = 3.7, 12.8 Hz, 2H), 4.63 (s, 4H), 4.77 (s, 2H), 5.14 (s, 2H), 6.85 (br s, 1H), 7.18 – 7.48 (m, 20H). ^{13}C NMR (101 MHz, $CDCl_3$) δ 167.0, 159.3, 138.5, 137.9, 128.4, 128.3, 128.2, 128.0, 127.8, 127.73, 127.70, 127.5, 83.8, 76.8, 74.6, 72.6, 66.6, 47.6, 46.5, 46.1, 44.3, 31.9, 31.8, 29.54, 29.51, 29.49, 29.4, 29.3, 28.5, 27.5, 27.0, 26.8, 22.7, 14.1. HRMS (ESI, $[M+H]^+$), calculated for $C_{57}H_{80}N_4O_6$, 917.6156; found, 917.6194.

*3.4.2.3 General procedure for Pd/C catalyzed hydrogenolysis for the synthesis of N-substituted guanidine compounds **14a-e***

The perbenzylated iminosugar was dissolved in a mixture of glacial AcOH in MeOH (1/1, v/v) and transferred to a Parr high-pressure hydrogenation flask. A catalytic amount of 10% palladium on carbon was added to the flask (ca. 10 mg catalyst/mg of benzylated starting material). The flask was put under reduced pressure and ventilated with hydrogen gas. This procedure was repeated twice after which the pressure was adjusted to 4.5-5.0 bar hydrogen pressure. The reaction was allowed to proceed for 6-12 h while mechanically shaken and the

pressure maintained at the value initially set. The mixture was filtered over Celite on a glass microfiber filter, followed by rinsing the filter with MeOH. The mixture was concentrated under reduced pressure. The crude products thus obtained were purified using RP-HPLC employing a preparative C8 column and an H_2O/MeCN gradient moving from 5% to 95% MeCN (0.1% TFA) over 60 min (flow rate, 18.0 mL/min). Product **14e** was purified using an H_2O/MeCN gradient moving from 50% to 95% MeCN (0.1% TFA) over 90 min (flow rate, 18.0 mL/min). Fractions containing the desired product were combined and lyophilized to yield the pure compounds as amorphous white powders. Analytical data for compounds **14a-e** and in-depth characterization data for all compounds are given below.

(2R,3R,4R,5S)-3,4,5-trihydroxy-2-(hydroxymethyl)-N-octylpiperidine-1-carboximidamide (14a).

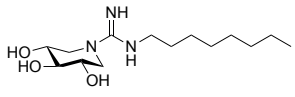

Yield: 10 mg, 86%. ^{1}H NMR (500 MHz, DMSO-d_6) δ 0.87 (t, J = 6.8 Hz, 3H), 1.19 – 1.36 (m, 10H), 1.42 – 1.58 (m, 2H), 2.89 (dd, J = 9.7, 13.3 Hz, 2H), 3.08 – 3.23 (m, 3H), 3.28 (d, J = 7.7 Hz, 2H), 3.69 (dd, J = 4.3, 12.9 Hz, 2H), 5.20 (s, 3H), 7.62 (s, 2H), 7.65 (t, J = 5.5 Hz, 1H). ^{13}C NMR (101 MHz, DMSO-d_6) δ 156.0, 77.5, 69.4, 49.9, 42.4, 31.6, 29.0, 29.0, 28.7, 26.5, 22.5, 14.4. HRMS (ESI, [M+H]$^+$), calculated for $C_{14}H_{29}N_3O_3$, 288.2287; found, 288.2320.

(2R,3R,4R,5S)-N-decyl-3,4,5-trihydroxy-2-(hydroxymethyl)piperidine-1-carboximidamide (14b).

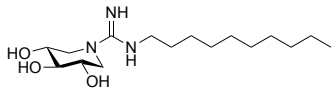

Yield: 12 mg, 81%. ^{1}H NMR (500 MHz, DMSO-d_6) δ 0.86 (t, J = 6.7 Hz, 3H), 1.19 – 1.34 (m, 14H), 1.42 – 1.56 (m, 2H), 2.89 (dd, J = 9.6, 13.3 Hz, 2H), 3.08 – 3.22 (m, 3H), 3.25 – 3.31 (m, 2H), 3.69 (dd, J = 4.3, 13.0 Hz, 2H), 5.18 (d, J = 4.6 Hz, 1H), 5.23 (d, J = 5.2 Hz, 2H), 7.62 (s, 2H), 7.66 (brs, 1H). ^{13}C NMR (101 MHz, DMSO-d_6) δ 156.0, 77.5, 69.4, 49.9, 42.4, 31.7, 29.4, 29.1, 29.1, 28.7, 26.5, 22.5, 14.4. HRMS (ESI, [M+H]$^+$), calculated for $C_{16}H_{33}N_3O_3$, 316.2600; found, 316.2539.

(2R,3R,4R,5S)-N-dodecyl-3,4,5-trihydroxy-2-(hydroxymethyl)piperidine-1-carboximidamide (14c).

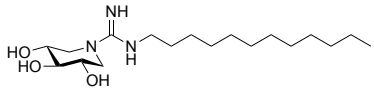

Yield: 8 mg, 87%. ^{1}H NMR (500 MHz, DMSO-d_6) δ 0.86 (t, J = 6.7 Hz, 3H), 1.19 – 1.34 (m, 18H), 1.43 – 1.54 (m, 2H), 2.89 (dd, J = 9.7, 13.3 Hz, 2H), 3.10 – 3.20 (m, 3H), 3.25 – 3.31 (m, 2H), 3.69 (dd, J = 4.3, 12.9 Hz, 2H), 5.19 (s, 3H), 7.62 (s, 3H). ^{13}C NMR (101 MHz, DMSO-d_6) δ 156.0, 77.5, 69.4, 49.9, 42.4, 31.7, 29.5, 29.44, 29.42, 29.37, 29.14, 29.06, 28.7, 26.5, 22.5, 14.4. HRMS (ESI, [M+H]$^+$), calculated for $C_{18}H_{37}N_3O_3$, 344.2913; found, 344.2853.

(2R,3R,4R,5S)-3,4,5-trihydroxy-2-(hydroxymethyl)-N-tetradecylpiperidine-1-carboximidamide (14d).

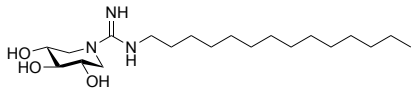

Yield: 9 mg, 83%. ^{1}H NMR (500 MHz, DMSO-d_6) δ 7.63, 5.24, 5.24, 5.18, 5.17, 3.71, 3.70, 3.69, 3.68, 3.29, 3.18, 3.17, 3.17, 3.16, 3.15, 3.15, 3.14, 3.13, 3.12, 2.91, 2.89, 2.88, 2.87, 1.49, 1.48, 1.47, 1.29, 1.27, 1.25, 1.24, 0.87, 0.86, 0.84. ^{13}C NMR (101 MHz, DMSO-d_6) δ 156.0, 77.5, 69.4, 49.9, 42.4, 31.7, 29.48, 29.47, 29.44, 29.42, 29.38, 29.13, 29.06, 28.7, 26.5, 22.5, 14.4. HRMS (ESI, [M+H]$^+$), calculated for $C_{20}H_{41}N_3O_3$, 372.3226; found, 372.3210.

N,N-didecyl-2-((2R,3R,4R,5S)-3,4,5-trihydroxy-2-(hydroxymethyl)piperidine-1-carboximidamido) acetamide (14e).

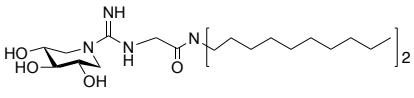

Yield: 16 mg, 92%. ^{1}H NMR (500 MHz, DMSO-d_6) δ 0.86 (t, J = 7.1 Hz, 6H), 1.17 – 1.38 (m, 28H), 1.40 – 1.48 (m, 2H), 1.48 – 1.57 (m, 2H), 2.96 (dd, J = 9.5, 13.3 Hz, 2H), 3.13 – 3.26 (m, 5H), 3.34 – 3.39 (m, 2H), 3.73 (dd, J = 4.3, 12.8 Hz, 2H), 4.08 (d, J = 5.7 Hz, 2H), 5.20 (d, J = 4.6 Hz, 1H), 5.26 (d, J = 5.2 Hz, 2H), 7.59 (t, J = 5.9 Hz, 1H), 7.71 (s, 2H). ^{13}C NMR (101 MHz, DMSO-d_6) δ 166.7, 157.1, 77.4, 69.4, 50.1, 46.7, 46.0, 43.9, 31.7, 29.42, 29.40, 29.38, 29.22, 29.19, 29.1, 28.6, 27.6, 26.8, 26.6, 22.5, 14.4. HRMS (ESI, [M+H]$^+$), calculated for $C_{28}H_{56}N_4O_4$, 513.4380; found, 513.4401.

*3.4.2.4 General procedure for the synthesis of Boc-amines **15a-d***

The amine of choice (1 eq) was dissolved in dry CH_2Cl_2 (50 mL) and NEt_3 (10 eq) was added to the solution at room temperature. Boc_2O (1.2 eq) was dissolved in 30 mL dry DCM and added to the mixture at 0°C. After stirring for 12 h at room temperature, TLC analysis indicated complete conversion of the starting material. The CH_2Cl_2 was then removed under reduced pressure, and the residue dissolved in EtOAc was then washed with 1 M HCl in water, saturated aq. $NaHCO_3$, and saturated aq. NaCl. The organic phase was dried over Na_2SO_4, filtered and concentrated under reduced pressure. Next, the residue was applied directly to a silica column, eluting with EtOAc/hexanes. Analytical data and characterization data for compounds **15a-c** are in accordance to previously published data. Analytical data and characterization data for compounds **15d-e** are given below.

***Tert*-butyl octylcarbamate (15a).**

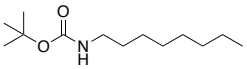

Compound **15a** was prepared according to the literature procedure.[41] Yield: 1.3 g, 92%. R_f(EtOAc/hexanes = 1:8) = 0.46

***Tert*-butyl decylcarbamate (15b).**

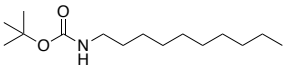

Compound **15b** was prepared according to the literature procedure.[42] Yield: 1.4 g, 97%. R_f(EtOAc/hexanes = 1:8) = 0.41.

***Tert*-butyl dodecylcarbamate (15c).**

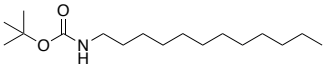

Compound **15c** was prepared according to the literature procedure.[40] Yield: 1.3 g, 87%. R_f(EtOAc/hexanes = 1:8) = 0.46.

***Tert*-butyl tetradecylcarbamate (15d).**

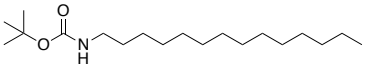

Yield: 1.5 g, 94%. R_f(EtOAc/hexanes = 1:8) = 0.6. ^{1}H NMR (400 MHz, $CDCl_3$) δ 0.88 (t, *J* = 6.6 Hz, 3H), 1.20 – 1.34 (m, 26H), 1.44 (s, 9H), 3.05 – 3.15 (m, 2H), 4.50 (s, 1H). 13C NMR (101 MHz, CDCl3) δ 146.7, 85.1, 40.6, 31.9, 30.0, 29.64, 29.63, 29.60, 29.54, 29.52, 29.31, 29.26, 28.4, 27.4, 26.8, 22.7, 14.1. HRMS (ESI, $[M+H]^+$), calculated for $C_{19}H_{39}NO_2$, 314.3059; found, 314.3038.

Tert-butyl (2-(didecylamino)-2-oxoethyl) carbamate (15e).

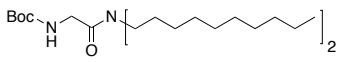

Compound **15e** is the same as compound **15** from **Chapter 2**. Boc-Gly-OH (0.88 g, 5 mmol, 1 eq) was dissolved in CH_2Cl_2 (60 mL). Didecylamine (1.64 g, 5.5 mmol, 1.1 eq) and EDCI (1.05 g, 5 mmol, 1 eq) were added and the reaction mixture was stirred for 24h. Consumption of starting material was confirmed with TLC analysis, followed by extraction with HCl (3x200 mL), sat. aq. $NaHCO_3$ (3x200 mL) and sat. aq. NaCl (200 mL). The combined organic phases were dried with Na_2SO_4, filtered and concentrated under reduced pressure. The residue was purified by silica gel column chromatography (EtOAc/hexanes = 4:1). Yield: 3.64 g, 92%. R_f(EtOAc/hexanes = 4:1) = 0.82. ^{1}H NMR (400 MHz, $CDCl_3$) δ 0.88 (2 x t, *J* = 7.1 Hz, 6H), 1.21 - 1.38 (m, 28H), 1.45 (s, 9H), 1.47 - 1.62 (m, 4H), 3.09 - 3.19 (m, 2H), 3.27 - 3.36 (m, 2H), 3.94 (d, *J* = 4.2 Hz, 2H), 5.57 (s, 1H). ^{13}C NMR (101 MHz, $CDCl_3$) δ 167.5, 155.8, 79.4, 77.3, 77.0, 76.7, 46.9, 46.1, 42.1, 31.83, 31.81, 29.50, 29.48, 29.4, 29.34, 29.28, 29.25, 29.2, 28.7, 28.3, 27.6, 26.94, 26.85, 22.6, 14.1. HRMS (ESI, $[M+H\text{-}Boc]^+$), calculated for $C_{27}H_{54}N_2O_3$, 355.3688; found, 355.3639.

3.4.2.5 *General procedure for the one-pot synthesis of benzyl protected ureas **16a-e** from Boc-protected amines **15a-e***

The Boc-protected amine of choice (**15a-e)** (1 eq), was dissolved in dry CH_2Cl_2 (20 mL), 2-chloropyridine (3 eq) was added, followed by the addition of triflic anhydride (1 M solution in methylene chloride, 1.5 eq). The reaction mixture was stirred for 12h at room temperature, after which TLC analysis confirmed total consumption of starting material into the isocyanate intermediate (EtOAc/hexanes = 1:8). Next, NEt_3 (10 eq) was added, followed by 2,3,4-Tri-O-benzyl-5-des(hydroxymethyl)-1-deoxynojirimycin (**11**, 1.2 eq) and the mixture was left stirring overnight at room temperature. The solvent was then removed under reduced pressure, and the residue, dissolved in $CHCl_3$, was applied directly to a silica column, eluting with hexanes and subsequently with EtOAc/hexanes gradient eluent. Analytical data and characterization data for compounds **16a-e** are given below.

(3S,4r,5R)-3,4,5-tris(benzyloxy)-N-octylpiperidine-1-carboxamide (16a).

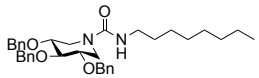

Yield: 321 mg, 84%. R_f (EtOAc/hexanes = 1:3) = 0.12 and (EtOAc/hexanes = 1:2) = 0.38. ^{1}H NMR (400 MHz, $CDCl_3$) δ 0.90 (t, *J* = 7.0 Hz, 3H), 1.20 – 1.33 (m, 10H), 1.35 – 1.44 (m, 2H), 2.71 (dd, *J* = 9.8, 13.1 Hz, 2H), 3.11 (td, *J* = 7.0, 13.1 Hz, 2H), 3.40 – 3.48 (m, 2H), 3.52 (t, *J* = 8.1 Hz, 1H), 3.87 (dd, *J* = 4.6, 13.1 Hz, 2H), 4.19 (br s, 1H), 4.66 (d, *J* = 11.6 Hz, 2H), 4.71 (d, *J* = 11.6 Hz, 2H), 4.86 (s, 2H), 7.22 – 7.38 (m, 15H). ^{13}C NMR (101 MHz, $CDCl_3$) δ 157.1, 138.7, 138.2, 128.4, 128.3, 128.0, 127.9, 127.8, 127.6, 85.0, 77.4, 75.3, 73.0, 46.3, 41.0, 40.6, 31.8, 31.8, 30.2, 30.1, 29.31, 29.29, 29.2, 26.9, 22.6, 14.1. HRMS (ESI, $[M+H]^+$), calculated for $C_{35}H_{46}N_2O_4$, 559.3536; found, 559.3520.

(3S,4r,5R)-3,4,5-tris(benzyloxy)-N-decylpiperidine-1-carboxamide (16b).

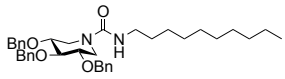

Yield: 292 mg, 73%. R_f (EtOAc/hexanes = 1:3) = 0.14 and (EtOAc/hexanes = 1:2) = 0.46. ^{1}H NMR (400 MHz, $CDCl_3$) δ 0.88 (t, *J* = 6.8 Hz, 3H), 1.20 – 1.33 (m, 14H), 1.34 – 1.45 (m, 2H), 2.71 (dd, *J* = 10.0, 13.1 Hz, 2H), 3.10 (td, *J* = 7.1, 13.0 Hz, 2H), 3.40 – 3.48 (m, 2H), 3.52 (t, *J* = 8.1 Hz, 1H), 3.86 (dd, *J* = 4.5, 12.7 Hz, 2H), 4.17 (br s, 1H), 4.64 (d, *J* = 11.6 Hz, 2H), 4.73 (d, *J* = 11.6 Hz, 2H), 4.86 (s, 2H), 7.24 – 7.38 (m, 15H). ^{13}C NMR (101 MHz, $CDCl_3$) δ 157.1, 138.7, 138.2, 128.4, 128.3, 128.0, 127.9, 127.8, 127.6, 85.0, 77.4, 75.3, 73.0, 46.3, 41.0, 31.9, 30.1, 29.6, 29.4, 29.3, 26.9, 22.7, 14.1. HRMS (ESI, $[M+H]^+$), calculated for $C_{37}H_{50}N_2O_4$, 587.3849; found, 587.3861.

(3S,4r,5R)-3,4,5-tris(benzyloxy)-N-dodecylpiperidine-1-carboxamide (16c).

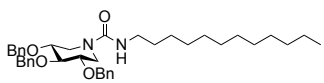

Yield: 313 mg, 78%. R_f (EtOAc/hexanes = 1:3) = 0.15 and (EtOAc/hexanes = 1:2) = 0.60. ^{1}H NMR (400 MHz, $CDCl_3$) δ 0.88 (s, *J* = 6.8 Hz, 3H), 1.17 – 1.33 (m, 18H), 1.32 – 1.46 (m, 2H), 2.72 (dd, *J* = 10.0, 13.3 Hz, 2H), 3.09 (td, *J* = 7.1, 12.8 Hz, 2H), 3.40 – 3.48 (m, 2H), 3.52 (t, *J* = 8.1 Hz, 1H), 3.85 (dd, *J* = 4.6, 12.6 Hz, 2H), 4.16 (brs, 1H), 4.66 (d, *J* = 11.4 Hz, 2H), 4.71 (d, *J* = 11.4 Hz, 2H), 4.86 (s, 2H), 7.24 – 7.38 (m, 15H). ^{13}C NMR (101 MHz, $CDCl_3$) δ 157.1, 138.7, 138.2, 128.4, 128.3, 128.0, 127.9, 127.8, 127.6, 85.0, 77.4, 75.3, 73.0, 46.3, 41.0, 31.9, 30.1, 29.64, 29.61, 29.60, 29.56, 29.4, 29.3, 26.9, 22.7, 14.1 HRMS (ESI, $[M+H]^+$), calculated for $C_{39}H_{54}N_2O_4$, 615.4162; found, 615.4171.

(3S,4r,5R)-3,4,5-tris(benzyloxy)-N-tetradecylpiperidine-1-carboxamide (16d).

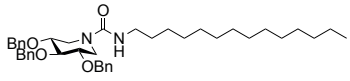

Yield: 291 mg, 81%. R_f (EtOAc/hexanes = 1:3) = 0.15 and (EtOAc/hexanes = 1:2.5) = 0.33. ^{1}H NMR (400 MHz, $CDCl_3$) δ 0.88 (t, *J* = 6.8 Hz, 3H), 1.18 – 1.34 (m, 22H), 1.32 – 1.47 (m, 2H), 2.71 (dd, *J* = 10.0, 13.2 Hz, 2H), 3.10 (dd, *J* = 6.0, 12.6 Hz, 2H), 3.44 (ddd, *J* = 4.7, 8.0, 10.0 Hz, 2H), 3.52 (t, *J* = 8.2 Hz, 1H), 3.86 (dd, *J* = 4.5, 13.2 Hz, 2H), 4.19 (t, *J* = 4.7 Hz, 1H), 4.64 (d, *J* = 11.6 Hz, 2H), 4.72 (d, *J* = 11.5 Hz, 2H), 4.86 (s, 2H), 7.21 – 7.39 (m, 15H). ^{13}C NMR (101 MHz, $CDCl_3$) δ 157.1, 138.7, 138.3, 128.4, 128.3, 128.0, 127.9, 127.8, 127.6, 85.0, 77.5, 77.3, 77.0, 76.7, 75.3, 73.0, 46.3, 41.0, 31.9, 30.2, 29.7, 29.67, 29.66, 29.64, 29.62, 29.58, 29.4, 29.3, 26.9, 22.7, 14.1. HRMS (ESI, $[M+H]^+$), calculated for $C_{41}H_{58}N_2O_4$, 643.4475; found, 643.4445.

(3S,4r,5R)-3,4,5-tris(benzyloxy)-N-(2-(didecylamino)-2-oxoethyl)piperidine-1-carboxamide (16e).

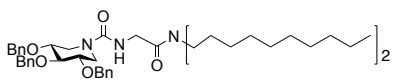

Yield: 355 mg, 89%. R_f (EtOAc/hexanes = 1:3) = 0.12 and (EtOAc/hexanes = 1:2) = 0.50. ^{1}H NMR (400 MHz, $CDCl_3$) δ 0.84 – 0.92 (m, 6H), 1.20 – 1.35 (m, 28H), 1.48 – 1.61 (m, 4H), 2.75 (dd, *J* = 9.5, 13.0 Hz, 2H), 3.16 (td, *J* = 8.1 Hz, 2H), 3.33 (td, *J* = 7.8 Hz, 2H), 3.45 – 3.57 (m, 3H),

4.00 (d, *J* = 3.5 Hz, 2H), 4.15 (dd, *J* = 3.7, 12.5 Hz, 2H), 4.70 (s, 4H), 4.85 (s, 2H), 5.72 (t, *J* = 3.6 Hz, 1H), 7.23 – 7.37 (m, 15H). ^{13}C NMR (101 MHz, $CDCl_3$) δ 168.1, 156.6, 138.7, 138.1, 128.4, 128.3, 127.9, 127.8, 127.7, 127.5, 85.5, 77.7, 75.3, 73.0, 46.8, 46.2, 46.0, 42.6, 31.84, 31.83, 29.53, 29.51, 29.49, 29.46, 29.4, 29.33, 29.26, 29.2, 28.7, 27.6, 27.0, 26.8, 22.6, 14.1. HRMS (ESI, $[M+H]^+$), calculated for $C_{49}H_{73}N_3O_5$, 784.5628; found, 784.5675.

*3.4.2.6 General procedure for Pd/C catalyzed hydrogenolysis for the synthesis of N-substituted urea compounds **17a-e***

Similarly to the guanidine compounds **14a-e**, the urea analogs **17a-e** were prepared using the same procedure to perform the final deprotection step. Analytical data and in-depth characterization data for urea compounds **17a-e** are given below.

(3S,4r,5R)-3,4,5-trihydroxy-N-octylpiperidine-1-carboxamide (17a).

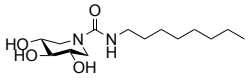

Yield: 16 mg, 88%. ^{1}H NMR (500 MHz, DMSO-d_6) δ 6.49, 6.48, 6.47, 4.88, 4.87, 4.82, 4.81, 3.89, 3.88, 3.86, 3.85, 3.10, 3.09, 3.08, 3.07, 3.07, 3.06, 3.05, 3.04, 2.97, 2.96, 2.95, 2.94, 2.93, 2.91, 2.38, 2.36, 2.36, 2.34, 1.36, 1.34, 1.33, 1.31, 1.27, 1.25, 1.22, 1.19, 1.17, 0.85, 0.84, 0.82. ^{13}C NMR (101 MHz, DMSO-d_6) δ 157.5, 79.6, 70.0, 48.7, 31.7, 30.2, 29.2, 29.1, 26.8, 22.5, 14.4. HRMS (ESI, $[M+H]^+$), calculated for $C_{14}H_{28}N_2O_4$, 289.2127; found, 289.2129.

(3S,4r,5R)-N-decyl-3,4,5-trihydroxypiperidine-1-carboxamide (17b).

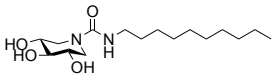

Yield: 12 mg, 85%. ^{1}H NMR (500 MHz, DMSO-d_6) δ 0.86 (t, *J* = 6.7 Hz, 3H), 1.17 – 1.31 (m, 14H), 1.31 – 1.40 (m, 2H), 2.38 (dd, *J* = 10.5, 12.9 Hz, 2H), 2.90 – 3.01 (m, 3H), 3.04 – 3.14 (m, 2H), 3.89 (dd, *J* = 4.9, 12.5 Hz, 2H), 4.83 (d, *J* = 4.5 Hz, 1H), 4.89 (d, *J* = 4.9 Hz, 2H), 6.50 (t, *J* = 5.4 Hz, 1H). ^{13}C NMR (101 MHz, DMSO-d_6) δ 157.5, 79.6, 70.0, 48.7, 39.3, 31.7, 30.2, 29.5, 29.4, 29.3, 29.1, 26.8, 22.5, 14.4. HRMS (ESI, $[M+H]^+$), calculated for $C_{16}H_{32}N_2O_4$, 317.2440; found, 317.2458.

(3S,4r,5R)-N-dodecyl-3,4,5-trihydroxypiperidine-1-carboxamide (17c).

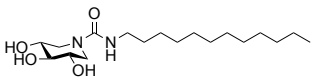

Yield: 11 mg, 82%. ^{1}H NMR (500 MHz, DMSO-d_6) δ 0.85 (t, *J* = 6.7 Hz, 3H), 1.16 – 1.31 (m, 18H), 1.31 – 1.44 (m, 2H), 2.38 (dd, *J* = 10.5, 12.9 Hz, 2H), 2.89 – 3.03 (m, 3H), 3.03 – 3.17 (m, 2H), 3.89 (dd, *J* = 4.8, 12.5 Hz, 2H), 4.88 (s, 3H), 6.50 (t, *J* = 5.4 Hz, 1H). ^{13}C NMR (101 MHz, DMSO-d_6) δ 157.5, 79.6, 70.0, 48.7, 31.7, 30.2, 29.49, 29.46, 29.45, 29.3, 29.1, 26.8, 22.5, 14.4. HRMS (ESI, $[M+H]^+$), calculated for $C_{18}H_{36}N_2O_4$, 345.2753; found, 345.2771.

(3S,4r,5R)-3,4,5-trihydroxy-N-tetradecylpiperidine-1-carboxamide (17d).

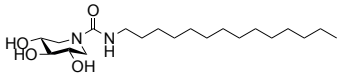

Yield: 12 mg, 79%. ^{1}H NMR (500 MHz, DMSO-d_6) δ 0.85 (t, *J* = 6.7 Hz, 3H), 1.16 – 1.31 (m, 22H), 1.31 – 1.44 (m, 2H), 2.38 (dd, *J* = 11.7 Hz, 2H), 2.90 – 3.02 (m, 3H), 3.03 – 3.16 (m, 2H), 3.89 (dd, *J* = 4.8, 12.8 Hz, 2H), 4.83 (d, *J* = 4.5 Hz, 1H), 4.89 (d, *J* = 4.8 Hz, 2H), 6.50 (t, *J* = 5.4 Hz, 1H). ^{13}C NMR (101 MHz, DMSO-d_6) δ 157.5, 105.0, 79.6, 70.0, 48.7, 31.7, 30.2, 29.48, 29.45, 29.4, 29.3, 29.1, 26.8, 22.5, 14.4. HRMS (ESI, $[M+H]^+$), calculated for $C_{20}H_{40}N_2O_4$, 373.3066; found, 373.3066.

(3S,4r,5R)-N-(2-(didecylamino)-2-oxoethyl)-3,4,5-trihydroxypiperidine-1-carboxamide (17e).

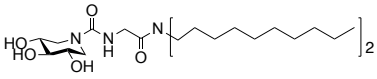

Yield: 11 mg, 82%. ^{1}H NMR (500 MHz, DMSO-d_6) δ 0.85 (t, *J* = 6.7 Hz, 6H), 1.14 – 1.33 (m, 28H), 1.37 – 1.46 (m, 2H), 1.44 – 1.55 (m, 2H), 2.43 (dd, *J* = 10.5, 13.0 Hz, 2H), 2.93 – 3.04 (m, 1H), 3.07 – 3.15 (m, 2H), 3.18 (t, *J* = 7.7 Hz, 4H), 3.77 (d, *J* = 5.4 Hz, 2H), 3.89 (dd, *J* = 4.9, 12.7 Hz, 2H), 4.87 (d, *J* = 4.4 Hz, 1H), 4.91 (d, *J* = 4.8 Hz, 2H), 6.58 (t, *J* = 5.5 Hz, 1H). ^{13}C NMR (101 MHz, DMSO-d_6) δ 169.2, 157.5, 105.0, 79.5, 69.9, 48.7, 46.6, 45.8, 42.2, 31.7, 29.39, 29.36, 29.24, 29.17, 29.1, 28.8, 27.7, 26.8, 26.6, 22.5, 14.4. HRMS (ESI, $[M+H]^+$), calculated for $C_{28}H_{55}N_3O_5$, 514.4220; found, 526.4239.

3.4.2.7 *Synthesis of bis-lipidated compound 18*

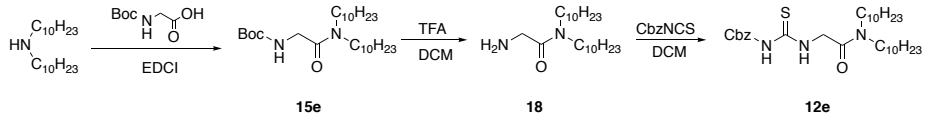

Scheme 3. Synthetic route towards thiourea compound **12e**.

2-amino-*N*,N-didecylacetamide (18).

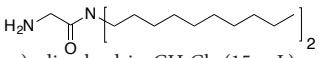

According to previously reported literature procedure.[35] TFA (15 mL) was added to previously isolated **15e** (3.27 g, 7.19 mmol, 1 eq), dissolved in CH_2Cl_2 (15 mL) and stirred for 24 h at room temperature. After consumption of starting material was observed with TLC, the residue was purified by flash column chromatography to obtain a yellow oil which was concentrated and co-evaporated with $CHCl_3$. Yield: 2.55 g, quant. yield, R_f (EtOAc/hexanes = 8:1) = 0.12. ^{1}H NMR (400 MHz, $CDCl_3$) δ 0.88 (2 x t, J = 7.0 Hz, 6H), 1.18 - 1.38 (m, 28H), 1.40 - 1.69 (m, 4H), 3.12 (t, J = 7.7 Hz, 2H), 3.30 (t, J = 7.6 Hz, 2H), 3.87 (s, 2H), 8.21 (s, 2H). ^{13}C NMR (101 MHz, $CDCl_3$) δ 164.9, 77.3, 77.0, 76.7, 47.2, 46.5, 40.0, 31.9, 31.8, 29.5, 29.44, 29.41, 29.34, 29.28, 29.21, 29.17, 28.3, 27.2, 26.9, 26.7, 22.63, 22.61, 14.0. HRMS (ESI, $[M+H]^+$), calculated for $C_{22}H_{46}N_2O$, 355.3688; found, 355.3633.

3.4.2.8 *Synthetic route for OBn protected DIX building block 11*

The synthetic route towards OBn proceted DIX building block is depicted in **Scheme 4**. First, commercially available D-xylopyranose **19** was treated with NaH and BnBr to yield 2,3,4-O-tribenzyl-D-xylopyranose (**20**). Next, treatment of **20** with sulfuric and acetic acids in dioxane selectively deprotected the anomeric benzyl group to yield compound **21**. The addition of allylamine in the presence of camphor-10-sulfonic acid and Na_2SO_4 gave compound **22**, which was then reduced with $LiAlH_4$ and immediately reacted with DEAD and PPh_3 to obtain the cyclized product **23**. Treatment of **23** with *t*BuOK as a base under reflux conditions with subsequent aqueous hydrochloric acid afforded 2,3,4-O-tribenzyl-1,5-dideoxy-1,5-iminoxylitol (**24**).

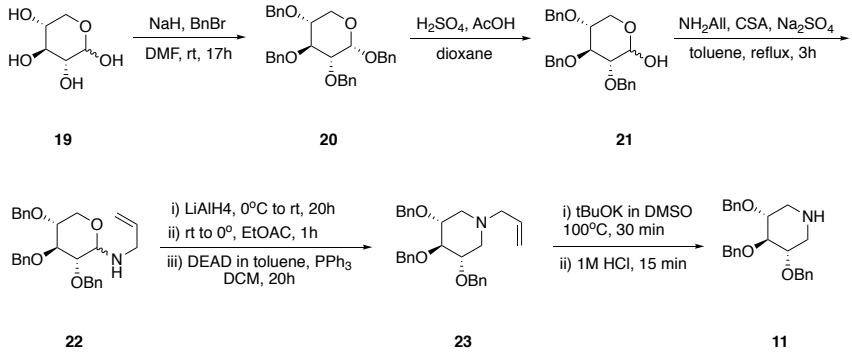

Scheme 4. Synthetic route towards OBn protected DIX species **11**.

(3S,4R)-2,3,4,5-tetrakis(benzyloxy)tetrahydro-2H-pyranose (20).

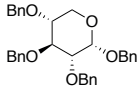

The compound was prepared according to previously published procedure.[37] D-xylose (**19**, 10 g, 0.066 mol, 1 eq) was dissolved in dry DMF (333 mL) and cooled to 0°C. NaH (60% in mineral oil, 18 g, 0.45 mol, 6.76 eq) was added carefully. The reaction mixture was stirred for 3h. BnBr (34 mL, 0.29 mol, 4.30 eq) was added drop-wise during the period of 30 min. The reaction mixture was stirred for 20 h at rt to obtain a dark brown mixture. Next, the reaction mixture was quenched with H_2O and a color change to orange was detected. The solvent was carefully removed under reduced pressure, followed by extraction with Et_2O (600 mL) and H_2O (700 mL). Organic

phases were combined, washed successively with a saturated aqueous solution of NaCl (200 mL), dried with Na_2SO_4 and concentrated under reduced pressure. TLC analysis confirmed complete consumption of starting material. The crude product was used in the next step without further purification. R_f: 0.75 (EtOAc:PE = 1:3).

(3S,5R)-3,4,5-tris(benzyloxy)tetrahydro-2H-pyran-2-ol (21).

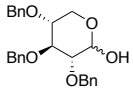

The compound was prepared according to a previously published procedure.[37] A suspension of crude compound **20** (38 g) in mixture of 1M HCl (93 mL) and AcOH (210 mL) was prepared and refluxed for 5h, after which TLC analysis confirmed complete consumption of the starting material. Solvent was removed under reduced pressure and the reaction mixture was co-evaporated with toluene (4 x 200 mL). Furthermore, the crude product was dissolved in a saturated aqueous solution of $NaHCO_3$ (650 mL) and extracted with EtOAc (4 x 300 mL). Combined organic phases were dried with Na_2SO_4 and concentrated. Next, the product was precipitated from solvent system (EtOAc/PE). Solid particles were filtered, washed with PE (300 mL) and dried under reduced pressure. The crude product was used in the next step without further purification. R_f: 0.18 (EtOAc:PE = 1:3).

(3S,4R)-N-allyl-3,4,5-tris(benzyloxy)tetrahydro-2H-pyran-2-amine (22).

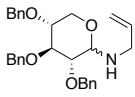

Camphor-10-sulfonic acid (5.61 g, 0.024 mol , 1 eq), Na_2SO_4 (16.46 g, 0.12 mol, 4.8 eq) and **21** (10 g, 0.025 mol, 1 eq) were suspended in toluene (240 mL). Allylamine (18 mL, 0.24 mol, 10 eq) was added and reaction mixture was refluxed for 4 h. Next, TLC analysis indicated complete consumption of starting material. After the residue was cooled to rt and dissolved in EtOAc (500 mL), it was extracted with a saturated aqueous solution of $NaHCO_3$ (500 mL). Organic phases were combined, successively washed with saturated aqueous solution of NaCl (500 mL), dried with Na_2SO_4 and concentrated. Crude product was subjected to the next step without further purification. R_f: 0.64 (EtOAc:PE, 1:3). A small sample was purified for characterization, which was in accordance with previously published data.[37] R_f = 0.61 (25% EtOAc in PE). ^{1}H NMR (400 MHz, $CDCl_3$) δ 7.39 – 7.22 (m, 15H), 5.96 – 5.80 (m, 1H), 5.24 – 5.01 (m, 2H), 4.96 – 4.56 (m, 6H), 4.46 (d, *J* = 4.0, 1H), 3.93 (d, *J* = 8.5, 1H), 3.91 – 3.12 (m, 7H), 1.96 (s, 1H, NH). ^{13}C NMR (100 MHz, $CDCl_3$) δ 138.9, 138.8, 138.6, 138.6, 138.4, 138.3, 136.9, 136.8, 128.6, 127.7, 115.9, 115.8, 90.8, 85.2, 84.4, 81.9, 79.4, 79.0, 78.6, 77.3, 75.8, 75.2, 74.8, 73.4, 73.3, 72.8, 65.1, 60.4, 48.6, 48.2. MS (ESI, $[M+H]^+$), calculated for $C_{29}H_{33}NO_4$, 460.2; found 460.4.

(3R,4R)-1-allyl-3,4,5-tris(benzyloxy)piperidine (23).

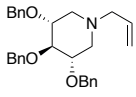

The compound was prepared according to previously published procedure.[37] Crude product **22** (14.3 g, 0.031 mol, 1 eq) was suspended in dry THF (952 mL) under a N_2 atmosphere. $LiAlH_4$ (3.55 g, 0.093 mol, 3 eq) was added carefully and stirred for 20 h, after which TLC analysis indicated complete consumption of starting material. Next, the reaction mixture was carefully quenched with EtOAc (300 mL) at 0°C and was stirred for additional 2 h. Furthermore, the reaction mixture was poured into a mixture of saturated aqueous solution of NH_4Cl (500 mL) and saturated aqueous NaCl (500 mL). The mixture was then extracted with EtOAc (3 x 300 mL). Combined organic phases were dried with Na_2SO_4 and concentrated. R_f: 0.33 (EtOAc + 2%NH_4OH). The crude product was used in the next step without further purification. Thus prepared crude intermediate (13 g, 0.029 mol, 1 eq) was suspended in dry DCM (286 mL) under a N_2 atmosphere, followed by addition of PPh_3 (8.34 g, 0.032 mol, 1.1 eq). Furthermore, DEAD (4.99 mL, 0.032 mol, 1.1 eq) in toluene (92 mL) was added drop wise and reaction mixture was stirred for 21 h. TLC analysis indicated complete consumption of starting material. Next, the reaction mixture was quenched with water (50 mL) and poured into DCM (20 mL), followed by extraction with water (250 mL). The combined organic phases were dried with Na_2SO_4 and concentrated. The remaining residue was purified by silica gel column chromatography (toluene » EtOAc:toluene = 1:4). Characterization data for compound **23** was in accordance with previously published data.[37] R_f = 0.73 (1:4; EtOAc:PE). ^{1}H NMR (400 MHz, $CDCl_3$) δ 7.40 – 7.21 (m, 15H), 5.79 (ddt, *J* = 6.5, 10.2, 16.8, 1H), 5.19 – 5.08 (m, 2H), 4.88 (s, 2H), 4.70 (d, *J* = 11.6, 2H), 4.64 (d, *J* = 11.6, 2H), 3.64 – 3.54 (m, 2H), 3.41 (dd, *J* = 8.7, 1H), 3.07 (dd, *J* = 3.7, 10.8, 2H), 3.01 (d, *J* = 6.5, 2H), 1.94 (t, *J* = 10.8, 2H). ^{13}C NMR (100 MHz, $CDCl_3$) δ 139.2, 138.7, 134.5, 128.7, 128.5, 128.4, 128.2, 128.1, 128.0, 127.9, 127.8, 127.7, 127.6, 127.5, 118.4, 86.4, 78.8, 75.5, 73.17, 73.14 60.9, 56.1. MS (ESI, $[M+H]^+$), calculated for $C_{29}H_{33}NO_3$, 444.3; found 444.3.

2,3,4-Tri-O-benzyl-5-des(hydroxymethyl)-1-deoxynojirimycin (10).

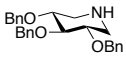

According to the literature procedure,[37] potassium *tert*-butoxide (32 mg, 0.29 mmol) was added to a solution of **23** (170 mg, 0.38 mmol) in DMSO (2 mL) and the resulting brown reaction mixture was heated at 100 °C for 30 minutes. The reaction mixture was charged with a 1M aqueous solution of HCl (2 mL) and stirred vigorously for 15 minutes. The mixture was poured into saturated aqueous $NaHCO_3$ (50 mL) and extracted with Et_2O (3×50 mL). The organic phase was isolated, dried over Na_2SO_4 and concentrated under reduced pressure. The residue was purified by silica gel column chromatography (33% » 100% EtOAc in PE + 2% NH_4OH) to produce **10** as yellow oil. Characterization data for compound **10** was in accordance with previously published data. Yield: 106 mg, 69%, R_f (EtOAc + 2% NH_4OH) = 0.72. ^1H NMR (400 MHz, CD_3OD) δ 1.51 (s, 1H), 2.48 (dd, *J* = 9.8, 12.3 Hz, 2H), 3.20 (dd, *J* = 4.8, 12.3 Hz, 2H), 3.35 – 3.58 (m, 3H), 4.60 – 4.76 (m, 4H), 4.88 (s, 2H), 7.16 – 7.44 (m, 15H). ^{13}C NMR (100 MHz, CD_3OD) δ 139.0, 138.6, 128.4, 128.3, 128.0, 127.7, 127.6, 127.5, 85.8, 79.8, 77.3, 77.0, 76.7, 75.5, 72.9, 49.2. HRMS (ESI, $[M+H]^+$), calculated for $C_{26}H_{29}NO_3$, 404.2226; found 404.2226.

3.4.3 Kinetic evaluation experimental details

Chemicals and Chromatography

Acetonitrile (ACN; LC-MS Chromasolv) was purchased from Biosolve BV (Valkenswaard, The Netherlands). Formic acid (FA; LC-MS grade) and ammonium acetate were acquired from Sigma-Aldrich (St. Louis, MA, USA). Ultra-pure water was obtained from a Synergy UV water delivery system from Millipore (Billerica, MA, USA). Buffer solutions of 200 mM ammonium acetate (pH 7.0) were prepared in ultra-pure water. Standard solutions of 1 mM guanidine **14a** and urea representative **17a** were prepared in buffer solution with pH 7.0. All experiments were achieved on a Zorbax Eclipse plus C_{18} column (4.6 x 50 mm, 1.8 µm particles). A 2-µL injection volume was used of all samples. UHPLC was performed on a 1290 Infinity UHPLC system (Agilent Technologies, Wald-bronn, BW, Germany) consisting of a binary pump and an autosampler. The optimal separation was achieved with a binary gradient with 0.5% FA (% v/v) in water (eluent A) and ACN (eluent B) at a flow rate of 0.5 mL/min. Detection was performed on a quadrupole-time-off-flight mass spectrometer, equipped with an electrospray ionization source (Bruker Daltonics, Bremen, HB, Germany). Masses were acquired from *m/z* 50-700 at a spectra rate of 1.5 Hz, nebulizer pressure was 4 bar, gas flow was 10 L/min, gas temperature was 2000 °C and capillary voltage was 3 kV. Guanidine compound **14a** and urea compound **17a** were detected as positive ions ($[M+H]^+$).

3.4.3.1 Stability indicating method procedure

The kinetic stability evaluation for compounds **14a** and **17a** in aqueous solutions was studied by ultra-high performance liquid chromatography – mass spectrometry (UHPLC-MS). A stability indicating method was developed and used to test the chemical stability of the compounds at pH 7.0 during a maximum period of time of 12 days. Both, guanidine representative **14a** and urea compound **17a**, proved to be stable compounds. The data reported in **Table 1** shows the values in % of total peak area for compounds **14a** and **17a** at pH 7.0 in researched time point. There was no degradation obtained for both sets of compounds even after 12 days.

3.4.4 Biological evaluation against commercial glycosidases

3.4.4.1 Inhibition assays against commercial glycosidases, human recombinant GBA (R&D 7410-GH) and human recombinant GALC (R&D 7310-GH)

Inhibition assays against commercial glycosidases were performed in either phosphate or acetate buffer at the optimum pH for each enzyme (See below for enzyme specific data). Determination of the IC_{50} values of the iminosugars was carried out by spectrophotometrically measuring the residual hydrolytic activities of the glycosidases on the corresponding p-nitrophenyl glycoside substrates in the presence of a concentration range of iminosugar derivatives. The incubation mixture consisted of 50 μL of inhibitor solution in buffer (0.1 U mL^{-1}) and 50 μL of enzyme solution. The concentrations of the enzyme were adjusted so that the reading for the final absorbance was in the range of 0.5–1.5 units. Inhibitor and enzyme solutions were mixed in a disposable 96-well microtiter plate and then incubated at room temperature for 5 minutes. Next, the reactions were initiated by addition of 50 μL of a solution of the corresponding p-nitrophenyl glycoside substrates solution in the appropriate buffer at the optimum pH for the enzyme. After the reaction mixture was incubated at 37 ^{0}C for 30 min, the reaction was quenched with 0.5 M Na_2CO_3 (150 μL) and the absorbance of 4-nitrophenol released from the substrate was read immediately at 405 nm using a BioTek mQuant Microplate Spectrophotometer. IC_{50} values were determined graphically with GraphPad Prism (version 6.0) by making a plot of percentage inhibition versus the log of inhibitor concentration, using at least 8 different inhibitor concentrations. IC_{50} values were presented as a concentration of the iminosugars that inhibits 50% of the enzyme activity under the assay conditions. NN-DNJ (**2**) was used as a reference compound. All materials were purchased from Sigma-Aldrich.

The commercial glycosidase solutions were prepared as following:

[b]For **α-glucosidase** (from *baker's yeast,* Sigma G5003, 0.05 U/mL) the activity was determined with p-nitrophenyl-α-D-glucopyranoside (0.7 mM final conc. in well) in sodium phosphate buffer (100 mM, pH 7.2). [c]For **α-galactosidase** (from *green coffee beans*, Sigma G8507, 0.05 U/mL) activity was determined with p-nitrophenyl-α-D-galactopyranoside (0.7 mM final conc. in well) in sodium phosphate buffer (100 mM, pH 6.8). [d]For **β-glucosidase** (from *almond*, Sigma G4511, 0.05 U/mL) the activity was determined with p-nitrophenyl-β-D-glucopyranoside (0.7 mM final conc. in well) in sodium acetate buffer (100 mM, pH 5.0). [e]For **β-galactosidase** (from *bovine liver*, Sigma G1875, 0.05 U/mL) activity was determined with p-nitrophenyl-β-D-galactopyranoside (0.7 mM final conc. in well) in sodium phosphate buffer (100 mM, pH 7.2). [f]For **Naringinase** (from *penicillium decumbens,* Sigma N1385, 0.06 U/mL) the activity was determined with p-nitrophenyl-β-D-glucopyranoside (0.7 mM final conc. in well) in sodium acetate buffer (100 mM, pH 5.0). [g]**Recombinant Human Glucosylceramidase/β-glucocerebrosidase/GBA** (7410-GH), purchased from R&D was also used in the inhibition studies. The used substrate 4-methylumbelliferyl-β-D-glucopyranoside was purchased by Sigma-Aldrich. GBA activity was determined with 4-methylumbelliferyl-β-D-glucopyranoside as reported in (A. Trapero, J. Med. Chem. 2012, 55, 4479-4488).[43] Briefly, enzyme solutions (25 μL from a stock solution containing 0.6 μg/mL) in the presence of 0.25% (w/v) sodium taurocholate and 0.1% (v/v) Triton X-100 in Mcllvaine buffer (100 mM sodium citrate and 200 mM sodium phosphate buffer, pH 5.2 or pH 7.0) were incubated at 37°C without (control) or with inhibitor at a final volume of 50 μL for 30 min. After addition of 25 μL 4-methylumbelliferyl-β-D-glucopyranoside (7.2 mM, Mcllvaine buffer pH 5.2 or pH 7.0), the samples were incubated at 37°C for 10 min. Enzymatic reactions were stopped by the addition of aliquots (100 μL) of Glycine/NaOH buffer (100 mM, pH 10.6). The amount of 4-methylumbelliferone formed was determined with a FLUOstar microplate reader (BMG Labtech) at / 355 nm (excitation) and / 460 nm (emission). [g]**Recombinant Human Galactosylceramidase/GALC** (7310-GH), purchased from R&D was used in the inhibition studies. The used substrate 4-methylumbelliferyl-β-D-galactopyranoside was purchased by Sigma-Aldrich. GALC activity was determined with 4-methylumbelliferyl-β-D-galactopyranoside as reported in assay procedure R&D product 7310-GH. Briefly, enzyme solutions (25 μL from a stock solution containing 60 ng/mL) in the presence of 0.5% (v/v) Triton X-100 in Assay buffer (50 mM sodium citrate and 125 mM NaCl, pH 4.5) were incubated at 37°C without (control) or with inhibitor at a final volume of 50 μL for 10 min. After addition of 25 μL 4-methylumbelliferyl-β-D-galactopyranoside (0.75mM, Assay buffer), the samples were incubated at 37°C for 20 min. Enzymatic reactions were stopped by the addition of aliquots (50 μL) of Glycine/NaOH buffer (100 mM, pH 10.6). The amount of 4-methylumbelliferone formed was determined with a FLUOstar microplate reader (BMG Labtech) at / 355 nm (excitation) and / 460 nm (emission).

3.4.4.2 IC_{50} curves for compounds 14a-e and NNDNJ against human recombinant GBA (R&D 7410-GH)

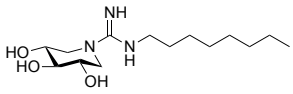

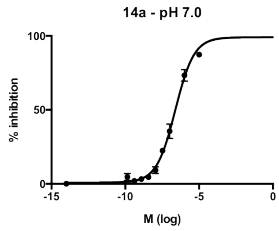

IC_{50} = 2.445e-007 ± 2.024e-008

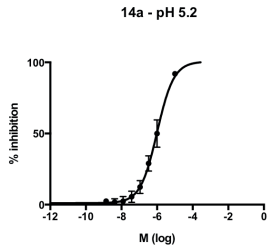

IC_{50} = 9.985e-007 ± 9.215e-008

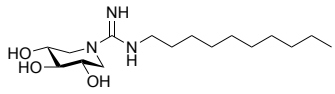

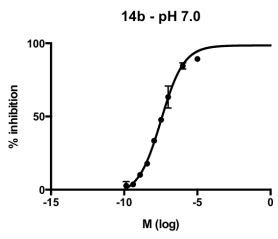

IC_{50} = 3.325e-008 ± 4.042e-009

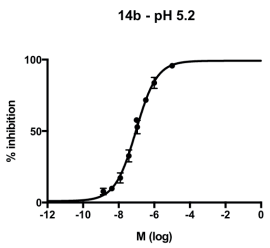

IC_{50} = 9.317e-008 ± 7.241e-009

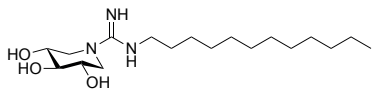

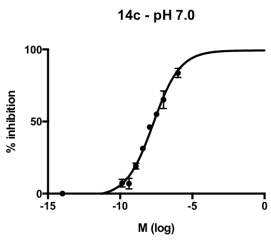

IC_{50} = 1.959e-008 ± 2.568e-009

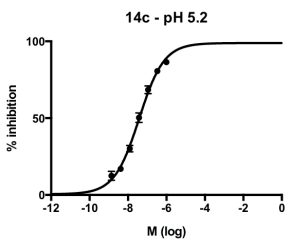

IC_{50} = 3.789e-008 ± 2.740e-009

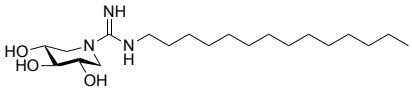

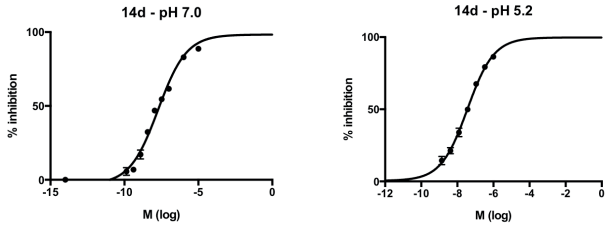

IC_{50} = 1.916e-008 ± 2.574e-009

IC_{50} = 3.610e-008 ± 2.253e-009

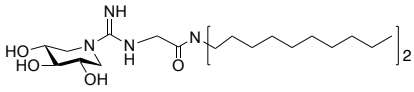

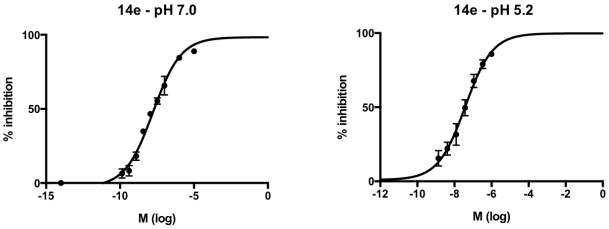

IC_{50} = 1.692e-008 ± 2.405e-009

IC_{50} = 3.806e-008 ± 5.219e-009

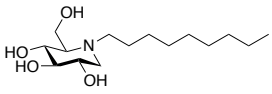

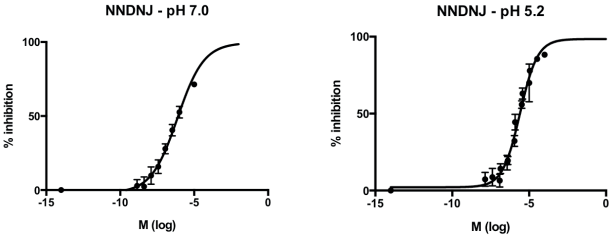

IC_{50} = 7.518e-007 ± 9.298e-008

IC_{50} = 2.564e-006 ± 2.874e-007

3.4.5 Fibroblast experiments

Cell lines and culture. Wild-type fibroblasts (GM 05659) and fibroblasts derived from Gaucher patients, homozygous for N370S GBA (GM00372) were obtained from Coriell Institute, Camden, USA. Fibroblast cells were cultured in Dulbecco's modified Eagle's medium (DMEM, Sigma-Aldrich) supplemented with 10% fetal bovine serum (FBS, Sigma-Aldrich) and penicillin-streptomycin (100 U/ml resp. 0.1 mg/ml, Sigma-Aldrich) at 37°C in 5% CO_2 and all cells used in this study were between the 5th and 15th passages. The Fibroblasts assay (*chaperone assay)* was performed according to a modified version as described in a paper published by Trapero, et. al.[43]

3.4.5.1 Experimental details for cytotoxicity assay in wild-type GD derived fibroblasts

All compounds were dissolved in DMSO (final concentration <1%) and control experiments were performed with DMSO. Cells were incubated at 37 °C in 5% CO_2 for 24 h. The cytotoxicity was measured by using the CytoTox 96 non-radioactive cytotoxicity assay and the Celltiter-Blue Cell viability assay from Promega.

3.4.5.2 Measurements of GBA activity in intact human (wild-type) fibroblasts

The chaperone assay was performed according to a modified version as previously described.[4] Fibroblasts were plated into 24-well assay plates and incubated at 37°C under 5% CO_2 atmosphere until a monolayer of at least 50% confluency was reached. The media were then replaced with fresh media with or without various concentrations of test compounds and incubated at 37°C in 5% CO_2 for 4 days. The enzyme activity assay was performed after removing media supplemented with the corresponding compound. The monolayers were washed twice with phosphate buffered saline (PBS) solution. Then, 80 µl of PBS and 80 µl of 200 mM acetate buffer (pH 4.0) were added to each well. The reaction was started by addition of 100 µl of 7.2 mM 4-methylumbelliferyl-β-D-glucopyranoside (200 mM acetate buffer pH 4.0) to each well, followed by incubation at 37°C for 2h. Enzymatic reactions were stopped by lysing the cells with 0.9 ml glycine/NaOH buffer (100 mM pH 10.6). Liberated 4-methylumbelliferone was measured (excitation 355 nm, emission at 460 nm) with the Fluoroskan Ascent FL plate reader (Labsystems) in 96-well format.

3.4.6 Experimental details for computational studies

The crystal structure of GBA with NN-DNJ (**2**) was downloaded from rcsb.org, code 2V3E.[44] Yasara 16.9.23 was used for all molecular manipulations and images, for example protonating GBA at pH 7.4 and 5.0.[45] Compound **14a** was globally docked with Vina to the original 2V3E structure of GBA and the best hits were close to the position of NN-DNJ (**2**) in the X-ray structure.[46] Then the compounds **14a** and NN-DNJ (**2**) were docked locally to GBA at the two pH values with Autodock local search.[47] The default macros for local docking from Yasara were used, except for the 50 dockings where ga_pop_size was set to 15000. Affinities were predicted as K_i-values. During all dockings the ligands were considered to be flexible. The Yasara energy minimization experiment (steepest descent followed by simulated annealing) was performed before the interactions were computed and the images were created.

*3.4.7 Analytical RP-HPLC traces for compounds **14a-e** and **17a-e***

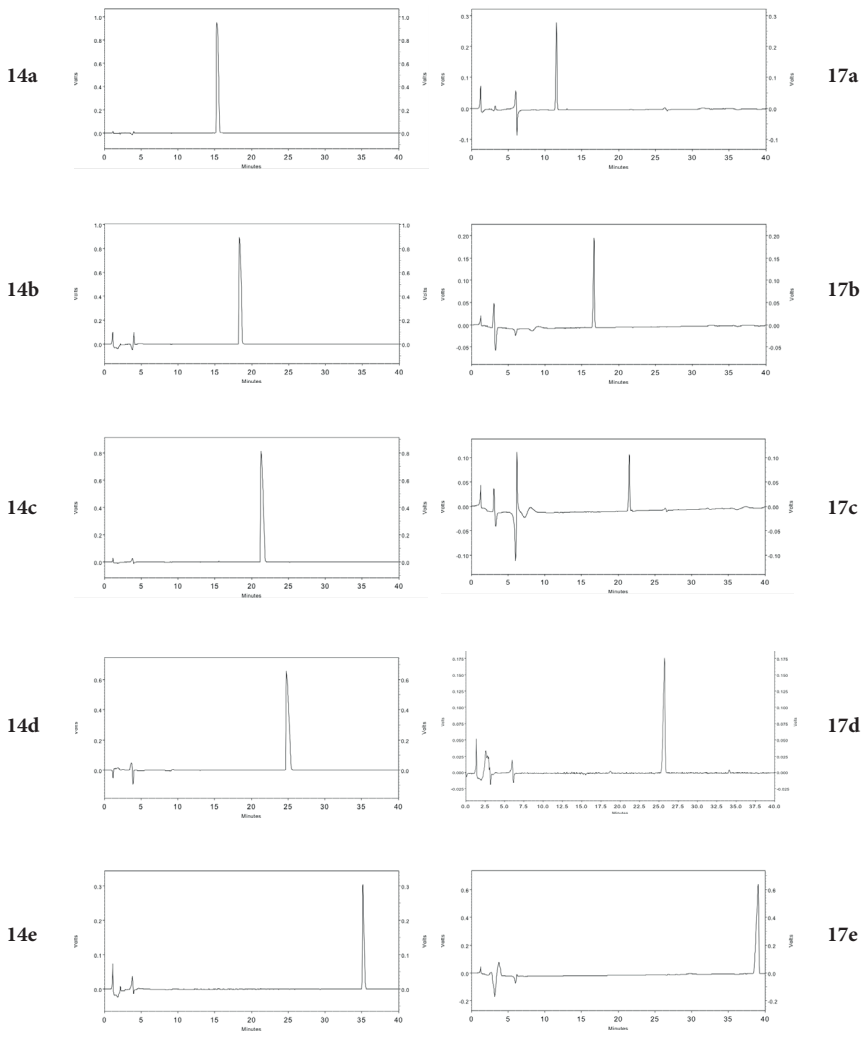

RP-HPLC experimental details

HPLC system (detection simultaneously at 214, 254 nm and evaporative light detection) equipped with an analytical C_{18} column (100 Å pore size, 4.6 mm (⌀) x 250 mm (l), 10 µm particle size) (for compounds **17a-e**) or C_8 column (100 Å pore size, 4.6 mm (⌀) x 250 mm (l), 10 µm particle size) (for compounds **14a-e**) in combination with buffers A: H_2O, B: MeCN, A and B with 0.1% aqueous trifluoroacetic acid (TFA), in some cases - coupled with an electrospray interface (ESI) was used. For RP-HPLC purifications (detection simultaneously at / 213, 254 nm), an automated HPLC system equipped with a preparative C_{18} column (20 mm (⌀) x 250 mm (l), 5 µm particle size) or C_8 column (20 mm (⌀) x 250 mm (l), 5 µm particle size) in combination with buffers A: H_2O, B: MeCN, A and B with 0.1% aqueous trifluoroacetic acid (TFA). Compounds **14a-e** and **17a-e** were purified using a 1 hour gradient, starting with 95% buffer A:5% buffer B (0.1%TFA) and 5% buffer A:95% buffer B (0.1%TFA) at the end mark.

3.4.8. *Graphical NMR example of compounds* ***14a*** *and* ***17a***

Compound 14a: ^{1}H NMR (500 MHz, DMSO-d_6)

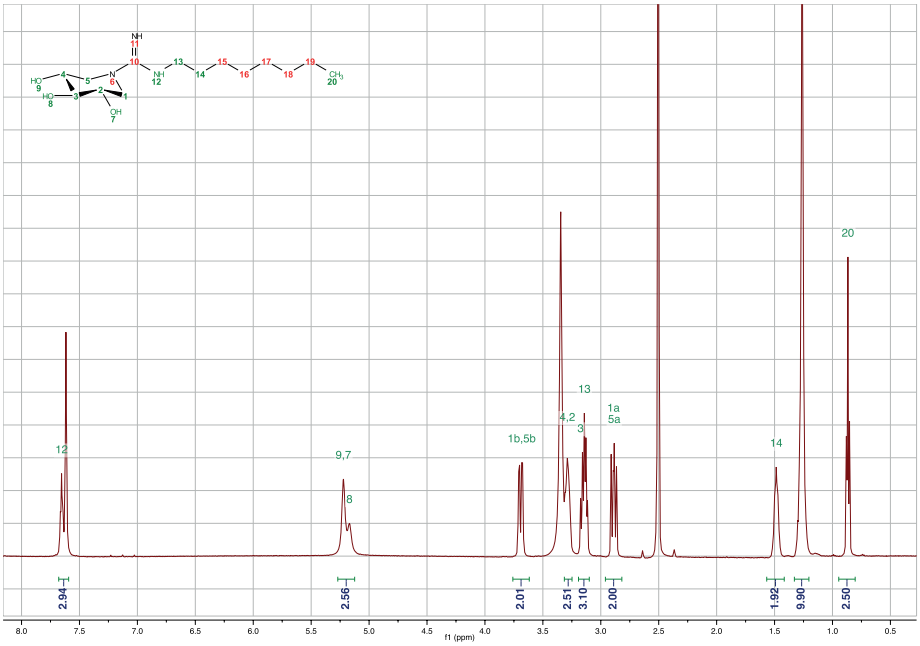

Compound 14a: ^{13}C NMR (126 MHz, DMSO-d_6)

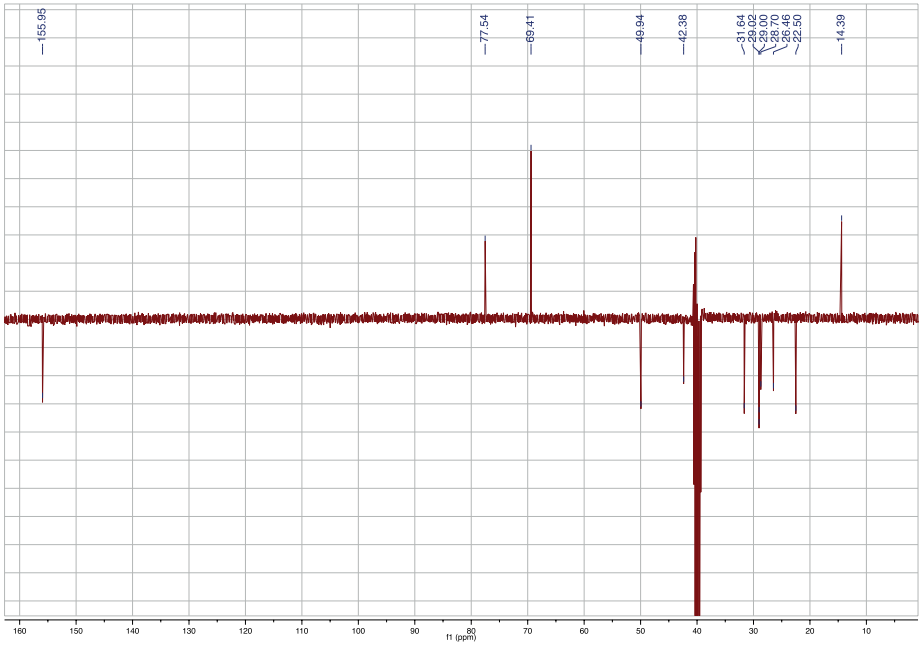

Compound 14a: $^{1}H - {}^{1}H$ COSY NMR (500 MHz, DMSO-d_6)

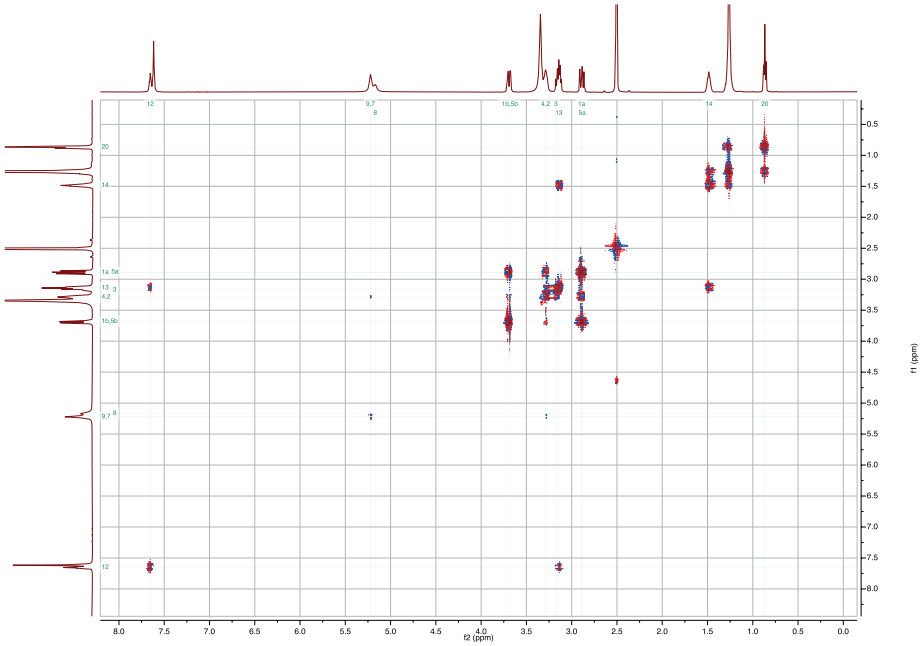

Compound 14a: $^{1}H - {}^{13}C$ HSQC NMR (126 MHz, DMSO-d_6)

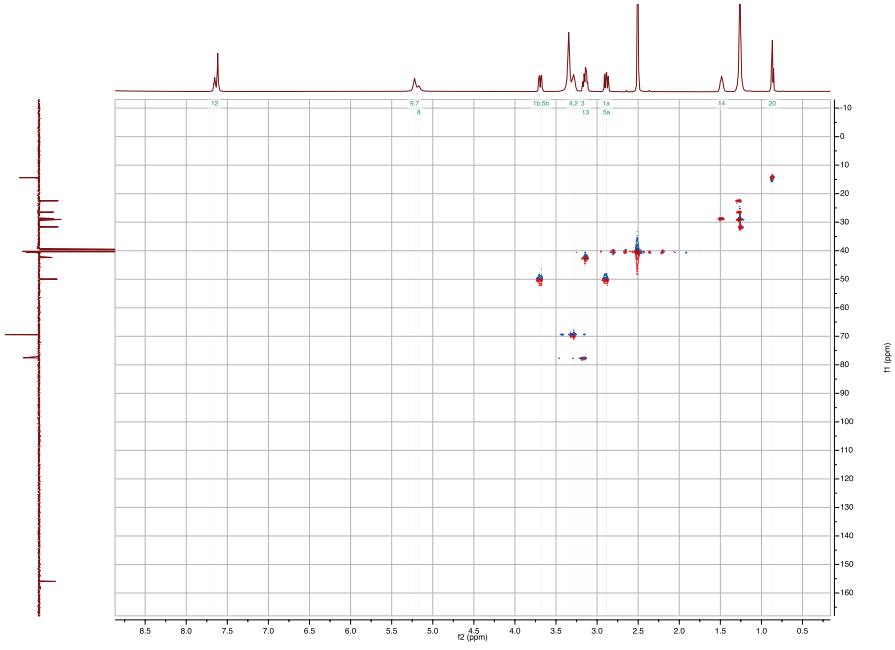

Compound 17a: ^{1}H NMR (500 MHz, DMSO-d_6)

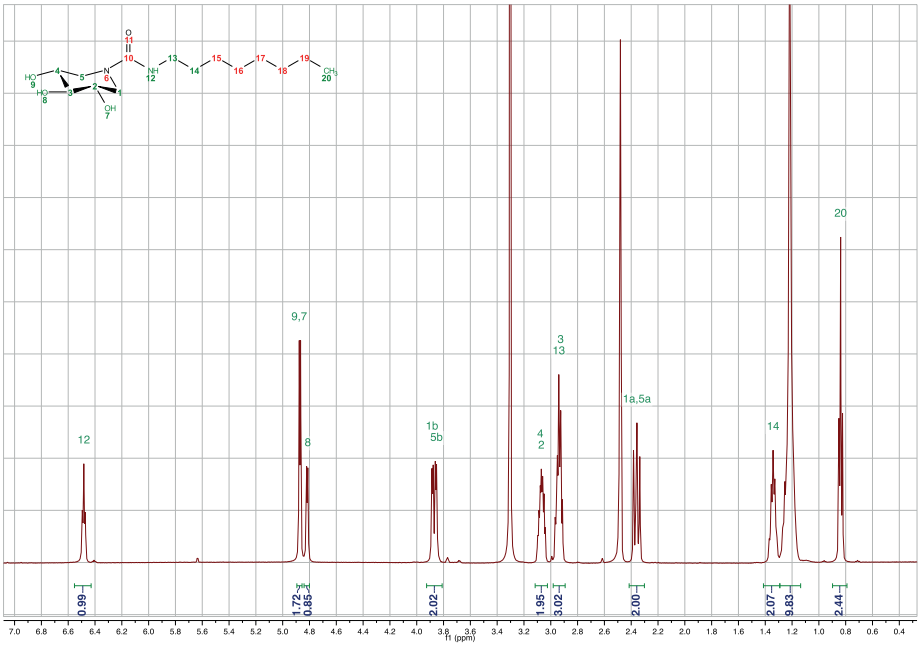

Compound 17a: ^{13}C NMR (101 MHz, $CDCl_3$)

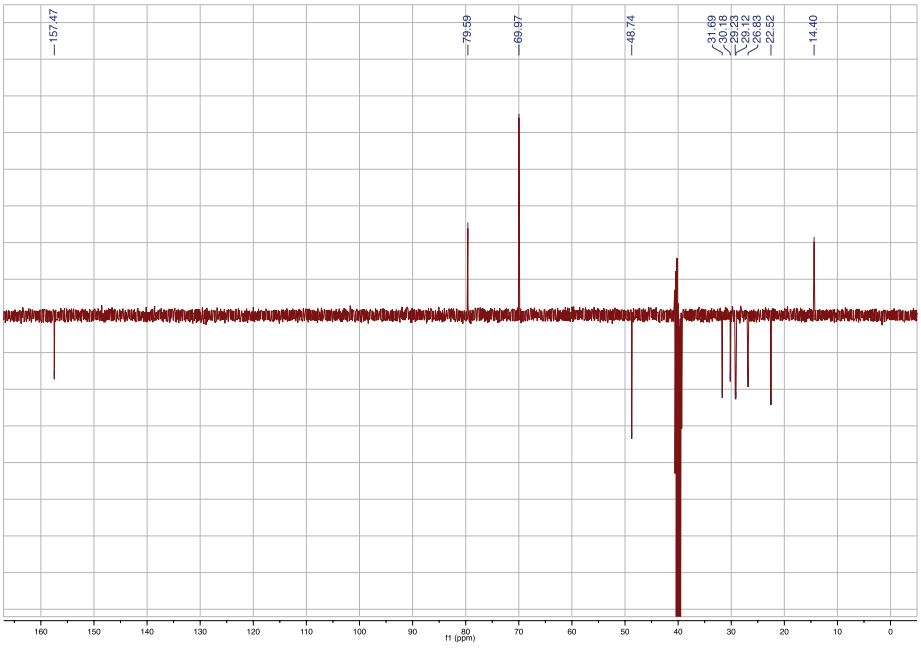

Compound 17a: ^{1}H – ^{1}H COSY NMR (500 MHz, DMSO-d_6)

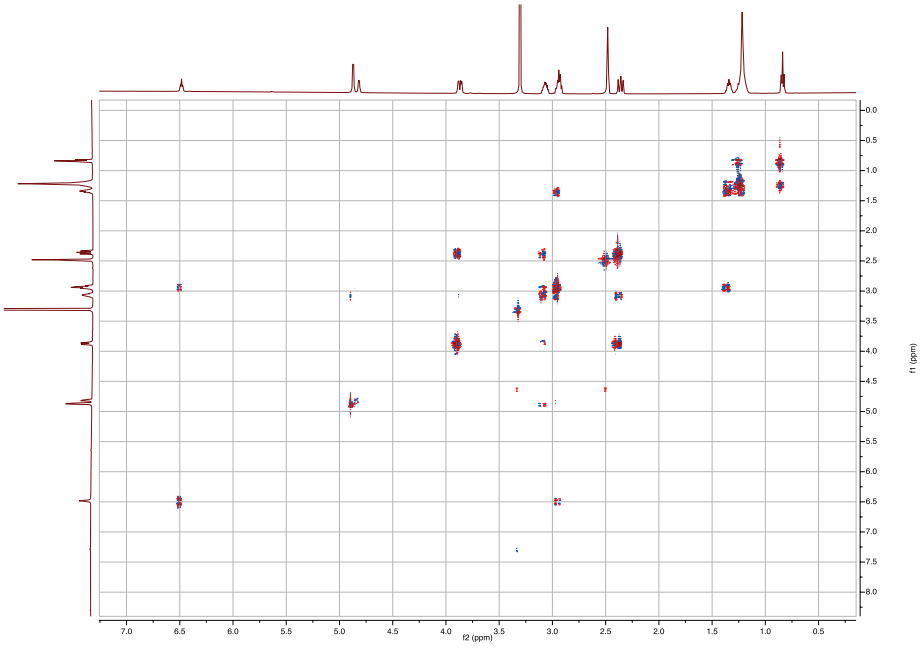

Compound 17a: ^{1}H – ^{13}C HSQC NMR (126 MHz, DMSO-d_6)

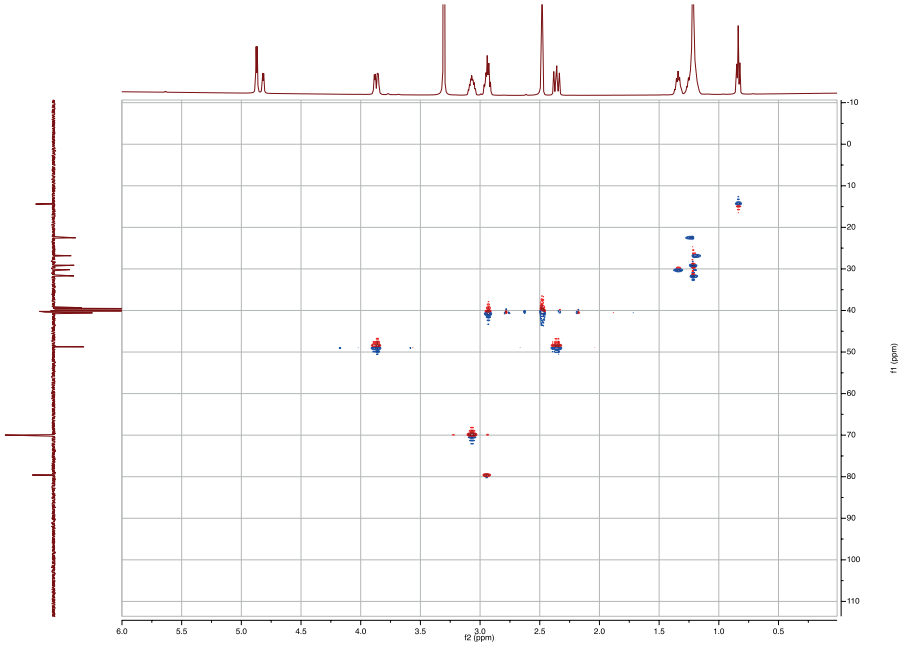

3.5 REFERENCES

1. Horne, G., Wilson, F. X., Tinsley, J., Williams, D. H. & Storer, R. Iminosugars past, present and future: medicines for tomorrow. *Drug Discov. Today* **16,** 107–118 (2011).
2. Churruca, J., Vigil Luis, Luna, E., Ruiz-Galiana, J. & Manuel, V. The route to diabetes: Loss of complexity in the glycemic profile from health through the metabolic syndrome to type 2 diabetes. *Diabetes, Metab. Syndr. Obes.* **1,** 3–11 (2008).
3. Gao, X. *et al.* International Immunopharmacology Iminosugar derivative WGN-26 suppresses acute allograft rejection via inhibiting the IFN- γ / p-STAT1 / T-bet signaling pathway. *Int. Immunopharmacol.* **23,** 688–695 (2014).
4. Ruhela, D., Chatterjee, P. & Vishwakarma, R. A. 1-Oxabicyclic beta-lactams as new inhibitors of elongating MPT–a key enzyme responsible for assembly of cell-surface phosphoglycans of Leishmania parasite. *Org. Biomol. Chem.* **3,** 1043–1048 (2005).
5. Hussain, S. *et al.* Strain-specific antiviral activity of iminosugars against human influenza A viruses. *J. Antimicrob. Chemother.* **70,** 136–152 (2015).
6. Wang, G. N., Xiong, Y., Ye, J., Zhang, L. H. & Ye, X. S. Synthetic N-alkylated iminosugars as new potential immunosuppressive agents. *ACS Med. Chem. Lett.* **2,** 682–686 (2011).
7. Kuntz, D. a *et al.* Structural investigation of the binding of 5-substituted swainsonine analogues to Golgi alpha-mannosidase II. *ChemBioChem* **11,** 673–680 (2010).
8. Platt, F. M. Sphingolipid Lysosomal Storage Disorders. *Nature* **510,** 68–75 (2014).
9. Parenti, G., Andria, G. & Valenzano, K. J. Pharmacological Chaperone Therapy: Preclinical Development, Clinical Translation, and Prospects for the Treatment of Lysosomal Storage Disorders. *Mol. Ther.* **23,** 1138–1148 (2015).
10. Convertino, M., Das, J. & Dokholyan, N. V. Pharmacological chaperones: design and development of new therapeutic strategies for the treatment of conformational diseases. *ACS Chem. Biol.* **11,** 1471–1489 (2016).
11. Kallemeijn, W. W. *et al.* A Sensitive gel-based method combining distinct cyclophellitol-based probes for the identification of acid/base residues in human retaining beta-glucosidases. *J. Biol. Chem.* **289,** 35351–35362 (2014).
12. Li, K.-Y. *et al.* Exploring functional cyclophellitol analogues as human retaining beta-glucosidase inhibitors. *Org. Biomol. Chem.* **12,** 7786–7791 (2014).
13. Compain, P. & Martin, O. R. *Iminosugars: From synthesis to therapeutic applications*. (Wiley, 2007).
14. Yagi M. Kouno T. Aoyagi Y. Murai H. The structure of moranoline, a piperidine alkaloid from Morus species. *J. Agric. Chem. Soc. Japan* **50,** 571–572 (1976).
15. Sekioka, T., Shibano, M. & Kusano, G. Three Trihydroxypiperidines, Glycosidase Inhibitors, from Eupatorium fotunei TURZ. *Nat. Med.* **49,** 332–335 (1995).
16. Hughes, A. B. & A. J. Rudge. Deoxynojirimycin: Synthesis and Biological Activity. *Nat. Prod. Rep.* **11,** 135–162 (1994).
17. Bernotas, R. C., Papandreou, G., Urbach, J. & Oanem, B. A new family of five-carbon iminoalditols which are potent glycosidase inhibitors. *Tetrahedron Lett.* **31,** 3393–3396 (1990).
18. Jespersen, T. M. & Bols, M. Synthesis of Isofagomine, a Novel Glycosidase Inhibitor. *Tetrahedron* **50,** 13449–13460 (1994).
19. Sanchez-Fernandez, E. M., Garcia Fernandez, J. M. & Mellet, C. O. Glycomimetic-based pharmacological chaperones for lysosomal storage disorders: lessons from Gaucher, GM1-gangliosidosis and Fabry diseases. *Chem. Commun.* **52,** 5497–5515 (2016).
20. Ghisaidoobe, A. T. *et al.* Identification and Development of Biphenyl Substituted Iminosugars as Improved Dual Glucosylceramide Synthase/Neutral Glucosylceramidase Inhibitors. *J. Med. Chem.* **57,** 9096–9104 (2014).
21. Hottin, A., Wright, D. W., Davies, G. J. & Behr, J. B. Exploiting the hydrophobic terrain in fucosidases with aryl-substituted pyrrolidine iminosugars. *ChemBioChem* **16,** 277–283 (2015).
22. Sawkar, A. R. *et al.* Chemical chaperones increase the cellular activity of N370S beta-glucosidase: a therapeutic strategy for Gaucher disease. *Proc. Natl. Acad. Sci. U. S. A.* **99,** 15428–15433 (2002).
23. Godin, G. *et al.* α-1-C-Alkyl-1-deoxynojirimycin derivatives as potent and selective inhibitors of intestinal isomaltase: remarkable effect of the alkyl chain length on glycosidase inhibitory profile. *Bioorg. Med. Chem. Lett.* **14,** 5991–5995 (2004).
24. Patil, N. T., John, S., Sabharwal, S. G. & Dhavale, D. D. 1-Aza-sugars from D-Glucose. Preparation of 1-Deoxy-5-dehydroxymethyl-Nojirimycin, its analogues and evaluation of glycosidase inhibitory

activity. *Bioorganic Med. Chem.* **10,** 2155–2160 (2002).
25. Pandey, G., Kapur, M., Khan, M. I. & Gaikwad, S. M. A new access to polyhydroxy piperidines of the azasugar class: synthesis and glycosidase inhibition studies. *Org. Biomol. Chem.* **1,** 3321–3326 (2003).
26. Han, H. A complete asymmetric synthesis of polyhydroxypiperidines. *Tetrahedron Lett.* **44,** 1567–1569 (2003).
27. Ouchi, H., Mihara, Y. & Takahata, H. A new route to diverse 1-azasugars from N-Boc-5-hydroxy-3-piperidene as a common building block. *J. Org. Chem.* **70,** 5207–5214 (2005).
28. Parmeggiani, C. *et al.* Human Acid beta-Glucosidase Inhibition by Carbohydrate Derived Iminosugars: Towards New Pharmacological Chaperones for Gaucher Disease. *ChemBioChem* **16,** 2054–2064 (2015).
29. Mccaig, A. E., Chomier, B. & Wightman, R. H. Hydroxylated piperidines: Synthesis of 1,5-alkylimino-1,5-dideoxy derivatives of xylitol, D- and L-arabinitol, and ribitol. *J. Carbohydr. Chem.* **13,** 397–407 (1994).
30. Wang, G.-N. *et al.* Rational Design and Synthesis of Highly Potent Pharmacological Chaperones for Treatment of N370S Mutant Gaucher Disease. *J. Med. Chem.* **52,** 3146–3149 (2009).
31. Zhu, X., Sheth, K. a, Li, S., Chang, H.-H. & Fan, J.-Q. Rational design and synthesis of highly potent beta-glucocerebrosidase inhibitors. *Angew. Chem. Int. Ed. Engl.* **44,** 7450–7453 (2005).
32. Compain, P. *et al.* Design and synthesis of highly potent and selective pharmacological chaperones for the treatment of Gaucher's disease. *ChemBioChem* **7,** 1356–1359 (2006).
33. Martin, N. I., Woodward, J. J. & Marletta, M. A. NG-hydroxyguanidines from Primary Amines. *Org. Lett.* **8,** 4035–4038 (2006).
34. Kooij, R. *et al.* Glycosidase inhibition by novel guanidinium and urea iminosugar derivatives. *Medchemcomm* **4,** 387–393 (2013).
35. Sevšek, A. *et al.* Bicyclic isoureas derived from 1-deoxynojirimycin are potent inhibitors of β-glucocerebrosidase. *Org. Biomol. Chem.* **14,** 8670–8673 (2016).
36. Lehmann, J. & Rob, B. N-amidino-3,4,5-trihydroxypiperidine, a new efficient competitive beta-glucosidase inhibitor. *Carbohydr. Res.* **272,** 5–7 (1995).
37. Boot, R. G. *et al.* Identification of the Non-lysosomal Glucosylceramidase as beta-Glucosidase 2. *J. Biol. Chem.* **282,** 1305–1312 (2007).
38. Martin, N. I., Beeson, W. T., Woodward, J. J. & Marletta, M. A. N-aminoguanidines from primary amines and the preparation of nitric oxide synthase inhibitors. *J. Med. Chem.* **51,** 924–931 (2008).
39. Martin, N. I. & Liskamp, R. M. J. Preparation of NG-Substituted L-Arginine Analogues Suitable for Solid Phase Peptide Synthesis. *J. Org. Chem.* **73,** 7849–7851 (2008).
40. Helgen, C. & Bochet, C. G. Photochemical protection of amines with Cbz and Fmoc groups. *J. Org. Chem.* **68,** 2483–2486 (2003).
41. Upadhyaya, D. J., Barge, A., Stefania, R. & Cravotto, G. Efficient, solventless N-Boc protection of amines carried out at room temperature using sulfamic acid as recyclable catalyst. *Tetrahedron Lett.* **48,** 8318–8322 (2007).
42. Sunitha, S., Kanjilal, S., Reddy, P. S. & Prasad, R. B. N. An efficient and chemoselective Bronsted acidic ionic liquid-catalyzed N-Boc protection of amines. *Tetrahedron Lett.* **49,** 2527–2532 (2008).
43. Trapero, A., González-Bulnes, P., Butters, T. D. & Llebaria, A. Potent aminocyclitol glucocerebrosidase inhibitors are subnanomolar pharmacological chaperones for treating gaucher disease. *J. Med. Chem.* **55,** 4479–4488 (2012).
44. Brumshtein, B. *et al.* Crystal structures of complexes of N-butyl- and N-nonyl-deoxynojirimycin bound to acid β-glucosidase: Insights into the mechanism of chemical chaperone action in Gaucher disease. *J. Biol. Chem.* **282,** 29052–29058 (2007).
45. Krieger, E. & Vriend, G. New ways to boost molecular dynamics simulations. *J. Comput. Chem.* **36,** 996–1007 (2015).
46. Garrett M. Morris *et al.* AutoDock4 and AutoDockTools4: Automated Docking with Selective Receptor Flexibility. *J. Comput. Chem.* **30,** 2785–2791 (2009).
47. Oleg Trott & Olson, A. J. AutoDock Vina: Improving the Speed and Accuracy of Docking with a New Scoring Function, Efficient Optimization, and Multithreading. *J. Comput. Chem.* **31,** 455–461 (2009).

CHAPTER 4

Orthoester Functionalized *N*-Guanidino Derivatives of 1,5-Dideoxy-1,5-imino-D-xylitol as pH-responsive Inhibitors of *β*-Glucocerebrosidase

Manuscript accepted for publication:

Sevšek, A.; Sastre Toraño, J.; Quarles van Ufford, L.; Pieters, R. J.; Martin, N. I. *MedChemComm,* **2017**.

ABSTRACT

Alkylated guanidino derivatives of 1,5-dideoxy-1,5-imino-D-xylitol bearing an orthoester moiety were prepared using a concise synthetic protocol. Inhibition assays with a panel of glycosidases revealed that one of the prepared compounds prepared displays potent inhibition against human *β*-glucocerebrosidase (GBA) at pH 7.0 with IC_{50} values in the low nanomolar range. Notably, a significant drop in inhibitory activity is observed when the same compound is tested at pH 5.2. This pH sensitive activity is due to degradation of the orthoester functionality at lower pH accompanied by loss of the alkyl group. This approach provides a degree of control in tuning enzyme inhibition based on the local pH. Compounds like those here described may serve as tools for studying various lysosomal storage disorders such as Gaucher disease. In this regard, the most active compound was also evaluated as a potential pharmacological chaperone by assessing its effect on GBA activity an assay employing fibroblasts from Gaucher patients.

4.1 INTRODUCTION

In recent years, the iminosugars have emerged as a class of promising compounds in medicinal chemistry due to their therapeutic potential in the treatment of a variety of carbohydrate-mediated diseases.[1–5] Certain iminosugars are highly potent and selective inhibitors of glycosidases and in some cases reversibly bind to their target enzyme through interactions involving the catalytic site or/and allosteric regions of the enzyme.[6,7] Of particular interest are glycomimetics that comprise an endocyclic nitrogen, such as the naturally occurring 1-deoxynojirimycin (DNJ, **1**, **Figure 1A**)[8] as well as 1,5-dideoxy-1,5-imino-D-xylitol (DIX, **4**)[9] and synthetically modified *N*-substituted iminosugars, such as **2**, **3** and **5** that often possess improved specificities and potent inhibition towards glycosidases.[10–21] Previous investigations in our group have evaluated iminosugar analogues with a partially sp^2 hybridized endocyclic nitrogen centre (compounds **6**-**8**, **Figure 1B**).[22,23] This structural feature affects both the conformation and charge delocalization of the endocyclic nitrogen and was found to result in changes in the glycosidase inhibition profile relative to the parent iminosugars.

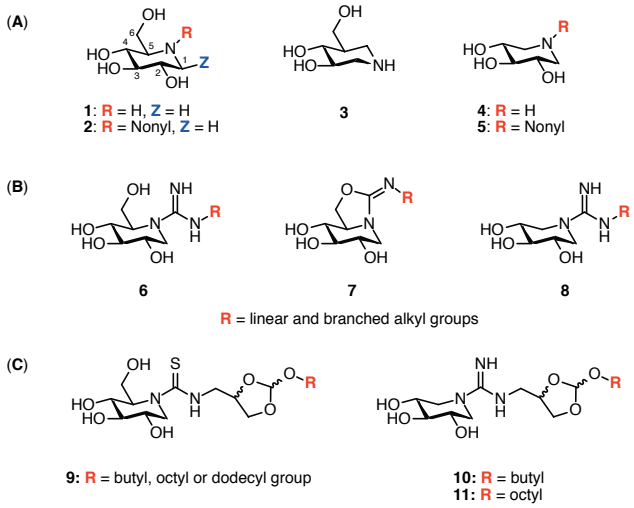

Figure 1. **A)** Chemical structures of selected iminosugar-based glycosidase inhibitors. **B)** Structures of derivatives previously prepared in our group. **C)** General structures of orthoester thiourea DNJ compounds previously published (**9**) and orthoester rich guanidine DIX compounds (**10**, **11**) presented in this work.

We recently reported the attempted synthesis of a series of lipidated DNJ guanidine compounds **6** and found that they were prone to spontaneous cyclization to generate the corresponding bicyclic isoureas **7**.[24] Gratifyingly, these compounds proved to be very potent and specific inhibitors of β-glucocerebrosidase (GBA, GCase, β-glucosidase, EC 3.2.1.45)[25] an enzyme responsible for the onset of Gaucher disease.[26–28] Gaucher disease is the most prevalent lysosomal storage disease (LSD) with 10,000 individuals affected worldwide and can result in the progressive accumulation of the undegraded glucosylceramide substrate leading to a variety of clinical symptoms.[29–31]

As a therapeutic strategy, iminosugars that bind a misfolded enzyme at neutral pH (pH 7.0) can provide an improvement in its folding and promote proper trafficking from the ER to the lysosome.[32] Such inhibitors can be used as pharmacological chaperones, which serve as one of the main options in treating lysosomal storage disorders.[33,34] Previous findings suggest that minor increases in mutant GBA activity, caused by chemical chaperoning, may be clinically useful.[35,36] More conservative research states that doubling N370S activity may be sufficient to raise activity levels above the critical threshold for the development of disease.[37] Ideally, an iminosugar-based pharmacological chaperone should have a lower binding affinity for the target glycosidase in the acidic environment of the lysosome (pH 5.2) allowing it to dissociate from the complex after which the enzyme can go on to degrade its substrate. Furthermore, the high initial substrate concentration in the lysosome of a patient with an LSD can further promote dissociation of the pharmacological chaperone-enzyme complex. In this regard, pharmacological chaperone approaches offers promising opportunities in the treatment of a broad range of inherited LSDs.[38] To this end, the development of potent, pH-dependent, glycosidase inhibitors presents an attractive target for the development of new therapeutics.[39] Recently we described the synthesis and evaluation of a new class of stable, guanidine-modified, DIX analogues **8**, both as GBA inhibitors and potential pharmacological chaperones.[40] We were able to show that incorporating an *N*-alkylated guanidino moiety into the DIX scaffold drastically improved inhibitor potency in contrast to *N*-alkylated DIX analogue **5**, which is only a moderate glycosidase inhibitor.[41] However, while DIX derived compounds such as **8** are potent, selective, and stable inhibitors of GBA at pH 7.0, they also maintain their inhibitory activity at pH 5.2. A similar lack of pH selective inhibition has also been implicated in the disappointing clinical trial failures of many other GBA inhibitors explored as pharmacological chaperones.[42] In building upon the GBA inhibitors developed in our group we therefore set out to develop analogues that maintain potent activity at neutral pH but show a significant decrease in activity at acidic pH. In this regard we were drawn to the recent report of *Ortiz Mellet and co-workers* who described the use of an acid sensitive orthoester functionality, which allowed for pH control in the design of other glycosidase inhibitors.[43] Specifically, they prepared the alkylated DNJ thiourea species **9** in which the alkyl was connected to the to the thiourea unit *via* the acid labile orthoester. This strategy led to GBA inhibitors with potent activity at pH 7.0 that was virtually abolished at pH 5.2 due to orthoester hydrolysis (**Figure 1C**).[43]

4.2 RESULTS AND DISCUSSION

*4.2.1 Synthetic approach towards the acetylated DIX building block **16***

We here apply a similar strategy in modifying the novel class of *N*-alkylated guanidino DIX analogues recently developed by our group. In doing so we introduced an orthoester moiety between the exocyclic guanidine group and the alkyl to arrive at compounds such as a **10** and **11**. First, benzyl protected DIX **12** was synthesized according to the literature procedure[44] and used as a starting material for the preparation of acetylated 1,5-dideoxy-1,5-imino-D-xylitol **16** used in this work (**Scheme 1**). This was done to avoid acidic environment needed to deprotect the benzyl protection groups, which would simultaneously affect the orthoester precursor, resulting in a prematurely hydrolysed

species discussed later. Acetylated species, on the other hand, needs basic conditions in the deprotection step and would not promote the hydrolysis. The *O*-perbenzylated 1,5-dideoxy-1,5-imino-D-xylitol **12** was prepared according to a literature protocol[44] and transformed in high yields to the corresponding per-acetylated species **16**. Conversion of **12** to Boc-protected **13** was followed by removal of the benzyl groups *via* hydrogenation under acidic conditions to yield triol **14**. Acetylation of **14** with acetic anhydride in pyridine gave **15** followed by treatment with trifluoroacetic acid to yield **16**, which served as a common precursor in the preparation of acid sensitive GBA inhibitors **10** and **11**.

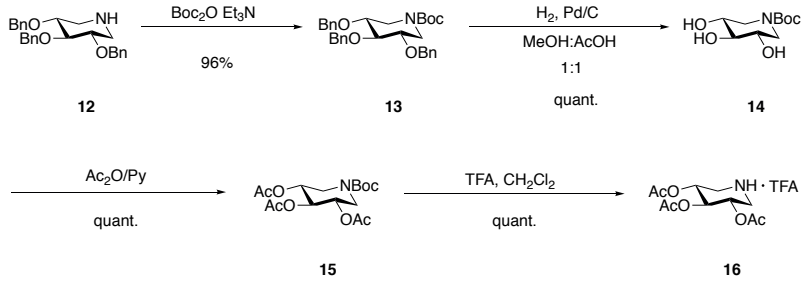

Scheme 1. Synthetic route towards acetylated DIX building block **16**.

4.2.2 *Synthesis of orthoester-rich DIX guanidines 10 and 11*

The synthetic approach used in preparing analogues **10** and **11** is outlined in **Scheme 2**. Two orthoester amines **18** and **19**, bearing simple linear alkyl chains containing four and eight carbon atoms respectively, were synthesized according to a literature procedure.[43,45] Treatment of **18** and **19** with CbzNCS[46,47] gave thioureas **20** and **21**, which provided a convenient means for incorporation of the DIX moiety. Activation of Cbz-protected thioureas **20** and **21** with EDCI followed by addition of **16** lead to clean formation of protected guanidines **22** and **23**. Interestingly, in the final deprotection step we observed simultaneous removal of both the Cbz and acetyl groups when performing the hydrogenation under basic conditions. It should be taken into account that the Cbz-deprotection step occurred in the presence of TEA and aprotic THF solvent that was not dried prior to use, which might be a plausible explanation for immediate deprotection of the acetyls. In doing so fully deprotected orthoester-armed guanidine products **10** and **11** were obtained in high yields.[48]

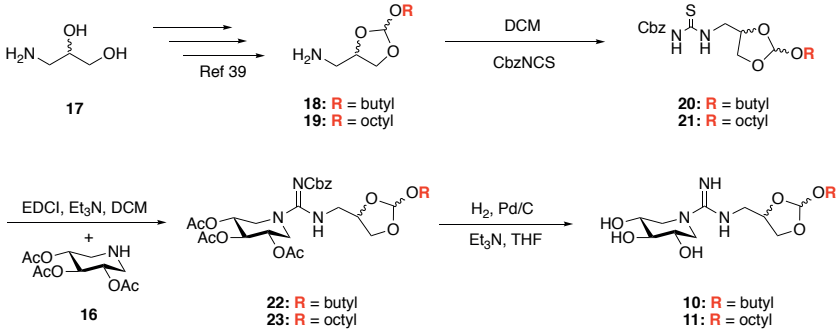

Scheme 2. Synthetic route towards orthoester rich DIX guanidines **10** and **11**.

4.2.3 *Acid hydrolysis of compounds 10 and 11*

The hydrolysis of compounds **10** and **11** was evaluated and revealed two major degradation products; corresponding to species **A** and **B** (**Scheme 3**).

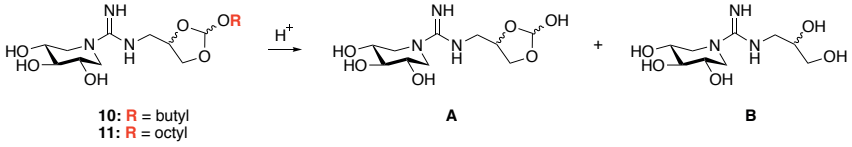

Scheme 3. Hydrolysis of **10** and **11** yields compounds **A** and **B**.

Proposed mechanisms for the hydrolysis of **10** and **11** are presented below in **Scheme 4** and **Scheme 5** to rationalize the formation of the two major degradation products with molecular weights 278 (**A**) and 250 (**B**).

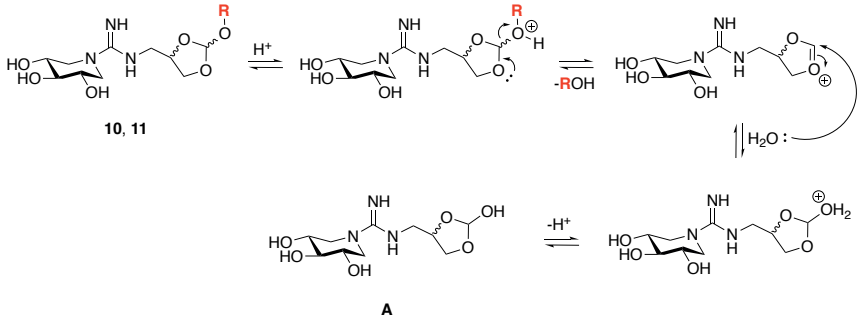

Scheme 4. Mechanism for the hydrolysis of **10** and **11** towards compound **A**.

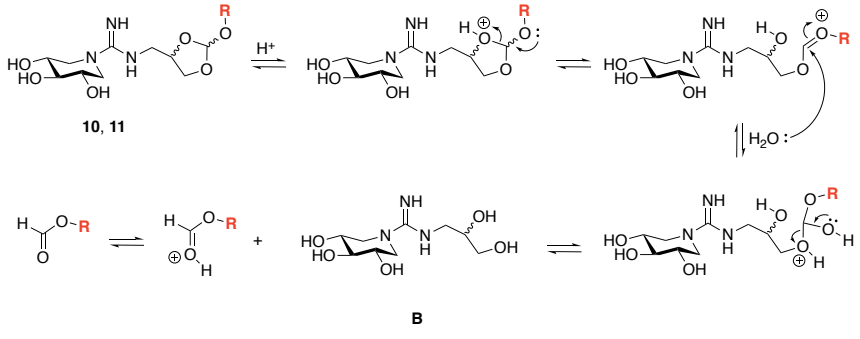

Scheme 5. Mechanism for the hydrolysis of **10** and **11** towards compound **B**.

4.2.4 Collision-induced dissociation mass spectrometry (CID MS-MS) studies

Accurate mass measurements of the degradation compounds showed a mass of *m/z* 278.1347 ([M+H]$^+$; compound **A**) and *m/z* of 250.1395 ([M+H]$^+$; compound **B**), corresponding to compounds with monoisotopic mass 277.1266 and 249.1325 and a molecular formula $C_{10}H_{19}N_3O_6$ and $C_9H_{19}N_3O_5$, respectively.

To fully confirm structures **A** and **B**, precursor ions corresponding to the peaks with *m/z* 278 and 250 were subjected to collision induced dissociation fragmentation to obtain fragments that could confirm the structures. After infusion, several fragments belonging to the guanidine iminosugar moiety were observed in both spectra (**Figure 2**, **Figure 3** and **Table 1**), confirming the presence of the same moiety in both compounds. The unique fragment ions *m/z* 120 and 102 (loss of water from *m/z* 120) for compound **A** and *m/z* 92 for compound **B** also indicated a similar fragmentation pathway for both compounds and confirmed the different branches attached to the guanidine iminosugar moiety.

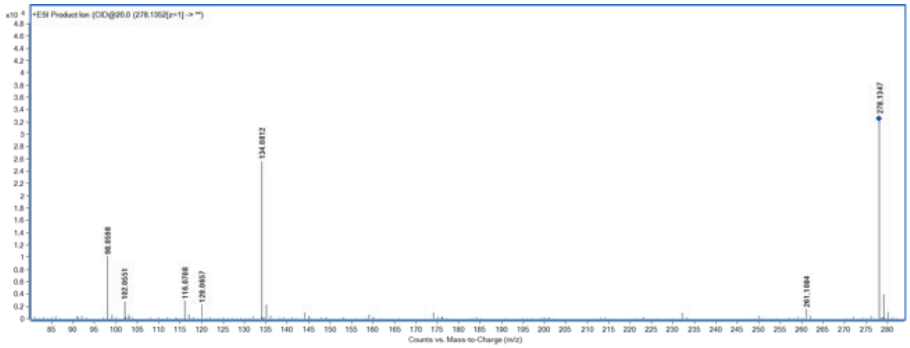

Figure 2. CID MS-MS spectrum of compound **A** with precursor ion *m/z* 278.

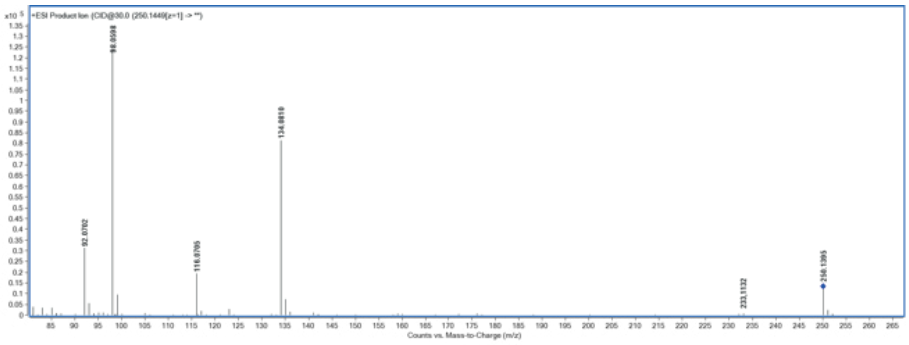

Figure 3. CID MS-MS spectrum of compound **B** with precursor ion *m/z* 250.

Measured *m/z* of compound **A** (278) fragment, proposed fragment structure and mass accurracy	Measured *m/z* of compound **B** (250) fragment, proposed fragment structure and mass accuracy	Molecular formula	Exact mass (Da)
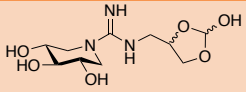 [M+H]$^+$ = 278.1347		$C_{10}H_{20}N_3O_6$+H	278.1347
	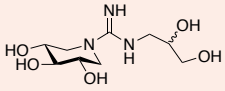 [M+H]$^+$ = 250.1395	$C_9H_{19}N_3O_5$+H	250.1397
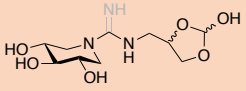 [M+H]$^+$ = 261.1084		$C_{10}H_{16}N_2O_6$+H	261.1081
	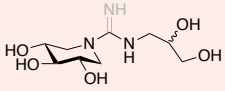 [M+H]$^+$ = 233.1132	$C_9H_{16}N_2O_5$+H	233.1132
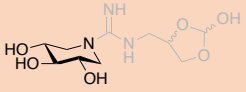 [M+H]$^+$ = 134.0812	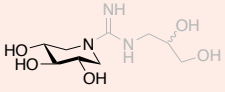 [M+H]$^+$ = 134.0810	$C_5H_{11}NO_3$+H	134.0812
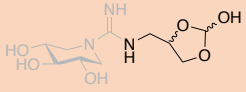 [M+H]$^+$ = 120.0657		$C_4H_9NO_3$+H	120.0655
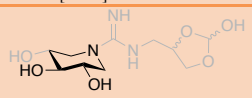 [M+H]$^+$ = 116.0708	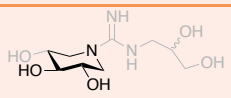 [M+H]$^+$ = 116.0705	$C_5H_9NO_2$+H	116.0706
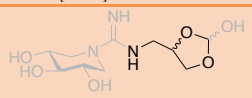 [M+H]$^+$ = 102.0551		$C_4H_7NO_2$+H	102.0550
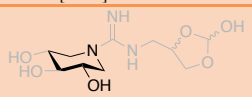 [M+H]$^+$ = 98.0598	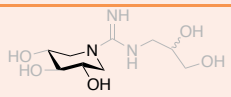 [M+H]$^+$ = 98.0598	C_5H_7NO+H	98.0600
	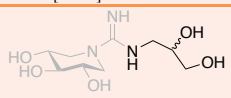 [M+H]$^+$ = 92.0702	$C_3H_9NO_2$+H	92.0706

Table 1. Fragments and proposed structures as observed in the MS-MS spectra of compounds **A** and **B**.

4.2.5 *UHPLC-MS method for kinetic hydrolysis experiments of orthoesters **10** and **11***

Next, the samples were degraded in a buffer solution (pH 5.2) at 21 °C for 6 hours and studied to develop the stability indicating method. The separation of compounds **10** and **11** and the degradation products **A** and **B** was optimized by adjusting the amount and type of acidifier and organic modifier and the gradient time and slope. Good selectivity for all high and low polar compounds was achieved in one run with 0.5% FA/ACN gradients. The optimized gradient started with a composition of 97% eluent A and 3% eluent B (% v/v) for 3 min, increased linearly to 100% B in 3.5 min and remained at 100% B for 2 min. MS settings were optimized to obtain maximum detector response for all compounds. Guanidine compounds **10** and **11** and their degradation products **A** and **B** (**Figure 4** and **Figure 5**), were detected as positive ions ($[M+H]^+$).

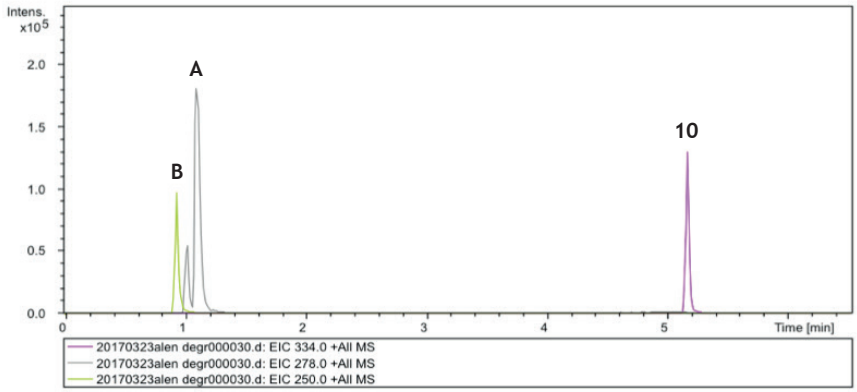

Figure 4. Extracted ion chromatogram for compound **10** obtained with the optimized UHPLC-MS method of a 1mM solution (pH 5.2), degraded at 21 °C for 6 hours. The following compounds were identified by their *m/z* value: **A**) *m/z* 278; **B**) *m/z* 250 and **10**) *m/z* 334.

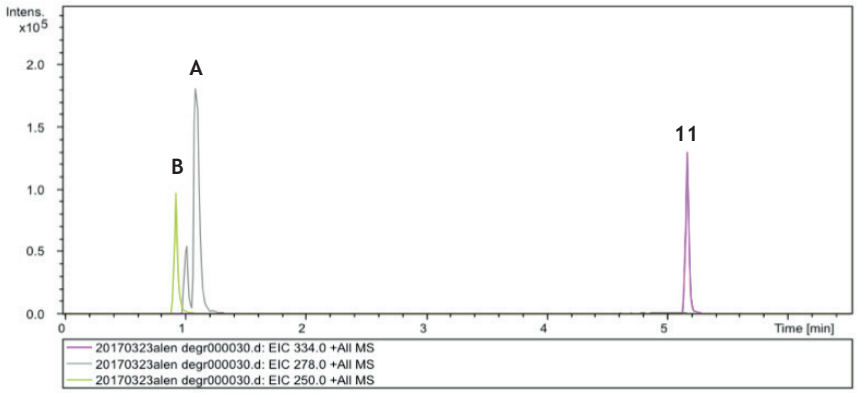

Figure 5. Extracted ion chromatogram for compound **11** obtained with the optimized UHPLC-MS method of a 1mM solution (pH 5.2), degraded at 21 °C for 6 hours. The following compounds were identified by their *m/z* value: **A**) *m/z* 278; **B**) *m/z* 250 and **11**) *m/z* 390.

In this respect, the collected data are consistent with the proposed orthoester hydrolysis mechanism of compounds **10** and **11** to their corresponding hydrolyzed products **A** and **B**.

The optimized method was used to study the time dependent degradation of the synthesized guanidine compounds. Thus, samples were dissolved in buffer solutions with pH 5.2 or pH 7.0, kept at 21 °C and analyzed at regular time intervals. The compounds **A** and **B** were identified by their *m/z* value as the main hydrolyzed products. The sum of peak areas in the chromatograms of the guanidines **10** and **11** and the hydrolyzed compounds **A** and **B** remained constant in time for the samples analyzed at different time points, which indicates that their detector responses are similar. This allows for the application of relative responses for quantitative analysis of these compounds to determine the degradation process. **Figure 6** and **Figure 7** show the first-order degradation data of **10** and **11** and the formation of **A** and **B** at pH 7.0, both expressed as % area. The half-life time, where the concentration of **10** and **11** decreased by 50%, was 157 min for compound **10** and 277 min for compound **11**, respectively. By using the logarithm (to base-e) of the concentration, a linear graph was obtained, confirming that the degradation of studied compounds was a first-order reaction with equation:

$$[\mathbf{10}, \mathbf{11}(t)] = [\mathbf{10}, \mathbf{11}]_0 \times e^{-k.t}$$

The slopes of the ln-linearized curves of all orthoester guanidine compounds were used to calculate the degradation rate constants (k) and the half-life times ($t_{0.5}$=(ln2/k)) for each compound.

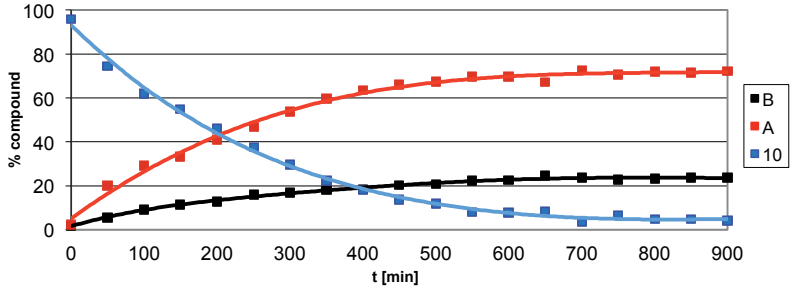

Figure 6. First-order kinetics of **10** and formation of **A** and **B** in pH 5.2 buffer solution at 21 °C.

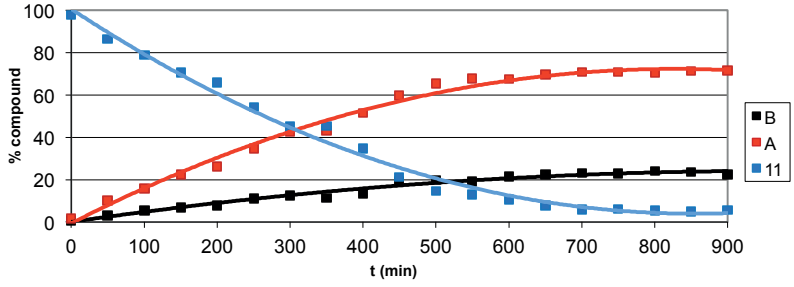

Figure 7. First-order kinetics of **11** and formation of **A** and **B** in pH 5.2 buffer solution at 21 °C.

The half-life time, where the concentration of **10** and **11** decreased by 50%, was 157 min for compound **10** and 277 min for compound **11**, respectively. **Table 2** shows the $t_{0.5}$ values for compounds **10** and **11** for the degradation at pH 5.2 and pH 7.0. Degradation was fast at pH 5.2, compared to pH 7.0. Compounds **10** and **11** showed no degradation at pH 7.0 during at least 15h.

Compound	$t_{0.5}$ in buffer pH 7.0 [min]	$t_{0.5}$ in buffer pH 5.2 [min]
10	>15	157
11	>15	277

Table 2. $t_{0.5}$ values for guanidine compounds **10** and **11** at pH 7.0 and 5.2.buffer solutions at 21 °C.

4.2.6 *Synthetic route towards compound B*

In order to confirm the structure of the orthoester adduct **B** we synthesized compound **B** and evaluated its structure by NMR and HRMS studies.

The synthetic approach used in preparing compound **B** is outlined in **Scheme 6**. Treatment of previously published amine **30**[43] was reacted with CbzNCS[46,47] and gave thiourea **31**, which provided a convenient means for incorporation of the DIX moiety. Activation of Cbz-protected thiourea **31** with EDCI followed by addition of **16** led to clean formation of protected guanidine **32**. Similar to previous deprotection procedures of our lead compounds, we observed simultaneously removal of both the Cbz and acetyl groups when performing the hydrogenation under basic conditions. Fully deprotected orthoester-armed guanidine product **B** was obtained in high yields and confirmed by NMR and MS studies.

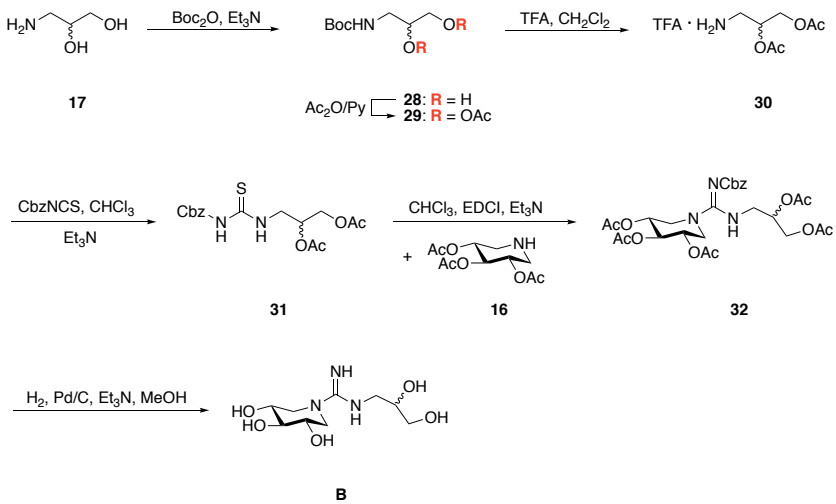

Scheme 6. Synthetic route towards compound **B**.

4.2.7 Enzyme inhibition studies against commercial glycosidases

The inhibitory potencies of DIX derived guanidine-orthoesters **10** and **11** were determined against a panel of readily available glycosidase enzymes as well as the human recombinant enzymes: *β*-glucocerebrosidase (GBA) and *β*-galactocerebrosidase (GALC) (**Table 3**). Inhibition of the plant *β*-glucosidases gave IC_{50} values in the low micromolar range for both compounds **10** and **11**. Conversely, no inhibition was seen with the other plant enzymes tested. However, when evaluated against human recombinant glycosidase enzymes, both **10** and **11** showed potent inhibition of GBA and no inhibition of GALC, indicating a high degree of selectivity among the human enzymes. Strikingly, very potent inhibition was observed against the human recombinant GBA for octyl analogue **11** with an inhibition constant that measured in the low nanomolar range ($IC_{50}^{(pH\ 7.0)}$: 25 nM). In stark contrast, butyl analogue **10** resulted in a 100-fold weaker inhibitor of GBA ($IC_{50}^{(pH\ 7.0)}$: 2561 nM) showing that the length of the alkyl group appended to the orthoester moiety has a large effect on GBA inhibition as previously found for this enzyme[49] and for the DIX series of compounds.[37] Compounds **10** and **11** were both found to be very stable in neutral aqueous solution at room temperature with less than 3% degradation after 6 days. Next, we tested the compounds at an acidic pH so as to mimic the environment of the lysosome. Compounds **10** and **11** were preincubated at pH 5.2 for 24 hours and tested under general assay conditions. Gratifyingly, after treatment at acidic pH, both **10** and **11** readily underwent hydrolysis leading to complete loss of inhibitory activity. As a reference we also assessed the effect of pH on the activity of the commonly used GBA inhibitor NN-DNJ (**2**). This revealed that at pH 7.0 NN-DNJ has an IC_{50} against GBA of 532 nM, while at pH 5.2 the IC_{50} value increases approximately 10-fold. Not only is compound **11** a more potent inhibitor of GBA, it also displays a much more significant pH dependence, a key consideration in the development of pharmacological chaperones.

Enzyme	10	11	NNDNJ
α-glu[b]	> 30000	> 30000	> 30000
α-gal[c]	> 30000	> 30000	> 30000
β-glu[d]	19150 ± 536	14570 ± 573	> 30000
β-gal[e]	> 30000	> 30000	> 30000
Nar[f]	> 30000	> 30000	85.4 ± 4.2
GBA[g] (pH 7.0)	**2561 ± 233**	**25.2 ± 2.6**	**532 ± 59**
GBA[g] (pH 5.2)	**> 30000**	**> 30000**	**5584 ± 731**
GALC[g]	> 30000	> 30000	> 30000

Table 3. Glycosidase inhibition values obtained for orthoester-armed guanidines **10** and **11**.[a]

[a]IC_{50} values are reported in nM and are averages obtained from triple independent duplicate analysis of each compound. [b]α-glucosidase (from baker's yeast, Sigma G5003): 0.05 U/mL, the activity was determined with p-nitrophenyl-α-D-glucopyranoside (0.7 mM final conc. in well) in sodium phosphate buffer (100 mM, pH 7.2). [c]α-galactosidase (from green coffee beans, Sigma G8507): 0.05 U/mL; α-galactosidase activity was determined with p-nitrophenyl-α-D-galactopyranoside (0.7 mM final conc. in well) in sodium phosphate buffer (100 mM, pH 6.8). [d]*β*-glucosidase (from almond, Sigma G4511): 0.05 U/mL; the activity was determined with p-nitrophenyl-*β*-D-glucopyranoside (0.7 mM final conc. in well) in sodium acetate buffer (100 mM, pH 5.0). [e]*β*-galactosidase (from bovine liver, Sigma G1875): 0.05 U/mL; activity was determined with p-nitrophenyl-*β*-D-galactopyranoside (0.7 mM final conc. in well) in sodium phosphate buffer (100 mM, pH 7.2). [f]Naringinase (from penicillium decumbens, Sigma N1385): 0.06 U/mL. the activity was determined with p-nitrophenyl-*β*-D-glucopyranoside (0.7 mM final conc. in well) in sodium acetate buffer (100 mM, pH 5.0). [g]*β*-glucocerebrosidase (GBA) and [g]*β*-galactocerebrosidase (GALC) activities were determined using 4-methylumbelliferyl-*β*-D-glucopyranoside and 4-methylumbelliferyl-*β*-D-galactopyranoside using assay conditions based on those previously reported.[50]

4.2.7.1 *Inhibition Assays against Human Recombinant GBA (R&D 7410-GH) for compounds **10** and **11** after immediate and 24 hour incubation period*

Based on our hydrolysis stability studies of compounds **10** and **11** we hypothesized that there would be no difference in inhibitory potency for samples left in solution at pH 7.0 and a complete inactivation of the samples that were left overnight at pH 5.2 would be observed. Since such claims were made, we found it necessary to determine whether these statements could be backed up with an additional, independent experiment.

For **pH 7.0**, samples were dissolved in buffers 24 hours prior to or right before the biological evaluation for GBA inhibition. As envisioned, only a minor difference for all compounds was obtained (approx. 10% in both cases), proving that these compounds did not undergo hydrolysis under neutral conditions and retained the inhibition properties (**Table 4**). It should be taken in consideration that the difference in inhibition at 0 min and 24 hours at pH 7.0 for compounds **10**, **11** and NNDNJ (**2**) occurs due to experiments fluctuations and is in the same order of magnitude as determined in regular GBA biological evaluations.

For **pH 5.2**, samples were dissolved in buffers 24 hours prior to or right before the biological evaluation for GBA inhibition. The inhibitory difference between time dependent hydrolysis is noticeable in both cases as presented in **Table 4**. A big jump in IC_{50} value was determined for compound **11** from 1934 nM to more than 30000 nM when left in the solution overnight.

Enzyme[a]	t [h]	10	11	NNDNJ
GBA[b] (pH 7.0)	0	3394±372	29.6±2.4	775±58
GBA[b] (pH 7.0)	24	2561±233	25.2±2.6	532±59
GBA[b] (pH 5.2)	0	> 30000	1934±178	3730±424
GBA[b] (pH 5.2)	24	> 30000	> 30000	5584±731

Table 4. Glycosidase inhibition values obtained for orthoester-armed guanidines **10** and **11** after immediate enzyme assay evaluation of after 24 hours incubation in the corresponding buffer solution.[a]

[a]IC_{50} values for GBA inhibition of compounds **10**, **11** and NNDNJ at pH 7.0 and pH 5.2 after immediate evaluation (t = 0 hours) and 24 hour incubation (t = 24 hours) in the corresponding buffer. IC_{50} Values are reported in nM and are averages obtained from triple independent duplicate analysis of each compound For ease of comparison, the IC_{50} values obtained for all compounds shown in Table 4 are compared to a reference compound NNDNJ. [b]β-glucocerebrosidase (GBA) activities were determined using 4-methylumbelliferyl-β-D-glucopyranoside assay conditions based on those previously reported.[50]

4.2.7.2 *Inhibition Assays against Human Recombinant GBA (R&D 7410-GH) in a time dependant fashion for compound **11***

To extend our studies, we prepared a series of sample **11** preincubated in the acidic buffer every two hours to illustrate the inactivation process of the enzyme during the period of 20 hours. Thus, 12 data points were plotted in **Figure 8** for a better graphical representation of the inactivation process as the hydrolysis of the orthoester occurs.

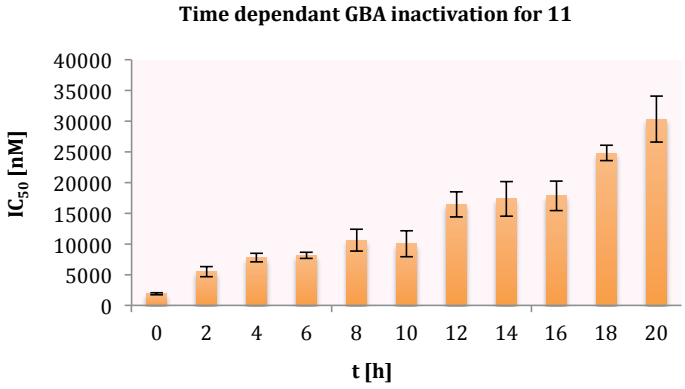

Figure 8. IC_{50} values for GBA inhibition for the orthoester-armed DIX derivative **11** at pH 5.2 determined immediately after addition and mixing and after every 2 hours incubation time, for 20 hours, at the acidic pH. The data reflect the inactivation of the chaperone **11**, thereby losing the inhibitory capacity, following hydrolysis to result in a completely inactive hydrolyzed species with IC_{50} of more than 30000 nM.

4.2.8 Fibroblast experiments

To investigate whether the inhibitory effect would translate into cellular pharmacological chaperone behavior, we examined the impact of compounds **10** and **11** on GBA activity in GD derived fibroblasts.

4.2.8.1 Enzyme enhancement activity in human N370S fibroblasts

Patient derived cells were incubated with compounds **10**, **11**, NN-DNJ (**2**) or isofagomine (**3**, IFG) for 4 days followed by measurement of GBA activity. The most prominent enzyme enhancement effects were seen with the N370S cell line. **Figure 9** summarizes the increase in GBA (N370S) activity measured at various concentrations of compounds **10** and **11** as well as NN-DNJ and IFG included as reference pharmacological chaperones.

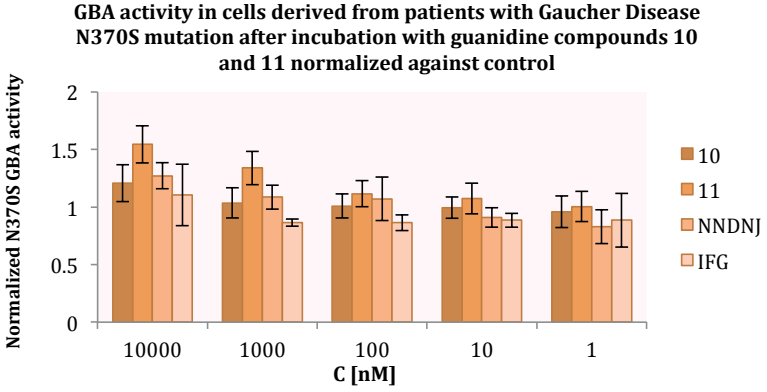

Figure 9. The effect of compounds **10**, **11**, **NNDNJ** and **IFG** on GBA activity in N370S fibroblasts (GM00372) from Gaucher patients. Cells were cultured for 4 days in the absence or presence of increasing concentrations (nM) of the compounds before GBA activity was measured. Experiments were performed in triplicate, and each bar represents the mean ± SD. Enzyme activity is normalized to untreated cells, assigned a relative activity of 1.

Assays using Gaucher patient-derived fibroblasts (homozygous for the most prevalent N370S mutation) indicate that **11** possesses a chaperone activity at least on par with that of NN-DNJ (**Figure 10**).[51] Furthermore, we observed a superior enhancement effect for **11** compared to that exhibited by the known pharmacological chaperone isofagomine (**3**, IFG), although low activity of IFG could be attributable to its poorer permeability.[52,53] We also note that the better GBA binder **11** is indeed the better chaperone in comparison to **10**. This chaperone effect of **11** is in contrast to our previous DIX derivatives, that were good GBA binders, but lacked the cleavable orthoester.[37]

4.2.9 Enzyme enhancement activity in human L444P fibroblasts

The effect of NN-DNJ (**2**), IFG and compounds **10** and **11** on the activity of the L444P GBA mutant was also measured using Gaucher disease Type 2 patient-derived fibroblast cell line. After a 4-day incubation, however, little-to-no enhancement in GBA activity was observed at all compound concentrations measured (**Figure 10**). The data do suggest a slight chaperone effect for compound **11** relative to IFG, however, the low basal GBA activity of the L444P cell line led to large fluctuations in the measured activity making it difficult to draw firm conclusions. When assays were performed with patient-derived fibroblasts homozygous for the L444P mutation, inhibition effects were observed for NN-DNJ but not for compound **11**. Nevertheless, our preliminary findings with Gaucher patient fibroblast are especially encouraging given that the two GBA mutations studied here have generally proven to be among the least responsive to chaperoning approaches.[43]

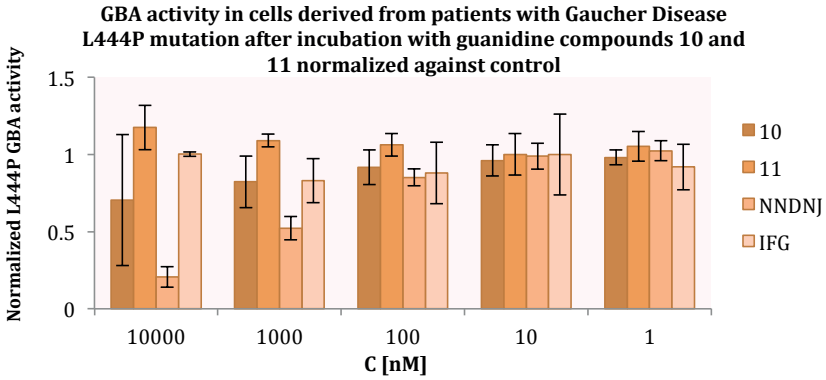

Figure 10. The effect of compounds **10**, **11**, **NNDNJ** and **IFG** on GBA activity in L444P fibroblasts (GM00877) from Gaucher patients. Cells were cultured for 4 days in the absence or presence of increasing concentrations (nM) of the compounds before GBA activity was measured. Experiments were performed in triplicate, and each bar represents the mean ± SD. Enzyme activity is normalized to untreated cells, assigned a relative activity of 1.

4.3 CONCLUSIONS & OUTLOOK

In summary, we here report a two new iminosugar based glycosidase inhibitors bearing an exocyclic guanidinium moiety that is alkylated *via* an acid labile orthoester. Our investigations revealed that DIX-derived analogue **11** is a particularly potent and selective inhibitor of the human *β*-glycosidase GBA. Our findings indicate that the addition of the guanidinium moiety leads to more potent GBA inhibition compared to NN-DNJ or the orthoester-linked alkylated DNJ thioureas reported by the group of *Ortiz Mellet*.[43] The inhibitory potency of the DIX analogues explored in our study are very dependent on the length of the alkyl substituent connected to the orthoester with compound **11** among the most potent GBA inhibitors reported to date. Importantly, while compound **11** was very active at neutral pH (IC_{50} 25.2 ± 2.6 nM), complete inactivation was observed at pH 5.2. These findings suggest that such compounds may have potential for application as pharmacological chaperones in LSDs such as Gaucher disease. More comprehensive studies examining the pharmacological chaperone activities of compound **11** and other guanidino iminosugars bearing an orthoester-linked lipid will be reported in due course.

4.4 EXPERIMENTAL SECTION

4.4.1 General methods and materials

Reagents, solvents and solutions. Unless stated otherwise, chemicals were obtained from commercial sources and used without further purification. All solvents were purchased from Biosolve (Valkenswaard, The Netherlands) and were stored on molecular sieves (4 Å). 2,3,4-Tri-O-benzyl-5-des(hydroxymethyl)-1-deoxynojirimycin[44] (**12**), Cbz-NCS[22] and compounds **18**[43] and **19**[43] were prepared as previously described.

Purification Techniques. All reactions and fractions from column chromatography were monitored by thin layer chromatography (TLC) using plates with a UV fluorescent indicator (normal SiO_2, Merck 60 F254). One or more of the following methods were used for visualization: 10% H_2SO_4 in MeOH, molybdenum blue, $KMnO_4$ or ninhydrine followed by warming until spots could be visible detected under UV light. Flash chromatography was performed using Merck type 60, 230–400 mesh silica gel. Removal of solvent was performed under reduced pressure using a rotary evaporator.

Instrumentation for Compound Characterization. For LC–MS analysis, an HPLC system (detection simultaneously at 214, 254 nm and evaporative light detection) equipped with an analytical C_{18} column (100 Å pore size, 4.6 mm (⌀) x 250 mm (l), 10 µm particle size) or C_8 column (100 Å pore size, 4.6 mm (⌀) x 250 mm (l), 10 µm particle size) in combination with buffers A: H_2O, B: MeCN, A and B with 1.0% aqueous trifluoroacetic acid (TFA), in some cases - coupled with an electrospray interface (ESI) was used. Formic acid (FA; LC-MS grade), acetic acid, sodium acetate and ammonium acetate were acquired from Sigma-Aldrich (St. Louis, MA, USA). Ultra-pure water was obtained from a Synergy UV water delivery system from Millipore (Billerica, MA, USA). For RP-HPLC purifications (detection simultaneously at 213, 254 nm), an automated HPLC system equipped with a preparative C_{18} column (20 mm (⌀) x 250 mm (l), 5 µm particle size) or C_8 column (20 mm (⌀) x 250 mm (l), 5 µm particle size) in combination with buffers A: H_2O, B: MeCN, A and B with 1.0% aqueous trifluoroacetic acid (TFA). High-resolution mass spectra were recorded by direct injection (2 µL of a 2 µM solution in H_2O/MeCN 50:50 *v/v* and 0.1% formic acid) on a mass spectrometer. ^1H and ^{13}C NMR spectra were recorded on 500–125 MHz or 400–100 MHz spectrometers. Chemical shifts (δ) are given in ppm relative to tetramethylsilane (TMS) as internal standard. All ^{13}C NMR spectra are proton decoupled. ^1H NMR data are reported in the following order: number of protons, multiplicity (*s*, singlet; *d*, doublet; *t*, triplet; *q*, quartet and *m*, multiplet) and coupling constant (*J*) in Hertz (*Hz*). When appropriate, the multiplicity is preceded by *br*, indicating that the signal was broad. ^{13}C NMR spectra were recorded at 75.5 MHz with chemical shifts reported relative to $CDCl_3$ δ 77.0. ^{13}C NMR spectra were recorded using the attached proton test (APT) sequence. All literature compounds had ^1H NMR and mass spectra consistent with the assigned structures.

4.4.2 Preparative details and analytical data for synthesized compounds

4.4.2.1 Synthetic approach towards the acetylated 1,5-dideoxy-1,5-imino-D-xylitol building block *16*

2,3,4-Tri-O-benzyl-5-des(hydroxymethyl)-1-deoxynojirimycin (12).

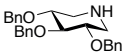

According to the literature procedure.[44] Characterization data for compound **12** is in accordance to previously published data. R_f (EtOAc + 2% NH_4OH) = 0.72. ^{1}H NMR (400 MHz, CD_3OD) δ 1.51 (s, 1H), 2.48 (dd, *J* = 9.8, 12.3 Hz, 2H), 3.20 (dd, *J* = 4.8, 12.3 Hz, 2H), 3.35 – 3.58 (m, 3H), 4.60 – 4.76 (m, 4H), 4.88 (s, 2H), 7.16 – 7.44 (m, 15H). ^{13}C NMR (100 MHz, CD_3OD) δ 139.0, 138.6, 128.4, 128.3, 128.0, 127.7, 127.6, 127.5, 85.8, 79.8, 77.3, 77.0, 76.7, 75.5, 72.9, 49.2. HRMS (ESI, $[M+H]^+$), calculated for $C_{26}H_{29}NO_3$, 404.2226; found 404.2226.

***Tert*-butyl 3,4,5-tris(benzyloxy)piperidine-1-carboxylate (13).**

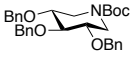

To a previously synthesised benzyl protected DIX **12** (2.00 g, 8.57 mmol) in DCM (50 mL), the mixture was cooled to 0 °C under Ar atmosphere. Next, Et_3N (1.25 mL, 9.00 mmol) and di-*tert*-butoxycarbonyl dicarbonate (Boc_2O, 2.42 g, 11.06 mmol) were added. The mixture was stirred until it reached the room temperature and additionally for 15 h under Ar atmosphere. The next day, the solvent was evaporated and the resulting residue washed with 2M HCl (2 x 30 mL) and saturated aqueous solution of $NaHCO_3$ (2 x 40 mL). The organic fractions were dried with Na_2SO_4 and the solvent was concentrated to give the residue, which was coevaporated several times with chloroform and purified by column chromatography. Yield: 4.13 g (96%). ^{1}H NMR (400 MHz, $CDCl_3$) δ 1.41 (s, 9H), 2.51 – 2.71 (m, 2H), 3.33 – 3.60 (m, 2H), 3.91 – 4.44 (m, 3H), 4.69 (s, 4H), 4.88 (s, 2H). ^{13}C NMR (101 MHz, $CDCl_3$) δ 154.4, 146.7, 138.2, 128.4, 128.3, 127.9, 127.7, 127.5, 85.7, 85.1, 80.2, 75.5, 72.8, 28.3, 27.4. HRMS (ESI, $[M+Na]^+$), calculated for $C_{31}H_{37}NO_5$, 526.2569; found 526.2564.

***Tert*-butyl 3,4,5-trihydroxypiperidine-1-carboxylate (14).**

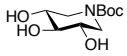

The benzylated boc protected iminosugar **13** was dissolved in a mixture of glacial AcOH in MeOH (1/1, v/v) and transferred to a Parr high-pressure hydrogenation flask. A catalytic amount of 10% palladium on carbon was added to the flask (ca. 10 mg catalyst/mg of benzylated starting material). The flask was put under reduced pressure and ventilated with hydrogen gas. This procedure was repeated twice after which the pressure was adjusted to 4.5-5.0 bar hydrogen pressure. The reaction was allowed to proceed for 12 h while mechanically shaken and the pressure maintained at the value initially set. The mixture was filtered over Celite on a glass microfiber filter, followed by rinsing the filter with MeOH. The mixture was concentrated under reduced pressure. The crude product thus obtained was immediately used in the next reaction. Yield: 1.91 g (quant.). ^{1}H NMR (400 MHz, DMSO) δ 1.35 (s, 9H), 2.36 – 2.45 (m, 2H), 2.96 (t, *J* = 8.4 Hz, 1H), 3.02 – 3.13 (m, 2H), 3.71 – 3.88 (m, 2H), 4.94 (s, 1H), 5.00 (s, 2H). ^{13}C NMR (101 MHz, DMSO) δ 154.3, 105.0, 79.3, 78.8, 69.9, 48.9, 28.4. HRMS (ESI, $[M+Na]^+$), calculated for $C_{10}H_{19}NO_5$, 256.1161; found 256.1162.

***Tert*-butoxycarbonyl-piperidine-3,4,5-triyl triacetate (15).**

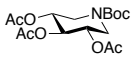

To a solution of **14** (1.91 g, 8.20 mmol), a mixture of Ac_2O and pyridine (1:1, 40 mL) was added and the resulting mixture was stirred at rt for 24 h. The reaction mixture was quenched with H_2O (30 mL), diluted with CH_2Cl_2 (100 mL) and washed with 2M HCl (30 mL) and saturated aqueous solution of $NaHCO_3$ (40 mL). The organic fractions were dried with Na_2SO_4 and the solvent was concentrated to give the residue, which was co-evaporated several times with toluene and purified by flash column chromatography (EtOAc:PE = 1:2). Yield: 2.95 g (quant.). ^{1}H NMR (400 MHz, $CDCl_3$) δ 1.47 (s, 9H), 2.05 (2x s, 9H), 3.06 (dd, *J* = 8.8, 13.6 Hz, 2H), 4.06 (dd, *J* = 8.8, 13.6 Hz, 2H), 4.82 (br s, 2H), 5.08 (t, *J* = 8.0 Hz, 1H). ^{13}C NMR (101 MHz, $CDCl_3$) δ 169.8, 154.2, 80.8, 72.4, 28.2, 20.74, 20.70. HRMS (ESI, $[M+Na]^+$), calculated for $C_{16}H_{25}NO_8$, 382.1478; found 382.1476.

3,4,5-Tri-*O*-acetyl piperidin trifluoroacetate (16).

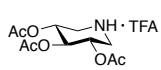

Compound **15** (2.95 g, 8.20 mmol) was treated with TFA-CH_2Cl_2 (9:1, 50 mL) at 0 °C for 30 min. After, the mixture was concentrated and co-evaporated several times with CH_2Cl_2. The resulting residue was purified by column chromatography (CH_2Cl_2:MeOH 2:1). Yield: 3.01 g (quant.). ^{1}H NMR (400 MHz, $CDCl_3$) δ 2.13 (s, 6H), 2.15 (s, 3H), 3.39 – 3.54 (m, 4H), 5.05 (td, *J* = 3.6 Hz, 2H), 5.17 (t, *J* = 4.0 Hz, 1H). ^{13}C NMR (101 MHz, $CDCl_3$) δ 169.3, 168.4, 64.6, 64.5, 43.3, 20.5, 20.3. HRMS (ESI, $[M+H\text{-}TFA]^+$), calculated for $C_{11}H_{17}NO_6$, 260.1134; found 260.1133.

*4.4.2.2 Synthetic route towards orthoester-armed DIX guanidines **10** and **11***

A series of orthoester amines **18** and **19**, comprised of simple alkyl chains with four and eight carbon atoms in length, were synthesized according to a literature procedure.[43] Treatment of the corresponding amines **18** or **19** with CbzNCS generated appropriate thioureas **20** and **21**, which served as an integral part of our approach to incorporate orthoester moiety through subsequent guanidine formation step (**Scheme 7**). Activation of the Cbz-protected thioureas **20** and **21** with EDCI followed by addition of previously prepared acetyl protected DIX **16**, led to clean formation of protected guanidines **22** and **23**. Hydrogenation under basic conditions yielded fully deprotected orthoester-armed guanidine products **10** and **11**. Analytical data and characterization data for compounds **17**-**27** are given below.

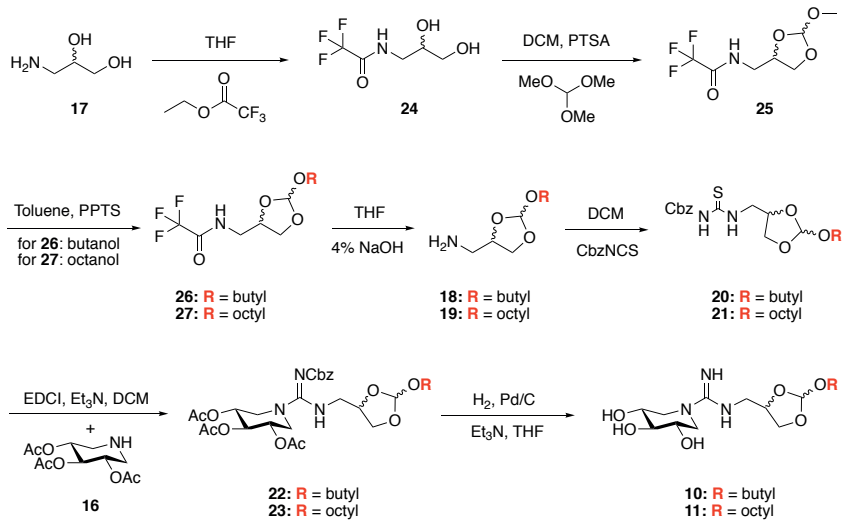

Scheme 7. Extended synthetic route towards orthoester rich DIX-guanidines **10** and **11**.

2,2,2-Trifluoro-*N*-(2,3-dihydroxy-propyl)-acetamide (24).[43]

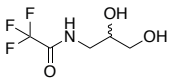

To a stirred solution of 3-amino-1,2-propanediol (**17**, 8.4 g, 0.090 mol) in THF (70 mL), ethyl trifluoroacetate (13 mL, 0.110 mol) was added dropwise at 0 ^{0}C. After 2 h, the mixture was evaporated and the residue dissolved in ethyl acetate (70 mL). It was washed with aqueous potassium hydrogen sulfate (0.5 M, 2 x 10 mL) and brine (30 mL), then dried over Na_2SO_4 and concentrated to obtain a colourless viscous liquid. Characterization data for compound **24** is in accordance to previously published data. Yield: 16 g (95%). ^{1}HNMR ($CDCl_3$, 300 MHz): δ 2.12 (t, *J* = 5.5 Hz, 1H), 2.61 (d, *J* = 5.0 Hz, 1H), 3.25–3.85 (m, 4H,), 3.92 (m, 1H), 6.88 (m, 1H). HRMS (ESI, $[M+H]^+$), calculated for $C_5H_8F_3NO_3$, 188.0535; found 188.0537.

2,2,2-Trifluoro-*N*-(2-methoxy-[1,3]dioxolan-4-ylmethyl)-acetamide (25).[43]

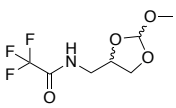

The diol **24** (14.5 g, 0.08 mol) was dissolved in dichloromethane (40 ml) and trimethyl orthoformate (38 ml, 0.70 mol); p-toluene sulfonic acid (PTSA; 0.3 g, 0.0017 mol) was then added. The solution was stirred at room temperature for 2 h. The solution was then diluted with dichloromethane (150 mL), washed successively with saturated aqueous sodium hydrogen carbonate (3 x 100 mL) and brine (100 mL). The organic phase was then dried over Na_2SO_4, filtered and concentrated to yield colourless oil. Characterization data for compound **25** is in accordance to previously published data. Yield: 15 g (86%). ^{1}H NMR ($CDCl_3$, 300 MHz): mixture of two diastereomers 50/50: δ 3.33 and 3.37 (s, 3H), 3.35–3.80 (m, 3H), 4.10–4.25 (m, 1H), 4.50 (m, 1H), 5.73 and 5.78 (s, 1H), 6.66 and 7.55 (s, 1H). HRMS (ESI, $[M+H]^+$), calculated for $C_7H_{10}F_3NO_4$, 230.0640; found 230.0

N-(2'-Butyloxy-[1',3']dioxolan-4'-ylmethyl)trifluoroacetamide (26).[3]

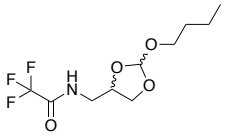

To a solution of **25** (2.5 g, 10.9 mmol) in toluene (20 mL), 1-butanol (0.81 g, 10.9 mmol) and pyridinium p-toluenesulfonate (PPTS, 28 mg, 0.11 mmol) were added. The resulting solution was stirred under reflux for 2 h. After addition of cyclohexane (100 mL), the organic layer was washed with saturated aqueous $NaHCO_3$ (3 x 30 mL) and brine (30 mL), dried (Na_2SO_4), filtered and the solvent was eliminated. The residue was purified by column chromatography (EtOAc:PE = 1:6). Yield: (2.46 g, 83%). Characterization data for compound **26** is in accordance to previously published data. R_f (EtOAc:PE = 1:4) = 0.40. ^{1}H NMR (400 MHz, $CDCl_3$) δ 0.89 (t, *J* = 7.4 Hz, 3 H), 1.39 (m, 2 H), 1.55 (m, 2 H), 3.37-3.73 (m, 4 H), 3.71-3.82 (m, 1 H), 4.03-4.16 (m, 1 H), 4.47 (m, 1 H), 5.79 and 5.83 (s, 1 H), 6.67 and 7.47 (br s, 1 H). ^{13}C NMR (100.6 MHz, $CDCl_3$) δ 14.0, 19.2, 19.4, 31.4, 31.5, 41.1, 42.2, 64.6, 65.8, 65.1, 65.9, 73.4, 73.9, 115.6, 115.71, 115.73, 157.8, 158.2. HRMS (ESI, $[M+H]^+$), calculated for $C_{10}H_{16}F_3NO_4$, 272.1110; found 272.1113.

2,2,2-Trifluoro-*N*-(2-octyl-[1,3]dioxolan-4-ylmethyl)-acetamide (27).[43]

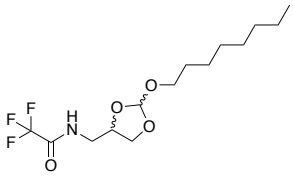

To a solution of **25** (2.5 g, 10.9 mmol) in toluene (17 mL), 1-octanol (1.42 g, 10.9 mmol) and pyridinium p-toluenesulfonate (PPTS, 28 mg, 0.11 mmol) were added. The resulting solution was stirred under reflux for 2 h. After addition of cyclohexane (100 mL), the organic layer was washed with saturated aqueous $NaHCO_3$ (3 x 30 mL) and brine (30 mL), dried (Na_2SO_4), filtered and the solvent was eliminated. The residue was purified by column chromatography (EtOAc:PE = 1:3). Yield: 2.63 g (74%). Characterization data for compound **27** is in accordance to previously published data. R_f (EtOAc:PE = 1:3) = 0.56. ^{1}H NMR (500 MHz, $CDCl_3$) δ 0.89 (t, *J* = 6.9 Hz, 3 H), 1.27 (m, 10 H), 1.59 (m, 2 H), 3.37-3.70 (m, 4 H), 3.73-3.80 (m, 1 H), 4.03-4.21 (m, 1 H), 4.48 (m, 1 H), 5.79 and 5.84 (s, 1 H), 6.68 and 7.47 (br s, 1 H). ^{13}C NMR (125.7 MHz, $CDCl_3$) δ 13.9, 22.6, 25.8, 25.9, 26.1, 26.3, 29.2, 29.4, 29.6, 31.6, 32.6, 41.0, 42.1, 64.5, 65.7, 65.1, 65.9, 73.4, 74.1, 115.6, 115.72, 115.73, 157.9, 158.1. HRMS (ESI, $[M+H]^+$), calculated for $C_{14}H_{24}F_3NO_4$, 328.1736; found 328.1741.

(2-Butyloxy-[1,3]dioxolan-4-yl)methylamine (18).[43]

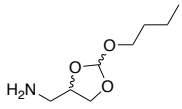

To a solution of **26** (1.9 g, 7.0 mmol) in THF (15 mL), a solution of 4% aqueous NaOH (16 mL) was added at 0 °C and the mixture reaction was stirred for 4 h at rt. The aqueous layer was extracted with CH_2Cl_2 (3 x 70 mL) and the combined organic layers were washed with brine (50 mL), dried (Na_2SO_4), then filtered and evaporated the solvent. The residue was purified by column chromatography (CH_2Cl_2:MeOH = 9:1). Characterization data for compound **18** is in accordance to previously published data. Yield: 0.99 g (81%). R_f (CH_2Cl_2:MeOH = 9:1) = 0.54. ^{1}H NMR (500 MHz, $CDCl_3$) δ 0.89 (m, 3 H), 1.31 (m, 2 H), 1.59 (m, 2 H), 2.73-2.95 (m, 2 H), 3.54 (m, 2 H), 3.71 and 3.79 (m, 1 H), 4.06 and 4.14 (m, 1 H), 4.19 and 4.35, (m, 1 H), 5.78 and 5.81 (s, 1 H). ^{13}C NMR (125.7 MHz, $CDCl_3$) δ 13.8, 19.3, 19.6, 31.1, 31.6, 44.5, 44.9, 64.82, 64.9, 66.1, 66.2, 78.3, 115.6, 115.9. HRMS (ESI, $[M+H]^+$), calculated for $C_8H_{17}NO_3$, 176.1287; found 176.1282.

(2-Octyloxy-[1,3]dioxolan-4-yl)methylamine 19.[43]

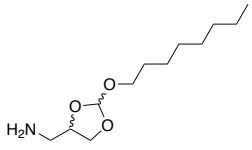

To a solution of **27** (2.4 g, 7.0 mmol) in THF (15 mL), a solution of 4% aqueous NaOH (16 mL) was added at 0 °C and the mixture reaction was stirred for 4 h at rt. The aqueous layer was extracted with CH_2Cl_2 (5 x 100 mL) and the combined organic layers were washed with brine (50 mL), dried (Na_2SO_4), then filtered and evaporated the solvent. The residue was purified by column chromatography (CH_2Cl_2:MeOH = 9:1). Characterization data for compound **19** is in accordance to previously published data. Yield: 1.28 g (79%). R_f (CH_2Cl_2:MeOH = 9:1) = 0.28. ^{1}H NMR (500 MHz, $CDCl_3$) δ 0.89 (m, 3 H), 1.31 (m, 10 H), 1.63 (m, 2 H), 2.72-2.96 (m, 2 H), 3.53 (m, 2 H), 3.70 and 3.79 (m, 1 H), 4.04 and 4.14 (m, 1 H), 4.26 and 4.34, (m, 1 H), 5.78 and 5.81 (s, 1 H). ^{13}C NMR (125.7 MHz, $CDCl_3$) δ 13.9, 22.6, 26.4, 29.4, 29.5, 31.1, 31.6, 44.5, 44.9, 64.82, 64.9, 66.1, 66.2, 78.3, 115.6, 115.9. HRMS (ESI, $[M+H]^+$), calculated for $C_{12}H_{25}NO_3$, 232.1913; found 232.1911.

N-(Benzyloxycarbonyl)-N'-(2'-Butyloxy-[1',3']dioxolan-4'-ylmethyl) thiourea (20).

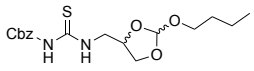

The amine **18** (250 mg, 1.4 mmol, 1eq) was dissolved in CH_2Cl_2 (100 mL) and treated with a 0.5 M solution of CbzNCS in CH_2Cl_2 (2.85 mL, 1 eq) and NEt_3 (10 eq). After stirring for 12 h at room temperature, TLC analysis indicated complete conversion to thiourea species. The CH_2Cl_2 was then removed under reduced pressure, and the residue dissolved in chloroform was applied directly to a silica column, eluting with EtOAc/PE mixture. Yield: 423 mg, 80%. R_f (EtOAc:PE = 1:4) = 0.32. ^{1}H NMR (400 MHz, $CDCl_3$) δ 0.90 (t, *J* = 7.4 Hz, 3H), 1.27 – 1.45 (m, 2H), 1.47 – 1.61 (m, 2H), 3.43 – 3.59 (m, 2H), 3.72 – 3.95 (m, 2H), 4.04 – 4.20 (m, 2H), 4.39 – 4.65 (m, 1H), 5.17 (s, 2H), 5.83 (2 x s, 1H), 7.28 – 7.45 (m, 2H), 8.02 (s, 1H), 9.90 (2 x s, 1H). ^{13}C NMR (101 MHz, $CDCl_3$) δ 179.7, 152.1, 134.4, 128.9, 128.9, 128.73, 128.71, 128.4, 115.9, 74.1, 73.1, 68.3, 68.2, 65.8, 65.7, 65.0, 64.8, 48.0, 47.5, 31.5, 31.4, 19.2, 19.2, 13.8, 13.7. HRMS (ESI, $[M+Na]^+$), calculated for $C_{17}H_{24}N_2O_5S$, 391.1304; found, 391.1287.

N-(Benzyloxycarbonyl)-N'-(2'-Octyloxy-[1',3']dioxolan-4'-ylmethyl) thiourea (21).

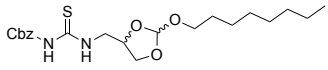

The amine **19** (300 mg, 1.3 mmol, 1eq) was dissolved in CH_2Cl_2 (100 mL) and treated with a 0.5 M solution of CbzNCS in CH_2Cl_2 (2.59 mL, 1 eq) and NEt_3 (10 eq). After stirring for 12 h at room temperature, TLC analysis indicated complete conversion to thiourea species. The CH_2Cl_2 was then removed under reduced pressure, and the residue dissolved in chloroform was applied directly to a silica column, eluting with EtOAc/PE mixture. Yield: 452 mg, 82%. R_f (EtOAc:PE = 1:4) = 0.28. ^{1}H NMR (400 MHz, $CDCl_3$) δ 0.78 – 0.96 (m, 3H), 1.17 – 1.42 (m, 10H), 1.49 – 1.69 (m, 2H), 3.48 – 3.69 (m, 2H), 3.74 – 3.98 (m, 3H), 4.07 – 4.21 (m, 2H), 4.39 – 4.70 (m, 1H), 5.19 (s, 2H), 5.85 (2 x s, 1H), 7.31 – 7.49 (m, 5H), 8.04 (s, 1H), 9.92 (2 x s, 1H). ^{13}C NMR (101 MHz, CDCl3) δ 179.9, 179.7, 152.1, 134.4, 128.94, 128.93, 128.73, 128.70, 128.4, 115.9, 77.3, 77.0, 76.7, 74.1, 73.1, 68.3, 68.2, 65.8, 65.7, 65.3, 65.1, 48.1, 47.5, 31.82, 31.80, 29.41, 29.40, 29.33, 29.31, 29.22, 29.21, 26.1, 26.0, 22.6, 14.1. HRMS (ESI, $[M+Na]^+$), calculated for $C_{21}H_{32}N_2O_5S$, 447.1930; found, 447.1921.

N'-((benzyloxy)carbonyl)-N-((2-(butoxy)-1,3-dioxolan-4-yl)methyl)-carbamimidoyl)piperidine-3,4,5-triyl triacetate (22).

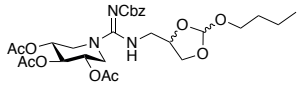

The thiourea **20** (150 mg, 0.41 mmol, 1 eq), OAc-DIX (**16**, 110 mg, 0.43 mmol, 1.05 eq) and EDCI (95 mg, 0.61 mmol, 1.5 eq) were dissolved in CH_2Cl_2 (40 mL), followed by addition of NEt_3 (0.17 mL, 1.2 mmol, 3 eq). Reaction mixture was stirred for 18h at room temperature, after which TLC analysis confirmed total consumption of starting material. The solvent was then removed under reduced pressure, and the residue, dissolved in $CHCl_3$, was applied directly to a silica column, eluting with hexanes chaser and subsequently with EtOAc/PE. Yield: 220 mg, 91%. R_f (EtOAc:PE = 1:1) = 0.31. ^{1}H NMR (400 MHz, $CDCl_3$) δ 0.88 – 0.96 (m, 3H), 1.31 – 1.44 (m, 2H), 1.50 – 1.62 (m, 2H), 2.04 (s, 9H), 2.82 – 3.02 (m, 2H), 3.26 – 3.49 (2 x m, 2H), 3.49 – 3.59 (m, 2H), 3.74 (2 x dd, J = 6.0, 8.2 Hz, 1H), 3.92 – 4.03 (m, 2H), 4.13 (2 x dd, J = 6.9, 8.2 Hz, 1H), 4.25 – 4.51 (2 x m, 1H), 4.81 – 4.94 (m, 2H), 5.12 (s, 2H), 5.14 – 5.22 (m, 1H), 5.83 (2 x s, 1H), 7.19 – 7.48 (m, 5H), 8.28 (2 x s, 1H). ^{13}C NMR (101 MHz, $CDCl_3$) δ 169.93, 169.91, 169.83, 169.82, 169.81, 169.7, 128.32, 128.31, 128.24, 128.22, 127.8, 127.7, 116.0, 115.5, 75.0, 73.8, 72.6, 72.5, 69.02, 69.01, 68.9, 68.8, 67.1, 67.0, 65.82, 65.81, 65.3, 64.8, 48.6, 48.4, 48.3, 48.2, 47.4, 46.9, 31.42, 31.40, 20.7, 19.23, 19.21, 13.8. HRMS (ESI, $[M+H]^+$), calculated for $C_{28}H_{39}N_3O_{11}$, 594.2663; found, 594.2657.

N'-((benzyloxy)carbonyl)-N-((2-(octyloxy)-1,3-dioxolan-4-yl)methyl)-carbamimidoyl)piperidine-3,4,5-triyl triacetate (23).

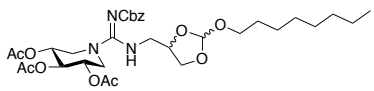

The thiourea **21** (240 mg, 0.57 mmol, 1 eq), OAc-DIX (**16**, 154 mg, 0.59 mmol, 1.05 eq) and EDCI (132 mg, 0.85 mmol, 1.5 eq) were dissolved in CH_2Cl_2 (40 mL), followed by addition of NEt_3 (0.24 mL, 1.7 mmol, 3 eq). Reaction mixture was stirred for 18h at room temperature, after which TLC analysis confirmed total consumption of starting material. The solvent was then removed under reduced pressure, and the residue, dissolved in $CHCl_3$, was applied directly to a silica column, eluting with hexanes chaser and subsequently with EtOAc/PE. Yield: 326 mg, 89%. R_f (EtOAc/PE = 1:1) = 0.27. ^{1}H NMR (400 MHz, $CDCl_3$) δ 0.79 – 0.99 (m, 3H), 1.18 – 1.42 (m, 10H), 1.49 – 1.68 (m, 2H), 2.04 (3 x s, 9H), 2.81 – 3.06 (m, 2H), 3.28 – 3.60 (2 x m, 4H), 3.74 (2 x dd, *J* = 6.1, 8.2 Hz, 1H), 3.90 – 4.03

(m, 2H), 4.13 (2 x dd, *J* = 6.1, 8.2 Hz, 1H), 4.24 – 4.52 (m, 1H), 4.82 – 4.93 (m, 2H), 5.12 (s, 2H), 5.13 – 5.23 (m, 1H), 5.83 (2 x s, 1H), 7.27 – 7.44 (m, 5H), 8.28 (2 x s, 1H). ^{13}C NMR (101 MHz, $CDCl_3$) δ 169.93, 169.91, 169.84, 169.83, 169.81, 169.7, 137.0, 128.32, 128.31, 128.2, 127.8, 127.7, 116.0, 75.0, 72.6, 72.5, 69.0, 68.83, 68.80, 67.0, 65.83, 65.82, 65.6, 65.2, 48.6, 48.3, 48.2, 47.4, 31.8, 29.43, 29.42, 29.3, 29.24, 29.21, 26.03, 26.01, 22.6, 20.7, 14.1, 14.0. HRMS (ESI, $[M+H]^+$), calculated for $C_{32}H_{47}N_3O_{11}$, 650.3289; found, 650.3283.

4.4.2.3 *General procedure for Pd/C catalyzed hydrogenolysis and deacetylation for the synthesis of N-substituted guanidine compounds **22** and **23***

The triacetylated iminosugars **22** and **23** were dissolved in a mixture of Et_3N in THF (1/5, v/v), and transferred to a Parr high-pressure hydrogenation flask. A catalytic amount of 10% palladium on carbon was added to the flask (ca. 10 mg catalyst per 100 mg of starting material). The flask was put under reduced pressure and ventilated with hydrogen gas. This procedure was repeated twice after which the pressure was adjusted to 1.5-2.0 bar hydrogen pressure. The reaction was allowed to proceed for 6-12 h while mechanically shaken and the pressure maintained at the value initially set. The mixture was filtered over Celite on a glass microfiber filter, followed by rinsing the filter with THF. The mixture was concentrated under reduced pressure. The crude product thus obtained was purified using RP-HPLC employing a preparative C8 column and a gradient moving from 95% to 5% eluent A (50mM NH_4HCO_3:5mM Et_3N, pH = 8.3) over 60 min (flow rate, 18.0 mL/min, eluent B: MeOH). Fractions containing the desired product were combined and lyophilized to yield the pure compounds as amorphous white powders. Analytical data for compounds **10** and **11** and in-depth characterization data for both final compounds are given below.

N-((2-butoxy-1,3-dioxolan-4-yl)methyl)-3,4,5-trihydroxypiperidine-1-carboximidamide (10).

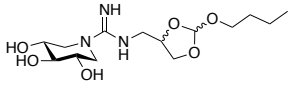

Yield: 32 mg, 92%. ^{1}H NMR (400 MHz, D_2O) δ 0.93 (br t, 3H), 1.29 – 1.48 (m, 2H), 1.52 – 1.67 (m, 2H), 3.09 (dd, *J* = 10.3, 13.4 Hz, 2H), 3.41 – 3.73 (m, 7H), 3.83 – 3.99 (m, 3H), 4.18 – 4.31 (m, 1H), 4.43 – 4.67 (2 x m, 1H), 6.00 (2 x s, 1H). ^{13}C NMR (101 MHz, D_2O) δ 157.13, 157.11, 115.6, 114.8, 76.9, 76.8, 75.1, 74.3, 68.54, 68.51, 68.50, 68.4, 65.9, 65.4, 65.3, 49.63, 49.61, 49.60, 44.5, 44.2, 30.7, 30.6, 18.6, 18.5, 12.93, 12.91. HRMS (ESI, $[M+H]^+$), calculated for $C_{14}H_{27}N_3O_6$, 334.1978; found, 334.1977.

N-((2-octyloxy-1,3-dioxolan-4-yl)methyl)-3,4,5-trihydroxypiperidine-1-carboximidamide (11).

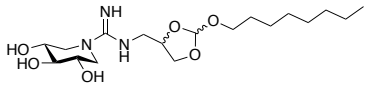

Yield: 26 mg, 89%. ^{1}H NMR (400 MHz, D_2O) δ 0.90 (br t, 3H), 1.22 – 1.47 (m, 10H), 1.52 – 1.72 (m, 2H), 3.10 (dd, *J* = 10.2, 13.4 Hz, 2H), 3.42 – 3.72 (m, 7H), 3.84 – 3.99 (m, 3H), 4.18 – 4.32 (m, 1H), 4.44 – 4.66 (2 x m, 1H), 6.01 (2 x s, 1H). ^{13}C NMR (101 MHz, D_2O) δ 157.1, 115.6, 76.9, 76.8, 75.1, 74.4, 68.55, 68.53, 68.52, 68.50, 66.2, 65.7, 65.33, 65.31, 49.62, 49.60, 44.6, 44.3, 31.02, 31.01, 28.5, 28.4, 28.33, 28.31, 28.22, 28.21, 25.2, 25.1, 21.92, 21.91, 13.33, 13.30. HRMS (ESI, $[M+H]^+$), calculated for $C_{18}H_{35}N_3O_6$, 390.2604; found, 390.2607.

4.4.2.4 *Experimental details for the synthesis of 2,3-di-O-acetylpropyl thiourea intermediate **B***

1-*N*-(*tert*-Butoxycarbonylamino)propane-2,3-diol (28). [43]

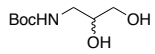

To a solution of commercial (±)-3-aminopropane-1,2-diol (**17**, 420 mg, 4.61 mmol) in DMF (5 mL) at 0 °C, Et_3N (704 µL, 5.07 mmol) and di-*tert*-butoxycarbonyl dicarbonate (Boc_2O) (1.21 g, 5.53 mmol) were added. The mixture was stirred at first at 0 °C and then at rt for 15 h, under Ar atmosphere. The solvent was evaporated and the resulting residue was purified by column chromatography (CH_2Cl_2:MeOH gradient 9:1 to 5:1). Characterization data for compound **28** is in accordance to previously published data. Yield: 835 mg (95%). R_f (CH_2Cl_2:MeOH = 5:1) = 0.63. ^{1}H NMR (300 MHz, CD_3OD) δ 1.44 (s, 9 H), 3.06 (m, 1 H), 3.21 (dd, 1 H), 3.49 (m, 2 H), 3.65 (m, 1 H). ^{13}C NMR (75.5 MHz, CD_3OD) δ 158.8, 80.1, 72.3, 65.1, 44.0, 28.7. HRMS (ESI, $[M+H]^+$), calculated for $C_8H_{17}NO_4$, 192.1236; found 192.1234.

2,3-Di-*O*-acetyl-1-N-((*tert*-butoxycarbonyl)amino)propane (29).[43]

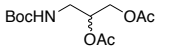

To a solution of **28** (783 mg, 4.10 mmol), a mixture of Ac_2O and pyridine (1:1, 12 mL) was added and the resulting mixture was stirred at rt for 24 h. The reaction mixture was quenched with H_2O (10 mL), diluted with CH_2Cl_2 (30 mL) and washed with 2M HCl (15 mL) and saturated aqueous solution of $NaHCO_3$ (20 mL). The organic fractions were dried with Na_2SO_4 and the solvent was concentrated to give the residue, which was coevaporated several times with toluene and purified by column chromatography (EtOAc:PE = 1:2). Characterization data for compound **29** is in accordance to previously published data. Yield: 1.15 g (quant.). R_f (EtOAc:PE = 1:2) = 0.48. ^{1}H NMR (300 MHz, CD_3OD) δ 1.43 (s, 9 H), 2.04 (2 x s, 6 H), 3.20 (dd, *J* = 14.4 Hz, *J* = 6.7 Hz, 1 H), 3.36 (d, *J* = 4.9 Hz, 1 H), 4.06 (dd, *J* = 3.0 Hz, 1 H), 4.27 (dd, *J* = 12.0 Hz, *J* = 4.0 Hz, 1H), 5.06 (m, 1 H). ^{13}C NMR (75.5 MHz, CD_3OD) δ 172.3, 172.2 (CO_{ester}), 158.7 ($CO_{carbamate}$), 80.4, 72.1, 64.1, 41.3, 28.9, 21.2, 20.5. HRMS (ESI, $[M+H]^+$), calculated for $C_{12}H_{21}NO_6$, 276.1447; found 276.1445.

1,2-Di-*O*-acetyl-3-aminopropane trifluoroacetic acid salt (30).[43]

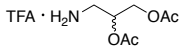

A solution of **29** (829 mg, 3.01 mmol) was treated with TFA-CH_2Cl_2 (9:1, 40 mL) at 0 °C for 20 min. After, the mixture was concentrated and coevaporated several times with CH_2Cl_2. The resulting residue was purified by column chromatography (CH_2Cl_2:MeOH gradient 15:1 to 9:1). Characterization data for compound **30** is in accordance to previously published data. Yield: 527 mg (quant.). R_f (CH_2Cl_2:MeOH = 9:1) = 0.39. ^{1}H NMR (300 MHz, CD_3OD) δ 2.04-2.11 (2 x s, 6 H), 3.25 (m, 2 H), 4.11 (dd, *J* = 4.7 Hz, 1 H), 4.41 (dd, *J* = 12.3 Hz, *J* = 4.5 Hz, 1 H), 5.26 (m, 1 H) . ^{13}C NMR (75.5 MHz, CD_3OD) δ 172.2, 171.9, 69.7, 63.6, 41.1, 20.6, 20.4. HRMS (ESI, $[M+H]^+$), calculated for $C_7H_{13}NO_4$, 176.0923; found 176.0922.

3-(3-((benzyloxy)carbonyl)thioureido)propane-1,2-diyl diacetate (31).

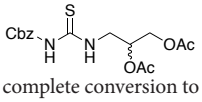

The amine salt **30** (440 mg, 1.52 mmol, 1eq) was dissolved in a mixture of NEt_3 (1.1 mL, 8 mmol) in $CHCl_3$ (100 mL) and treated with a 0.5 M solution of CbzNCS in CH_2Cl_2 (3.04 mL, 1 eq). After stirring for 12 h at room temperature, TLC analysis indicated complete conversion to thiourea species. The solvent was then removed under reduced pressure, and the residue dissolved in chloroform was applied directly to a silica column, eluting with EtOAc/PE mixture. Yield: 526 mg, 94%. ^{1}H NMR (400 MHz, $CDCl_3$) δ 2.10 (2 x s, 6H), 3.85 (ddd, *J* = 7.1, 13.2 Hz, 1H), 4.05 – 4.13 (m, 1H), 4.16 (dd, *J* = 4.4, 12.1 Hz, 1H), 4.34 (dd, *J* = 4.4, 12.1 Hz, 1H), 5.19 (s, 2H), 5.26 – 5.34 (m, 1H), 7.30 – 7.44 (m, 5H), 8.14 (s, 1H), 9.87 (s, 1H). ^{13}C NMR (101 MHz, $CDCl_3$) δ 180.0, 170.5, 170.1, 152.3, 134.3, 128.9, 128.7, 128.3, 69.3, 68.3, 62.9, 45.8, 20.9, 20.7. HRMS (ESI, $[M+Na]^+$), calculated for $C_{16}H_{20}N_2O_6S$, 391.094; found, 391.097.

N'-((benzyloxy)carbonyl)-N-(2,3-diacetoxypropyl)carbamimidoyl)piperidine-3,4,5-triyl triacetate (32).

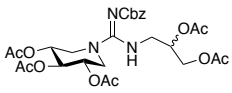

The thiourea **31** (210 mg, 0.57 mmol, 1 eq), OAc-DIX (**16**, 162 mg, 0.62 mmol, 1.1 eq) and EDCI (133 mg, 0.86 mmol, 1.5 eq) were dissolved in CH_2Cl_2 (40 mL), followed by addition of NEt_3 (0.24 mL, 1.7 mmol, 3 eq). Reaction mixture was stirred for 18h at room temperature, after which TLC analysis confirmed total consumption of starting material. The solvent was then removed under reduced pressure, and the residue, dissolved in $CHCl_3$, was applied directly to a silica column, eluting with hexanes chaser and subsequently with CH_2Cl_2:MeOH mixture (CH_2Cl_2:MeOH gradient 2:1 to 4:1). Yield: 296 mg, 87%. R_f (CH_2Cl_2:MeOH = 4:1) = 0.34. ^{1}H NMR (400 MHz, $CDCl_3$) δ 2.05 (5 x s, 15H), 2.78 – 2.91 (m, 2H), 3.39 – 3.56 (m, 2H), 3.91 – 4.05 (m, 2H), 4.12 – 4.31 (m, 2H), 4.77 – 4.96 (m, 2H), 5.03 – 5.13 (m, 3H), 5.12 – 5.25 (m, 1H), 7.22 – 7.42 (m, 5H), 8.52 (s, 1H). ^{13}C NMR (101 MHz, $CDCl_3$) δ 170.5, 170.3, 169.93, 169.91, 169.90, 136.8, 128.3, 128.2, 127.8, 72.8, 69.9, 69.0, 68.9, 67.1, 62.7, 48.6, 48.5, 45.2, 20.72, 20.71, 20.6. HRMS (ESI, $[M+H]^+$), calculated for $C_{27}H_{35}N_3O_{12}$, 594.2299; found, 594.2302.

*4.4.2.5 Deprotection of compound **32** and experimental details for compound **B***

The pentacetylated iminosugar **32** was dissolved in a mixture of Et_3N in THF (1/5, v/v), and transferred to a Parr high-pressure hydrogenation flask. A catalytic amount of 10% palladium on carbon was added to the flask (ca. 10 mg catalyst per 100 mg of starting material). The flask was put under reduced pressure and ventilated with hydrogen gas. This procedure was repeated twice after which the pressure was adjusted to 1.5-2.0 bar hydrogen pressure. It should be taken into account, that the Cbz-deprotection step occurred in the presence of aprotic THF solvent that was not dried prior to use, and might be a plausible explanation for simultaneous

deprotection of the acetyls. The reaction was allowed to proceed for 12 h while mechanically shaken and the pressure maintained at the value initially set. The mixture was filtered over Celite on a glass microfiber filter, followed by rinsing the filter with THF. The mixture was concentrated under reduced pressure. The crude product thus obtained was first analysed using LCMS and resulted in a fully deprotected species **B**, which were further purified using C_8 column (100 Å pore size, 4.6 mm (⌀) x 250 mm (l), 10 µm particle size) in combination with buffers A: H_2O, B: MeCN, A and B with 1.0% aqueous trifluoroacetic acid (TFA). Fractions containing the desired product **B** were combined and lyophilized to yield the pure compound as amorphous white powder. Analytical data and in-depth characterization data for final compound **B** are given below.

N-(2,3-dihydroxypropyl)-3,4,5-trihydroxypiperidine-1 carboximidamide (B)

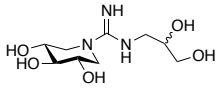

Yield: 3 mg, 84%. ^{1}H NMR (400 MHz, D_2O) δ ^{1}H NMR (400 MHz, $CDCl_3$) δ 3.10 (dd, *J* = 10.1, 13.4 Hz, 2H), 3.36 – 3.44 (m, 1H), 3.45 – 3.54 (m, 2H), 3.59 – 3.72 (m, 4H), 3.88 – 3.99 (m, 3H). ^{13}C NMR (101 MHz, D_2O) δ 171.0, 76.9, 70.2, 68.5, 62.8, 49.6, 49.6, 45.1.HRMS (ESI, $[M+H]^+$), calculated for $C_9H_{19}N_3O_5$, 250.1403; found, 250.1395.

*4.4.3 Experimental details for UHPLC-MS hydrolysis studies of orthoesters **10** and **11***

The kinetic evaluation of the in-house synthesized guanidine compounds **10** and **11** in aqueous solutions was studied by ultra-high performance liquid chromatography – mass spectrometry (UHPLC-MS).

Chemicals
Acetonitrile (ACN; LC-MS Chromasolv) was purchased from Biosolve BV (Valkenswaard, The Netherlands). Formic acid (FA; LC-MS grade), acetic acid, sodium acetate and ammonium acetate were acquired from Sigma-Aldrich (St. Louis, MA, USA). Ultra-pure water was obtained from a Synergy UV water delivery system from Millipore (Billerica, MA, USA). Buffer solutions of 200 mM ammonium acetate (pH 7.0) and 21 mM acetic acid with 85 mM sodium acetate (pH 5.2) were prepared in ultra-pure water. Standard solutions of 1 mM guanidine compounds **10** and **11** were prepared in buffer solutions with pH 5.2 and pH 7.0.

Chromatography
Separation of guanidine compounds and their degradation products was achieved on a Zorbax Eclipse plus C_{18} column (4.6 x 50 mm, 1.8 µm particles). A 2-µL injection volume was used of all samples. UHPLC was performed on a 1290 Infinity UHPLC system (Agilent Technologies, Wald-bronn, BW, Germany) consisting of a binary pump and an autosampler. The optimal separation was achieved with a binary gradient with 0.5% FA (% v/v) in water (eluent A) and ACN (eluent B) at a flow rate of 0.5 mL/min. Detection was performed on a quadrupole-time-off-flight mass spectrometer, equipped with an electrospray ionization source (Bruker Daltonics, Bremen, HB, Germany). Masses were acquired from *m/z* 50-700 at a spectra rate of 1.5 Hz, nebulizer pressure was 4 bar, gas flow was 10 L/min, gas temperature was 2000 °C and capillary voltage was 3 kV. Guanidine compounds **10** and **11** and their degradation products **A** and **B** were detected as positive ions ($[M+H]^+$).

4.4.3.1 Stability indicating method procedure

A sample of **10** and **11**, degraded in buffer solution (pH 5.2) at 21 °C for 5 hours, was used to develop the stability indicating method. The separation of compounds **10** and **11** and the degradation products **A** and **B** was optimized by adjusting the amount and type of acidifier and organic modifier and the gradient time and slope. Good selectivity for all high and low polar compounds was achieved in one run with 0.5% FA/ACN gradients. The optimized gradient started with a composition of 97% eluent A and 3% eluent B (% v/v) for 3 min, increased linearly to 100% B in 3.5 min and remained at 100% B for 2 min. MS setting were optimized to obtain maximum detector response for all compounds. The optimized method was used to study the degradation of the synthesized guanidine compounds. Samples were dissolved in buffer solutions with pH 5.2 or pH 7.0, kept at 21 °C and analyzed at regular time intervals.

We observed that the hydrolysis resulted in an additional product with a molecular mass of 278 in hydrolysis experiments for both compounds **10** and **11**.

4.4.3.2 LC-MS monitored hydrolysis

In order to confirm that these are indeed two independent compounds **A** and **B** we decided to try to develop a method to separate the species using HILIC column conditions (**Figure 11**).

For this purpose, we first prepared 1 mM solution of compound **10** using TFA 0.1 % H_2O in 10 mL to fully result in the hydrolyzed species A and B, which were separated using LC-MS HILIC technique. LC–MS analysis was performed on an amide HILIC column (XBridge, 4.6 mm (⌀) x 250 mm (l), 5 µm particle size) coupled to an ESI-iontrap mass spectrometer to develop the suitable method for preparative NP-HPLC with 90-55% MeCN in 60 min. For analytical runs the following buffers were used: A: H_2O (30 mM NH_4HCOO, pH 4), B: MeCN, (solvents and additives in LCMS grade). Preparative NP-HPLC purifications (detection at 210 nm) was accomplished on a semi-preparative amide HILIC column (XBridge, 10 mm (⌀) x 250 mm (l), 3.5 µm particle size) in combination with buffers A: H_2O (10 mM NH_4HCOO, pH 4), B: 10% H_2O in MeCN (10 mM NH_4HCOO, pH 4). Preparative purification was performed isocratically with 71 % buffer B.

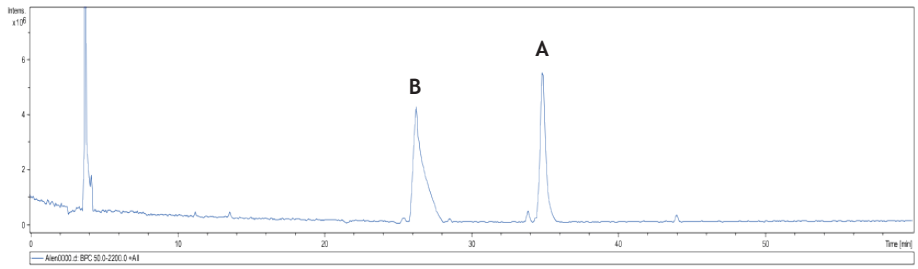

Figure 11. Extracted ion chromatogram for compound (**10**) obtained with the optimized UHPLC-MS method of a 1mM solution in 0.1 % TFA in water and MeCN mixture (pH 3.0), degraded at 21 °C for 12 hours. The following compounds were identified by their *m/z* value: **A)** *m/z* 278 **B)** *m/z* 250.

4.4.3.3 Collision-induced dissociation mass spectrometry (CID MS-MS) details

To fully confirm structures **A** and **B**, precursor ions corresponding to the compounds with *m/z* 278 and 250 were subjected to collision induced dissociation fragmentation to obtain fragments that could approve the structures. Purified samples were dissolved in water:acetonitrile 1:1 (% v/v) with 0.1% formic acid and infused on an Agilent 6560 ion mobility-quadrupole time-off-flight mass spectrometer (Agilent technologies, Waldbronn, Germany). Spectra were acquired in positive ion mode with a capillary voltage of 3.5 kV, nebulizer pressure of 0.8 bar, drying gas flow of 5 L/min, temperature of 320 °C, and CID energies of 20 and 30 V for compound **A** and **B**, respectively.

4.4.4 Biological evaluation against commercial glycosidases

4.4.4.1 Inhibition assays against commercial glycosidases, human recombinant GBA (R&D 7410-GH) and human recombinant GALC (R&D 7310-GH)

Inhibition assays against commercial glycosidases were performed in either phosphate or acetate buffer at the optimum pH for each enzyme (See below for enzyme specific data). Determination of the IC_{50} values of the iminosugars was carried out by spectrophotometrically measuring the residual hydrolytic activities of the glycosidases on the corresponding p-nitrophenyl glycoside substrates in the presence of a concentration range of iminosugar derivatives. The incubation mixture consisted of 50 µL of inhibitor solution in buffer (0.1 U mL^{-1}) and 50 µL of enzyme solution. The concentrations of the enzyme were adjusted so that the reading for the final absorbance was in the range of 0.5–1.5 units. Inhibitor and enzyme solutions were mixed in a disposable 96-well microtiter plate and then incubated at room temperature for 5 minutes. Next, the reactions were initiated by addition of 50 µL of a solution of the corresponding p-nitrophenyl glycoside substrates solution in the appropriate buffer at the optimum pH for the enzyme. After the reaction mixture was incubated at 37 °C for 30 min, the reaction was quenched with 0.5 M Na_2CO_3 (150 µL) and the absorbance of 4-nitrophenol released from the substrate was read immediately at 405 nm using a BioTek mQuant Microplate Spectrophotometer.

IC_{50} values were determined graphically with GraphPad Prism (version 6.0) by making a plot of percentage inhibition versus the log of inhibitor concentration, using at least 8 different inhibitor concentrations. IC_{50} values were presented as a concentration of the iminosugars that inhibits 50% of the enzyme activity under the assay conditions. NN-DNJ was used as a reference compound. All materials were purchased from Sigma-Aldrich.

The commercial glycosidase solutions were prepared as following:

[b]For **α-glucosidase** (from *baker's yeast,* Sigma G5003, 0.05 U/mL) the activity was determined with p-nitrophenyl-α-D-glucopyranoside (0.7 mM final conc. in well) in sodium phosphate buffer (100 mM, pH 7.2).

[c]For **α-galactosidase** (from *green coffee beans*, Sigma G8507, 0.05 U/mL) activity was determined with p-nitrophenyl-α-D-galactopyranoside (0.7 mM final conc. in well) in sodium phosphate buffer (100 mM, pH 6.8).

[d]For **β-glucosidase** (from *almond*, Sigma G4511, 0.05 U/mL) the activity was determined with p-nitrophenyl-β-D-glucopyranoside (0.7 mM final conc. in well) in sodium acetate buffer (100 mM, pH 5.0).

[e]For **β-galactosidase** (from *bovine liver*, Sigma G1875, 0.05 U/mL) activity was determined with p-nitrophenyl-β-D-galactopyranoside (0.7 mM final conc. in well) in sodium phosphate buffer (100 mM, pH 7.2).

[f]For **Naringinase** (from *penicillium decumbens,* Sigma N1385, 0.06 U/mL) the activity was determined with p-nitrophenyl-β-D-glucopyranoside (0.7 mM final conc. in well) in sodium acetate buffer (100 mM, pH 5.0).

[g]**Recombinant Human Glucosylceramidase/β-glucocerebrosidase/GBA** (7410-GH), purchased from R&D was also used in the inhibition studies. The used substrate 4-methylumbelliferyl-β-D-glucopyranoside was purchased by Sigma-Aldrich. GBA activity was determined with 4-methylumbelliferyl-β-D-glucopyranoside as reported in (A. Trapero, J. Med. Chem. 2012, 55, 4479-4488).[50] Briefly, enzyme solutions (25 µL from a stock solution containing 0.6 µg/mL) in the presence of 0.25% (w/v) sodium taurocholate and 0.1% (v/v) Triton X-100 in Mcllvaine buffer (100 mM sodium citrate and 200 mM sodium phosphate buffer, pH 5.2 or pH 7.0) were incubated at 37°C without (control) or with inhibitor at a final volume of 50 µL for 30 min. After addition of 25 µL 4-methylumbelliferyl-β-D-glucopyranoside (7.2 mM, Mcllvaine buffer pH 5.2 or pH 7.0), the samples were incubated at 37°C for 10 min. Enzymatic reactions were stopped by the addition of aliquots (100 µL) of Glycine/NaOH buffer (100 mM, pH 10.6). The amount of 4-methylumbelliferone formed was determined with a FLUOstar microplate reader (BMG Labtech) at / 355 nm (excitation) and / 460 nm (emission). Samples for GBA inhibition studies were dissolved in buffers 24 hours prior to the start of the experiment. This was done to determine the inhibitory potency of fully hydrolyzed species **10** and **11** at pH 5.2. Experiments at pH 7.0 were done in the same fashion knowing that no difference in inhibitory potency would be obtained, since minor hydrolysis would occur in such time period.

[g]**Recombinant Human Galactosylceramidase/GALC** (7310-GH), purchased from R&D was used in the inhibition studies. The used substrate 4-methylumbelliferyl-β-D-galactopyranoside was purchased by Sigma-Aldrich. GALC activity was determined with 4-methylumbelliferyl-β-D-galactopyranoside as reported in assay procedure R&D product 7310-GH. Briefly, enzyme solutions (25 µL from a stock solution containing 60 ng/mL) in the presence of 0.5% (v/v) Triton X-100 in Assay buffer (50 mM sodium citrate and 125 mM NaCl, pH 4.5) were incubated at 37°C without (control) or with inhibitor at a final volume of 50 µL for 10 min. After addition of 25 µL 4-methylumbelliferyl-β-D-galactopyranoside (0.75mM, Assay buffer), the samples were incubated at 37°C for 20 min. Enzymatic reactions were stopped by the addition of aliquots (50 µL) of Glycine/NaOH buffer (100 mM, pH 10.6). The amount of 4-methylumbelliferone formed was determined with a FLUOstar microplate reader (BMG Labtech) at 355 nm (excitation) and 460 nm (emission).

4.4.4.2 IC_{50} curves for compounds **10**, **11** and **NNDNJ** against human recombinant GBA (R&D 7410-GH)

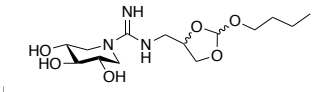

10 - pH 7

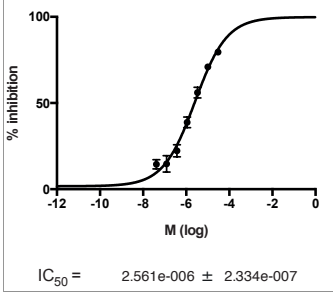

IC_{50} = 2.561e-006 ± 2.334e-007

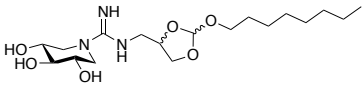

11 - pH 7

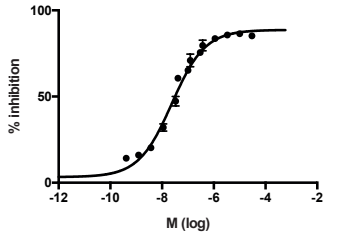

IC_{50} = 2.392e-008 ± 2.500e-009

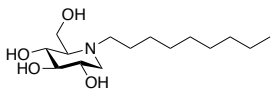

NNDNJ - pH 7

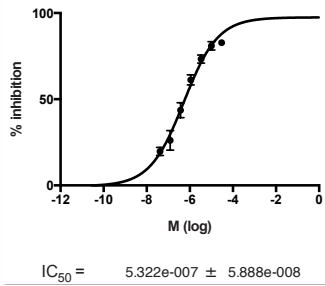

IC_{50} = 5.322e-007 ± 5.888e-008

4.4.5 Fibroblast experiments

Cell lines and culture. Wild-type fibroblasts (GM 05659) and fibroblasts derived from Gaucher patients, homozygous for N370S GBA (GM00372) and L444P GBA (GM00877) were obtained from Coriell Institute, Camden, USA. Fibroblast cells were cultured in Dulbecco's modified Eagle's medium (DMEM, Sigma-Aldrich) supplemented with 10% fetal bovine serum (FBS, Sigma-Aldrich) and penicillin-streptomycin (100 U/ml resp. 0.1 mg/ml, Sigma-Aldrich) at 37°C in 5% CO_2 and all cells used in this study were between the 5th and 15th passages. The Fibroblasts assay (*chaperone assay)* was performed according to a modified version as described in a paper published by Trapero, et. al.[50]

4.4.5.1 Measurements of N370S and L444P GBA activity in fibroblasts derived from patients with GD

The chaperone assay was performed according to a modified version as previously described.[4] Fibroblasts were plated into 24-well assay plates and incubated at 37°C under 5% CO_2 atmosphere until a monolayer of at least 50% confluency was reached. The media were then replaced with fresh media with or without various concentrations of test compounds and incubated at 37°C in 5% CO_2 for 4 days. The enzyme activity assay was performed after removing media supplemented with the corresponding compound. The monolayers were washed twice with phosphate buffered saline (PBS) solution. Then, 80 µl of PBS and 80 µl of 200 mM acetate buffer (pH 4.0) were added to each well. The reaction was started by addition of 100 µl of 7.2 mM 4-methylumbelliferyl-β-D-glucopyranoside (200 mM acetate buffer pH 4.0) to each well, followed by incubation at 37°C for 2h. Enzymatic reactions were stopped with 0.9 ml glycine/NaOH buffer (100 mM pH 10.6). Liberated 4-methylumbelliferone was measured (excitation 355 nm, emission at 460 nm) with the Fluoroskan Ascent FL plate reader (Labsystems) in 96-well format.

4.4.6 Analytical RP-HPLC traces for compounds **10** and **11**

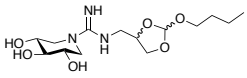

10

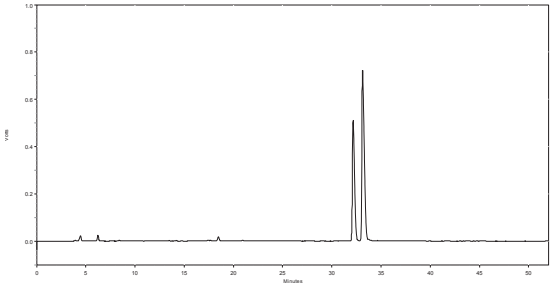

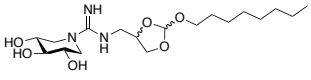

11

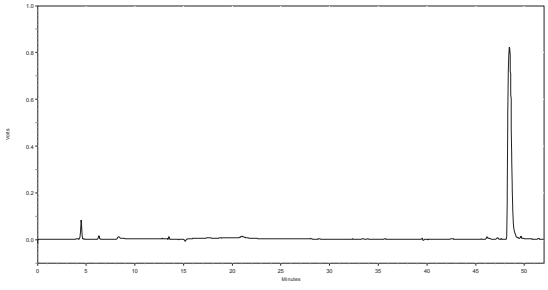

RP-HPLC experimental details

HPLC system (detection simultaneously at 214, 254 nm and evaporative light detection) equipped with an analytical C_8 column (100 Å pore size, 4.6 mm (⌀) x 250 mm (l), 10 µm particle size) in combination with buffers A: H_2O, B: MeCN, A and B with 0.1% aqueous trifluoroacetic acid (TFA). For RP-HPLC purifications (detection simultaneously at 213, 254 nm), an automated HPLC system equipped with a preparative C_8 column (20 mm (⌀) x 250 mm (l), 5 µm particle size) and gradient moving from 95% to 5% eluent A (50mM NH_4HCO_3:5mM Et_3N, pH = 8.3) over 60 min (flow rate, 18.0 mL/min, eluent B: MeOH).

4.4.7. Graphical NMR example of compound 11

Compound 11: ^{1}H NMR (400 MHz, D_2O)

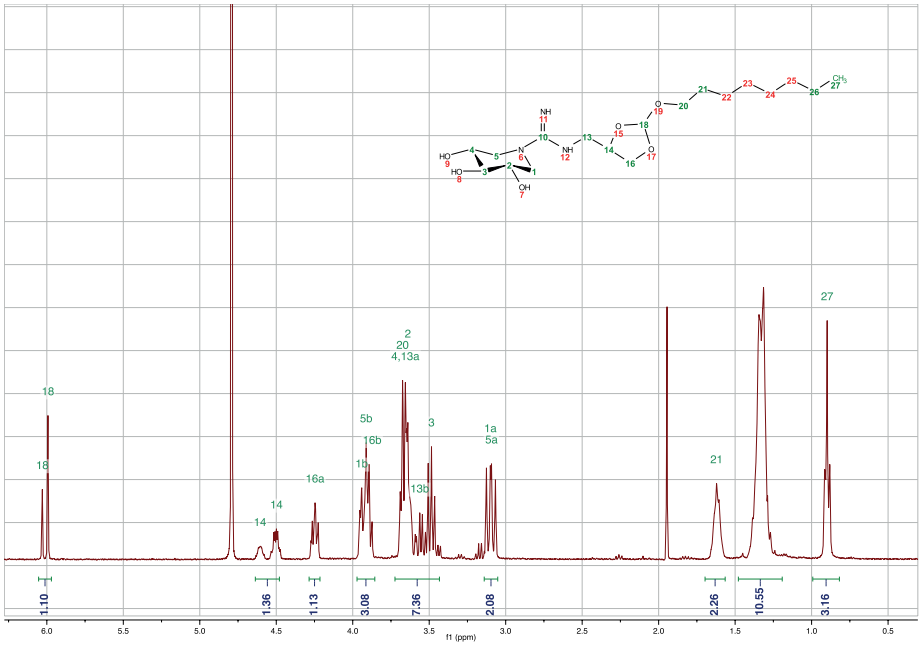

Compound 11: ^{13}C NMR (101 MHz, D_2O)

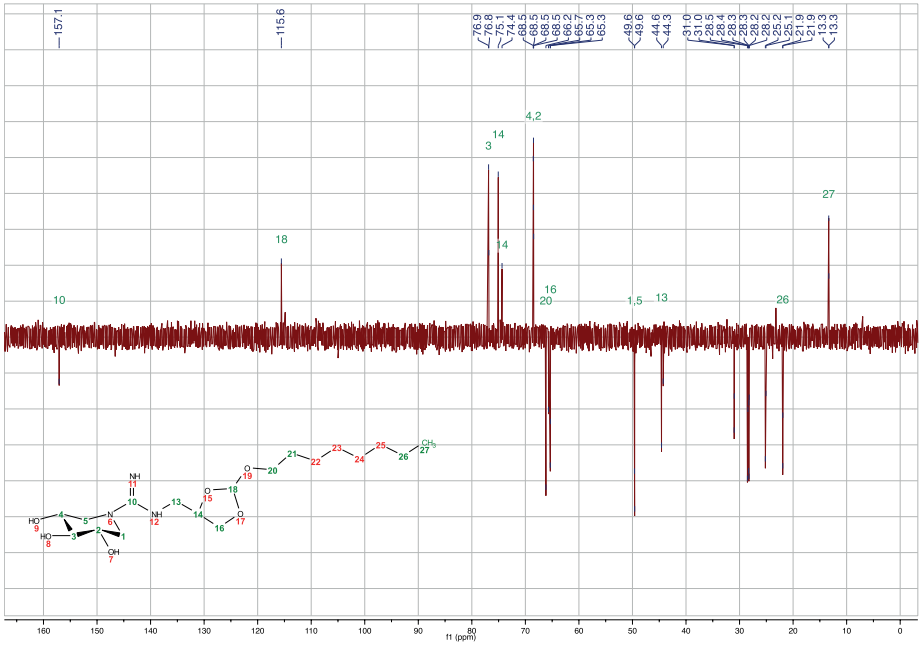

Compound 11: ^{1}H – ^{1}H COSY NMR (400 MHz, D_2O)

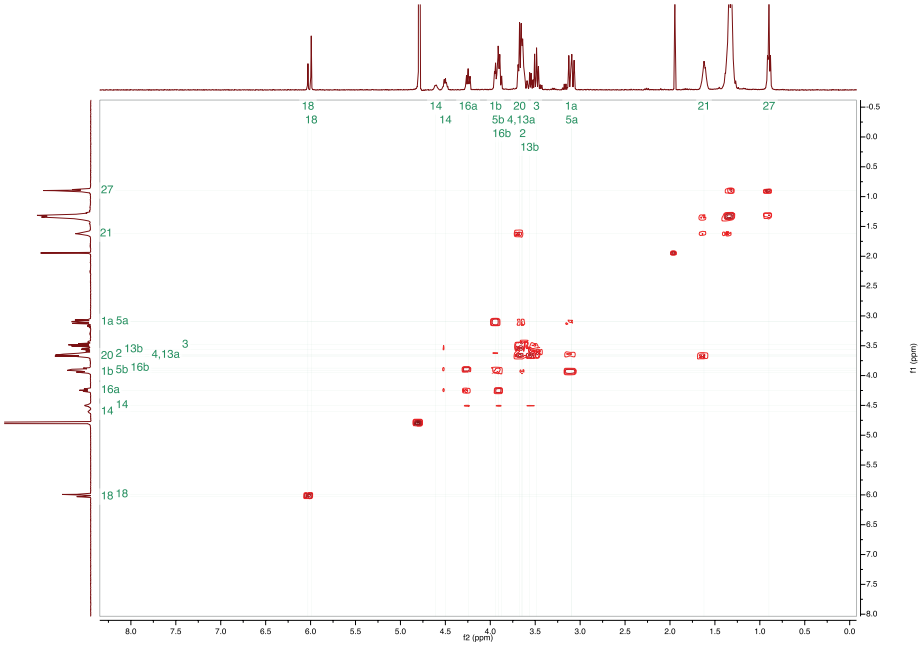

Compound 11: ^{1}H – ^{13}C HSQC NMR (101 MHz, D_2O)

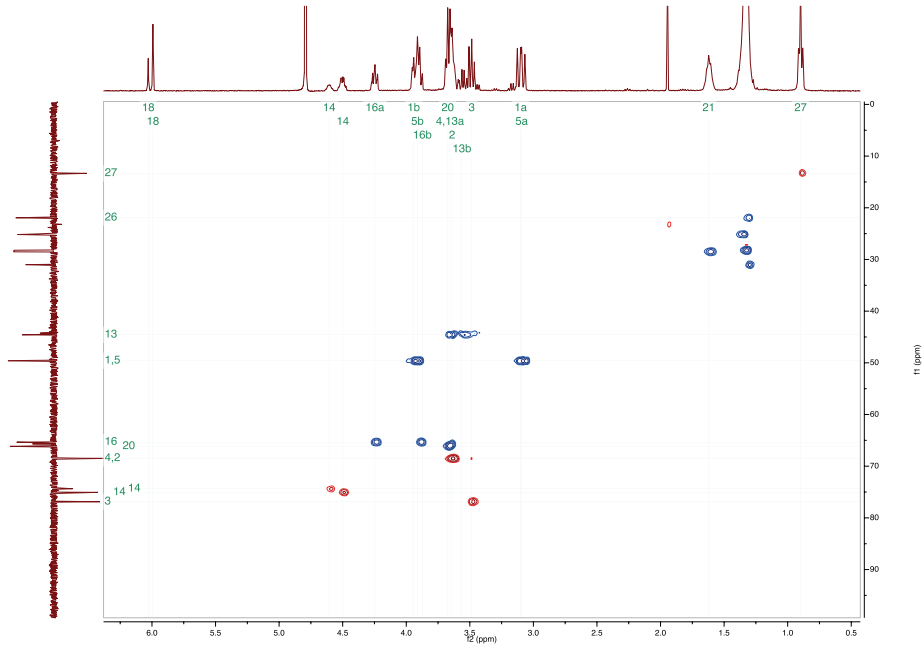

4.5 REFERENCES

1. Platt, F. M. Sphingolipid Lysosomal Storage Disorders. *Nature* **510,** 68–75 (2014).
2. Convertino, M., Das, J. & Dokholyan, N. V. Pharmacological chaperones: design and development of new therapeutic strategies for the treatment of conformational diseases. *ACS Chem. Biol.* **11,** 1471–1489 (2016).
3. Parenti, G., Andria, G. & Valenzano, K. J. Pharmacological Chaperone Therapy: Preclinical Development, Clinical Translation, and Prospects for the Treatment of Lysosomal Storage Disorders. *Mol. Ther.* **23,** 1138–1148 (2015).
4. Hussain, S. *et al.* Strain-specific antiviral activity of iminosugars against human influenza A viruses. *J. Antimicrob. Chemother.* **70,** 136–152 (2015).
5. Wennekes, T. *et al.* Glycosphingolipids - Nature, Function, and Pharmacological Modulation. *Angew. Chemie Int. Ed.* **48,** 8848–8869 (2009).
6. Compain, P. & Martin, O. R. *Iminosugars: From synthesis to therapeutic applications*. (Wiley, 2007).
7. Parenti, G., Moracci, M., Fecarotta, S. & Andria, G. Pharmacological chaperone therapy for lysosomal storage diseases. *Future Med. Chem.* **6,** 1031–1045 (2014).
8. Gao, K. *et al.* 1-Deoxynojirimycin: Occurrence, Extraction, Chemistry, Oral Pharmacokinetics, Biological Activities and In Silico Target Fishing. *Molecules* **21,** 1600–1614 (2016).
9. Sekioka, T., Shibano, M. & Kusano, G. Three Trihydroxypiperidines, Glycosidase Inhibitors, from Eupatorium fotunei TURZ. *Nat. Med.* **49,** 332–335 (1995).
10. Parmeggiani, C. *et al.* Human Acid beta-Glucosidase Inhibition by Carbohydrate Derived Iminosugars: Towards New Pharmacological Chaperones for Gaucher Disease. *ChemBioChem* **16,** 2054–2064 (2015).
11. Sanchez-Fernandez, E. M., Garcia Fernandez, J. M. & Mellet, C. O. Glycomimetic-based pharmacological chaperones for lysosomal storage disorders: lessons from Gaucher, GM1-gangliosidosis and Fabry diseases. *Chem. Commun.* **52,** 5497–5515 (2016).
12. Ghisaidoobe, A. T. *et al.* Identification and Development of Biphenyl Substituted Iminosugars as Improved Dual Glucosylceramide Synthase/Neutral Glucosylceramidase Inhibitors. *J. Med. Chem.* **57,** 9096–9104 (2014).
13. Hottin, A., Wright, D. W., Davies, G. J. & Behr, J. B. Exploiting the hydrophobic terrain in fucosidases with aryl-substituted pyrrolidine iminosugars. *ChemBioChem* **16,** 277–283 (2015).
14. Godin, G. *et al.* α-1-C-Alkyl-1-deoxynojirimycin derivatives as potent and selective inhibitors of intestinal isomaltase: remarkable effect of the alkyl chain length on glycosidase inhibitory profile. *Bioorg. Med. Chem. Lett.* **14,** 5991–5995 (2004).
15. Patil, N. T., John, S., Sabharwal, S. G. & Dhavale, D. D. 1-Aza-sugars from D-Glucose. Preparation of 1-Deoxy-5-dehydroxymethyl-Nojirimycin, its analogues and evaluation of glycosidase inhibitory activity. *Bioorganic Med. Chem.* **10,** 2155–2160 (2002).
16. Pandey, G., Kapur, M., Khan, M. I. & Gaikwad, S. M. A new access to polyhydroxy piperidines of the azasugar class: synthesis and glycosidase inhibition studies. *Org. Biomol. Chem.* **1,** 3321–3326 (2003).
17. Zhu, X., Sheth, K. a, Li, S., Chang, H.-H. & Fan, J.-Q. Rational design and synthesis of highly potent beta-glucocerebrosidase inhibitors. *Angew. Chem. Int. Ed. Engl.* **44,** 7450–7453 (2005).
18. Compain, P. *et al.* Design and synthesis of highly potent and selective pharmacological chaperones for the treatment of Gaucher's disease. *ChemBioChem* **7,** 1356–1359 (2006).
19. Brumshtein, B. *et al.* 6-Amino-6-deoxy-5,6-di-N-(N'-octyliminomethylidene)nojirimycin: Synthesis, Biological Evaluation, and Crystal Structure in Complex with Acid β-Glucosidase. *ChemBioChem* **10,** 1480–1485 (2009).
20. García-Moreno, M. I., Díaz-Pérez, P., Mellet, O. & García Fernández, J. M. Castanospermine-trehazolin hybrids: a new family of glycomimetics with tuneable glycosidase inhibitory properties. *Chem. Commun.* **45,** 848–849 (2002).
21. Compain, P. Searching for glycomimetics that target protein misfolding in rare diseases: Successes, failures, and unexpected progress made in organic synthesis. *Synlett* **25,** 1215–1240 (2014).
22. Martin, N. I., Woodward, J. J. & Marletta, M. A. NG-Hydroxyguanidines from Primary Amines. *Org. Lett.* **8,** 4035–4038 (2006).
23. Kooij, R. *et al.* Glycosidase inhibition by novel guanidinium and urea iminosugar derivatives. *Medchemcomm* **4,** 387–393 (2013).
24. Sevšek, A. *et al.* Bicyclic isoureas derived from 1-deoxynojirimycin are potent inhibitors of β-glucocerebrosidase. *Org. Biomol. Chem.* **14,** 8670–8673 (2016).

25. Fabrega, S. *et al.* Human Glucocerebrosidase: Heterologous Expression of Active Site Mutants in Murine Null Cells. *Glycobiology* **10,** 1217–1224 (2000).
26. Zeller, J. L. Gaucher Disease. *J. Am. Med. Assoc.* **298,** 1358 (2007).
27. Jmoudiak, M. & Futerman, A. H. Gaucher Disease: Pathological Mechanisms and Modern Management. *Br. J. Haematol.* **129,** 178–188 (2005).
28. Brady, R. O. Gaucher's Disease : Past , Present and Future. *Baillieres. Clin. Haematol.* **10,** 621–634 (1997).
29. Charrow, J. *et al.* The Gaucher Registry. *Arch Intern Med.* **160,** 2835–2843 (2000).
30. Pastores, G. M., Patel, M. J. & Firooznia, H. Bone and Joint Complications Related to Gaucher Disease. *Curr. Rheumatol. Rep.* **2,** 175–180 (2000).
31. Beutler, E. Gaucher Disease: Multiple Lessons from a Single Gene Disorder. *Acta Paediatr.* **95,** 103–109 (2006).
32. Nash, R. J., Kato, A., Yu, C.-Y. & Fleet, G. W. Iminosugars as therapeutic agents: recent advances and promising trends. *Futur. Sci.* **3,** 1513–1521 (2011).
33. Trapero, A. & Llebaria, A. Glucocerebrosidase inhibitors for the treatment of Gaucher disease. *Futur. Sci.* **5,** 573–590 (2013).
34. Trapero, A. & Llebaria, A. Glucocerebrosidase inhibitors: future drugs for the treatment of Gaucher disease? *Futur. Sci.* **6,** 975–978 (2014).
35. Beutler, E., Kuhl, W. & Vaughan, L. M. Failure of Alglucerase Infused into Gaucher Disease Patients to Localize in Marrow Macrophages. **1,** 320–324 (1995).
36. Schueler, U. H., Olter, T. K., Kaneski, C. R. & Zirzow, G. C. Correlation between enzyme activity and substrate storage in a cell culture model system for Gaucher disease. *J. Inherit. Metab. Dis.* **27,** 649–658 (2004).
37. Sawkar, A. R. *et al.* Gaucher Disease-Associated Glucocerebrosidases Show Mutation-Dependent Chemical Chaperoning Profiles. *Chem. Biol.* **12,** 1235–1244 (2005).
38. Gavrin, L. K., Denny, R. A. & Saiah, E. Small molecules that target protein misfolding. *J. Med. Chem.* **55,** 10823–10843 (2012).
39. Fan, J. Q. A counterintuitive approach to treat enzyme deficiencies: use of enzyme inhibitors for restoring mutant enzyme activity. *Biol Chem* **389,** 1–11 (2008).
40. Sevšek, A. *et al.* N-Guanidino Derivatives of 1,5-Dideoxy-1,5-imino-D-xylitol are Potent, Selective, and Stable Inhibitors of β-Glucocerebrosidase. *ChemMedChem* **12,** 483–486 (2017).
41. Wang, G.-N. *et al.* Rational Design and Synthesis of Highly Potent Pharmacological Chaperones for Treatment of N370S Mutant Gaucher Disease. *J. Med. Chem.* **52,** 3146–3149 (2009).
42. Shayman, J. A. & Larsen, S. D. The development and use of small molecule inhibitors of glycosphingolipid metabolism for lysosomal storage diseases. *J. Lipid Res.* **55,** 1215–1225 (2014).
43. Mena-Barragán, T. *et al.* pH-Responsive Pharmacological Chaperones for Rescuing Mutant Glycosidases. *Angew. Chemie - Int. Ed.* **54,** 11696–11700 (2015).
44. Boot, R. G. *et al.* Identification of the Non-lysosomal Glucosylceramidase as - Glucosidase 2. *J. Biol. Chem.* **282,** 1305–1312 (2007).
45. Bruyère, H., Westwell, A. D. & Jones, A. T. Tuning the pH sensitivities of orthoester based compounds for drug delivery applications by simple chemical modification. *Bioorganic Med. Chem. Lett.* **20,** 2200–2203 (2010).
46. Martin, N. I., Beeson, W. T., Woodward, J. J. & Marletta, M. A. N-aminoguanidines from primary amines and the preparation of nitric oxide synthase inhibitors. *J. Med. Chem.* **51,** 924–931 (2008).
47. Martin, N. I. & Liskamp, R. M. J. Preparation of NG-Substituted L-Arginine Analogues Suitable for Solid Phase Peptide Synthesis. *J. Org. Chem.* **73,** 7849–7851 (2008).
48. Meier, L., Monteiro, G. C., Baldissera, R. A. M. & Sá, M. M. Simple method for fast deprotection of nucleosides by triethylamine-catalyzed methanolysis of acetates in aqueous medium. *J. Braz. Chem. Soc.* **21,** 859–866 (2010).
49. Brumshtein, B. *et al.* Crystal structures of complexes of N-butyl- and N-nonyl-deoxynojirimycin bound to acid β-glucosidase: Insights into the mechanism of chemical chaperone action in Gaucher disease. *J. Biol. Chem.* **282,** 29052–29058 (2007).
50. Trapero, A., González-Bulnes, P., Butters, T. D. & Llebaria, A. Potent aminocyclitol glucocerebrosidase inhibitors are subnanomolar pharmacological chaperones for treating gaucher disease. *J. Med. Chem.* **55,** 4479–4488 (2012).
51. Sawkar, A. R. *et al.* Chemical chaperones increase the cellular activity of N370S beta-glucosidase: A therapeutic strategy for Gaucher disease. *Proc. Natl. Acad. Sci. U. S. A.* **99,** 15428–15433 (2002).

52. Steet, R. A. *et al.* The iminosugar isofagomine increases the activity of N370S mutant acid beta-glucosidase in Gaucher fibroblasts by several mechanisms. *Proc. Natl. Acad. Sci. U. S. A.* **103,** 13813–13818 (2006).
53. Sun, Y. *et al.* Ex vivo and in vivo effects of isofagomine on acid β-glucosidase variants and substrate levels in Gaucher disease. *J. Biol. Chem.* **287,** 4275–4287 (2012).

CHAPTER 5

SUMMARIZING DISCUSSION

AND

FUTURE OUTLOOK

5.1 INTRODUCTION

Effective drug design to modulate biological processes requires knowledge of how substrates and ligands are recognized by their complementary enzymes and receptors. Glycoside trimming enzymes are crucially important in a broad range of metabolic pathways, including glycoprotein and glycolipid processing and carbohydrate digestion. Thus, inhibitors of glycan-processing enzymes can be used to target an enzyme in a specific pathway to induce predictable changes in glycosylation.[1] The outcomes of such alterations can then be studied and the information obtained is important to understand what makes an inhibitor useful in the biological process, and how inhibitors having these features can be designed in a way that can then be applied into future therapeutics.[2] Lysosomal catabolic pathways involve the well-orchestrated actions of a series of enzymes for proper functioning.[3] Lysosomal enzymes carry out precise biochemical reactions in breaking the substrates into smaller components, which need to be either recycled or excreted by the cell. Abnormal excessive accumulation of non-degraded substrates causes a variety of cellular dysfunctions that can potentially lead to a range of pathologies commonly known as lysosomal storage disorders, generally abbreviated as LSDs.[4,5]

Gaucher disease (GD) is the most dominant lysosomal storage disease.[6,7] The condition is caused by a mutation in the glucocerebrosidase gene, which can lead to reduced activity of β-glucocerebrosidase (GBA, GBA1) the enzyme responsible for the hydrolysis of glucosylceramide (GlcCer).[8] A deficiency in GBA activity can result in the progressive accumulation of undegraded glucosylceramide substrate leading to serious clinical symptoms and in some cases neurological complications.[9–11]

The primary focus for therapeutic strategies has been on reducing the cellular concentration of glycosphingolipids within the lysosome.[12] Among the different therapeutic approaches under investigation at present, pharmacological chaperone therapy (PCT) is an interesting technique in order to restore the balance between the influx and degradation of the accumulated substrate. Pharmacological chaperones are small molecules capable of stabilizing a misfolded enzyme and thus prevent degradation by the Endoplasmic Reticulum Associated Degradation machinery (ERAD).[13] In the case of GD, the mutant GBA enzyme is predisposed to misfolding and premature degradation in the ER but often still retains some degree of catalytic activity.[14] An effective pharmacological chaperone-based treatment for GD would involve the pharmacologically active compound binding to and stabilize the misfolded GBA enzyme, thus facilitating its trafficking from the ER to the lysosome where it can degrade GlcCer. Certain iminosugars are highly potent and selective inhibitors of glycosidases[15] and in some cases reversibly bind to the active site of their target enzyme in a pH-dependent manner.[16] It may seem paradoxical to use an inhibitor to stabilize an enzyme, however, the positive outcomes of such therapeutic approaches proved to be beneficial for patients and can result in final enzyme enhancements. Competitive inhibitors, such as iminosugars, have the ability to template the folding of the affected protein and can be used to prevent misfolding and accelerate its transport to the lysosome.

In this regard, the development of potent, preferably pH-dependent glycosidase inhibitors presents an attractive target for the development of new therapeutics.[17]

5.2 SUMMARIZING DISCUSSION

5.2.1 Chapter 2

C**hapter 2** describes the preparation of a series of bicyclic isourea derivatives from 1-deoxynojirimycin using a concise synthetic protocol proceeding *via* a guanidino intermediate (**Scheme 1**). Inhibition assays with a panel of glycosidases revealed deoxynojirimycin-derived bicyclic isoureas to be among the most potent known inhibitors of GBA, a human lysosomal β-glucosidase. While we initially set out to explore exocyclic guanidine analogues of DNJ it was found that such compounds are prone to intramolecular cyclization yielding instead the corresponding bicyclic isoureas. The DNJ-derived bicyclic isourea analogues described in this study are a novel class of glycosidase inhibitors. Our data indicate that compounds prepared in this chapter are among the most potent GBA inhibitors reported to date. It is known that mutations in GBA can lead to serious lysosomal storage disorders such as GD. Interestingly, in some cases GBA inhibitors can serve to counteract the loss of GBA activity by functioning as pharmacological chaperones. Preliminary data from experiments using Gaucher patient derived fibroblasts bearing the N370S GBA mutation indicate that the most promising compound prepared in this work possesses chaperone activity on par with that of the known chaperone NN-DNJ. Further investigations into the potential for DNJ-derived bicyclic isoureas like compounds prepared in this chapter may be warranted.

5.2.2 Chapter 3

Our previous studies established that formation of the cyclic isourea proceeds *via* the guanidine species, which is prone to cyclization by action of the 6-OH group. **Chapter 3** reports a strategy designed to circumvent this process wherein N-substituted guanidine analogues of DIX, lacking the 6-OH group of DNJ, were prepared and found to be stable (**Scheme 1**). Thus, a series of lipidated guanidino and urea derivatives of 1,5-di-deoxy-1,5-imino-D-xylitol were prepared from D-xylose using a concise synthetic protocol. Inhibition assays with a panel of glycosidases revealed that the guanidino analogues display potent inhibition against human recombinant β-glucocerebrosidase with IC_{50} values in the low nanomolar range. The inhibitory potency is increased with longer alkyl substituents. In addition, a bis-lipidated analogue served as a close substrate mimic for β-glucocerebrosidase and proved to be on par with our most potent inhibitors evaluated in this study. Our study clearly indicates that the addition of a guanidinium moiety leads to more potent inhibition of GBA when compared to the reported alkylated amine compound. Docking studies also point to additional cation-π_interactions, as well as an extra hydrogen bond/salt bridge to the guanidinium group, as a plausible explanation for the enhanced glycosidase inhibition exhibited by guanidine analogues. Related urea analogues of 1,5-dideoxy-1,5-imino-D-xylitol were also synthesized and evaluated in the same fashion and found to be selective for β -galactosidase from bovine liver. No inhibition of human recombinant β-glucocerebrosidase was observed for the urea analogues.

5.2.3 Chapter 4

As a continuation of our previous studies, **chapter 4** describes the preparation of new DIX-iminosugar based glycosidase inhibitors that contain both; an exocyclic *N*-alkylated guanidine and an acid labile orthoester moiety (**Scheme 1**). We considered such compounds interesting due to the pH-responsive orthoester capable of hydrolysis in the

mildly acidic lysosomal environment, thereby transforming itself from a hydrophobic to a hydrophilic species. Therefore, the study discusses the development of analogues that maintain potent activity at neutral pH but show a significant decrease in activity at acidic pH. A lack of pH selective inhibition might have also been implicated in the disappointing clinical trial failures of many other GBA inhibitors explored as pharmacological chaperones. Inhibition assays with a panel of glycosidases revealed that many of the compounds prepared displayed potent inhibition against human *β*-glucocerebrosidase at pH 7.0 with IC_{50} values in the low nanomolar range. Notably, a significant drop in inhibitory activity was achieved when the same compound was tested at pH 5.2. This pH sensitive activity is due to degradation of the orthoester functionality at lower pH accompanied by loss of the lipid. This approach provides a degree of control in tuning enzyme inhibition based on the local pH. Orthoester compounds like those described here may serve as tools for studying various lysosomal storage disorders such as GD.

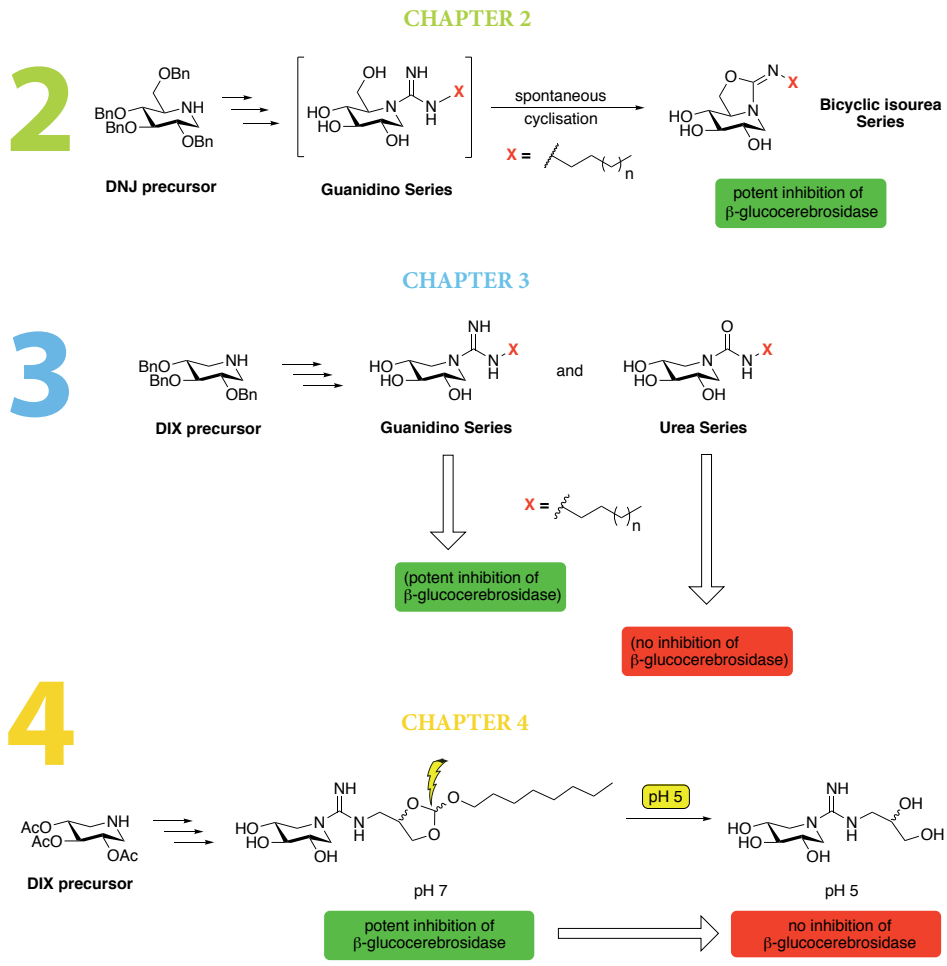

Scheme 1. Overview scheme of compounds prepared in **Chapter 2**, **3** and **4** of this thesis.

5.3 FUTURE DIRECTIONS

The research described in this thesis resulted in many novel inhibitors of GBA following a trend of increased inhibition profile with longer lipophilic substituents. Furthermore, guanidinium incorporation seemed to improve the inhibition profile in most cases when compared to non-guanidinylated species, showing a superior effect in this respect. A remaining challenge still lies in the development of a lipophilic iminosugar that solely inhibits GBA without affecting other relatives of a similar biological pathway, such as glucosylceramide synthase (GCS). Only in cases where compounds would not show activity against GCS, conclusions can be made that these compounds really hold the promise to act as pharmacological chaperones rather than substrate reduction agents.[18] Extended selectivity profile of all compounds should be evaluated on non-lysosomal GBA2 and GBA3 to specify exact inhibition selectivity profile, although neither of these are present in the lysosome and consequently are not involved in the lysosomal degradation of glycolipids.[19] Nonetheless, evaluations to distinguish between the lysosomal GBA1, GCS and non-lysosomal GBA2 cellular β-glucosidases should be addressed in the future to fully establish the prospects of compounds prepared in this work.

Compounds like those described in this thesis may serve as tools for studying various lysosomal storage disorders. In this regard, the most active compounds were evaluated as potential pharmacological chaperones by assessing its effect on GBA activity in an assay employing fibroblasts from Gaucher patients. To investigate whether the inhibitory effect would translate into cellular pharmacological chaperone behavior, we examined the impact of all compounds on GBA activity in GD derived fibroblasts. The effect of the compound activity of the two most prevalent mutations, N370S and L444P GBA mutant was measured using GD patient-derived fibroblast cell line. Since it is assumed that the threshold for lysosomal diseases to develop is at around 10% of normal enzyme activity, therefore only a relatively small increase in enzyme activity is needed to have a large positive outcome for patients.[14] Our preliminary findings with Gaucher patient fibroblast are encouraging given that the two GBA mutations studied here have generally proven to be among the least responsive to chaperoning approaches.[20] However, more comprehensive studies examining the pharmacological chaperone activities of compounds against other cell-line mutations to evaluate their ability to enhance the enzyme activity in broader human derived fibroblast is necessary. Furthermore, we think its imperative to not only repeat the experiments on different mutations but to include various donors of the same mutation in independent fibroblast experiments. Such a broad profile would give a better insight in the actual result of pharmacological chaperones since some patient's cells could produce minute amounts of the enzyme while others tend to have higher basal concentrations.

Overall, additional experiments are needed to fully determine the potential of inhibitors ability to act as pharmacological chaperones prepared in this thesis. The development of more reliable methods to assess chaperoning activity warranting that the measured enzyme increases translates into significant activity enhancements and substrate processing rates in the lysosomes is needed to establish initiatives for the reliable comparison of glycomimetics from different research groups that would allow confident selection of the best leads for preclinical studies.

A number of mouse models that would resemble human GD manifestations have already been developed and could serve as an addition to biological evaluations.[21] Despite the unprecedented value of mouse models for modeling GD, they still suffer from the disadvantage of simply not being human. More recently, the discovery of direct reprograming has allowed the derivation of induced pluripotent stem cells (iPSc) from fibroblasts obtained from GD patients, which might show a more direct line to resemble GD conditions.[22,23]

One already established technique to better understand the pharmacology of pharmacological chaperones and confirm their capability of stabilizing the enzyme is thermal denaturation assay. The recovery of recombinant GBA activity after thermal denaturation is generally used as an *in vitro* model to evaluate the potential of the tested compounds as pharmacological chaperones.[14] Complexes with bound inhibitors can stabilize GBA relative to the free enzyme and heighten the temperature needed to result in a denaturated enzyme.

In order to ascertain whether or not the iminosugars complexes are internalized in cells, experiments with fluorescent attached tag to trace inhibitors internalization in fibroblasts can also be performed.[24] In a similar fashion, compounds with appropriate antibodies can be monitored with confocal microscopy, which gives insight into intracellular distribution within the cell. However, the presence of the relatively large fluorescent moiety may significantly alter the membrane-crossing and diffusion properties of the molecule as compared with the un-labeled chaperone, limiting the scope of such conclusions.

Recently, more comprehensive studies to ameliorate LSD associated discomforts are devoted to the study of a small molecule agent in combination therapy with recombinant enzymes.[13] A PC given as a single administration immediately prior to ERT infusion can help stabilize the recombinant enzyme.[25] Potential increased stabilization may also ameliorate the immune response caused by many ERTs and such stabilization could help extend the ERT circulating half-life and thereby improve cellular uptake and efficacy.

In conclusion, the complexity of LSDs made the development of therapies a major challenge and none of the therapeutic approaches that are already approved for clinical settings is suitable to treat all patients with a specific disorder but rather requires individual approach based on the mutation that patients hold. PCT appears to have the potential to offer a new approach in ameliorating the disease, however, further development and innovation of new agents that target a broader set of mutations as well as development of more reliable methods that translate into significant activity enhancements in laboratory settings are crucial for the development of future therapeutics.

Much exciting work remains to be done in optimizing, understanding, and extending the scope of the inhibitory effects of guanidine rich compounds in general and iminosugars in particular. Since the guanidinium incorporation seems to alter both the steric and electronic properties of the iminosugar, future efforts will be aimed at exploring the incorporation of the guanidine center into other iminosugar structures as a means of further enhancing both the potency and selectivity of glycoside inhibition. Future investigations will explore the use of guanidinium-modified iminosugars for inhibiting different enzymes of medicinal interest or develop them into fluorescent probes to label appropriate enzymes.[26] Targets may include trehalase enzymes for development of antifungal or antibiotic agents,

β-glucosidases located in the endoplasmic reticulum towards anti-cancer agents and targets related to hepatitis and diabetes.[27] Longer side chain analogues, or different spacers could also be prepared to potentially improve potency against certain enzymes and investigate if maximum inhibtion was already reached. Strategies used in this thesis could also be implicated on various scaffolds such as C-alkylated iminosugars, amphiphilic pyrrolidine-type iminosugars, aminosugars and aminocyclitols prototypes with the key nitrogen functionality at an exocyclic location, might also show considerable promise in the future.[28–30]

Convenient synthetic route enables chemists to exploit guanidine modifications in design of other potential inhibitors and evaluate their activity against broader therapeutically relevant targets. Guanidinium scaffolds could also be exploited in designing multivalent compounds with the desire to target multiple glycosidases at once or heighten the final effect in comparison to monovalent inhibitors, which already proved to be fruitful option to this date.[31–34]

5.4 REFERENCES

1. Gloster, T. M. & Vocadlo, D. J. Developing inhibitors of glycan processing enzymes as tools for enabling glycobiology. *Nat. Chem. Biol.* **8,** 683–694 (2012).
2. Brás, N. F., Cerqueira, N. M., Ramos, M. J. & Fernandes, P. A. Glycosidase inhibitors: a patent review (2008-2013). *Expert Opin. Ther. Pat.* **24,** 857–874 (2014).
3. Winchester, B. Lysosomal metabolism of glycoproteins. *Glycobiology* **15,** 1–15 (2005).
4. Futerman, A. H. & van Meer, G. The cell biology of lysosomal storage disorders. *Nat. Rev.* **5,** 554–565 (2004).
5. Aerts, J. M. F. G. *et al.* Biomarkers in the diagnosis of lysosomal storage disorders: Proteins, lipids, and inhibodies. *J. Inherit. Metab. Dis.* **34,** 605–619 (2011).
6. Rosenbloom, B. E. & Weinreb, N. J. Gaucher disease: a comprehensive review. *Crit. Rev. Oncog.* **18,** 163–175 (2013).
7. Grabowski, G. A. Phenotype, diagnosis, and treatment of Gaucher's disease. *Lancet* **372,** 1263–1271 (2008).
8. Fabrega, S. *et al.* Human Glucocerebrosidase: Heterologous Expression of Active Site Mutants in Murine Null Cells. *Glycobiology* **10,** 1217–1224 (2000).
9. Charrow, J. *et al.* The Gaucher Registry. *Arch Intern Med.* **160,** 2835–2843 (2000).
10. Pastores, G. M., Patel, M. J. & Firooznia, H. Bone and Joint Complications Related to Gaucher Disease. *Curr. Rheumatol. Rep.* **2,** 175–180 (2000).
11. Beutler, E. Gaucher Disease: Multiple Lessons from a Single Gene Disorder. *Acta Paediatr.* **95,** 103–109 (2006).
12. Boustany, R.-M. N. Lysosomal storage diseases—the horizon expands. *Nat. Rev. Neurol.* **9,** 583–598 (2013).
13. Parenti, G., Andria, G. & Valenzano, K. J. Pharmacological Chaperone Therapy: Preclinical Development, Clinical Translation, and Prospects for the Treatment of Lysosomal Storage Disorders. *Mol. Ther.* **23,** 1138–1148 (2015).
14. Sawkar, A. R. *et al.* Chemical chaperones increase the cellular activity of N370S beta-glucosidase: A therapeutic strategy for Gaucher disease. *Proc. Natl. Acad. Sci. U. S. A.* **99,** 15428–15433 (2002).
15. Ichikawa, Y., Igarashi, Y., Ichikawa, M. & Suhara, Y. 1-N-Iminosugars: Potent and Selective Inhibitors of β-Glycosidases. *J. Am. Chem. Soc.* **120,** 3007–3018 (1998).
16. Horne, G. Iminosugars: Therapeutic Applications and Synthetic Considerations. *Top. Med. Chem.* **12,** 23–51 (2014).
17. Fan, J. Q. A counterintuitive approach to treat enzyme deficiencies: use of enzyme inhibitors for restoring mutant enzyme activity. *Biol Chem* **389,** 1–11 (2008).
18. Wennekes, T. *et al.* Glycosphingolipids - Nature, Function, and Pharmacological Modulation. *Angew. Chemie Int. Ed.* **48,** 8848–8869 (2009).
19. van Scherpenzeel, M. *et al.* Nanomolar affinity, iminosugar-based chemical probes for specific labeling of lysosomal glucocerebrosidase. *Bioorg. Med. Chem.* **18,** 267–273 (2010).
20. Mena-Barragán, T. *et al.* pH-Responsive Pharmacological Chaperones for Rescuing Mutant Glycosidases. *Angew. Chemie - Int. Ed.* **54,** 11696–11700 (2015).
21. Kanferl, J., Legler, G., Sullivan, J., Raghavan, S. S. & Mumfog, A. The Gaucher mouse. **67,** 85–90 (1975).
22. Tiscornia, G. *et al.* Neuronopathic Gaucher's disease: induced pluripotent stem cells for disease modelling and testing chaperone activity of small compounds. *Hum. Mol. Genet.* **22,** 633–645 (2013).
23. Santos, D. & Tiscornia, G. Induced Pluripotent Stem Cell Modeling of Gaucher's Disease: What Have We Learned? *Int. J. Mol. Sci.* **18,** 1–18 (2017).
24. Kallemeijn, W. W. *et al.* Endo-β-Glucosidase Tag Allows Dual Detection of Fusion Proteins by Fluorescent Mechanism-Based Probes and Activity Measurement. *ChemBioChem* **17,** 1698–1704 (2016).
25. Platt, F. M. Sphingolipid Lysosomal Storage Disorders. *Nature* **510,** 68–75 (2014).
26. Witte, M. D. *et al.* Ultrasensitive in situ visualization of active glucocerebrosidase molecules. *Nat. Chem. Biol.* **6,** 907–913 (2010).
27. Mehta, A., Zitzmann, N., Rudd, P. M., Block, T. M. & Dwek, R. A. Alpha Glucosidase Inhibitors As Potential Broad Based Anti Viral Agents. *Febs Lett.* **430,** 17–22 (1998).
28. Compain, P., Chagnault, V. & Martin, O. R. Tactics and strategies for the synthesis of iminosugar C-glycosides: a review. *Tetrahedron Asymmetry* **20,** 672–711 (2009).
29. Sanchez-Fernandez, E. M., Garcia Fernandez, J. M. & Mellet, C. O. Glycomimetic-based pharmacological

chaperones for lysosomal storage disorders: lessons from Gaucher, GM1-gangliosidosis and Fabry diseases. *Chem. Commun.* **52,** 5497–5515 (2016).

30. Trapero, A., González-Bulnes, P., Butters, T. D. & Llebaria, A. Potent aminocyclitol glucocerebrosidase inhibitors are subnanomolar pharmacological chaperones for treating gaucher disease. *J. Med. Chem.* **55,** 4479–4488 (2012).
31. Stauffert, F. *et al.* Understanding multivalent effects in glycosidase inhibition using C-glycoside click clusters as molecular probes. *New J. Chem.* **40,** 7421–7430 (2016).
32. Decroocq, C. *et al.* The multivalent effect in glycosidase inhibition: probing the influence of valency, peripheral ligand structure, and topology with cyclodextrin-based iminosugar click clusters. *ChemBioChem* **14,** 2038–2049 (2013).
33. Lepage, M. L. *et al.* Iminosugar-Cyclopeptoid Conjugates Raise Multivalent Effect in Glycosidase Inhibition at Unprecedented High Levels. *Chemistry* **22,** 5151–5155 (2016).
34. Compain, P. & Bodlenner, A. The multivalent effect in glycosidase inhibition: A new, rapidly emerging topic in glycoscience. *ChemBioChem* **15,** 1239–1251 (2014).

APPENDICES

SAMENVATTING

Effectief design van nieuwe medicijnen die biologische processen moduleren vereist kennis van hoe substraten en liganden door hun complementaire enzymen en receptoren worden herkend. **Glycoside trimmende enzymen** zijn van cruciaal belang in een breed scala van metabole routes, waaronder de verwerking van glycoproteïne en glycolipide, en het verteren van koolhydraten. **Remmers** van glycaan-verwerkende enzymen kunnen zodoende worden gebruikt om een enzym in een specifieke route te beinvloeden, om voorspelbare veranderingen in glycosylering van substraten te veroorzaken. De resultaten van het bestuderen van dergelijke veranderingen en de hieruit verkregen inzichten zijn belangrijk om te kunnen begrijpen wat een inhibitor nuttig maakt in het biologische proces en hoe remmers die deze eigenschappen hebben zo kunnen worden ontworpen dat ze vervolgens in toekomstige therapieën kunnen worden toegepast. Het functioneren van **lysosomale katabolische routes** hangt af van goed georkestreerde acties van een reeks enzymen. Lysosomale enzymen voeren hier precieze biochemische reacties uit die de substraten in kleinere componenten breken, welke vervolgens door de cel gerecycled of uitgescheiden moeten worden. Abnormale overmatige accumulatie van niet-gedegradeerde substraten veroorzaakt een verscheidenheid aan cellulaire disfuncties die mogelijk kunnen leiden tot een reeks pathologieën. Deze pathologieën staan algemeen bekend als lysosomale opslagstoornissen, of **LSDs**. (**Schema 1**)

De ziekte van Gaucher (**GD**) is de meest dominante lysosomale opslagziekte. De aandoening wordt veroorzaakt door een mutatie in het glucocerebrosidase-gen, dat kan leiden tot verminderde activiteit van ***β*-glucocerebrosidase** (**GBA**, GBA1), het enzym dat verantwoordelijk is voor de hydrolyse van **glucosylceramide** (**GlcCer**). Een tekort aan GBA-activiteit kan resulteren in de progressieve accumulatie van ongedegradeerd glucosylceramide substraat, wat leidt tot ernstige klinische symptomen, en in sommige gevallen neurologische complicaties. De primaire focus voor therapeutische strategieën

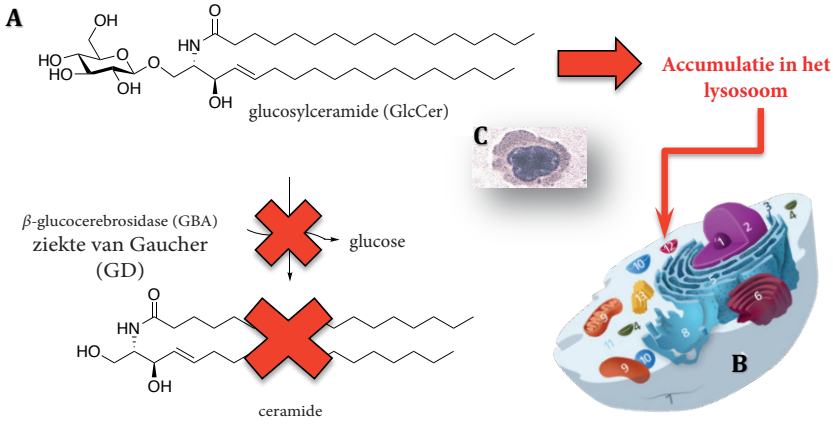

Schema 1. Illustratie van de etiologie van de ziekte van Gaucher. A) Onvoldoende hydrolyse van glucosylceramide door *β*-glucocerebrosidase. **B)** Accumulatie van substraat in het lysosoom. **C)** Gaucher cel met geaccumuleerd glucosylceramide.

is het reduceren van de cellulaire concentratie van glycosphingolipiden in het lysosoom. Onder de verschillende therapeutische benaderingen die momenteel onderzocht worden, is **farmacologische chaperontherapie** (**PCT**) een interessante techniek om het evenwicht tussen de opname en de afbraak van het geaccumuleerde substraat te herstellen. **Farmacologische chaperones** (**PC**) zijn kleine moleculen die in staat zijn om een verkeerd gevouwen enzym te stabiliseren, en zo de afbraak door de **Endoplasmatische Reticulum Associated Degradation** (**ERAD**) te voorkomen. In het geval van GD is het mutant GBA-enzym sterk vatbaar voor misvouwing en voortijdige afbraak in het ER, hoewel het in deze staat vaak nog wel een mate van katalytische activiteit behoudt. Een effectieve farmacologische chaperone-gebaseerde behandeling voor GD zou de farmacologisch actieve verbinding binden aan het verkeerd gevouwen GBA-enzym, en deze zo stabiliseren. Hierdoor wordt het transport van het ER naar het lysosoom vergemakkelijkt, wat vervolgens afbraak van GlcCer in het lysosoom mogelijk maakt. Bepaalde iminosuikers zijn zeer krachtige en selectieve remmers van glycosidasen en binden in sommige gevallen omkeerbaar op de actieve plaats van specifieke enzymen op een pH-afhankelijke manier. Hoewel het paradoxaal lijkt om een remmer te gebruiken om een enzym te stabiliseren, bleken de resultaten van dergelijke therapeutische benaderingen gunstig te zijn voor patiënten. Dit kan vervolgens leiden tot verbeteringen van het uiteindelijke enzym. Inhibitoren, zoals **iminosugaren**, kunnen de vouwing van GBA te beïnvloeden en kunnen daarom worden gebruikt om misvouwing te voorkomen en het transport naar het lysosoom bevorderen. In dit proefschrift zijn krachtige inhibitoren intwikkeld voor het GD eiwit gebaseerd op twee architecturen. Eén hiervan is verder ontwikkeld zodat het in de lysozoom uiteenvalt en het getransporteerde eiwit z'n werk kan doen. Deze stof gaf in celstudies de gewenste toename van de enzymactiviteit te zien en is een stap in de richting van een geneesmiddel voor de ziekte van Gaucher. (**Schema 2**)

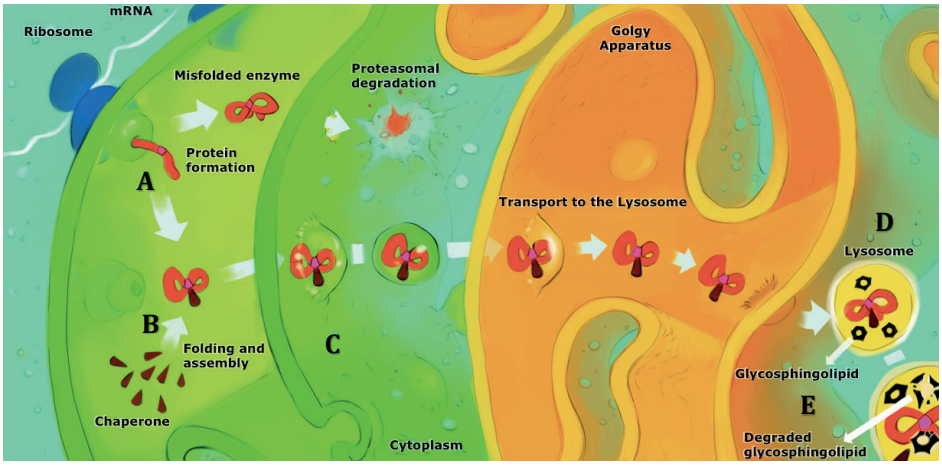

Schema 2. Voorgesteld mechanisme van farmacologische chaperonnes. A) Een missense mutatie resulteert in een verkeerd gevouwen maar nog steeds katalytisch actief enzym. **B)** Een farmacologische chaperonne bindt en stabiliseert het verkeerd gevouwen enzym. **C)** Het chaperonne-enzym complex wordt getransporteerd naar het lysosoom zonder voortijdige degradatie. **D)** Aangekomen in het lysosoom, dissocieert de chaperonne van het complex dankzij de zure pH en hogere substraatconcentratie. **E)** Het vrije enzym is nu in staat om het in het lysosoom geaccumuleerde substraat te hydrolyseren.

2 *Hoofdstuk 2*

Hoofdstuk 2 beschrijft de bereiding van een reeks bicyclische isoureumederivaten uit 1-deoxynojirimycine volgens een specifiek synthese protocol dat *via* een guanidino-intermediair ging. Remmingsbepalingen met een reeks van glycosidasen onthulden dat deoxynojirimycine (DNJ) afgeleide bicyclische isoureas tot de meest krachtige bekende remmers van GBA (een menselijk lysosomaal *β*-glucosidase) behoren. Hoewel we aanvankelijk exocyclische guanidine analogen van DNJ onderzochten, bleek dat dergelijke verbindingen gevoelig zijn voor intramoleculaire cyclisatie. De DNJ-afgeleide bicyclische isourea-analogen die in deze studie zijn beschreven, zijn een nieuwe klasse van glycosidase-remmers. Onze gegevens laten zien dat de verbindingen die in dit hoofdstuk zijn beschreven tot de meest krachtige GBA-remmers horen die tot op heden zijn gerapporteerd. Voorlopige resultaten van experimenten met uit Gaucher-patiënt afgeleide fibroblasten met de N370S GBA mutatie, wijzen erop dat de meest veelbelovende verbinding die in dit werk werd bereid chaperonactiviteit bezit die vergelijkbaar is met die van de bekende chaperon NN-DNJ (**Schema 3**).

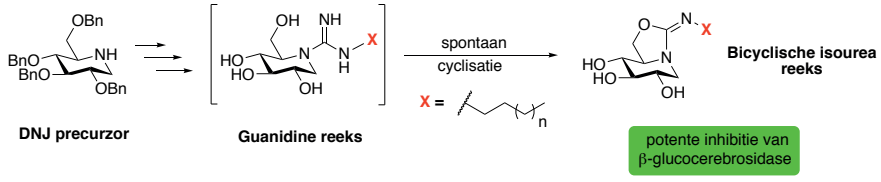

Schema 3. Overzicht van het reactieschema van de verbindingen zoals beschreven in hoofdstuk 2.

3 *Hoofdstuk 3*

Uit onze eerdere studies bleek dat de vorming van het cyclische isoureum *via* de guanidine soort verloopt, welke gevoelig is voor cyclisatie door middel van activiteit van de 6-OH-groep. **Hoofdstuk 3** geeft een strategie aan om dit proces te omzeilen waarin *N*-gesubstitueerde guanidine-analogen van DIX, waarbij de 6-OH-groep van DNJ ontbraken, bereid waren en stabiel bleken. Zo werden een reeks gelipideerde guanidino- en ureumderivaten van 1,5-di-deoxy-1,5-imino-D-xylitol bereid uit D-xylose volgens een specifiek synthese protocol. Inhiberingsassays met een reeks van glycosidasen onthulden dat de guanidino-analogen krachtige remming tonen van humaan recombinant *β*-glucocerebrosidase met IC_{50}-waarden in het lage nanomolaire domein (**Schema 4**).

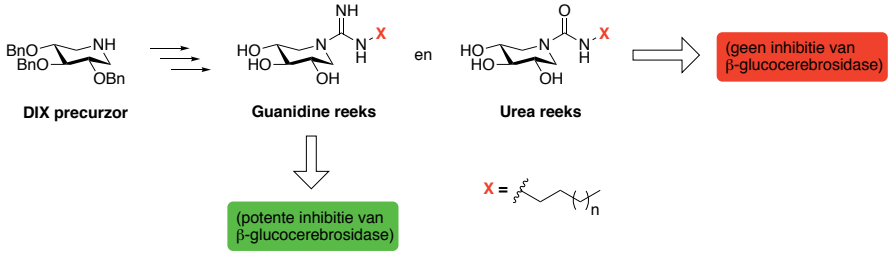

Schema 4. Overzicht van het reactieschema van de verbindingen zoals beschreven in hoofdstuk 3.

De remmende kracht wordt verhoogd naarmate de alkylsubstituenten langer worden. Onze studie wijst duidelijk aan dat de toevoeging van een guanidiniumgedeelte leidt tot een sterkere remming van GBA in vergelijking met de gerapporteerde gealkyleerde amineverbinding. Verwante ureumanalogen van 1,5-dideoxy-1,5-imino-D-xylitol werden ook op dezelfde wijze gesynthetiseerd en geëvalueerd, en bleken selectief te zijn voor β-galactosidase van runderlever. Geen remming van humaan recombinant β-glucocerebrosidase werd waargenomen voor de ureumanalogen.

Hoofdstuk 4

Als vervolg op onze eerdere studies beschrijft **hoofdstuk 4** de voorbereiding van nieuwe DIX-iminosuiker gebaseerde glycosidase remmers zowel een exocyclische N-gealkyleerde guanidine als en een zuurlabiel orthoestergedeelte. We beschouwden dergelijke verbindingen als interessant door de pH-responsieve orthoester die in staat is om hydrolyse te veroorzaken in de lichtzure lysosomale omgeving, waardoor deze zich van een hydrofobe naar een hydrofiele soort transformeert. Daarom bespreekt de studie de ontwikkeling van analogen die krachtige activiteit behouden bij neutrale pH, maar een significante afname van de activiteit bij zure pH tonen. In het bijzonder werd een significante daling in remmende activiteit bereikt wanneer dezelfde verbinding werd getest bij pH 5.2. Deze pH-gevoelige activiteit is te danken aan de afbraak van de orthoesterfunctionaliteit bij lagere pH, vergezeld van verlies van het lipide. Deze aanpak zorgt voor een mate van controle bij het afstemmen van enzyminhibitie op basis van de lokale pH (**Schema 5**).

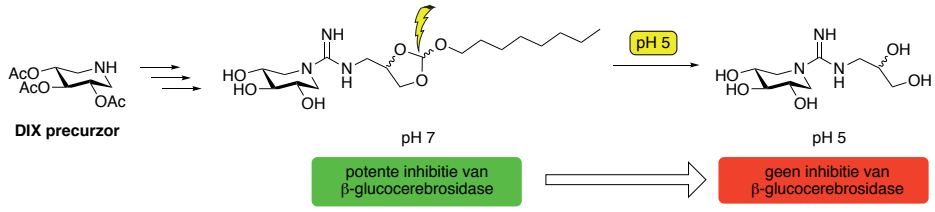

Schema 5. Overzicht van het reactieschema van de verbindingen zoals beschreven in hoofdstuk 4.

Hoofdstuk 5

Afsluitend is in **hoofdstuk 5** een samenvatting van het onderzoek uit hoofdstukken 2-4 beschreven, gevolgd door een discussie over de vooruitzichten voor toekomstig onderzoek en mogelijke toepassingen in biologisch en klinisch onderzoek.

"Je gaat het pas zien als je het doorhebt."

— *Johan Cruijff* —

explaining pharmacological chaperones

POVZETEK

Efektiven dizajn zdravil za modulacijo bioloških procesov zahteva detajlno poznavanje substratov in ligandov, ki jih prepoznavajo njihovi komplementarni encimi in receptorji. **Glikozidni encimi** so ključnega pomena pri procesu razgrajevanja tekom širokega spektra metabolnih poti, vključno z obdelavo glikoproteinov in glikolipidov ter prebavo ogljikovih hidratov. **Inhibitorje** encimov lahko uporabimo za manipulacijo encima na določeni poti in s tem povzročimo predvidljive spremembe glikozilacije. Rezultate takih sprememb lahko nato preučimo in pridobljene informacije uporabimo za razumevanje, kaj naredi specifičen inhibitor pri biološki proces in kako se lahko inhibitorji, ki imajo te lastnosti, oblikujejo na način za implementacijo v bodoči terapiji. Življenjsko pomembne **lizosomske katabolične poti** vključujejo perfektno orkestrirane akcije serije encimov za pravilno delovanje. Lizozomski encimi izvajajo natančne biokemične reakcije pri razgrajevanju substratov na manjše sestavine, ki jih mora celica reciklirati ali izločati. Nenormalno, čezmerno kopičenje ne-degradiranih substratov, povzroči različne celične disfunkcije, ki lahko vodijo v vrsto neželenih patologij, splošno znanih kot motnje shranjevanja lizosomatskih produktov, običajno skrajšane z **LSD** (Lysosomal Storage Disorders).

Gaucherjeva bolezen (Gaucher disease, **GD**) je najbolj prevladujoča bolezen lizosomskega shranjevanja. V tem primeru gre za posledico mutacije v genu glukocerebrozidaze, kar lahko privede do zmanjšane aktivnosti ***β*-glukocerebrosidaze** (**GBA**, GBA1), encima, ki je odgovoren za hidrolizo **glukozilceramida** (**GlcCer**). Pomanjkanje aktivnosti GBA lahko povzroči postopno akumulacijo nerazgrajenega glukozilceramidnega substrata, ki vodi do resnih kliničnih simptomov in v nekaterih primerih tudi do nevroloških zapletov. Primarni poudarek, na terapevtskih strategijah za zdravljenje takšnih bolezni, se osredotoča na zmanjšanje celične koncentracije glikosfingolipidov v lizosomu (**Shema 1**).

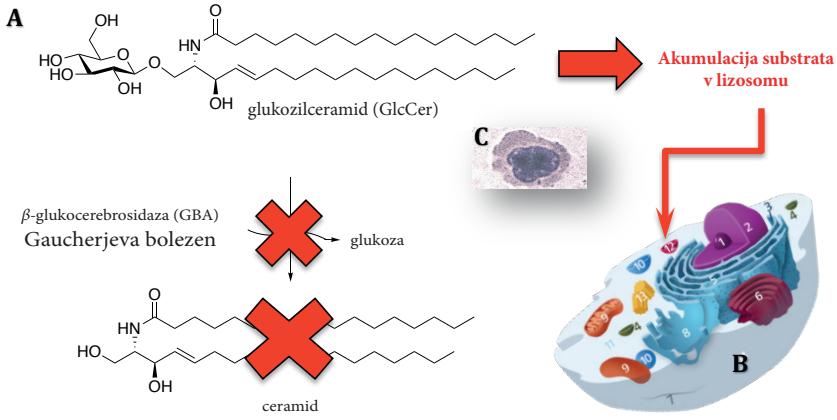

Shema 1. Ilustracija nastanka Gaucherjeve bolezni. A) Neuspešna hidroliza GlcCer substrata, zaradi motnje delovanja encima *β*-glukocerebrosidaze. **B)** Akumulacija nerazgrajenega substrata v lizosomu. **C)** Gaucherjeva celica s povišano koncentracijo GlcCer.

Med različnimi terapevtskimi pristopi, ki jih trenutno preučujemo, je **farmakološka terapija s šaperoni** (Pharmacological Chaperone Therapy, **PCT**), kjer gre za zanimivo tehniko za vzpostavitev ravnovesja med prilivom in degradacijo nakopičenega substrata. **Farmakološki šaperoni** (Pharmacological Chaperone, **PC**) so majhne molekule, ki lahko stabilizirajo napačno sestavljen encim in s tem preprečijo predčasno degradacijo, čigar naloga je **endoplazemskega retikuluma** (**ER**). V primeru Gaucherjeve bolezni je mutiran GBA encim odgovoren za napačno presnovo substrata zaradi prezgodnje razgradnje encima v ER, kljub temu, da encim pogosto še vedno ohranja določeno stopnjo katalitične aktivnosti. Učinkovito zdravljenje na osnovi zdravljenja s šaperoni vključuje farmakološko aktivno spojino, ki se veže in stabilizira napačno sestavljen encim, s čimer se omogoči transport encima do lizosoma, kjer lahko nato razgrajuje presežen GlcCer (**Shema 2**).

Nekateri **iminosladkorji** so zelo močni in selektivni zaviralci glikozidaz in se v nekaterih primerih reverzibilno vežejo na aktivno mesto njihovega ciljnega encima na pH-odvisen način. Morda se zdi paradoksalno uporabiti inhibitor za stabilizacijo encima, vendar so pozitivni izidi takih terapevtskih pristopov pokazali, da gre za koristno tehniko, ki lahko povzroči končno izboljšanje bolnikov z lizosomskimi komplikacijami. Konkurenčni inhibitorji, kot so iminosladkorji, imajo neprecenljivo možnost, da stabilizirajo prizadeti encim in kot rezultat preprečijo predčasno degradacijo encima in pospešijo njihov transport do lizosomov.

Kot posledica zgoraj omenjenih razlog je razvoj potentnih zaviralcev glikozidaze, katerih delovanje je preferirano odvisno od pH okolja v katerem sodelujejo tekom procesa, privlačna tema za razvoj novih terapevtskih sredstev.

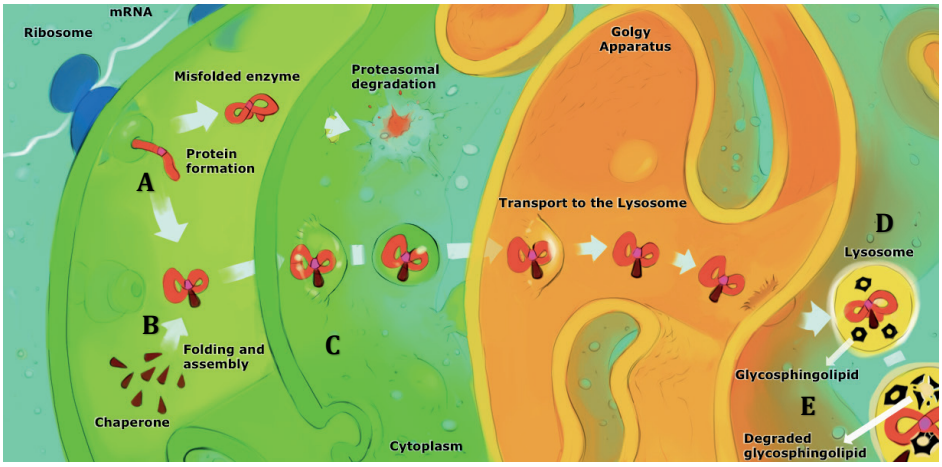

Shema 2. Predlagan mehanizem delovanja farmakoloških šaperonov. A) Mutiran encim je v nepravilni obliki, vendar je še vedno katalitsko aktiven. **B)** Farmakološki šaperon se veže na encim in ga pri tem stabilizira. **C)** Kompleks je nato transportiran do lizosoma brez predčasne degradacije encima. **D)** V lizosomu, se šaperon, zaradi nižjega pH in višje koncentracije substrata, disocira iz kompleks. **E)** Sedaj prost encim lahko posledično razgradi substrat v presežku.

2 *Poglavje 2*

V **2. poglavju** smo iz 1-deoksinojirimicina (DNJ) pripravili niz derivatov bicikličnih izosečnin, s sintetskim protokolom, ki je potekal preko gvanidinskega intermediata. Biološki testi inhibicije glikozidaz so pokazali, da gre za biciklične spojine, ki spadajo med najmočnejše znane inhibitorje GBA. Medtem ko smo prvotno raziskovati eksociklične gvanidinske analoge DNJ, je bilo ugotovljeno, da so takšne spojine nagnjene k intramolekularni ciklizaciji, ki se preobrazijo v ustrezne biciklične derivate. Naši podatki kažejo, da so biciklične izosečnine, pripravljene v tem poglavju, med najmočnejšimi zaviralci GBA doslej. Preliminarni podatki eksperimentov z uporabo fibroblastov iz GD pacientov, ki nosijo mutacijo N370S GBA, kažejo, da ima najbolj obetavna spojina, pripravljena v tem delu, lastnosti šaperona, na enaki ravni kot pri že znanem šaperonu NN-DNJ (**Shema 3**).

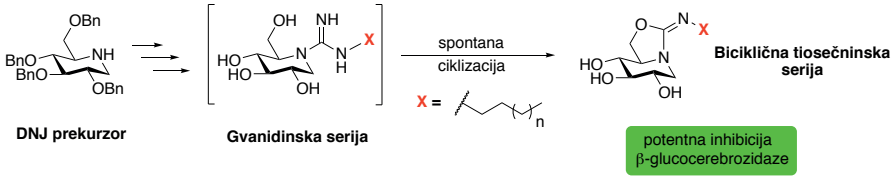

Shema 3. Povzetek sintetskega dela, ki je opisan v 2. poglavju.

3 *Poglavje 3*

Naše prejšnje študije so pokazale, da nastajanje ciklične izosečnine poteka preko gvanidinske vrste, ki je nagnjena k ciklizaciji z delovanjem skupine 6-OH. **3. poglavje** poroča o strategiji za izogib intramolekularne ciklizacije, pri čemer so bili pripravljeni *N*-substituirani gvanidinski analogi DIX, ki nimajo 6-OH skupine, kot pri DNJ. Raziskave inhibicije s serijo glikozidaz so pokazali, da gvanidinski analogi močno inhibirajo človeško rekombinantno GBA z IC_{50} vrednostmi v nanomolarnem območju, kar potrjuje njihovo potentnost, zaviralna moč inhibitorjev pa se še poveča z daljšimi alkilnimi substituenti. Naša študija jasno kaže, da dodatek gvanidinijevega dela vodi k močnejši inhibiciji GBA v primerjavi s poročanim alkiliranim aminskim analogom. Sečninski analogi DIX-a so bili prav tako sintetizirani in ovrednoteni na enak način in pokazali, da so selektivni za *β*-galaktozidazo iz govejih jeter. Pri analogih sečnine nismo opazili inhibicije človeške GBA.

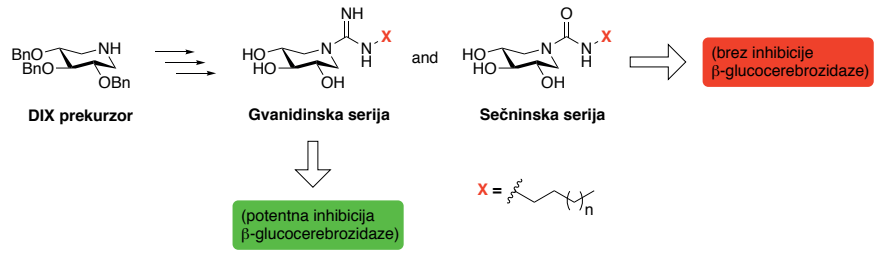

Shema 4. Povzetek sintetskega dela, ki je opisan v 3. poglavju.

Poglavje 4

4

Kot nadaljevanje prejšnjih študij, **4. poglavje** opisuje pripravo novih inhibitorjev glikozidaz na osnovi DIX-iminosladkorja, ki vsebujejo; eksociklični N-alkilirani gvanidin in kislinsko labilen ortoesterni del. Kislinsko labilen ortoester je še posebej zanimiv adukt zaradi pH-odzivnih lastnosti, ki je sposoben hidrolizirati v blago kislem lizosomskem okolju, s čimer se preoblikuje iz aktivnega hidrofobnega inhibitorja v neaktino hidrofilno spojino, brez inhibitorskih lastnosti. V ta namen študija razpravlja o razvoju analogov, ki ohranjajo močno aktivnost pri nevtralnem pH, ter kažejo znatno zmanjšanje aktivnosti pri kislem pH v lizosomu. pH-občutljiva aktivnost je posledica degradacije funkcionalnosti ortoesterskih spojin pri nižjem pH, ki jo spremlja izguba lipida. Ta pristop zagotavlja stopnjo nadzora pri uravnavanju inhibicije encimov na osnovi lokalnega pH in nudi eleganten pristop za zdravljenje lizosomskih bolezni v prihodnosti.

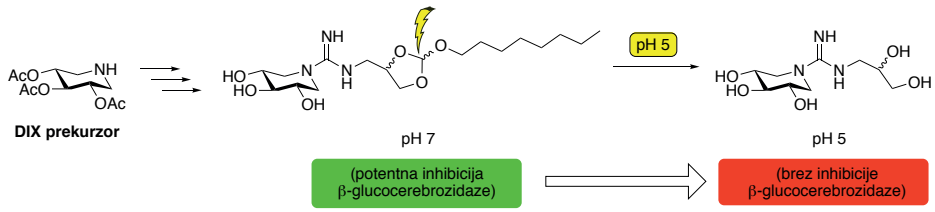

Shema 5. Povzetek sintetskega dela, ki je opisan v 4. poglavju.

Poglavje 5

5

Zadnje raziskovalno poglavje zajema pregled trenutnih molekul, ki so že na tržišču ali pozitivno dosegajo terapevtsko normo v znanstvenih raziskavah. Poglavje se zaključi z vizijo prihodnosti ter potencialom znanstvene raziskave, ki zajema to doktorsko disertacijo.

"Na tem mestu bi se rad zahvalil svojim staršem.

Še posebej mami in očetu."

— *Sebastjan Cimirotič - Cime* —

trying to understand human biology

CURRICULUM VITAE

Alen Sevšek was born in Celje, Slovenia on the 30th of April in 1987. After completing an eight year primary school program and four years of general gymnasium highschool, he started with a masters equivalent education in chemistry at the Faculty of Chemistry and Chemical Technology in Ljubljana, Slovenia. As a part of this program he conducted a five month diploma thesis internship at the organic chemistry synthesis group of prof. dr. Branko Stanovnik and prof. dr. Jurij Svete in 2010. During this internship he was working on stereoselective synthesis and rearrangements of camphor derivatives with dr. Uroš Grošelj. After completing the practical part of his diploma thesis, he continued his education at Utrecht University as a part of the Erasmus internship program in 2011, with financial support from the Slovene HR Scholarship Fund. Research was conducted at the Medicinal Chemistry and Chemical Biology Department of prof. dr. Rob Liskamp, under the supervision of dr. Jeroen van Ameijde. Five months scientific internship resulted in a thesis equivalent project, researching novel nitrotyrosine-containing peptides as kinase substrates for development of kinase/phosphatase dynamic microarrays in close cooperation with dr. Rob van Ruijtenbeek of PamGene. Before receiving his degree in 2012, Alen spent a month at Universidade Federal de Pernambuco in Recife, Brasil, working on calixarenes as anticancer compounds with prof. Severino Alves Júnior as a part of Slovene Development Study Visit program.

Alen was affiliated with Utrecht University as a Ph.D. candidate from February 2013 until October 2017 in the group of prof. dr. Roland J. Pieters under supervision of associate prof. dr. Nathaniel I. Martin working on glycosidase inhibition. Parts of the work described in this thesis were communicated by means of oral and poster presentations on various international and domestic symposia.

During his doctoral studies he was a Ph.D. committee board member of Utrecht Institute for Pharmaceutical Sciences (UIPS) from 2014 until February 2017.

LIST OF PUBLICATIONS

Orthoester Functionalized N-guanidino Derivatives of 1,5-Dideoxy-1,5-imino-D-xylitol as pH-responsive Inhibitors of β-Glucocerebrosidase

Sevšek, A.; Sastre Toraño, J.; Quarles van Ufford, L.; Pieters, R. J.; Martin, N. I. *Manuscript accepted for publication in MedChemComm.*

***N*-guanidino Derivatives of 1,5-Dideoxy-1,5-imino-D-xylitol are Potent, Selective and Stable Inhibitors of β-Glucocerebrosidase**

Sevšek, A.; Šrot, L.; Rihter, J.; Čelan, M.; Quarles van Ufford, L.; Moret, E. E.; Martin, N. I.; Pieters, R. J. *ChemMedChem*. **2017**, *12*, 483–486.

Bicyclic Isoureas Derived from 1-Deoxynojirimycin are Potent Inhibitors of β-Glucocerebrosidase

Sevšek, A.; Čelan, M.; Erjavec, B.; Quarles van Ufford, L.; Sastre Toraño, J.; Moret, E. E.; Pieters, R. J.; Martin, N. I. *Org. Biomol. Chem.* **2016**, *14*, 8670–8673.

CONFERENCES

Potent, Selective, and Stable Inhibitors of β-Glucocerebrosidase

Poster Presentation at 4th Chains Symposium
Veldhoven, The Netherlands, 7th of December - 8th of December *2016*

Enhancing Enzyme Activity with Isourea and Guanidino Derived Iminosugars

Poster Presentation at 3rd Chains Symposium
Veldhoven, The Netherlands, 30th of November - 2nd of December *2015*

Enhancing Enzyme Activity with Inhibitors

Oral Presentation at 1st Science for Life Conference
Utrecht, The Netherlands, 9th of November *2015*
Awarded with the Young Scientist Award for best oral presentation.

Inhibitors as Potential Pharmacological Chaperones

Poster Presentation at 18th EuroCarb Symposium
Moskow, Russia, 2nd of August - 6th of August *2015*
Awarded with the 1st poster prize.

Guanidinium Modified Iminosugars are Potent Glucosidase Inhibitors with Potential as Pharmacological Chaperones

Oral Presentation at 2nd Chains Symposium
Veldhoven, The Netherlands, 17th of November - 18th of November *2014*

Glycosidase Inhibition by Novel Guanidinium and Urea Iminosugar Derivatives

Poster Presentation at 17th EuroCarb Symposium
Tel Aviv, Israel, 7th of July - 11th of July *2013*

ACKNOWLEDGEMENTS / ZAHVALA

"Sreča je srečati prave ljudi, ki v tebi pustijo dobre sledi."

— *Tone Pavček* —

Roland or **Nathaniel**? Who to address first? Both of you contributed equally to the making of this thesis and provided me with great guidance though the whole project. I could not be more lucky with having you both on the team. I met both of you during my first appearance in the group during my Erasmus exchange and immediately felt a good connection, which was one of the main reason to come back and obtain the PhD degree under your supervision. **Roland**, thank you for always taking time to listen and discuss different topics in detail, whether it was work related or not, when rushing to your office unannounced. It has been a pleasure working with you - one could not ask for a better professor to work with. **Nathaniel**, your energy and optimism always kept me going forward and you always found a way for me to thrive, steering my attention towards finding solutions for various obstacles that first appeared unsolvable. One cannot forget one of your best life tips: "Work smart, not hard" - although I have sometimes tried to combine them both - :). It is my pleasure to address that our connection brought us together, not only as colleagues at work, but also as friends that shared joyful after-work drinks on multiple occassions. I wish you both good luck in the future, on both professional and personal levels, and hope to eventually show you around in Slovenia.

Dear **Linda**, you have been a big part of my project, and of tremendous help with taking a lead on the biochemical field. We have had many problems to solve, mainly associated with the assay conditions, and it was always a pleasure to solve those enigmas together. Appart from professional discussions, I have also enjoyed many suggestions about where to spend our holidays in the future.

Javier, my Spanish amigo - thanks for contributing with all the degradation assays and concluding the behavour of our peculiar molecules. Our curiosity has brought us to some interesting results. Most of all, thanks for convincing Madrid to let Dončić play for Slovenia - I have a feeling you made some calls there.

Mr. van Haren, my paranimf, a fumehood neighbour and a close friend. Without a doubt, we have made these synched PhD-years properly entertaining by sharing project discussions during work and many late, fun-oriented Magical evenings. Heck, we started strong even before working in the lab by uninttentionally syncing our Django seats together. It was great to share many gastro-explorations together and accompany those by random topics that brought us together through the years. The sailboat will be waiting ;)!

This brings me to my other paranimf - **Frank**. We have been through some amazing *experiences* together; festivals, nights out, morning gym sessions and a plethora of discussions, where nothing was off-limits. You are a trully great friend and I am sure we will keep in touch and schedule many more of *such* in the future - planned a few weeks in advance of course :).

A special thanks goes to **Dirk** for welcoming me to the CPS program, where I gained valuable teaching experiences and got to be a part of a nice tandem with you and **Johan**. In addition - Johan, thanks for all the help with the spectra and an opportunity to make use of the private NMR downstairs. **John**, thanks for always being around the LCMS room and for finding an immediate solution for my problem. I have also enjoyed our discussions on meat, and hope you don't burn your house down just to get that "extra smokiness". **Ed**, it has been a pleasure working with you on the computational side of my project and on the board of the UIPS PhD committee. A big part of the committee was **Paul**, which I thank for welcoming me on the board and for a nice overall experience during these three years on the board. **Tom W.**, you havent been in the group for that long, but long enough to shed some light on important obstacles along the crucial phases of my project in a very friendly fashion. I hope the work in this thesis can be a welcoming, although minute, addition to your bible of Lipophilic Iminosugars. **Gert-Jan** thank you for the input in the final stages of my thesis, and good luck with the youngsters that are yet to join the group.

To all lab-colleagues: it seems difficult to find a word in English that nicely sums up your presence, so I will have to search elsewhere and thank you for the *gezellig* vibe, both inside and outside of the lab. **Marjon**, we've managed to keep in touch after your departure and to accompany our sessions with nice talks, which I am sure we will continue. Thank you for adding the icing on the cake with your artistic contribution to this thesis. **Timo**, you were a great roomate at the end of my program and a great laugh during the coffee breaks with your nifty humor. Don't let that ship sink, arr! **Tom**, you have brought a valuable freshness to the group but unfortunately joined way to late, so I will have to experience the full potential of The Woody Joker off work, and catch up every now and then ;). **Peter Taart**, it doesn't get old :). Despite the fact you have enlightened me with the difference between colleagues and friends, I still insist we are better friends due to plenty of nice occasions we spent off-work. Alles gute in Deutschland für dich und **Nikki**! **Ingrid**, the sweeter of the cake family, keep on smiling and feeding me those whiskeys! **Joost**, it has been way to long since we have seen each other, which is just one more reason to arrange another fun session and catch up properly. **Paul**, such a relief when you left the group. Not only I have gained more leg room, but was finally able to stare at Laurens's pretty back when your solid-stone presence moved from my sight. Jokes aside, beer in Groningen once they move it closer to Utrecht! **Laurens**, the diplomat of the bunch, I have enjoyed many one-on-one conversations with you and wish you and your family all the best in the future. Take care of them, papa! **Hao**, you get nothing! NOTHING! **Charlotte**, I would prefer if you would've changed sits with Laurens after Paul left the building :p. Good luck with the project and all your gastro-explorations that are yet to come. **Barbara**, it is somewhat self explanatory that we have to climb Zugspitze together once the lowlands are not our home grounds anymore ;). **Suhela**, **Diksha**, **Xin**, **Jie**, **Wenjing**, **Guangyun**, **Yongzi**, **Apoorva**, **Ivan**, **Mehman**, **Pieter**, **Tim**, **Jack**, **Frederik**, **Yvette**, **Núria, Victor** and **Seino** it was fun to have you around in the lab and I wish you good luck wherever you end up being. And now, the most beautifully written paragraph in Persian:

lamaK,ک م ال، د ر م ورد ف ره ن گ خ ود ب س ی ارخ وش ح ال ش د م ود وس ت دارم ب ه ش م ای
س ف رب پ ردازم آگ ر د ره م ان ز م ان ه م د ر ای ران ه س ت ی م. م وف ق ب اش ی د!

Arvin, I have enjoyed working with you, especially on a well-orchestrated beauty of GROS and prank-calling **Hans** many times, who I also thank for bearing with us and not destroying the phone during our annoying conversations. **Edwin**, not much to say here other than that you have to take me and Nathaniel to one of your late night adventures. **Rob**, still dreaming of the suckling lamb you've roasted on the yard of your house - epic! **Jeroen**, you were my first supervisor in Utrecht and I appreciate you showing me around and your supervision during these five months. **Rob R.**, we have not been working together too much, apart from my Erasmus project, but it is always a pleasure talking with you and absorbing the optimism you are so subtly sharing with others. Good luck with PamGene and travels around the World! **Jack**, **Steffen**, **Francesca**, **Rik**, **Hilde**, **Loek**, **Núria** and **Gwen**, you were in the group at the very start of my program, and yet you helped tremendously by welcoming me to the group with great vibes. **Sam** and **Ramon**, the jolly duo from the fourth floor! Thanks for some awesome talks and parties together. I am sure, we did not yet say our finals words.

Bibi, **Maša**, **Luka**, **Jakob**, **Rens**, moji študentje, ki ste drastično pripomogli k nastajanju te doktorske naloge. Verjamem, da ste se tekom projekta veliko naučili predvsem pa upam da sem vam vmes omogočil tudi dovolj časa za uživancijo. Dodatna zahvala gre **Bibi**, in sicer za krasno slikovno reprezentacijo mehanizma farmakoloških šaperonov. Srečno vsem! **Rens**, Google it! :)

Joep, we needed three months to start talking to each other - being fumehood neighbours and all - but boy, we made sure to catch up for the missing months, hehe. To many more! **Clémence**, my French hedonist friend and chaterbox with a fine accent. We had some great times together, and I hope to share a few more before the old building fall on you while you're asleep. **Adrien**, my roomate and a true friend that needs to pay a visit again, because it has simply been to long! **Tino** for life! A fast around the world cheers goes to my Erasmus companions **Austen**, **Yone**, **Conor**, **Morgann**, **Samir**, **Peter** and **Nikster**! **Gruson**, your raw humor brought some dynamics into our evenings together and a big thanks for taking care of me looking good on the promotion pictures! Good luck to you and **Eva** in your new nest. **Jan Peke**, the Dutch pizza aficionado! A great addition to the Dutch crew that need to reunite soon after this thesis is finalized. All the best to you and **Elisa**. **Pieter**, festivals were never as fun as when together, so I propose we duo again on Fusion if the Germans decide to reopen it again. **Sara**, the energetic superwoman - always a pleasure to share your Polish delights and honest one-on-one conversations. **Michael**, it's hard to pin point for what I am grateful the most; Our friendship, or the fact that you gave us a roof above our heads when the notorious Betty Chang canceled our reservation while driving to the Netherlands. **Rami**, Shalom! Words hardly describe what we have grown into during these years. You have been my housemate, my 12m^2-roommate my evening consort and overall associate when fun was on schedule. I simply don't see an end to it, so how about you ditch your girlfriend - **Devi**, and we start our life together.

A big shout out to my SBU mates that made these few years epic: **Tim**, **Joost**, **Charley**, **The Stel Brothers**, **Jannes**, **Kris**, **Derek**, **Zanny**, **Ruirt**, **Sjaun**, **Johan**, **Pim**, **Siebe**, **Kenny**, **Richard**, **Luc**, **Yorrick**, **Tomas**, **Tom**, **Jelmer**, **Matthijs**, **Corwin**, **Guy**, **Maurice**, **Melchior**, **Poes**, **Eriiik** and the entire female counterpart that made the whole SBU prettier.

Na tem mestu gre zahvala slovenski delegaciji, ki mi je vedno stala ob strani in ob tem pripomogla k zabavnim dogodivščinam tekom večkratnih obiskov v Slovenijo. **Virtič**, The Beatbox Machine, kolega pri katerem je kavč vedno na razpolago in čevapčiči vedno na meniju! Sedaj pa še na eno frikandelo na Nizozemsko - perfektno! **Jurič** in **Brezovnik**, savinjska predstavnika, ki ju zaradi naglasa malokdo zastopi pa kljub temu naveza z velemestnim intelektualcem neustavljivo cveti. Predlagam, da od sedaj naprej rezervirata letno karto in prijavita 5-dnevne dopuste za leta vnaprej. **Huš**, cimer, sošolec, sotrpin na faksu, dober prijatelj in fanatik atletike. Še dalje izpopolnjuj, že tako širok spekter atributov, da me lahko ob priliki na kratko naučiš bistva, kot že mnogokrat. **Klara**, vedno prikupna a **Retko** visoka - še vedno čakam na obisk najnižje predstavnice Evrope - pa kar dve šali naenkrat :). Kljub temu, pa nikoli ni treba čakati na kavo v Ljubljani, ker si vedno za akcijo! Še na mnogo teh! **Kek**, ruski predstavnik slovenskih podjetnikov in kolega že iz srednješolskih časov. Na zadnje sva se srečala v Moskvi in pristala v klubu s karakterjem. Čas, da drugi del nadaljujeva v Amsterdamu! **Bobinac**, vedno v veselje, ko se vidiva in nadaljujeva standardne pogovore srednješolskega obdobja, ki pa počasi rastejo v resne *fotrovske* debate, čeprav naju še vedno rado zanese v igrive teme. Ni je teme, ki je ne bi prežvečila in prav čas je da kmalu spet vrževa nekaj na žar.

Nazadnje gre zahvala, verjetno najpomembnejšemu členu za nastanek te doktorske disertacije, moji družini. Hvala za razumevanje, za podporo, finančno kontribucijo brez katere ta naloga ne bi bila izvedljiva in hvala za vedno dobrodošel prihod. Vem, da lahko vedno računam na vas v rutinskih in težkih trenutkih za kar sem izredno hvaležen. Hvala ker ste, ste bili in še boste! **Mami**, hvala za vse podporne besede in vse slastne prigrizke, ki jih vedno pripraviš za na pot. Hvala za vse izlete v Zagreb in vse vikende, ki smo jih preživeli skupaj z **dedijem** in **bako**, ki sta mi med drugimi resnično pokazala kaj pomeni iskrena ljubezen. **Ati**, hvala za pohorske gene, za humor tekom teh trideset let in za vse dogodivščine, ki še pridejo. Verjamem da kmalu skupaj obesima mreže v vinogradu, da ne bojo ptiči spet vsega pojedli. **Mitja**, hvala ker si najboljši brat kar si ga kdor lahko zaželi, predvsem pa hvala ker si ob tem tudi nezamenjiv prijatelj. Upam, da v prihodnosti še nadoknadiva kar je bilo zamujeno in nadaljujeva avanturo v najboljšem možnem *bratskem stilu na nož*. Vedno nasmejana **Anja**, hvala za vse podporne besede in optimistično nabito energijo. Res si dobrodošel žarek pozitive in verjamem da boš takšna še naprej. **Lea**, prva vnukinja, in **Mark**, prvi vnuk, hvala za vse smešne prigode in neprespane noči, ker me cel časa rukata v rebra. **Cveta**, hvala za estetsko inspiracijo interiornega dizajna, za vse dobrodošle obiske pri vas doma in na morju ter dodatno ekvivalentno-materinsko podporo. **Aleš**, hvala za vse gastronomske pokušine, še posebej tiste, ki so naročeni pri sosednjih mizah v retavraciji, predvsem pa obema hvala za kolegialni občutek, ko čas preživimo doma. **Klarisa**, hvala ker nisi tečna, ker imeti dve sestri v familiji pač ni najboljši recept za najbolj lahkotno-umirjene vibracije :). Ti sam glej, da me povabiš na 18-ko. **Patricija**, **Anže** in **Žak**, vam se zahvalim, ko Žaku razložite bistvo te doktorske. Do takrat pa srečno vsem na vseh šprtanskih avanturah. **Žuži** in **Ollie**, hvala ker me vedno *tak fajn* grejeta ko gledamo televizijo pa čeprav vem da se primarno grejeta sama. In nasvezadnje, hvala **Romina**, ker si vedno ob meni, ker me pri vsem vedno podpiraš, ker se rada vrneš domov po napornem dnevu in ker si vedno v top-kondiciji in se z leti, praktično vizualno, ne spreminjaš :). Ti si bistvo mojega življenja zato sem srečen, da sva skupaj že tako zgodaj najine skupne življenjske poti. Rad vas imam!

A